

**13ª. ESCOLA LATINO-AMERICANA DE VERÃO EM EPILEPSIA
13ª. ESCUELA LATINO-AMERICANA DE VERANO EN EPILEPSIA
13th. LATIN-AMERICAN SUMMER SCHOOL ON EPILEPSY
(LASSE)**

**SÃO PAULO, BRASIL 7 – 15 DE Março DE 2019
Centro de Convenções Santa Mônica**

COORDENAÇÃO GERAL
Prof. Dr. Esper A. Cavalheiro

**COMISSÃO LATINO AMERICANA DA DA INTERNATIONAL
LEAGUE AGAINST EPILEPSY (ILAE)**
Prof. Dr. Roberto Caraballo

**ACADEMIA LATINO AMERICANA DE EPILEPSIA DA INTERNATIONAL
LEAGUE AGAINST EPILEPSY**
Prof. Dr. Alejandro Scaramelli

PRESIDENTE DA LIGA BRASILEIRA DE EPILEPSIA (LBE)
Profa. Dra. Vera Terra

PRESIDENTE DA ILAE
Prof. Dr. Samuel Wiebe

COMISSÃO ORGANIZADORA
Elza Márcia Yacubian - UNIFESP
Esper A. Cavalheiro - UNIFESP
Fernando Cendes - UNICAMP
Fulvio Alexandre Scorza - UNIFESP
Jaime Carrizosa - Universidade de Antioquia

LASSE XIII – EPILEPSIA COMO UMA DOENÇA DE REDES NEURAIS

A 13ª Escola Latino-Americana de Verão em Epilepsia (Lasse) é uma atividade educacional da International League against Epilepsy (Ilae) e da Academia Latino-Americana de Epilepsia (Alade) com o apoio da Liga Brasileira de Epilepsia (LBE).

Com início em 2002, as Escolas de verão em epilepsia, organizadas pela Ilae, tornaram-se referência como experiência didática. Como professores e alunos permanecem em contato próximo por cerca de dez dias consecutivos, esse tipo de Escola tem facilitado a integração entre pesquisadores básicos, clínicos, cirurgiões na área de epilepsia e alunos, permitindo uma melhor compreensão das novas descobertas para o benefício das pessoas com epilepsia.

A 13ª Escola Latino-Americana de Verão em Epilepsia (Lasse) a ser realizada em Guarulhos, entre 7 e 15 de março de 2019, abordará o tema Redes neurais em epilepsia _ Da conectividade ao conectoma, uma mudança de paradigmas cuja abordagem é necessária à atualização de jovens epileptologistas latino-americanos.

Agradecemos aos professores e tutores que, de forma tão generosa, abandonam seus afazeres e oferecem-se seu tempo e damos boas-vindas aos alunos da LASSE XIII, razão maior do nosso trabalho.

A COMISSÃO ORGANIZADORA

**13th. Latin-American Summer School on Epilepsy (LASSE IX)
7 – 15 March 2019 – São Paulo, Brazil**

PROGRAM

07/03 – Thursday

09:00 – 10:00 Welcome and Introduction to LASSE – Esper Cavalheiro (Brazil) 6
 10:30 – 12:00 From structural brain connectivity to the connectome: paradigm shifts in approaches and concepts – Marina Bentivoglio (Italy) 7
 14:00 – 15:00 Brain wiring: from circuits to systems – Giuseppe Bertini (Italy) 18
 15:00 – 16:00 Parahippocampal-hippocampal networks in the healthy and diseased brain – Menno Witter (Norway) 19
 16:30 – 17:30 The 5 critical elements of a connectome: nodes, links, topology, dynamics and multiplex scaling - Jean Faber (Brazil) 78

08/03 – Friday

09:00 – 10:00 Imaging presynaptic activity – Philippe Mendonça (UK) 99
 10:00 – 11:00 Strength and weaknesses of some basic methods: correlation, coherence, Granger causality – Jean Gotman (Canada) 105
 11:30 – 12:30 Inferring effective connectivity from EEG recordings – Adenauer Casali (Brazil) 106
 14:00 – 15:00 Quantitative methods in neuroimaging: basis for connectivity measures – Edson Amaro (Brazil) 118
 15:00 – 16:00 Consciousness and brain complexity: perturb-and-measure approaches - Adenauer Casali (Brazil) 119
 16:30 – 17:30 Theta-gamma coupling in the hippocampus – Adriano Tort (Brazil) 128
 17:30 – 20:00 Epilepsy revealed: the history of epilepsy through paintings – Jaime Carrizosa (Colombia) 129

09/03 – Saturday

09:00 – 10:00 The diffusion MRI-based connectome: promises and pitfalls – Matteo Mancini (UK) 150
 10:00 – 11:00 Connectomes: what can they tell us about brain function and dysfunction – Christophe Bernard (France) .. 162
 11:30 – 12:30 From electrophysiological recordings to connectivity: how to construct a graph and how to analyze it? – Jean Faber (Brazil) 163
 14:00 – 15:00 Neuroimaging and big data: beyond the ‘omics’ revolution – Edson Amaro (Brazil) 168
 15:00 – 16:00 Novel insights into the mechanisms of spatial coding by hippocampal neurons – Adriano Tort (Brazil) 169
 16:30 – 17:30 Structure-function relationships in epileptic networks – Maxime Guye (France) 170
 17:30 – 18:30 How unique are structural and functional connectomes? Towards personalized medicine – Christophe Bernard (France) 183
 18:30 – 20:00 The historical background: body-body, body-mind, mind-brain connectivity from ancient Mesopotamia to the rise of modernity – Mario Fales (Italy) 184

10/03 – Sunday

09:00 – 10:00 Mapping brain networks in patients with focal epilepsy – Imad Najm (USA) 185
 10:00 – 11:00 Brain connectivity in focal onset epilepsies – Fernando Cendes (Brazil) 186
 11:30 – 12:30 Connectivity in nodular heteropia – Jean Gotman (Canada) 187
 14:00 – 16:00 Group A – Case Study – Peter Wolf (Denmark) 188
 Group B – Case Study – Katia Lin (Brazil) 189
 Group C – Case Study – Rūta Mameniskienė (Lithuania) 190
 Group D – Concepts in Neural Design – Philippe Mendonça (UK) 191
 16:30 – 17:15 Functional and epileptic networks: building hypothesis based on clinical descriptions – Patricia Braga (Uruguay) 192
 17:15 – 20:00 Mapping epileptic networks (Case discussions) - Imad Najm (USA), Patricia Braga (Uruguay) 204

11/03 – Monday

09:00 – 10:00	EEG as basis for understanding connectivity in epilepsies – Elza Marcia Yacubian (Brazil).....	205
10:00 – 11:00	Brain connectivity in generalized epilepsies - Clarissa Lin Yasuda (Brazil)	224
11:30 – 12:30	Neuroplasticity in refractory epilepsy: is it a protective or risk factor? – Loreto Rios (Chile)	225
14:00 – 16:00	Group B – Case Study – Peter Wolf (Denmark).....	238
	Group C – Case Study – Katia Lin (Brazil)	239
	Group A – Case Study – Rūta Mameniskienė (Lithuania)	240
	Group D – Connectivity modelling - Jean Faber (Brazil)	241
16:30 – 20:00	Clinical correlation of connectivity alterations in childhood Epilepsy with centrottemporal spikes – Guilca Contreras (Venezuela)	242
21:00 – 22:00	Science in the 21st century: achievements, problems, need for integrity - Marina Bentivoglio (Italy)	252

12/03 – Tuesday

09:00 – 10:00	Is seizure classification compatible with the connectome concept? – Alicia Bogacz (Uruguay)	253
10:00 – 11:00	Hyperexcitable and hyper synchronous neural networks in animal models of epilepsy: aspects of the temporal dynamics of neural recruitment in epileptogenesis – Márcio Flávio Dutra de Moraes (Brazil)	265
11:30 – 12:30	Transition in epilepsy - Jaime Carrizosa (Colombia).....	266
14:00 – 16:00	Group C – Case Study – Peter Wolf (Denmark).....	281
	Group A – Case Study – Katia Lin (Brazil).....	282
	Group B – Case Study – Rūta Mameniskienė (Lithuania)	283
	Group D – How to keep and report your research activity? – Giuseppe Bertini (Italy).....	284
16:30 – 20:00	Identification of epileptic zone from stereoEEG: a connectivity based approach – Ferruccio Panzica (Italy)	285

13/03 – Wednesday

09:00 – 10:00	Understanding the vagus afferent network and its role in translational connectomics – Isabella D’Andrea Meira (Brazil)	296
10:00 – 11:00	Effect of pharmacological and surgical interventions on cognitive networks – Matthias Koepp (England)....	297
11:30 – 12:30	Connectivity derived from EEG and neuroimaging in focal epilepsies – Lilia Morales (Cuba)	298
14:00 – 15:00	Structural and functional connectivity during epileptogenesis – Matthias Koepp (England).....	311
15:00 – 16:00	Using structural and functional connectomes to improve neurosurgery outcome – Christophe Bernard (France).....	312
16:30 – 17:30	Future trends in neuronal circuitry imaging - Matheus de Castro Fonseca (Brazil)	313

14/03 – Thursday

	Neurostimulation in the treatment of drug-resistant epilepsy – Guilca Contreras (Venezuela)	322
09:00 – 10:30	Groups 1, 3, 5, 7.....	323
10:30 – 12:00	Groups 2, 4, 6, 8.....	324
14:00 – 15:00	The wide spectrum of metabolic encephalopathies – Maria Luiza Manreza (Brazil)	325

15/03 – Friday

09:00 – 11:00	Presentation of research projects.....	343
14:00 – 16:00	Presentation of research projects.....	344
17:00 – 20:00	Goodbye to the 13th LASSE	345

FROM STRUCTURAL BRAIN CONNECTIVITY TO THE CONNECTOME: PARADIGM SHIFTS IN APPROACHES AND CONCEPTS

(Part of the article *Methods for analysis of brain connectivity: an IFCN-sponsored review* submitted to Clinical Neurophysiology by Rossini PM, Di Iorio, Bentivoglio M, Bertini G, Ferreri F, Gerloff C, Ilmoniemi RJ, Miraglia F, Nitsche MA, Pestilli F, Rosanova M, Shirota Y, Tesoriero C, Ugawa Y, Vecchio, Ziemann U Hallett M)

Structural brain connectivity: experimental approaches and *in vivo* studies of the human brain

(by Marina Bentivoglio, Chiara Tesoriero, Giuseppe Bertini)

Chasing neuronal circuits: a never-ending story

Over the centuries, many paradigm shifts have occurred in the views on neuronal connections, their behavioral output and their alterations in diseases (Bentivoglio and Mazzeo, 2010). The “neuron doctrine”, which extended cell theory to the nervous system, was enunciated in 1891 (Shepherd, 2015). A breakthrough in the visualization of neurons was provided by the “black reaction”, the metallic impregnation introduced in 1873 by Camillo Golgi (1843-1926). Golgi staining revealed neurons, including their processes, in their entirety and with unprecedented detail. This allowed studies of neuronal circuits (Golgi, 1885), and still allows the investigations of the local neuronal circuitry of randomly impregnated neurons (**Fig. 1A**), also in tissue blocks of *post-mortem* human brain. The revelation power of the Golgi method is only matched after more than one century by genetic cell tagging with fluorescent proteins, or intracellular neuron filling (e.g., in surgically resected tissue blocks of the human brain) (**Fig. 1B,C**).

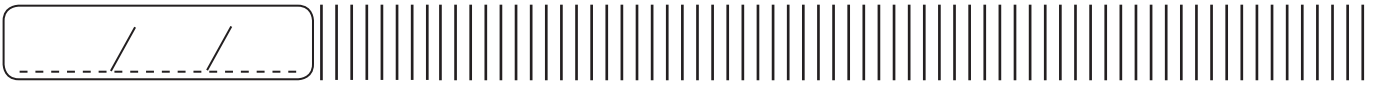
The champion of the “neuron doctrine” was Santiago Ramón y Cajal (1852–1934), who accomplished a monumental work, largely based on the Golgi stain, in which he provided a map of neuronal connectivity in the mammalian brain (Cajal, 1909, 1995). The debate between Cajal and Golgi—who had adhered to the reticular theory of nervous system organization—boosted neuroscience studies, focusing interest on the gray matter. White matter investigations were essentially descriptive, based on manual dissections and on the study of brain sections with the myelin stain introduced by Carl Weigert (1845–1904). Seminal contributions on the organization of fiber bundles in the human brain were provided by Carl Wernicke (1848–1900) and Joseph Jules Déjérine (1849–1917) (Schmahmann and Pandya, 2007).

The second half of the twentieth century witnessed a revolution in the experimental studies of neuronal connections, together with the explosion of neuroscience in the last decades of the century. As briefly discussed below, novel powerful techniques were introduced. The exploration of connectivity in the human brain remained, however, a challenging problem until the introduction of *in vivo* imaging.

Long-range neuronal connectivity

Anterograde and retrograde degeneration techniques

Pioneering early studies revealed that retrograde degeneration (“secondary atrophy”) of neuronal cell bodies and anterograde degeneration of fibers can provide effective tools to trace neuronal connections (Bentivoglio and Mazzeo, 2010) (**Fig. 2A**). Towards the end of the nineteenth century, neuronal alterations consequent to retrograde damage could be assessed by the cell stain (with thionin or toluidine blue) introduced in 1884 by Franz Nissl (1860–1919). Especially influential was the observation of anterograde degeneration of nerve fibers after transection reported in 1851 by Auguste Volney Waller (1816–1870) and named after him “Wallerian degeneration” (**Fig. 2A**).



Besides its implications for the trophic dependence of the axon from the cell body, this finding paved the way to the introduction of anterograde tract tracing methods based on silver impregnation of degenerating fibers after experimental lesions (Nauta and Gyax, 1951; Fink and Heimer, 1967). Metal impregnation stains are capricious and laborious, and degeneration methods have limited sensitivity, but these techniques gave a great impulse to experimental neuroanatomical studies. Importantly, anterograde degeneration revealed by modifications of silver impregnation was also applied to *post-mortem* investigations on the human brain, especially after restricted lesions occurring a few weeks before death (Mesulam, 1979).

Classical experimental tract tracing techniques based on axonal transport

A turning point in the study of structural brain connectivity was the discovery of anterograde and retrograde axonal transport (Bentivoglio, 1999). Axonal transport requires live axons; the active transport of tracers obviously cannot be applied to the human brain. Findings obtained with tract tracing based on axonal transport represent nowadays the "ground truth" for studies of the human brain based on *in vivo* imaging, and in particular on diffusion tractography.

Anterograde tract tracing based on the use of tritiated amino acids revealed by autoradiography was introduced in the early 1970s (Cowan et al., 1972). With this approach, trajectories and terminal fields of fibers originating from the tracer injection site (**Fig. 3**) could be delineated in detail. Anterograde tract tracing approaches have then been implemented (Gerfen and Sawchenko, 1984; Glover et al., 1986). In the same years, the discovery of retrograde axonal transport (Kristensson, 1970; Kristensson and Olsson, 1971) introduced as a tool the enzyme horseradish peroxidase (HRP), visualized by a histochemical reaction, which was soon applied to experimental retrograde tracing of the origin of projections to the tracer injection site (LaVail and LaVail, 1972) (**Fig. 3**).


The introduction of other retrograde tracers rapidly followed to increase sensitivity, combine tracers for multiple retrograde labeling for the study of branched connections, combine retrograde tracing with immunohistochemistry or *in situ* hybridization for the neurochemical characterization of pathways, and so forth. Fluorescent retrograde tracers turned out to be especially effective and versatile for these applications (e.g. Bentivoglio et al., 1980; Kuypers et al., 1980; Schmued and Fallon, 1986).

Conventional tract tracing has been implemented in recent years with genetic tracing for the study of the connectivity of specific neurons using cell-type-specific promoters (Oh et al., 2009). Most anterograde and retrograde tracers explore monosynaptic connections since they can cross synapses only in minute amounts, ineffective for transsynaptic tracing unless a bolus is injected, which is not feasible in the brain. Neurotropic viruses, which travel through axons and replicate in infected neurons, can instead provide tracing tools (Kristensson et al., 1974) applicable to trans-synaptic tract tracing (Kuypers and Ugolini, 1990) thanks to their propagation across synapses (**Fig. 3**).

Novel approaches to experimental tract tracing: optogenetics and chemogenetics

These innovative techniques are increasingly used to investigate the relationship between neuronal activity, neuronal circuits, and behavior.

The term optogenetics was introduced in 2006 (Deisseroth et al., 2006) referring to the general optogenetic discovery (Boyden et al., 2005). By combining genetic and optical methods, optogenetics utilizes molecular light-sensors to switch on and off neuronal electrical activity. Optogenetics thus allow to investigate neurons and neuronal circuits underlying specific behaviors at the time scale of milliseconds. By this approach, functional effects of defined neuronal cell types can be controlled in living tissue and in freely moving animals (Deisseroth, 2015). Optogenetics has also been combined with functional MRI for the experimental study of cell-type-specific contributions to behavioral output together with a "whole brain read-out" at the millimeter scale (Lee et al., 2017). From the translational point of view, applications of optogenetics in humans for therapeutic purposes are currently envisaged. Clinical applications of the optogenetic system will require obvious implementation and cross-disciplinary know-how (Delbeke et al., 2017).



The term “chemogenetics” was used to describe experiments of site-specific functional group modifications for the analysis of DNA-protein interactions (Strobel, 1998). Currently, the term is used to indicate the processes by which “designer macromolecules” interact with previously unrecognized small molecules (Roth, 2016). Over the past two decades, chemogenetically engineered molecules (kinases, non-kinase enzymes, G protein-coupled receptors, ligand-gated ion channels) have been used experimentally for cell-specific targeting; these molecules modulate cell signaling, turning neuronal circuits on and off. Among chemogenetically engineered protein classes, the most commonly used are the so-called Designer Receptors Exclusively Activated by Designer Drugs (DREADDs) (Roth, 2016).

Local neurocircuitry in the human brain

Diffusion of dyes

An attempt to trace connections in the human brain using *in vitro* diffusion of wheat germ agglutinin conjugated with HRP gave very limited results (Haber, 1988). More interesting findings were obtained using the diffusion of lipophilic dyes along cell membranes in fixed tissue blocks (**Fig. 2E**). The fluorescent dyes carbocyanines, and in particular DiI and DiO (Honig and Hume, 1989) proved useful for this application. However, dye diffusion can label axons only for a few millimeters, requiring a tracing time of several weeks. Other dyes have been introduced (Heilingoetter and Jensen, 2016), and in particular NeuroVue dyes, which can trace axons for slightly longer distances and at faster diffusion rates than carbocyanines (Fritsch et al., 2005). The limitations of *ex vivo* tracing, however, hamper its application for extensive fiber tracking in the human brain.

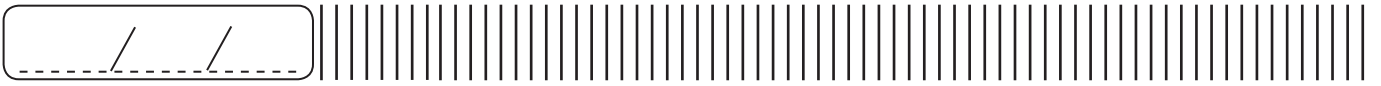
Seeing through: tissue clarification

The natural 3D structure of cells – especially neurons and glial cells, which extend their ramifications in many directions – requires volumetric imaging. The heterogeneous chemical composition of biological tissues (mostly water, proteins, and lipids) generates substantial scattering of the transmitted light, especially at the interface between aqueous protoplasm and membrane lipids, thereby hindering microscopic observation of histological sections beyond a certain thickness. Replacing lipids with a medium characterized by the same refractive index as proteins can effectively render tissues transparent while preserving the native molecular profile and tissue structure, allowing the microscopic observation of the microcircuitry of labeled (e.g., by immunohistochemistry or fluorescent protein tagging) elements.

Aqueous-based clearing techniques are currently widely used and are based on the reduction of light scattering by immersion in a high-refractive-index molecule solution. A breakthrough has been provided by a brain-hydrogel hybrid formed by the so-called CLARITY (Clear Lipid-exchanged Acrylamide-hybridized Rigid Imaging / immunostaining / *in situ* hybridization-compatible Tissue Hydrogel) (Chung et al., 2013). The clarification of thick tissue blocks, such as those useful for the study of the human brain (**Fig. 1D**) remains, however, a challenge. A method to adapt CLARITY to human brain samples with a thickness up to 8 mm has been recently proposed (Morawski et al., 2018). Of note, bridging historical and modern approaches to microcircuits, the Golgi (Golgi-Cox) stain is currently optimized for the use with CLARITY approaches, and could be useful for the study of microcircuitry and the comparison with microstructure MRI data (Kassem et al., 2017).

Diffusion tractography

Diffusion-weighted imaging (DWI), a computational reconstruction method of diffusion-weighted MR images (tractography), allows quantitative estimates *in vivo* of the organization of fiber bundles (tractograms). The characteristic color coding of reconstructed fiber bundles results in images attractive also to the public at large, thus making this approach a very popular insight in the human




brain. (*This method is extensively presented in another part of the review from which this text has been extracted*).

The diffusion coefficient measures the ease of the translational motion of water in tissues. Main DWI acquisition schemes are provided by diffusion tensor imaging (DTI) (**Fig. 2B**), diffusion spectrum imaging (DSI), and high angular resolution diffusion imaging (HARDI). DTI utilizes a tensor model (a matrix of measured diffusion in three orthogonal planes) to characterize the water diffusion properties through myelinated nerve fibers (Basser et al., 1994). Fiber orientation profiles derive from the statistical profile of the displacement of water molecules at a voxel scale and fiber trajectories are inferred from adjacent similar diffusion profiles (Thomas et al., 2014). DSI adds to DTI the capability of resolving multiple directions in each voxel (Wedeen et al., 2005), thus improving also the tracking of intersecting fibers. HARDI improves the accuracy of tractography by using a large number of diffusion-encoding gradients with a reasonable scanning time.

After the first validation study in the macaque brain (Parker et al., 2002), a number of validation studies have been performed, with rather positive or more critical conclusions. For example, the comparison of DSI in the light of extensive autoradiographic tract tracing data on long association pathways in the monkey cerebral hemispheres was found to replicate main features of these fiber tracts (Schmahmann et al., 2007). This comparison proved useful and effective for major cortical fiber bundles (superior, middle and inferior longitudinal fasciculi, fronto-occipital fasciculus, uncinate and arcuate fasciculi, cingulum bundle) (Schmahmann et al., 2007). Another study, based on DWI approaches to the monkey brain, reached more critical conclusions on the potential for accurate fiber tracing (Thomas et al., 2014). The results of a recent “open international tractography challenge”, tractograms produced by 20 research groups turned out to contain 90% of the ground truth bundles, but were also reported to “contain many more invalid than valid bundles” (Maier-Hein et al., 2017). These results encourage innovation.

References

- Basser PJ, Mattiello J, LeBihan D. MR diffusion tensor spectroscopy and imaging. *Biophys J* 1994; 66:259-67.
- Bentivoglio M, Kuypers HGJM, Catsman-Berrevoets CE, Loewe H, Dann O. Two new fluorescent retrograde neuronal tracers which are transported over long distances. *Neurosci Lett* 1980; 18:25-30.
- Bentivoglio M, Mazzarello P. Chapter 12: the anatomical foundations of clinical neurology. *Handb Clin Neurol* 2010; 95:149-68.
- Bentivoglio M. The discovery of axonal transport. *Brain Res Bull* 1999; 50:383-4.
- Cajal SR y. *Cajal’s histology of the nervous system of man and vertebrates*. New York: Oxford University Press 1995.
- Boyden ES, Zhang F, Bamberg E, Nagel G, Deisseroth K. Millisecond-timescale, genetically targeted optical control of neural activity. *Nat Neurosci* 2005; 8:1263-8.
- Cajal SR. *Histologie du système nerveux de l’homme et des vertébrés*. Maloine, Paris 1909.
- Cowan WM, Gottlieb DI, Hendrickson AE, Price JL, Woolsey TA. The autoradiographic demonstration of axonal connections in the central nervous system. *Brain Res* 1972; 37:21-51.
- Chung K, Wallace J, Kim S-Y, Kalyanasundaram S, Andalman AS, Davidson TJ, et al. Structural and molecular interrogation of intact biological systems. *Nature* 2013; 497:332-7.
- Deisseroth K, Feng G, Majewska AK, Miesenböck G, Ting A, Schnitzer MJ. Next-generation optical technologies for illuminating genetically targeted brain circuits. *J Neurosci* 2006; 26:10380-6.
- Deisseroth K. Optogenetics: 10 years of microbial opsins in neuroscience. *Nat Neurosci* 2015; 18:1213-25.

- 
- Delbeke J, Hoffman L, Mols K, Braeken D, Prodanov D. And Then There Was Light: Perspectives of Optogenetics for Deep Brain Stimulation and Neuromodulation. *Front Neurosci* 2017; 11:663.
 - Fink RP, Heimer L. Two methods for selective silver impregnation of degenerating axons and their synaptic endings in the central nervous system. *Brain Res* 1967; 4:369-74.
 - Fritzsche B, Muirhead KA, Feng F, Gray BD, Ohlsson-Wilhelm BM. Diffusion and imaging properties of three new lipophilic tracers, NeuroVue Maroon, NeuroVue Red and NeuroVue Green and their use for double and triple labeling of neuronal profile. *Brain Res Bull* 2005; 66:249-58.
 - Gerfen CR, Sawchenko PE. An anterograde neuroanatomical tracing method that shows the detailed morphology of neurons, their axons and terminals: immunohistochemical localization of an axonally transported plant lectin, Phaseolus vulgaris leucoagglutinin (PHA-L). *Brain Res* 1984; 290:219-38.
 - Glover JC, Petursdottir G, Jansen JK. Fluorescent dextran-amines used as axonal tracers in the nervous system of the chicken embryo. *J Neurosci Methods* 1986; 18:243-54.
 - Golgi C. Sulla fina anatomia degli organi centrali del sistema nervoso. Reggio Emilia: S. Calderini 1885.
 - Haber S. Tracing intrinsic fiber connections in postmortem human brain with WGA-HRP. *J Neurosci Methods* 1988; 23:15-22.
 - Heilingoetter CL, Jensen MB. Histological methods for ex vivo axon tracing: A systematic review. *Neurol Res* 2016; 38:561-9.
 - Honig MG, Hume RI. Dil and DiO: versatile fluorescent dyes for neuronal labelling and pathway tracing. *Trends Neurosci* 1989; 12:333-41.
 - Kassem MS, Fok SYY, Smith KL, Kuligowski M, Balleine BW. A novel, modernized Golgi-Cox stain optimized for CLARITY cleared tissue. *J Neurosci Methods* 2017; 294:102-10.
 - Kristensson K, Olsson Y. Retrograde axonal transport of protein. *Brain Res* 1971; 29:363-5.
 - Kristensson K. Transport of fluorescent protein tracer in peripheral nerves. *Acta Neuropathol* 1970; 16:293-300.
 - Kuypers HG, Bentivoglio M, Catsman-Berrevoets CE, Bharos AT. Double retrograde neuronal labeling through divergent axon collaterals, using two fluorescent tracers with the same excitation wave length which label different features of the cell. *Exp Brain Res* 1980; 40:383-92.
 - Kuypers HG, Ugolini G. Viruses as transneuronal tracers. *Trends in the Neurosciences* 1990; 13:71-5.
 - LaVail JH, LaVail MM. Retrograde axonal transport in the central nervous system. *Science* 1972; 176:1416-7.
 - Maier-Hein KH, Neher PF, Houde J-C, Côté M-A, Garyfallidis E, Zhong J, et al. The challenge of mapping the human connectome based on diffusion tractography. *Nat Commun* 2017; 8:1349.
 - Lee JH, Kreitzer AC, Singer AC, Schiff ND. Illuminating Neural Circuits: From Molecules to MRI. *J Neurosci* 2017; 37:10817-25.
 - Mesulam MM. Tracing neural connections of human brain with selective silver impregnation. Observations on geniculocalcarine, spinothalamic, and entorhinal pathways. *Arch Neurol* 1979; 36:814-8.
 - Morawski M, Kirilina E, Scherf N, Jäger C, Reimann K, Trampel R, et al. Developing 3D microscopy with CLARITY on human brain tissue: Towards a tool for informing and validating MRI-based histology. *Neuroimage* 2018; 182:417-428.
 - Nauta WJH, Gyax PA. Silver impregnation of degenerating axon terminals in the central nervous system: (1) Technic (2) Chemical notes. *Stain Technol* 1951; 26:3-9.
 - Oh MS, Hong SJ, Huh Y, Kim K-S. Expression of transgenes in midbrain dopamine neurons using the tyrosine hydroxylase promoter. *Gene Ther* 2009; 16:437-40.



- Parker GJM, Stephan KE, Barker GJ, Rowe JB, MacManus DG, Wheeler-Kingshott CAM, et al. Initial demonstration of in vivo tracing of axonal projections in the macaque brain and comparison with the human brain using diffusion tensor imaging and fast marching tractography. *Neuroimage* 2002; 15:797-809.
- Roth BL. DREADDs for Neuroscientists. *Neuron* 2016; 89:683-94.
- Schmahmann JD, Pandya DN, Wang R, Dai G, D'Arceuil HE, de Crespigny AJ, et al. Association fiber pathways of the brain: parallel observations from diffusion spectrum imaging and autoradiography. *Brain* 2007; 130:630-53.
- Schmahmann JD, Pandya DN. Cerebral white matter--historical evolution of facts and notions concerning the organization of the fiber pathways of the brain. *J Hist Neurosci* 2007; 16:237-67.
- Schmued LC, Fallon JH. Fluoro-Gold: a new fluorescent retrograde axonal tracer with numerous unique properties. *Brain Res* 1986; 377:147-54.
- Shepherd GM. *Foundations of the Neuron Doctrine: 25th Anniversary Edition*. Oxford University Press 2015.
- Sporns O, Zwi, JD. The small world of the cerebral cortex. *Neuroinformatics* 2004; 2:145-62.
- Strobel SA. Ribozyme chemogenetics. *Biopolymers* 1998; 48:65-81.
- Thomas C, Ye FQ, Irfanoglu MO, Modi P, Saleem KS, Leopold DA, et al. Anatomical accuracy of brain connections derived from diffusion MRI tractography is inherently limited. *Proc Natl Acad Sci USA* 2014; 111:16574-9.
- Wedeen VJ, Hagmann P, Tseng W-YI, Reese TG, Weisskoff RM. Mapping complex tissue architecture with diffusion spectrum magnetic resonance imaging. *Magn Reson Med* 2005; 54:1377-86.

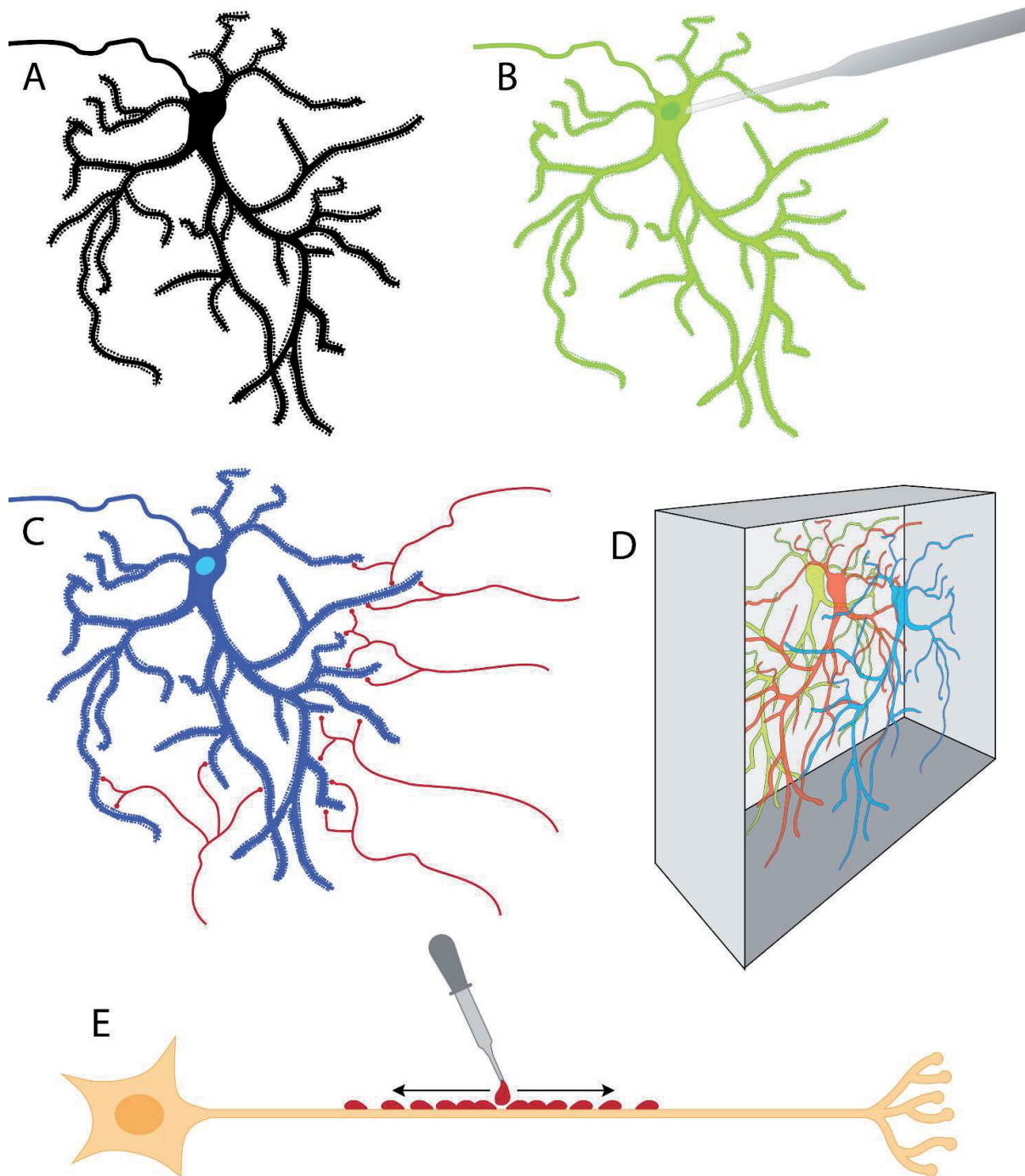


Fig. 1 Histological methods to study local neuronal connectivity and applicable to human brain samples. **A.** The Golgi silver impregnation entirely fills neuronal cell bodies and their processes, allowing detailed visualization and reconstructions; on the other hand, with the Golgi stain it is impossible to predict which cells will be impregnated in any given preparation. **B.** Filling neurons with fluorophores, as part of *in-vitro* electrophysiological experiments (for example in surgically resected brain tissue), allows correlating microscopic morphology with the functional properties of individual neurons. **C.** Immunocytochemistry targets specific cellular markers, and combining different labels allows the study, for example, of connectivity at the individual synapse level. **D.**



Schematic representation of the clarification approach in which brain tissue blocks are rendered transparent and immunocytochemically labeled neurons can be visualized in 3D. **E.** Lipophilic dyes applied on *ex-vivo* samples of nervous tissue are taken up by cell membranes and diffuse to a certain distance, thereby tracing short-range connections, also in human preparations.

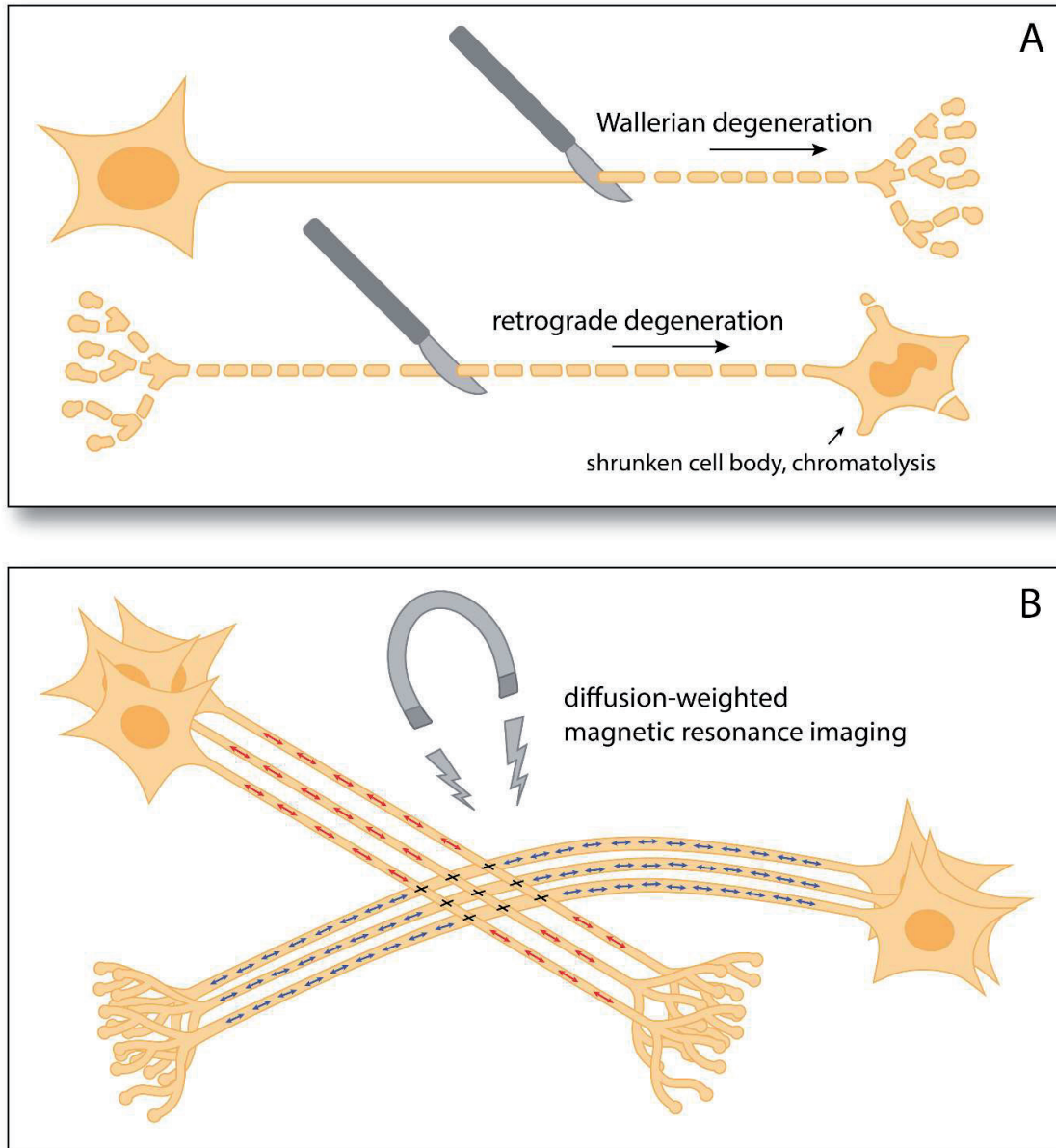


Fig. 2 Methods to study long-range connections in the human brain. **A.** Transections of nerves or CNS fiber bundles invariably cause anterograde (Wallerian) degeneration, i.e. destruction and elimination of the portions of axons and terminal ramifications distal to the lesion; depending on lesion location and size, degeneration can also follow a retrograde path and involve neuronal cell bodies. **B.** Diffusion-weighted magnetic resonance imaging is used to identify *in vivo* the spatial orientation of fiber bundles in the brain, making it possible to reconstruct central pathways. An important limitation of the technique is that in areas where fibers intersect, the signal averages out and accurate directions cannot be established.

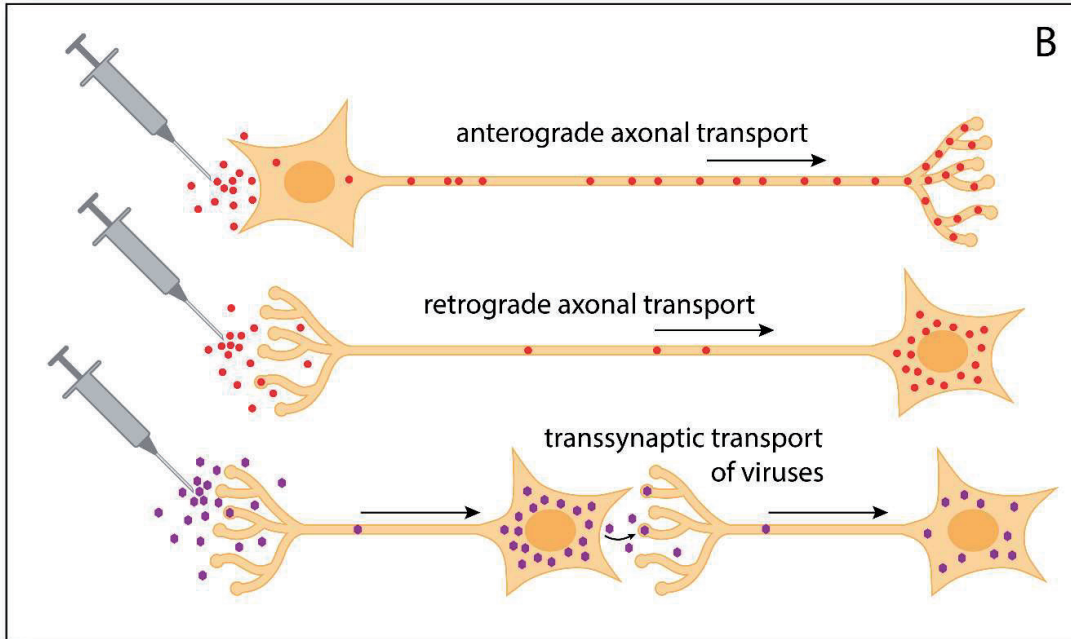
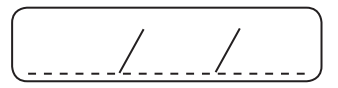
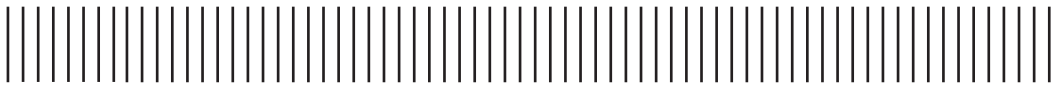


Fig. 3 (added for LASSE Syllabus) Experimental tract-tracing methods based on axonal transport. Axonal transport, the physiological mechanism by which cell bodies exchange cytosolic and membrane-bound components with distant terminals, has been exploited to obtain the most accurate reconstructions of neuronal connections to date. Substances surgically injected into a region of interest are taken up by neurons and are actively transported along axons, thereby acting as tracers. A few days after tracer administration, different visualization techniques allow the precise identification of connections. **Anterograde tracers** enter cell bodies and travel down the axons. Staining reveals fiber bundles and terminal fields. **Retrograde tracers** are taken up by terminals and are carried to the cell body, where they accumulate and produce intense staining of neurons that project to the injected area. Finally, **neurotropic viruses** have been used to trace multisynaptic pathways by exploiting their biological ability to infect peripheral tissues, enter nerve terminals and travel along the fibers, replicate in the cell body, and spread to nearby terminals to repeat the process. Careful determination of time intervals between experimental infection and histological staining of viruses allows to effectively trace synaptic chains.



A series of horizontal lines for handwriting practice, consisting of 20 evenly spaced lines extending across the width of the page.



A series of horizontal lines for writing, consisting of 20 evenly spaced lines.

REVIEWS

MEMORY SYSTEMS

The anatomy of memory: an interactive overview of the parahippocampal–hippocampal network

N. M. van Strien*^{||}, N. L. M. Cappaert*^{||} and M. P. Witter*[§]

Abstract | Converging evidence suggests that each parahippocampal and hippocampal subregion contributes uniquely to the encoding, consolidation and retrieval of declarative memories, but their precise roles remain elusive. Current functional thinking does not fully incorporate the intricately connected networks that link these subregions, owing to their organizational complexity; however, such detailed anatomical knowledge is of pivotal importance for comprehending the unique functional contribution of each subregion. We have therefore developed an interactive diagram with the aim to display all of the currently known anatomical connections of the rat parahippocampal–hippocampal network. In this Review, we integrate the existing anatomical knowledge into a concise description of this network and discuss the functional implications of some relatively underexposed connections.

In the more than 100 years since the first explorations of the parahippocampal–hippocampal network by Ramon y Cajal¹, numerous detailed anatomical tract-tracing analyses (BOX 1) have been published. These studies were sparked by the discovery of a prominent relationship between declarative memory and structures in the human medial temporal lobe, in particular the hippocampal formation (HF)²; the importance of the parahippocampal region (PHR) for memory was established only later³. An increasingly complex picture of the connectivity within and between the HF and the PHR has emerged over the years, and comprehensive knowledge of the PHR–HF network lies at the basis of understanding its functions⁴.

The level of anatomical detail at which an experiment must be carried out or results interpreted depends on the questions under investigation. In some instances, the effects of experimental manipulations can be interpreted using connectivity data at an overall network level (without taking the details of local networks into account). Other studies require more detail, but even those studies that benefit from a detailed understanding of the circuitry often do not, for a variety of reasons, take all the known connections into consideration. Sometimes connections are simply overlooked, whereas other times connections are intentionally left out because they seem to have no function and are therefore considered irrelevant for a particular theoretical interpretation. Eventually, such

underexposed connections tend to be erased from the common scientific memory. For this Review, we have assembled the extensive anatomical PHR–HF connectivity literature, focusing on all known connections of one frequently used experimental animal: the rat. We introduce a new approach to describe the network connectivity that uses an interactive diagram to display the complete PHR–HF connectivity (see [Supplementary information S1](#) (figure) and [Supplementary information S2](#) (box)). The complex and detailed connectivity patterns in this diagram are made accessible through the ability to switch on and off individual or groups of network connections between cortical layers and/or anatomical areas. The information this diagram provides could prove to be useful at a time when research is moving beyond the functional explanations that can be provided by a PHR–HF circuitry model that contains only a subset of the connections; moreover, it might lead to a re-evaluation of the functional importance of connections that have previously been ignored.

This Review first describes the anatomical concepts that are essential to understanding the PHR–HF circuitry (for an extensive description, see [REFS 5–7](#)). Next, it presents an overview of the main PHR–HF circuits as well as of some of the lesser-known aspects of the circuitry, using the interactive diagram ([Supplementary information S1](#) (figure)). Subsequently, it shows how having detailed knowledge of the PHR–HF circuitry can

*Department of Anatomy and Neurosciences, VU University Medical Center, P.O. BOX 7057, 1007 MB Amsterdam, The Netherlands.

^{||}SILS Center for Neuroscience, University of Amsterdam, 1098 SM Amsterdam, The Netherlands.

[§]Kavli Institute for Systems Neuroscience, and Centre for the Biology of Memory, Department of Neuroscience, Norwegian University of Science and Technology, N-7489 Trondheim, Norway.

^{||}These authors contributed equally to this work.

Correspondence to N.M.v.S. e-mail:

n.vanstrien@temporal-lobe.com

doi:10.1038/nrn2614

Box 1 | Neuroanatomical tract-tracing methods

Most of what is known today about the pathways that connect neurons in different brain regions has been discovered by using neuroanatomical tract-tracing techniques¹⁵⁶. A tracer is a substance that allows such pathways to be visualized. Tracers can be injected intracellularly to label the dendrites and axons of a neuron. Both autofluorescent dyes (for example, Lucifer yellow and Alexa dyes) and biotin-derived dyes are often used for intracellular labelling, as they can be easily visualized using fluorescent microscopy. Alternatively, a tracer can be injected at a stereotaxically defined extracellular location in the *in vivo* brain. The tracer is taken up by neurons at the injection site and is transported or diffuses within cells. A tracer substance can be transported anterogradely from the soma towards the axon terminals (for example, *Phaseolus vulgaris* leucoagglutinin), retrogradely from the axon terminals towards the soma (for example, Fast Blue), or it can be transported in both directions (for example, horseradish peroxidase). Another tract-tracing method involves creating small lesions and visualizing the resulting degeneration; the labelled connections are generally assessed using light microscopy. Electron microscopy can be used to visualize whether a presynaptic axon contacts a postsynaptic element. This is a very accurate but time-consuming method because only small pieces of tissue can be examined at one time. Alternatively, confocal microscopy allows three-dimensional reconstruction of larger pieces of tissue and can indicate whether pre- and postsynaptic elements are likely to form a synapse. A question of current interest is whether confocal microscopy is reliable enough for indicating such contacts. In order to increase our understanding of the connectivity of the brain and its related function, accurate numbers that provide information about pathways' projection intensity and termination density are needed. To achieve this, techniques using viral tracers¹⁵⁷ and new genetic tools¹⁵⁸ are being developed.

aid one's understanding of some of the functional processes that engage the PHR–HF regions, such as memory formation, spatial navigation and temporal dynamics.

Hippocampal–parahippocampal anatomy

The rat HF is a C-shaped structure that is situated in the caudal part of the brain. Three distinct subregions can be distinguished (FIG. 1): the dentate gyrus (DG), the hippocampus proper (consisting of CA3, CA2 and CA1) and the subiculum. The cortex that forms the HF has a three-layered appearance. The first layer is a deep layer, comprising a mixture of afferent and efferent fibres and interneurons. In the DG this layer is called the hilus, whereas in the CA regions it is referred to as the stratum oriens. Superficial to this polymorph layer is the cell layer, which is composed of principal cells and interneurons. In the DG this layer is called the granule layer, whereas in the CA regions and the subiculum it is referred to as the pyramidal cell layer (stratum pyramidale). The most superficial layer is referred to as the molecular layer (the stratum moleculare) in the DG and the subiculum. In the CA region the molecular layer is subdivided into a number of sublayers. In CA3, three sublayers are distinguished: the stratum lucidum, which receives input from the DG; the stratum radiatum, comprising the apical dendrites of the neurons located in the stratum pyramidale; and, most superficially, the stratum lacunosum-moleculare, comprising the apical tufts of the apical dendrites. The lamination in CA2 and CA1 is similar, with the exception that the stratum lucidum is missing.

The PHR lies adjacent to the HF, bordering the subiculum. It is divided into five subregions: the presubiculum, the parasubiculum, the entorhinal cortex (EC,

consisting of medial (MEA) and lateral (LEA) areas), the perirhinal cortex (PER, consisting of Brodmann areas (A) 35 and 36) and the postrhinal cortex (POR). The PHR is generally described as having six layers. The coordinate systems that define position within the HF and the PHR are explained in FIG. 1.

Circuitry of the PHR–HF region

In the interactive diagram (FIG. 2; Supplementary information S1 (figure)) we attempted to display all of the PHR–HF connections that have been reported in the anatomical literature concerning the rat (for references see [Supplementary information S3](#) (table)). The interactive diagram contains almost 1,600 connections, which can be displayed at a customizable level of complexity. This allows easy comparisons between the detailed PHR–HF circuitry illustrated by the diagram and a 'standard' model of this circuitry (FIG. 3), which displays the subset of connections that are currently most often used in the field (based on an analysis of a selection of recent key studies^{8–15}).

Connectivity within the PHR. In the standard model (FIG. 3), the projections from the PER and the POR to the EC are often depicted with a topology that emphasizes PER-to-LEA and POR-to-MEA relationships. However, as can be seen in the interactive diagram, the available data indicate (see figure 1a in [Supplementary information S4](#) (figure)) that the POR also projects to the LEA, although quantitatively to a lesser extent than the PER (4.9% versus 15.6%, respectively, of the total cortical input)¹⁶. Likewise, the PER also projects to the MEA (see figure 1b in [Supplementary information S4](#) (figure)), contributing a level of cortical input equal to that of the POR (7.5%)¹⁶. Neurons in layers II, III, V and VI of A35 and A36 of the PER project in a convergent way to LEA layers II and III¹⁷, whereas the PER projection to the MEA arises mainly from A36 (REFS 16, 17). The POR projection to the LEA arises from layers II, III, V and VI and terminates in layers II and III^{16,17}. The POR projection to the MEA originates from the same layers and terminates preferentially in the superficial layers, although some fibres can be seen in the deep layers of the MEA^{16,18}.

The EC reciprocates the projections from the PER and the POR, as depicted in the standard model. A detailed look at the interactive diagram shows that there are projections from layers III and V of the LEA to all layers of A35 and A36 (REFS 16, 17, 19), and from the MEA to all layers of A35 (REFS 16, 17, 20) (see figure 2a in [Supplementary information S4](#) (figure)). The MEA also projects to A36 (REFS 16, 21). Both the MEA and the LEA project to the POR, but details of the topography of this connection in the rat are currently not available^{16,21,22} (see figure 2b in [Supplementary information S4](#) (figure)).

Traditionally, little attention has been paid to the connections between the PER and the POR, although there is extensive connectivity between these regions. POR layers II and V project to all layers of A35 and A36; POR layer III also projects to A36 (see figure 3a in [Supplementary information S4](#) (figure)). Rostral levels of the POR provide the densest projection to caudal levels of A35 and

Temporal dynamics

Properties of neurons in a network, such as precise spike times and firing rates, that facilitate information transfer.

Convergence

When inputs from different brain regions converge on single cells or on a local network in another region.

REVIEWS

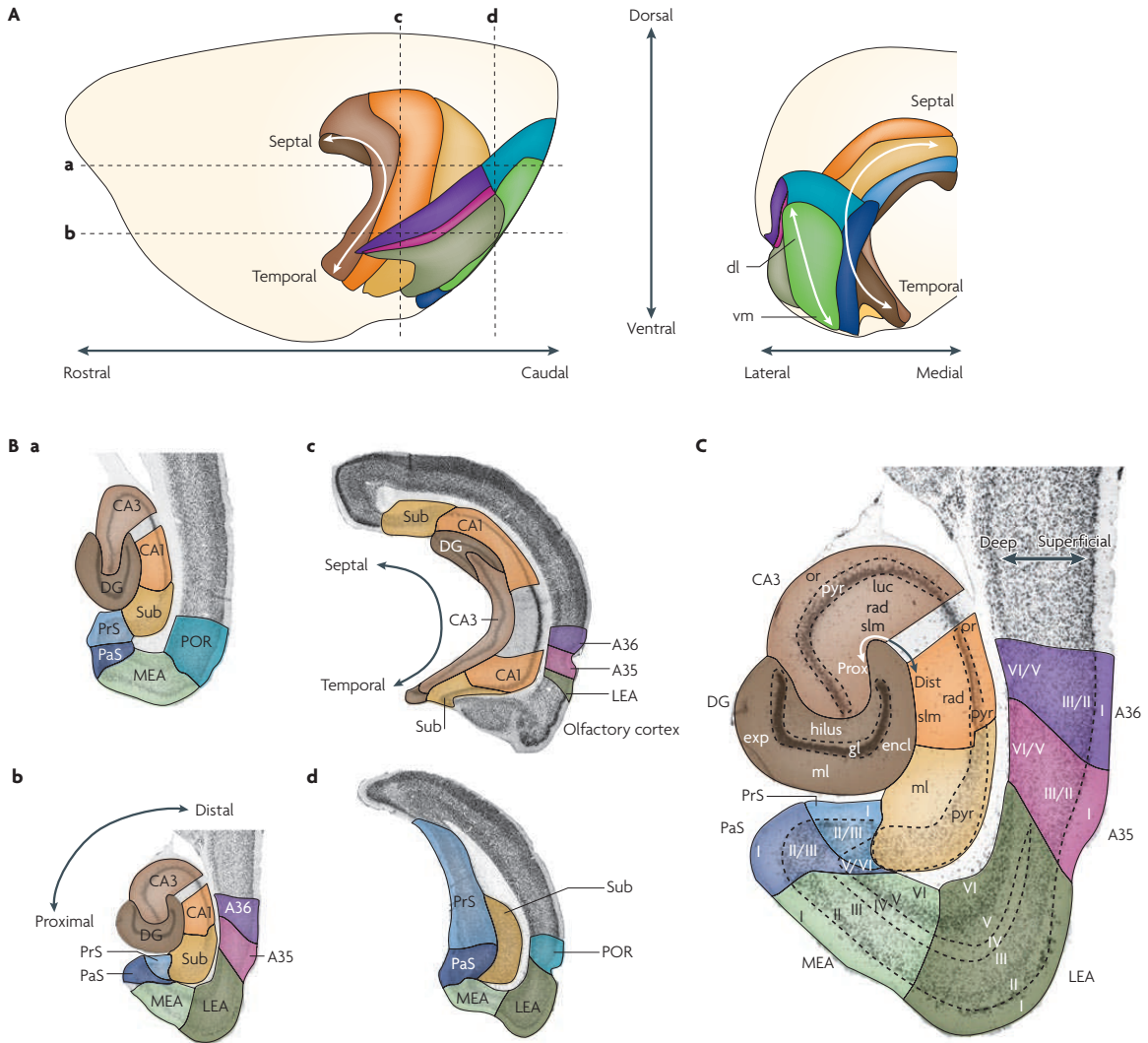


Figure 1 | Representations of the hippocampal formation and the parahippocampal region in the rat brain.
A | Lateral (left panel) and caudal (right panel) views. For orientation in the hippocampal formation (consisting of the dentate gyrus (DG; dark brown), CA3 (medium brown), CA2 (not indicated), CA1 (orange) and the subiculum (Sub; yellow)), three axes are indicated: the long or septotemporal axis (also referred to as the dorsoventral axis); the transverse or proximodistal axis, which runs parallel to the cell layer and starts at the DG; and the radial or superficial-to-deep axis, which is defined as being perpendicular to the transverse axis. In the parahippocampal region (green, blue, pink and purple shaded areas), a similar superficial-to-deep axis is used. Additionally, the presubiculum (PrS; medium blue) and parasubiculum (PaS; dark blue) are described by a septotemporal and proximodistal axis. The entorhinal cortex, which has a lateral (LEA; dark green) and a medial (MEA; light green) aspect, is described by a dorsolateral-to-ventromedial gradient and a rostrocaudal axis. The perirhinal cortex (consisting of Brodmann areas (A) 35 (pink) and 36 (purple)) and the postrhinal cortex (POR; blue-green) share the latter axis with the entorhinal cortex and are additionally defined by a dorsoventral orientation. The dashed lines in the left panel indicate the levels of two horizontal sections (a,b) and two coronal sections (c,d), which are shown in part B. All subfields of the parahippocampal-hippocampal region are colour-coded in correspondence with the interactive diagram in [Supplementary information S1](#) (figure). A further description of the anatomical features of each subfield is provided in the legend of this supplementary information.
C | A Nissl-stained horizontal cross section (enlarged from part Bb) in which the cortical layers and three-dimensional axes are marked. The Roman numerals indicate cortical layers. CA, cornu ammonis; dist, distal; dl, dorsolateral part of the entorhinal cortex; encl, enclosed blade of the DG; exp, exposed blade of the DG; gl, granule cell layer; luc, stratum lucidum; ml, molecular layer; or, stratum oriens; prox, proximal; pyr, pyramidal cell layer; rad, stratum radiatum; slm, stratum lacunosum-moleculare; vm, ventromedial part of the entorhinal cortex.

Reciprocal connections
Bidirectional, equivalent connections between two areas, networks or neurons.

Perforant pathway
Axons that originate in the superficial layers of the EC and are distributed to all fields of the hippocampus.

A36. Additionally, the POR projection to A36 is stronger than that to A35 (REFS 16,17,23). The PER projection to the POR originates in PER layers II, V and VI^{16,17,21,23} (see figure 3b in Supplementary information S4 (figure)). The densest projection connects the rostral PER with the caudal POR¹⁷.

A set of intra-PHR connections that is also underexposed in the standard model is the connections between the EC, the presubiculum and the parasubiculum. The dorsolateral MEA projects to septal levels of the presubiculum and the parasubiculum (see figure 4a in Supplementary information S4 (figure)), whereas the ventromedial MEA projects to the temporal presubiculum and parasubiculum^{20,22,24–28} (see figure 4b in Supplementary information S4 (figure)). The LEA also projects to the presubiculum and the parasubiculum, but precise topographical information for this projection is absent^{19,20,22,25,29,30}. Both the presubiculum and the parasubiculum send projections to the EC. The septal presubiculum projects to the dorsolateral and intermediate part of the MEA (see figure 5a in Supplementary information S4 (figure)), whereas the temporal presubiculum projects to the ventromedial part of the MEA (see figure 5b in Supplementary information S4 (figure)). The superficial layers of the presubiculum project to the deep layers of the LEA³¹ and to layers I, II and III of the MEA^{27,32–34}.

The deep layers of the presubiculum project to all layers of the MEA and predominantly to the deep layers of the LEA^{27,34,35}. A detailed topography for the parasubiculum-to-EC connection has not yet been described, but it is known that all layers of the parasubiculum converge on to layer II of the MEA^{21,24,30,32,33,36}.

Several other connections have been described that have not been incorporated into the standard model shown in FIG. 3. For example, reciprocal connections between the presubiculum/parasubiculum and the PER/POR have been described^{21,23}, but details are limited. Other connections, such as the intrinsic connections of the EC, are better anatomically characterized, but they remain outside the scope of most models. For example, the MEA and the LEA are strongly interconnected: cells in layers II, III, V and VI of the MEA project to the superficial layers of the LEA^{20,37}; LEA layers II and V project to the superficial layers of the MEA^{17,20,29,37}, whereas LEA layers III and VI project to superficial and deep layers of the MEA^{29,37}.

PHR projections to the HF. There is a prominent and topologically arranged circuitry between the PHR and the HF. The EC-to-HF circuitry is known as the perforant pathway (FIG. 3). According to the standard view only EC layer II projects to the entire transverse

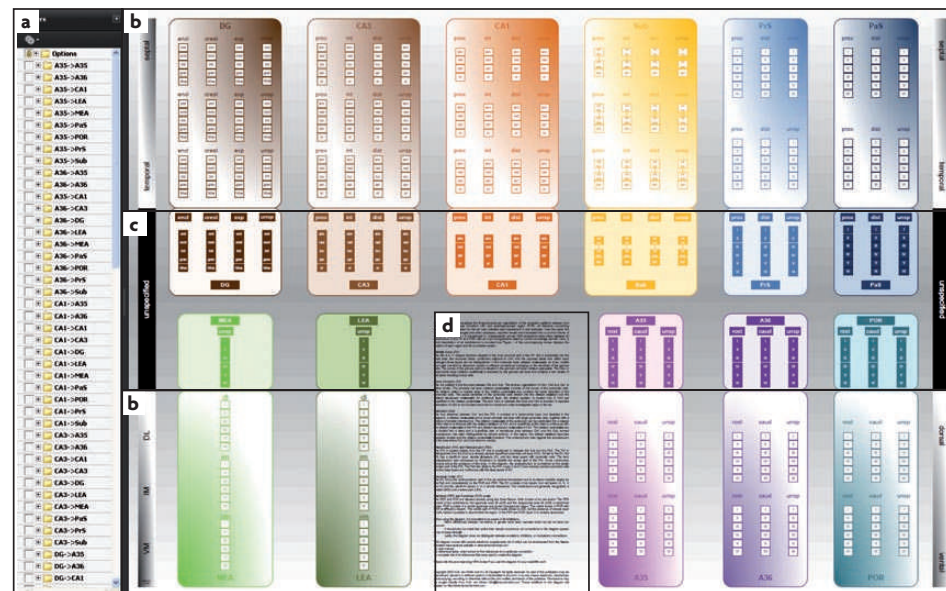


Figure 2 | Interactive diagram. The interactive diagram (see Supplementary information S1 (figure)) shows the details of the connectivity in the parahippocampal–hippocampal network, including the topology of the connections. All regions and their three-dimensional axes (for example, the septotemporal axis; see FIG. 1) are included in the diagram.

a | An alphabetically sorted list of ‘from-to’ connection groups that can be switched on or off. In front of each group is a + sign. Clicking this expands the list of individual connections that make up the group, allowing one to select connections originating from a specific cortical layer or according to a specific three-dimensional projection pattern (for example, only dorsolateral entorhinal cortex to septal hippocampus connections). **b |** In this area of the diagram the selected connectivity within and between subregions is displayed with full topological detail. **c |** In some cases topological detail is not available; these connections are displayed with a reduced level of topological detail in the centre of the diagram. Connections between diagram elements in parts **b** and **c** also exist. **d |** The diagram legend provides a detailed anatomical description of all subregions. Refer to the diagram manual in Supplementary information S2 (box) for detailed instructions.

REVIEWS

Divergence

When one brain region sends projections to several different brain regions.

Mossy fibres

The main projection of DG granular cells to CA3; characterized by high concentrations of zinc.

Schaffer collaterals

The axon collaterals of the CA3 pyramidal cells that project to CA1.

extent of the DG. In fact, EC layers III, V and VI also contribute to this projection, although to a lesser extent. The details of the EC-to-DG^{19,22,24–26,38–51} and EC-to-CA3^{19,20,22,25,29,38,41,42,44,48–50,52} projections might provide clues to their function. For example, in the molecular layer of the DG and the stratum lacunosum-moleculare of CA3, projections from the EC converge on to the apical dendrites of dentate principal cells and interneurons. Specifically, the LEA projects to the outer third of the molecular layer of the DG, and the MEA projects to the middle third of this layer. A similar pattern of convergence⁵³ is observed in CA3, where the LEA projection terminates in the superficial part of the stratum lacunosum-moleculare and the MEA projection terminates in the deep part of this layer. In addition to convergence, divergence⁵³ of the EC projections to the DG and CA3 also occurs, as individual layer II cells project to both the DG and CA3 (REFS 48,54).

The organization of the EC projection to CA1 and the subiculum is markedly different from that of the EC-to-DG or EC-to-CA3 projection. The origin of the main projection from the EC to the stratum lacunosum-moleculare of CA1 and the molecular layer of the subiculum lies in layer III although, again, other layers (II, V and VI) contribute to a lesser extent to this projection^{20,22,25,26,29,38,41–43,46,49,51,52,55–57}. Another striking feature of this pathway is the difference between the LEA and MEA projections along the transverse axis. The LEA projects to the distal part of CA1 and the proximal subiculum, whereas the MEA projects to the proximal part of CA1 and the distal subiculum^{38,49,52}. This segregation suggests that the input from the LEA and the MEA is processed in different parts of CA1 and the subiculum. This idea is supported by the observation that the segregation of the EC input to CA1 and the subiculum is maintained in the intra-HF projection from CA1 to the subiculum (see next subsection).

In addition to this topology along the transverse axis of the HF, there is a topological organization of connections between the dorsolateral–ventromedial axis of the EC and the longitudinal axis of the HF: the dorsolateral parts of the LEA and the MEA project to the septal HF, the intermediate part of the EC projects to intermediate septotemporal levels, and the ventromedial EC projects to the temporal HF^{40,58,59}. According to some reports, the actual organization of the perforant pathway is more widespread (see figure 6 in Supplementary information S4 (figure)), such that this topography relates to the densest projections, whereas weaker components show a more divergent distribution along the septotemporal axis^{46,50}. Such a broader projection pattern along the septotemporal axis of the HF may affect information processing.

The EC-to-HF projection forms the main PHR connection to the HF. Other PHR subregions have also been observed to project to the HF directly, although less strongly than the EC and most of them are not included in the standard view. Neurons in all layers of the presubiculum and the parasubiculum project to the stratum moleculare of the DG^{32,44,60} and the subiculum^{24,32,60,61} and to the stratum lacunosum-moleculare of CA3 (REFS 32,44) and CA1 (REFS 32,44,60) (see figures 7a and 7b

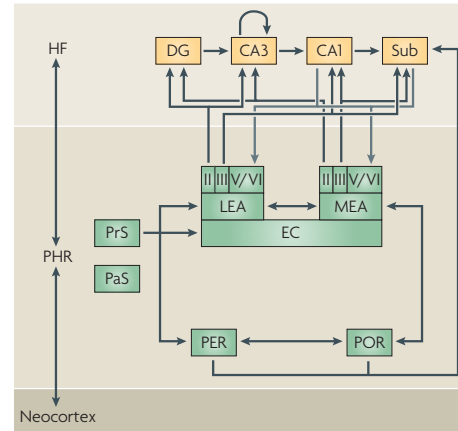


Figure 3 | The standard view of parahippocampal-hippocampal circuitry. The standard view that is presented here is based on various circuitry models from recent articles^{8–15}. According to this standard view, neocortical projections are aimed at the parahippocampal region (PHR), which in turn provides the main source of input to the hippocampal formation (HF). In the PHR, two parallel projection streams are discerned: the perirhinal cortex (PER) projects to the lateral entorhinal cortex (LEA), and the postrhinal cortex (POR) projects to the medial entorhinal cortex (MEA). The entorhinal cortex (EC) reciprocates the connections from the PER and the POR. Additionally, the EC receives input from the presubiculum (PrS). The EC is the source of the perforant pathway, which projects to all subregions of the hippocampal formation. Entorhinal layer II projects to the dentate gyrus (DG) and CA3, whereas layer III projects to CA1 and the subiculum (Sub). The polysynaptic pathway, an extended version of the traditional trisynaptic pathway, describes a unidirectional route that connects all subregions of the HF sequentially. In short, the DG granule cells give rise to the mossy fibre pathway, which targets CA3. The CA3 Schaffer collaterals project to CA1 and, lastly, CA1 projects to the Sub. Output from the HF arises in CA1 and the Sub and is directed to the PHR, in particular to the deep layers of the EC. The Roman numerals indicate cortical layers.

in Supplementary information S4 (figure)). Another example of underexposed circuitry is the direct projection from the PER and the POR to the HF. Both A35 and A36 have been reported to project to CA1 and the subiculum^{23,62}. The POR has been suggested to project to all sub-areas of the HF²³, but another report indicates only direct projections to CA1 and the subiculum⁵⁷.

Connectivity within the HF. In the standard model the first step of the polysynaptic HF pathway (FIG. 3; see also figure 8a in Supplementary information S4 (figure)) is formed by a unidirectional projection from the DG to CA3: the mossy fibres. The Schaffer collaterals, which originate in CA3 and project to CA1, are the next step in the polysynaptic loop. A detailed look at these connections shows an interesting topology along the transverse axis. The distal part of CA3 projects to proximal CA1 and, conversely, the proximal part of CA3 projects to distal

CA1 (REFS 63–65). The topography of the projections that arise from mid-proximodistal portions of CA3 lies between that of these two projection patterns. The last step in the polysynaptic pathway is the projection from CA1 to the subiculum. The proximal part of the CA1 pyramidal cell layer projects to the distal subiculum, whereas the distal CA1 projects to the proximal part of the subiculum^{52,66–69}.

In contrast to what is depicted in the standard model, there are several backprojections in the HF. Pyramidal cells in CA3 project back to the hilus and the inner molecular layer of the DG^{64,70–74}, and all septotemporal levels have this backprojection (see figure 8b in Supplementary information S4 (figure)). The strongest backprojection originates in the temporal levels of CA3 and projects to the temporal part of the DG⁷¹. Again contrasting the standard idea of unidirectionality, a backprojection from CA1 to CA3 has also been reported; this backprojection most likely arises from inhibitory neurons in the stratum radiatum and stratum oriens of CA1 and projects to the same layers in CA3 (REFS 64,66,67,75) (see figure 8b in Supplementary information S4 (figure)). A backprojection from the subiculum to CA1 has also been reported (see figure 8b in Supplementary information S4 (figure)). This backprojection arises from neurons in the stratum pyramidale of the subiculum and projects to all layers of CA1 (REFS 32,76). Currently, it is not known whether this backprojection is of an excitatory or an inhibitory nature.

Recurrent collaterals of the CA3 region^{63,64,70–73,77–81} are well acknowledged in the literature (FIG. 3), and they have been described in the other HF subregions as well (see figure 9 in Supplementary information S4 (figure)); these intrinsic recurrent networks are less extensive and are also less investigated in terms of their anatomy and function (see the ‘Functional implications’ section). In the polymorphic layer of the DG, each granule cell establishes contact with the proximal dendrites of several mossy cells, which return excitatory synapses to granule cell dendrites in the molecular layer^{47,64,65,70,80,82–85}. CA1 has recurrent loops that are restricted to one septotemporal level^{66,69,75,76,79,86}. In the subiculum, principal cells extend axon collaterals to a substantial part of the subiculum that lies ventral to the site of origin; these collaterals terminate on pyramidal cells and interneurons^{32,76,87,88}.

HF projections to the PHR. The HF output to the PHR arises from CA1 and the subiculum and, according to the standard view, terminates primarily in the deep layers of the EC. In contrast to this view, several authors have reported direct projections from CA1 (REFS 72,75) and the subiculum^{32,89,90} to the superficial layers of both the LEA and the MEA.

There are reciprocal connections between the EC and CA1/the subiculum. The CA1-to-EC projection is organized such that the septotemporal axis of the HF is mapped topologically on to the dorsolateral–ventromedial axis of the EC, comparable to the organization of the strongest EC-to-HF projection^{52,72,75}. The transverse output organization also mimics the input — that is, the proximal part of CA1 projects to the MEA (see figure

10a in Supplementary information S4 (figure)) and the distal part of CA1 projects to the LEA^{49,52} (see figure 10b in Supplementary information S4 (figure)). The subiculum-to-EC projections have a similar topography along the long^{89,91} and transverse axes^{49,88,89,91,92}, although they seem to be less sharply defined. Moreover, along the transverse axis the organization is opposite to that of the CA1-to-EC connections: the proximal subiculum sends a stronger projection to the LEA and the distal subiculum sends a stronger projection to the MEA, again in line with the overall organization of the EC projections to the subiculum.

Although the CA1/subiculum-to-EC projections form the main part of the HF output to the PHR, other connections to the PHR also exist. For example, CA3 (REFS 24,44,72,78), CA1 (REFS 24,31,44,69,75) and the subiculum^{24,31,32,88,89,91,92} all project to the presubiculum and the parasubiculum (see figure 11 in Supplementary information S4 (figure)). The projection from the subiculum to the presubiculum is the best described of these. It follows a septotemporal gradient, such that the septal part of the subiculum projects to the septal presubiculum^{31,88,89,91} and the temporal part of the subiculum projects to the temporal presubiculum^{24,91}. A projection from the subiculum to the parasubiculum exists, but no detailed information about it is known^{24,32,89}. Finally, CA1 and the subiculum project to both the PER and the POR, although no detailed information about the organization of this projection is currently available^{21,23}.

Functional implications

In the preceding section we compared the details of the PHR–HF circuitry to the standard view, highlighting several underexposed connections. To provide a functional perspective on some of these connections, we now discuss them in the context of three topics that have long been associated with the HF: memory formation, navigation and temporal dynamics.

Memory formation. The first example of how increased knowledge of connections in the PHR and the HF might change our views on the memory function of the HF concerns the idea that the HF is the region in which different types of information are associated in memory. By contrast, the EC is generally defined as a simple input–output structure that keeps the incoming information flows separate by way of two parallel pathways (FIG. 3): the PER-to-LEA-to-HF pathway conveys non-spatial information about external stimuli, whereas the POR-to-MEA-to-HF pathway conveys spatial information¹⁸.

However, there are four arguments that support the notion that, rather than being a simple input–output structure, the EC has a role in more complex associations. First, anatomical evidence shows that PER and POR projections to the EC overlap (see the ‘Circuitry’ section). Second, there is an extensive network in the EC that reciprocally connects the LEA and the MEA^{17,20,29,37}. These first two anatomical characteristics suggest that non-spatial information in the LEA and spatial information in the MEA can become associated at the level of the EC, which is supported by the observation that the LEA

is involved in odour–place associations⁹³. Third, deep and superficial layers of the EC are also anatomically interconnected^{20,26,29,37,94}, and this connection is likely to explain the observation that the firing characteristics of cells in all layers of the MEA have a clear correlation across layers during the performance of spatial tasks⁹⁵. Fourth, according to the classical view (FIG. 3), the superficial EC layers are the input layers to the HF, whereas the deep layers receive hippocampally processed information that they convey back to the cortex. However, the anatomical data summarized in this Review show projections from the deep layers of the EC to the HF, consistent with the finding that activation of the deep layers of the EC is sufficient to activate the DG⁹⁶. Additionally, the HF projects to both deep and superficial EC layers (see the ‘Circuitry’ section).

We therefore propose that the notion that the EC is a simple, laminated input–output structure needs revision: information becomes integrated before it enters the HF. This suggests that both the HF and the EC associate information that is relevant to memory. As the same types of information are processed by the two structures, the question remains how their functions compare. One way to view the distinctive roles of the regions is that the EC holds a more universal memory representation of the associated information, whereas the HF is involved in processing details of this information through processes such as pattern separation and pattern completion. The observation that activity in the HF increases when a person is recalling details from memory supports the proposal that the HF has a role in processing detailed information⁹⁷. The idea that the EC processes information at an earlier and more generic level than the HF (in which detailed information is processed) corresponds to the idea that the EC holds a universal map that is important to the HF in navigation, as discussed below.

Associative networks and, in particular, the auto-associative network of CA3 have been proposed to be essential for encoding and storing episodic memories^{98,99}. The recurrent connections in this area can be theoretically arranged into a number of discrete patterns of activation, called stable states or attractors, and the synaptic strengths of the recurrent connections determine the stable states of this network⁹⁸. Incoming information presumably directs the network into one of its stable states, thus enabling pattern completion¹⁰⁰. Although the CA3 recurrent network is currently thought to be the most elaborate in the HF, CA1, the DG hilus region and the subiculum also contain recurrent collateral networks (see figure 9 in Supplementary information S4 (figure)) and are likely to exhibit computational characteristics comparable to those of the CA3 recurrent network. One striking feature of the CA1 recurrent network that emerges from the diagram is that the recurrent loops are restricted to one septotemporal level (see figure 9 in Supplementary information S4 (figure)). For example, the input to the septal CA1 from CA3 arises from both septal and intermediate levels of CA3, whereas the input to the temporal CA1 arises from the temporal and intermediate CA3. This input is then processed independently in both the septal and the temporal CA1. It would be interesting to know whether there is also regional specificity of CA1 recurrenents along

the transverse axis, as the MEA and the LEA project preferentially to different proximodistal regions of CA1 (see the ‘PHR projections to the HF’ subsection). Preliminary data from recordings in the septal CA1 are in line with this idea and show that cells at different transverse positions have different firing characteristics¹⁰¹ that are related to the type of information provided by the MEA or LEA inputs (spatial and non-spatial, respectively). We propose that CA1 is divided into subdomains along the combination of the septotemporal and proximodistal axes, and that each subdomain independently processes different, specific combinations of information originating from different input areas. In theory, each of these subdomains would thus be able to encode and store unique input patterns, which may be instrumental in discriminating subtle differences in input cues and may aid pattern separation and completion. This prediction awaits further experimental data, such as detailed recordings along both axes in freely behaving animals.

Navigation. Different types of spatial information, discussed below, are represented in the PHR–HF circuitry, and the circuitry may facilitate the exchange of these different types of information in order to make navigation through an environment possible. The same circuitry may mediate the formation of memories for the spatial position of behaviourally relevant cues. Place cells, which encode place fields, provide essential information for navigation. They are found in CA1 (REF. 102) and CA3 (REF. 103), but cells with similar functional properties have been found in the subiculum^{104–106}, the septal pre-subiculum¹⁰⁷ and the parasubiculum^{108,109}. In the HF, the size of a place field is related to the septotemporal position of the place cells: place cells in the septal HF have the smallest place fields, at intermediate septotemporal levels place fields are twice as big¹¹⁰ and in the temporal HF they become even larger^{103,110,111}. Place field size can be interpreted as a measure of spatial scale, indicating that environments might be represented at different spatial resolutions along the septotemporal axis of the HF.

A large number of non-overlapping, unique spatial representations of the environment are stored in the rather limited network of the HF, which creates a storage problem. It has been argued that in order to solve this problem the HF might make use of a universal map, presumably located outside the HF^{102,112,113}, that can be applied across environments. Based on the strong reciprocal connectivity between the EC and the HF, the EC (in particular the MEA) was considered a likely candidate for the location of this map, as this area was shown to receive predominantly visuospatial information from the POR¹⁶. Indeed, a disruption of the monosynaptic information flow from MEA layer III to CA1 affected long-term spatial-memory performance¹¹⁴ and impaired place cell firing in CA1 (REF. 115). However, initial recordings in the EC did not reveal cells with a striking spatially modulated firing pattern^{116,117}, probably because these recordings did not cover the most dorsolateral portion of the MEA. The dorsolateral MEA was predicted to contain such cells because it is reciprocally connected both to the septal hippocampus (see the ‘Circuitry’ section), in which place cells are

Auto-associative network
A network of neurons with axon collaterals that terminate on dendrites of the parent cell.

Place cells
Principal neurons in the hippocampus and parahippocampus that fire whenever an animal is in a specific location in an environment (corresponding to the cell’s ‘place field’).

most conspicuous, and to visuospatial cortical domains — for example, the POR^{17,18}. Subsequent recordings in the dorsolateral part of the MEA indeed revealed grid cells¹¹⁸. Like place cells, grid cells show a gradual increase in grid field size from the dorsolateral MEA towards the ventromedial MEA¹¹⁹ and, because of the predominant topology of the perforant path, the grid cells with the smallest grid field scale in the dorsolateral MEA connect to the place cells in the septal HF with the smallest place field scale. Similarly, the grid cells with the largest grid field scale in the ventromedial MEA connect to the place cells in the temporal HF with the largest place field scale.

Head-direction cells are a third class of cells involved in navigation. Head-direction cells were first discovered in the septal presubiculum^{109,120}, but directionally tuned cells have also been observed in the EC⁹⁵, the anterior and lateral dorsal thalamic nuclei^{121–123}, the lateral mammillary nucleus¹²⁴, the retrosplenial cortex¹²⁵ and the striatum¹²⁶. This indicates that the directional signal is probably computed in brain networks outside the HF. The head-direction information from the mammillary bodies is crucial for place and grid cell functioning¹²⁴, and head-direction information from the presubiculum is important, although not indispensable, for the functional characteristics of place fields in CA1 (REF. 127). As the septal presubiculum also projects to other HF sub-regions, we propose that the firing properties of neurons in the DG, CA3 and the subiculum might also be affected by presubiculum lesions.

What more can the details of the circuitry tell us about the space-related functional properties of the network? A first hypothesis is that information from the head-direction system may enter the HF through at least two different routes. One route projects from the presubiculum directly to the HF and a second route runs indirectly to the HF through the projections from layers II and III of the EC. In order to decide which of these routes provides the predominant directional input to the HF, the reported effects of presubiculum lesions on CA1 place cell firing¹⁰⁷ should be compared with the effect of presubiculum lesions on the spatial-firing properties of MEA neurons. If MEA neuron firing is not affected by such lesions, the direct route from the presubiculum to CA1 is more likely to be the predominant input pathway for directional information to the HF. However, if the firing properties of MEA neurons do change as a result of presubiculum lesions, the CA1 firing properties after a presubiculum lesion should be compared with the CA1 firing properties after a selective MEA lesion¹¹⁵ and after a combined presubiculum and MEA lesion.

Another prediction based on the PHR–HF network characteristics is that the place-specific firing of CA1 should be stronger at its proximal end than at its distal end, as the MEA preferentially projects to the proximal portion of CA1 and place-specific firing in CA1 strongly depends on the direct input from the MEA^{115,128,129}. By contrast, the preferential LEA-to-CA1 projection pattern predicts that non-spatial information about external stimuli is processed in the distal CA1. Preliminary data show that the firing of cells in the proximal (MEA-recipient) CA1 is indeed significantly more affected

by spatial information than the firing of cells in the distal CA1 (REF. 101). A similar type of prediction can be made for the subiculum, as the LEA projects to the proximal part of the subiculum and the MEA projects to its distal part. On the basis of this topology, the most prominent place cells are expected to be found in the distal subiculum. One study found subtle differences in the spatial properties of cells in the proximal versus the distal subiculum¹⁰⁴. There are several explanations for why the difference was only small, but the best explanation is probably the extensive but underexposed and not very well studied intrinsic recurrent network in the subiculum¹³⁰.

Temporal dynamics. Some of the underexposed PHR–HF connections are likely to be involved in the temporal synchronization of neuronal firing between brain areas. Synchronized firing is essential for the coordination of spatially distributed networks and is generally achieved through neuronal oscillations. By synchronizing excitatory periods across regions, oscillations may facilitate the transfer of information in the PHR–HF network¹³¹. Furthermore, oscillations promote coincident firing among cells, which is likely to be important for inducing synaptic plasticity (for example, see REF. 132) and memory consolidation¹³³. One of the prerequisites for the occurrence of oscillations is the interaction between excitatory glutamatergic neurons and inhibitory GABA (γ -aminobutyric acid)-ergic interneurons¹³⁴. Different classes of GABAergic neurons can be characterized in the hippocampus according to their distinct firing patterns during behaviourally relevant oscillations such as theta oscillations, gamma oscillations and sharp wave ripples^{135–138}, projections from these interneurons to different targets synchronize the firing of large numbers of pyramidal cells¹³⁵. Although most research on GABAergic cells is carried out on interneurons that project locally in one sub-area, recent evidence showed the existence of long-range GABAergic projection neurons that cross the sub-area border and are involved in the coordination of spike timing across sub-areas¹³⁹.

Although most tract-tracing studies do not reveal whether a projection is excitatory or inhibitory, an indication of the excitatory or inhibitory nature of a connection can be derived from the layers of origin and termination. For example, the CA1-to-CA3 backprojections discussed in the ‘Circuitry’ section arise not from the (excitatory) glutamatergic principal cell layer, but mainly from neurons located in the stratum oriens of CA1 (REFS 64,66,67,75), and project to the stratum radiatum and stratum oriens of CA3. An *in vivo* labelling study showed the same locus of origin and termination for CA1 GABAergic neurons projecting to CA3 (REFS 77,140–142). Also, in the stratum radiatum of CA1, cells project to the DG and the subiculum. GABAergic cells have been reported to reside in the CA1 stratum radiatum with axons that radiate to the molecular layer of the DG and the subiculum¹⁴³.

Because the layer of origin of these CA1 neurons seems to be a reliable predictor of GABAergic connections, it is likely that other projections that do not start

Grid cells

Neurons in the entorhinal cortex that fire strongly when an animal is at one of several specific locations in an environment and that are organized in a grid-like fashion.

Head-direction cells

Neurons that fire only when the animal's head points in a specific direction in an environment.

Mammillary bodies

A pair of nuclei in the hypothalamus, strongly connected to the HF and the anterior complex of the thalamus, that are involved in recognition memory.

Theta oscillations

Rhythmical changes at 5–12 Hz in network activity, as observed in the electroencephalogram, characteristic of the hippocampal network communicating with various cortical and subcortical networks in the brain.

Gamma oscillations

Rhythmical oscillations of 25–70 Hz observed in the electroencephalogram.

Ripple oscillations

Short-lasting bursts of field oscillations (~ 140 – 200 Hz) in the mammalian hippocampus and parahippocampus that occur during rest or slow-wave sleep.

in the principal cell layer are also GABAergic. This can be used to discover the existence of other inhibitory projections. In the interactive diagram (see Supplementary information S1 (figure)) one can observe that, in the hippocampus, cells in the hilus of the DG project to CA1. There are also reports of projections from the HF to the PHR that do not start in the principal cell layer of the HF: cells in the molecular layer of the subiculum project to the parasubiculum, the presubiculum and the POR. Moreover, cells in the stratum oriens and the stratum radiatum of CA1 and the molecular layer of the subiculum project to the LEA and the MEA. We suggest that these connections indeed originate from long-range GABAergic neurons, and are capable of functionally coupling the PHR–HF subregions and coordinate oscillations over the entire PHR–HF network.

Conclusions and future directions

Comprehensive knowledge of the organization of the PHR–HF connectivity is of pivotal importance for elucidating PHR–HF function. Such detailed knowledge of PHR–HF circuits will help us to understand how these circuits are engaged in spatial processing and temporal dynamics, as well as in other functions that have been associated with the region, such as episodic memory¹⁴⁴, crossmodal memory¹⁴⁵, recollection and recognition¹⁴⁶, memory for the temporal order of events^{147–150} and visual perception of conjunctions¹⁵¹. Moreover, the PHR and HF are implicated in various disorders, such as Alzheimer's disease¹⁵², epilepsy¹⁵³, schizophrenia¹⁵⁴ and depression¹⁵⁵. Knowing the changes in connection patterns within and between these regions may help us to understand the underlying mechanisms of these PHR–HF-related disorders and consequently enhance the possibilities for treating them. This Review and the complementary knowledge base may facilitate the study of altered connectivity in animal models for diseases that involve the PHR and HF.

Although topological information is available in the interactive diagram for a large number of connections, increasing the knowledge base of PHR–HF connectivity is an important requirement for future functional understanding of these regions. Although currently all connections in the interactive diagram are displayed as if they are of equal density, we aim for future versions of the diagram (which will be available on [our website](#)) to differentiate between strong and weak connections. Unfortunately, connectional density is often not reported quantitatively in the anatomical literature, and even when it is reported it is a subjective observation that is difficult to compare between studies. Second, we aim to incorporate *in vivo* and *in vitro* electrophysiological data into future versions of this knowledge base so that it will contain information about the excitatory or inhibitory role of connections. Third, the current version of the diagram displays only the layers of origin and termination, but each region and layer consists of several cell types. We aim for future versions of the diagram to contain a description of pre- and postsynaptic cell types. Implementing these improvements requires extensive fundamental research into the cytoarchitectonic and connectional properties of the region, but this investment will have a tremendous impact on advancing our functional understanding.

An ever-increasing amount of anatomical knowledge brings with it several difficulties. One consequence of the overwhelming number of reported connections is that attention focuses on a selection of the connections whereas others fall into disuse, especially those for which the functional relevance is not entirely clear, such as some of the recurrent collaterals in the HF subregions. A knowledge base such as the one presented in this Review can help to prevent the loss of valuable knowledge and inspire creative minds to come up with new solutions for outstanding problems in the field.

- Ramón y Cajal, S. Estructura del asta de Ammon y fascia dentata. *Anales de la Sociedad Española de Historia Natural* **22**, 53–126 (1893).
- Scoville, W. B. & Milner, B. Loss of recent memory after bilateral hippocampal lesions. *J. Neurol. Neurosurg. Psychiatry* **20**, 11–21 (1957).
- Zola-Morgan, S., Squire, L. R., Amaral, D. G. & Suzuki, W. A. Lesions of perirhinal and parahippocampal cortex that spare the amygdala and hippocampal formation produce severe memory impairment. *J. Neurosci.* **9**, 4355–4370 (1989).
- Crick, F. & Koch, C. A framework for consciousness. *Nature Neurosci.* **6**, 119–126 (2003).
- Amaral, D. G. & Lavenex, P. In *The Hippocampus Book* (eds Andersen, P., Morris, R., Amaral, D. G., Bliss, T. & O'Keefe, J.) 37–114 (Oxford Univ. Press, New York, 2007).
- Witter, M. P. & Amaral, D. G. In *The Rat Nervous System* 3rd edn (ed. Paxinos, G.) 637–703 (Elsevier Academic Press, San Diego, 2004).
This book chapter gives an extensive description of cells and projections in the HF and the PHR.
- Burwell, R. D. & Witter, M. P. In *The Parahippocampal Region: Organization and Role in Cognitive Function* (eds Witter, M. P. & Wouterlood, F. G.) 35–60 (Oxford Univ. Press, New York, 2002).
- Bird, C. M. & Burgess, N. The hippocampus and memory: insights from spatial processing. *Nature Rev. Neurosci.* **9**, 182–194 (2008).
This paper provides a comprehensive summary of arguments that support the thesis that studies on the role of the rodent hippocampus in navigation bear on our understanding of memory.
- Brown, M. W. & Aggleton, J. P. Recognition memory: what are the roles of the perirhinal cortex and hippocampus? *Nature Rev. Neurosci.* **2**, 51–61 (2001).
- Bussey, T. J. & Saksida, L. M. Memory, perception, and the ventral visual-perirhinal-hippocampal stream: thinking outside of the boxes. *Hippocampus* **17**, 898–908 (2007).
This paper provides a critical but stimulating perspective on the idea that the medial temporal lobe system is involved only in memory, with special emphasis on the functions of the perirhinal cortex.
- Eichenbaum, H. A cortical-hippocampal system for declarative memory. *Nature Rev. Neurosci.* **1**, 41–50 (2000).
- Eichenbaum, H., Yonelinas, A. P. & Ranganath, C. The medial temporal lobe and recognition memory. *Annu. Rev. Neurosci.* **30**, 123–152 (2007).
This paper reviews current concepts of how familiarity and recollection memory are supported by regions in the medial temporal lobe and proposes that there is a distinction between recollection and familiarity in specific regions of the medial temporal lobe.
- Hasselmo, M. E., Fransén, E., Dickson, C. & Alonso, A. A. Computational modeling of entorhinal cortex. *Ann. NY Acad. Sci.* **911**, 418–446 (2000).
- Martin, S. J. & Clark, R. E. The rodent hippocampus and spatial memory: from synapses to systems. *Cell. Mol. Life Sci.* **64**, 401–431 (2007).
- Squire, L. R., Stark, C. E. & Clark, R. E. The medial temporal lobe. *Annu. Rev. Neurosci.* **27**, 279–306 (2004).
- Burwell, R. D. & Amaral, D. G. Cortical afferents of the perirhinal, postrhinal, and entorhinal cortices of the rat. *J. Comp. Neurol.* **398**, 179–205 (1998).
- Burwell, R. D. & Amaral, D. G. Perirhinal and postrhinal cortices of the rat: interconnectivity and connections with the entorhinal cortex. *J. Comp. Neurol.* **391**, 293–321 (1998).
- Naber, P. A., Caballero-Bleda, M., Jorritsma-Byham, B. & Witter, M. P. Parallel input to the hippocampal memory system through peri- and postrhinal cortices. *Neuroreport* **8**, 2617–2621 (1997).
- Swanson, L. W. & Kohler, C. Anatomical evidence for direct projections from the entorhinal area to the entire cortical mantle in the rat. *J. Neurosci.* **6**, 3010–3023 (1986).
- Kohler, C. Intrinsic connections of the retrohippocampal region in the rat brain. II. The medial entorhinal area. *J. Comp. Neurol.* **246**, 149–169 (1986).
- Deacon, T. W., Eichenbaum, H., Rosenberg, P. & Eckmann, K. W. Afferent connections of the perirhinal cortex in the rat. *J. Comp. Neurol.* **220**, 168–190 (1983).
- Kerr, K. M., Agster, K. L., Furtak, S. C. & Burwell, R. D. Functional neuroanatomy of the parahippocampal region: the lateral and medial entorhinal areas. *Hippocampus* **17**, 697–708 (2007).
- Furtak, S. C., Wei, S. M., Agster, K. L. & Burwell, R. D. Functional neuroanatomy of the parahippocampal region in the rat: the perirhinal and postrhinal cortices. *Hippocampus* **17**, 709–722 (2007).
- van Groen, T. & Wyss, J. M. The connections of presubiculum and parasubiculum in the rat. *Brain Res.* **518**, 227–243 (1990).

25. Wyss, J. M. An autoradiographic study of the efferent connections of the entorhinal cortex in the rat. *J. Comp. Neurol.* **199**, 495–512 (1981).
26. Lingenhohl, K. & Finch, D. M. Morphological characterization of rat entorhinal neurons *in vivo*: soma-dendritic structure and axonal domains. *Exp. Brain Res.* **84**, 57–74 (1991).
27. Honda, Y. & Ishizuka, N. Organization of connectivity of the rat presubiculum. I. Efferent projections to the medial entorhinal cortex. *J. Comp. Neurol.* **473**, 463–484 (2004).
28. Van Haeften, T., Wouterlood, F. G., Jorritsma-Byham, B. & Witter, M. P. GABAergic presubicular projections to the medial entorhinal cortex of the rat. *J. Neurosci.* **17**, 862–874 (1997).
29. Kohler, C. Intrinsic connections of the retrohippocampal region in the rat brain: III. The lateral entorhinal area. *J. Comp. Neurol.* **271**, 208–228 (1988).
30. Segal, M. Afferents to the entorhinal cortex of the rat studied by the method of retrograde transport of horseradish peroxidase. *Exp. Neurol.* **57**, 750–765 (1977).
31. van Groen, T. & Wyss, J. M. The postsubicular cortex in the rat: characterization of the fourth region of the subicular cortex and its connections. *Brain Res.* **529**, 165–177 (1990).
32. Kohler, C. Intrinsic projections of the retrohippocampal region in the rat brain. I. The subicular complex. *J. Comp. Neurol.* **236**, 504–522 (1985).
33. Caballero-Bleda, M. & Witter, M. P. Regional and laminar organization of projections from the presubiculum and parasubiculum to the entorhinal cortex: an anterograde tracing study in the rat. *J. Comp. Neurol.* **328**, 115–129 (1993).
34. Honda, Y., Umitsu, Y. & Ishizuka, N. Organization of connectivity of the rat presubiculum: II. Associational and commissural connections. *J. Comp. Neurol.* **506**, 640–658 (2008).
35. Van Haeften, T., Wouterlood, F. G. & Witter, M. P. Presubicular input to the dendrites of layer-V entorhinal neurons in the rat. *Ann. NY Acad. Sci.* **911**, 471–473 (2000).
36. Kohler, C., Shipley, M. T., Srebro, B. & Harkmark, W. Some retrohippocampal afferents to the entorhinal cortex. Cells of origin as studied by the HRP method in the rat and mouse. *Neurosci. Lett.* **10**, 115–120 (1978).
37. Dolorfo, C. L. & Amaral, D. G. Entorhinal cortex of the rat: organization of intrinsic connections. *J. Comp. Neurol.* **398**, 49–82 (1998).
38. Baks-Te-Bulte, L., Wouterlood, F. G., Vinkenoog, M. & Witter, M. P. Entorhinal projections terminate onto principal neurons and interneurons in the subiculum: a quantitative electron microscopic analysis in the rat. *Neuroscience* **136**, 729–739 (2005).
39. Deller, T., Martinez, A., Nitsch, R. & Frotscher, M. A novel entorhinal projection to the rat dentate gyrus: direct innervation of proximal dendrites and cell bodies of granule cells and GABAergic neurons. *J. Neurosci.* **16**, 3322–3333 (1996).
- This paper described an underexposed projection from the deep layers of the EC to the DG, which should fundamentally alter our concept of the EC (see also reference 96).**
40. Dolorfo, C. L. & Amaral, D. G. Entorhinal cortex of the rat: topographic organization of the cells of origin of the perforant path projection to the dentate gyrus. *J. Comp. Neurol.* **398**, 25–48 (1998).
41. Hjorth-Simonsen, A. Projection of the lateral part of the entorhinal area to the hippocampus and fascia dentata. *J. Comp. Neurol.* **146**, 219–232 (1972).
42. Kajiwara, R. *et al.* Convergence of entorhinal and CA3 inputs onto pyramidal neurons and interneurons in hippocampal area CA1 - An anatomical study in the rat. *Hippocampus* **18**, 266–280 (2007).
43. Kohler, C. A projection from the deep layers of the entorhinal area to the hippocampal formation in the rat brain. *Neurosci. Lett.* **56**, 13–19 (1985).
44. Nafstad, P. H. An electron microscope study on the termination of the perforant path fibres in the hippocampus and the fascia dentata. *Z. Zellforsch. Mikrosk. Anat.* **76**, 532–542 (1967).
45. Ruth, R. E., Collier, T. J. & Routtenberg, A. Topography between the entorhinal cortex and the dentate septotemporal axis in rats: I. Medial and intermediate entorhinal projecting cells. *J. Comp. Neurol.* **209**, 69–78 (1982).
46. Ruth, R. E., Collier, T. J. & Routtenberg, A. Topographical relationship between the entorhinal cortex and the septotemporal axis of the dentate gyrus in rats: II. Cells projecting from lateral entorhinal subdivisions. *J. Comp. Neurol.* **270**, 506–516 (1988).
47. Segal, M. & Landis, S. Afferents to the hippocampus of the rat studied with the method of retrograde transport of horseradish peroxidase. *Brain Res.* **78**, 1–15 (1974).
48. Steward, O. Topographic organization of the projections from the entorhinal area to the hippocampal formation of the rat. *J. Comp. Neurol.* **167**, 285–314 (1976).
49. Tamamaki, N. & Nojo, Y. Preservation of topography in the connections between the subiculum, field CA1, and the entorhinal cortex in rats. *J. Comp. Neurol.* **353**, 379–390 (1995).
50. Tamamaki, N. Organization of the entorhinal projection to the rat dentate gyrus revealed by Dil anterograde labeling. *Exp. Brain Res.* **116**, 250–258 (1997).
51. Witter, M. P., Griffioen, A. W., Jorritsma-Byham, B. & Krijnen, J. L. Entorhinal projections to the hippocampal CA1 region in the rat: an underestimated pathway. *Neurosci. Lett.* **85**, 193–198 (1988).
52. Naber, P. A., Lopes da Silva, F. H. & Witter, M. P. Reciprocal connections between the entorhinal cortex and hippocampal fields CA1 and the subiculum are in register with the projections from CA1 to the subiculum. *Hippocampus* **11**, 99–104 (2001).
53. Sporns, O. & Tononi, G. In *Handbook of Brain Connectivity* (eds Jirsa, V. K. & McIntosh, A. R.) 117–147 (Springer, Berlin, 2007).
- In this book chapter the authors clearly explain segregation and integration and describe a method for quantifying structural connection patterns as global measures of brain dynamics.**
54. Tamamaki, N. & Nojo, Y. Projection of the entorhinal layer II neurons in the rat as revealed by intracellular pressure-injection of neurobiotin. *Hippocampus* **3**, 471–480 (1993).
55. Braak, H. On the structure of the human archicortex. I. The cornu ammonis. A Golgi and pigmentarchitectonic study. *Cell Tissue Res.* **152**, 349–383 (1974).
56. Honda, Y., Umitsu, Y. & Ishizuka, N. Topographic projections of perforant path from entorhinal area to CA1 and subiculum in the rat. *Neurosci. Res.* **24** (Suppl.), S101 (2000).
57. Naber, P. A., Witter, M. P. & Lopes da Silva, F. H. Evidence for a direct projection from the postrhinal cortex to the subiculum in the rat. *Hippocampus* **11**, 105–117 (2001).
58. Witter, M. P. & Groenewegen, H. J. Laminar origin and septotemporal distribution of entorhinal and perirhinal projections to the hippocampus in the cat. *J. Comp. Neurol.* **224**, 371–385 (1984).
59. Witter, M. P. A survey of the anatomy of the hippocampal formation, with emphasis on the septotemporal organization of its intrinsic and extrinsic connections. *Adv. Exp. Med. Biol.* **203**, 67–82 (1986).
60. Witter, M. P., Holtrop, R. & van de Loosdrecht, A. A. Direct projections from the periallocortical subicular complex to the fascia dentata in the rat. *Neurosci. Res. Commun.* **2**, 61–68 (1988).
61. Beckstead, R. M. Afferent connections of the entorhinal area in the rat as demonstrated by retrograde cell-labeling with horseradish peroxidase. *Brain Res.* **152**, 249–264 (1978).
62. Kosel, K. C., Van Hoesen, G. W. & Rosene, D. L. A direct projection from the perirhinal cortex (area 35) to the subiculum in the rat. *Brain Res.* **269**, 347–351 (1983).
63. Ishizuka, N., Weber, J. & Amaral, D. G. Organization of intrahippocampal projections originating from CA3 pyramidal cells in the rat. *J. Comp. Neurol.* **295**, 580–623 (1990).
64. Laurberg, S. Commissural and intrinsic connections of the rat hippocampus. *J. Comp. Neurol.* **184**, 685–708 (1979).
65. Laurberg, S. & Sorensen, K. E. Associational and commissural collaterals of neurons in the hippocampal formation (hilus fasciae dentatae and subfield CA5). *Brain Res.* **212**, 287–300 (1981).
66. Amaral, D. G., Dolorfo, C. & varez-Royo, P. Organization of CA1 projections to the subiculum: a PHA-L analysis in the rat. *Hippocampus* **1**, 415–435 (1991).
67. Swanson, L. W., Sawchenko, P. E. & Cowan, W. M. Evidence for collateral projections by neurons in Ammon's horn, the dentate gyrus, and the subiculum: a multiple retrograde labeling study in the rat. *J. Neurosci.* **1**, 548–559 (1981).
68. Tamamaki, N. & Nojo, Y. Disposition of the slab-like modules formed by axon branches originating from single CA1 pyramidal neurons in the rat hippocampus. *J. Comp. Neurol.* **291**, 509–519 (1990).
69. van Groen, T. & Wyss, J. M. Extrinsic projections from area CA1 of the rat hippocampus: olfactory, cortical, subcortical, and bilateral hippocampal formation projections. *J. Comp. Neurol.* **302**, 515–528 (1990).
70. Buckmaster, P. S., Strowbridge, B. W. & Schwartzkroin, P. A. A comparison of rat hippocampal mossy cells and CA3c pyramidal cells. *J. Neurophysiol.* **70**, 1281–1299 (1993).
71. Li, X. G., Somogyi, P., Ylinen, A. & Buzsaki, G. The hippocampal CA3 network: an *in vivo* intracellular labeling study. *J. Comp. Neurol.* **339**, 181–208 (1994).
72. Swanson, L. W., Wyss, J. M. & Cowan, W. M. An autoradiographic study of the organization of intrahippocampal association pathways in the rat. *J. Comp. Neurol.* **181**, 681–715 (1978).
73. Wittner, L., Henze, D. A., Zaborszky, L. & Buzsaki, G. Hippocampal CA3 pyramidal cells selectively innervate aspiny interneurons. *Eur. J. Neurosci.* **24**, 1286–1298 (2006).
74. Wittner, L., Henze, D. A., Zaborszky, L. & Buzsaki, G. Three-dimensional reconstruction of the axon arbor of a CA3 pyramidal cell recorded and filled *in vivo*. *Brain Struct. Funct.* **212**, 75–83 (2007).
75. Cenuizca, L. A. & Swanson, L. W. Spatial organization of direct hippocampal field CA1 axonal projections to the rest of the cerebral cortex. *Brain Res. Rev.* **56**, 1–26 (2007).
76. Finch, D. M., Nowlin, N. L. & Babb, T. L. Demonstration of axonal projections of neurons in the rat hippocampus and subiculum by intracellular injection of HRP. *Brain Res.* **271**, 201–216 (1983).
77. Sik, A., Tamamaki, N. & Freund, T. F. Complete axon arborization of a single CA3 pyramidal cell in the rat hippocampus, and its relationship with postsynaptic parvalbumin-containing interneurons. *Eur. J. Neurosci.* **5**, 1719–1728 (1993).
78. Siddiqui, A. H. & Joseph, S. A. CA3 axonal sprouting in kainate-induced chronic epilepsy. *Brain Res.* **1066**, 129–146 (2005).
79. Hjorth-Simonsen, A. Some intrinsic connections of the hippocampus in the rat: an experimental analysis. *J. Comp. Neurol.* **147**, 145–161 (1973).
80. Van, G. T. & Wyss, J. M. Species differences in hippocampal commissural connections: studies in rat, guinea pig, rabbit, and cat. *J. Comp. Neurol.* **267**, 322–334 (1988).
81. Lorente de N6, R. Studies on the structure of the cerebral cortex. II. Continuation of the study of the ammonic system. *J. Psychol. Neurol.* **46**, 113–177 (1934).
82. Claiborne, B. J., Amaral, D. G. & Cowan, W. M. A light and electron microscopic analysis of the mossy fibers of the rat dentate gyrus. *J. Comp. Neurol.* **246**, 435–458 (1986).
83. Frotscher, M., Seress, L., Schwedtfeger, W. K. & Buhl, E. The mossy cells of the fascia dentata: a comparative study of their fine structure and synaptic connections in rodents and primates. *J. Comp. Neurol.* **312**, 145–163 (1991).
84. Deller, T., Nitsch, R. & Frotscher, M. Heterogeneity of the commissural projection to the rat dentate gyrus: a Phaseolus vulgaris leucoagglutinin tracing study. *Neuroscience* **75**, 111–121 (1996).
85. Swanson, L. W. & Cowan, W. M. An autoradiographic study of the organization of the efferent connections of the hippocampal formation in the rat. *J. Comp. Neurol.* **172**, 49–84 (1977).
86. Finch, D. M. & Babb, T. L. Demonstration of caudally directed hippocampal efferents in the rat by intracellular injection of horseradish peroxidase. *Brain Res.* **214**, 405–410 (1981).
87. Harris, E., Witter, M. P., Weinstein, G. & Stewart, M. Intrinsic connectivity of the rat subiculum. I. Dendritic morphology and patterns of axonal arborization by pyramidal neurons. *J. Comp. Neurol.* **435**, 490–505 (2001).
88. Witter, M. P., Ostendorf, R. H. & Groenewegen, H. J. Heterogeneity in the dorsal subiculum of the rat. Distinct neuronal zones project to different cortical and subcortical targets. *Eur. J. Neurosci.* **2**, 718–725 (1990).
89. Kloosterman, F., Witter, M. P. & Van Haeften, T. Topographical and laminar organization of subicular projections to the parahippocampal region of the rat. *J. Comp. Neurol.* **455**, 156–171 (2003).
90. Van Haeften, T., Jorritsma-Byham, B. & Witter, M. P. Quantitative morphological analysis of subicular terminals in the rat entorhinal cortex. *Hippocampus* **5**, 452–459 (1995).
91. Naber, P. A. & Witter, M. P. Subicular efferents are organized mostly as parallel projections: a double-labeling, retrograde-tracing study in the rat. *J. Comp. Neurol.* **393**, 284–297 (1998).

REVIEWS

92. Honda, Y., Umitsu, Y. & Ishizuka, N. Efferent projections of the subiculum to the retrohippocampal and retrosplenial cortices of the rat. *Neurosci. Res.* **22** (Suppl.), S265 (1999).
93. Mayeux, D. J. & Johnston, R. E. Discrimination of social odors and their locations: role of lateral entorhinal area. *Physiol. Behav.* **82**, 653–662 (2004).
94. Van Haeflen, T., Baks-Te-Bulte, L., Goede, P. H., Wouterlood, F. G. & Witter, M. P. Morphological and numerical analysis of synaptic interactions between neurons in deep and superficial layers of the entorhinal cortex of the rat. *Hippocampus* **13**, 943–952 (2003).
95. Sargolini, F. *et al.* Conjunctive representation of position, direction, and velocity in entorhinal cortex. *Science* **312**, 758–762 (2006). **This study provided evidence that information on location, direction and distance is integrated and updated in the grid cell network during navigation.**
96. Koganezawa, N. *et al.* Significance of the deep layers of entorhinal cortex for transfer of both perirhinal and amygdala inputs to the hippocampus. *Neurosci. Res.* **61**, 172–181 (2008).
97. Viskontas, I. V., Carr, V. A., Engel, S. A. & Knowlton, B. J. The neural correlates of recollection: hippocampal activation declines as episodic memory fades. *Hippocampus* **19**, 265–272 (2008).
98. Rolls, E. T. An attractor network in the hippocampus: theory and neurophysiology. *Learn. Mem.* **14**, 714–731 (2007). **This paper provided a clear definition of the characteristic features of attractor networks and summarized data in support of the view that the hippocampus comprises an attractor network relevant for fast and efficient encoding and retrieval of trial-unique memories.**
99. Nakazawa, K. *et al.* Requirement for hippocampal CA3 NMDA receptors in associative memory recall. *Science* **297**, 211–218 (2002).
100. Gold, A. E. & Kesner, R. P. The role of the CA3 subregion of the dorsal hippocampus in spatial pattern completion in the rat. *Hippocampus* **15**, 808–814 (2005).
101. McNaughton, B. L. *et al.* Distinct characteristics of CA1 place cells correlated with medial or lateral entorhinal cortex layer III input. *Society for Neuroscience Abstracts* **391.3** (2008).
102. O'Keefe, J. Place units in the hippocampus of the freely moving rat. *Exp. Neurol.* **51**, 78–109 (1976).
103. Kjelstrup, K. B. *et al.* Finite scale of spatial representation in the hippocampus. *Science* **321**, 140–143 (2008).
104. Sharp, P. E. & Green, C. Spatial correlates of firing patterns of single cells in the subiculum of the freely moving rat. *J. Neurosci.* **14**, 2359–2356 (1994).
105. Sharp, P. E. Subicular cells generate similar spatial firing patterns in two geometrically and visually distinctive environments: comparison with hippocampal place cells. *Behav. Brain Res.* **85**, 71–92 (1997).
106. Sharp, P. E. Subicular place cells expand or contract their spatial firing pattern to fit the size of the environment in an open field but not in the presence of barriers: comparison with hippocampal place cells. *Behav. Neurosci.* **113**, 643–662 (1999).
107. Sharp, P. E. Multiple spatial/behavioral correlates for cells in the rat postsubiculum: multiple regression analysis and comparison to other hippocampal areas. *Cereb. Cortex* **6**, 238–259 (1996).
108. O'Keefe, J. in *The Hippocampus Book* (eds Andersen, P., Morris, R., Amaral, D. G., Bliss, T. & O'Keefe, J.) 475–579 (Oxford Univ. Press, New York, 2007).
109. Taube, J. S. Place cells recorded in the parasubiculum of freely moving rats. *Hippocampus* **5**, 569–583 (1995).
110. Jung, M. W., Wiener, S. I. & McNaughton, B. L. Comparison of spatial firing characteristics of units in dorsal and ventral hippocampus of the rat. *J. Neurosci.* **14**, 7347–7356 (1994).
111. Maurer, A. P., Vanhoads, S. R., Sutherland, G. R., Lipa, P. & McNaughton, B. L. Self-motion and the origin of differential spatial scaling along the septo-temporal axis of the hippocampus. *Hippocampus* **15**, 841–852 (2005).
112. Touretzky, D. S. & Redish, A. D. Theory of rodent navigation based on interacting representations of space. *Hippocampus* **6**, 247–270 (1996).
113. Sharp, P. E. Complimentary roles for hippocampal versus subicular/entorhinal place cells in coding place, context, and events. *Hippocampus* **9**, 432–443 (1999).
114. Remondes, M. & Schuman, E. M. Role for a cortical input to hippocampal area CA1 in the consolidation of a long-term memory. *Nature* **431**, 699–703 (2004).
115. Brun, V. H. *et al.* Impaired spatial representation in CA1 after lesion of direct input from entorhinal cortex. *Neuron* **57**, 290–302 (2008).
116. Quirk, G. J., Muller, R. U., Kubie, J. L. & Ranck, J. B. Jr. The positional firing properties of medial entorhinal neurons: description and comparison with hippocampal place cells. *J. Neurosci.* **12**, 1945–1963 (1992).
117. Frank, L. M., Brown, E. N. & Wilson, M. Trajectory encoding in the hippocampus and entorhinal cortex. *Neuron* **27**, 169–178 (2000).
118. Fyhn, M., Molden, S., Witter, M. P., Moser, E. I. & Moser, M. B. Spatial representation in the entorhinal cortex. *Science* **305**, 1258–1264 (2004).
119. Brun, V. H. *et al.* Progressive increase in grid scale from dorsal to ventral medial entorhinal cortex. *Hippocampus* **18**, 1200–1212 (2008).
120. Taube, J. S., Muller, R. U. & Ranck, J. B. Jr. Head-direction cells recorded from the postsubiculum in freely moving rats. II. Effects of environmental manipulations. *J. Neurosci.* **10**, 436–447 (1990).
121. Mizumori, S. J. & Williams, J. D. Directionally selective mnemonic properties of neurons in the lateral dorsal nucleus of the thalamus of rats. *J. Neurosci.* **13**, 4015–4028 (1993).
122. Taube, J. S. Head direction cells recorded in the anterior thalamic nuclei of freely moving rats. *J. Neurosci.* **15**, 70–86 (1995).
123. Stackman, R. W. & Taube, J. S. Firing properties of head direction cells in the rat anterior thalamic nucleus: dependence on vestibular input. *J. Neurosci.* **17**, 4349–4358 (1997).
124. Sharp, P. E. & Koester, K. Lesions of the mammillary body region severely disrupt the cortical head direction, but not place cell signal. *Hippocampus* **18**, 766–784 (2008). **This study provides evidence that the mammillary bodies provide important information for the head-direction cells but not for the place cells in the hippocampus.**
125. Chen, L. L., Lin, L. H., Green, E. J., Barnes, C. A. & McNaughton, B. L. Head-direction cells in the rat posterior cortex. I. Anatomical distribution and behavioral modulation. *Exp. Brain Res.* **101**, 8–23 (1994).
126. Wiener, S. I. Spatial and behavioral correlates of striatal neurons in rats performing a self-initiated navigation task. *J. Neurosci.* **13**, 3802–3817 (1993).
127. Calton, J. L. *et al.* Hippocampal place cell instability after lesions of the head direction cell network. *J. Neurosci.* **23**, 9719–9731 (2003).
128. McNaughton, B. L., Barnes, C. A., Meltzer, J. & Sutherland, R. J. Hippocampal granule cells are necessary for normal spatial learning but not for spatially-selective pyramidal cell discharge. *Exp. Brain Res.* **76**, 485–496 (1989).
129. Brun, V. H. *et al.* Place cells and place recognition maintained by direct entorhinal-hippocampal circuitry. *Science* **296**, 2243–2246 (2002).
130. Witter, M. P. Connections of the subiculum of the rat: topography in relation to columnar and laminar organization. *Behav. Brain Res.* **174**, 251–264 (2006).
131. Buzsáki, G. & Draguhn, A. Neuronal oscillations in cortical networks. *Science* **304**, 1926–1929 (2004).
132. Levy, W. B. & Steward, O. Synapses as associative memory elements in the hippocampal formation. *Brain Res.* **175**, 233–245 (1979).
133. Wilson, M. A. & McNaughton, B. L. Reactivation of hippocampal ensemble memories during sleep. *Science* **265**, 676–679 (1994).
134. Mann, E. O. & Paulsen, O. Role of GABAergic inhibition in hippocampal network oscillations. *Trends Neurosci.* **30**, 343–349 (2007). **This paper reviews the mechanism by which GABAergic interneurons control the spike timing of other neurons and synchronize network activity.**
135. Cobb, S. R., Buhl, E. H., Halasy, K., Paulsen, O. & Somogyi, P. Synchronization of neuronal activity in hippocampus by individual GABAergic interneurons. *Nature* **378**, 75–78 (1995).
136. Klausberger, T. *et al.* Brain-state- and cell-type-specific firing of hippocampal interneurons *in vivo*. *Nature* **421**, 844–848 (2003).
137. Klausberger, T. *et al.* Spike timing of dendrite-targeting bistratified cells during hippocampal network oscillations *in vivo*. *Nature Neurosci.* **7**, 41–47 (2004).
138. Tukker, J. J., Fuentealba, P., Hartwich, K., Somogyi, P. & Klausberger, T. Cell type-specific tuning of hippocampal interneuron firing during gamma oscillations *in vivo*. *J. Neurosci.* **27**, 8184–8189 (2007).
139. Jinno, S. *et al.* Neuronal diversity in GABAergic long-range projections from the hippocampus. *J. Neurosci.* **27**, 8790–8804 (2007).

This paper provides evidence that particular long-range GABAergic projection neurons are important for coordinating oscillation across brain areas.

140. Gulyás, A. I., Hajos, N., Katona, I. & Freund, T. F. Interneurons are the local targets of hippocampal inhibitory cells which project to the medial septum. *Eur. J. Neurosci.* **17**, 1861–1872 (2003).
141. Losonczy, A., Zhang, L., Shigemoto, R., Somogyi, P. & Nusser, Z. Cell type dependence and variability in the short-term plasticity of EPSCs in identified mouse hippocampal interneurons. *J. Physiol.* **542**, 193–210 (2002).
142. Sik, A., Penttonen, M., Ylinen, A. & Buzsáki, G. Hippocampal CA1 interneurons: an *in vivo* intracellular labeling study. *J. Neurosci.* **15**, 6651–6665 (1995).
143. Vida, I., Halasy, K., Szinyei, C., Somogyi, P. & Buhl, E. H. Unitary IPSPs evoked by interneurons at the stratum radiatum-stratum lacunosum-moleculare border in the CA1 area of the rat hippocampus *in vitro*. *J. Physiol.* **506**, 755–773 (1998).
144. Tulving, E. in *Organization of Memory* (eds Tulving, E. & Donaldson, W.) 381–403 (Academic, New York, 1972).
145. Goulet, S. & Murray, E. A. Neural substrates of crossmodal association memory in monkeys: the amygdala versus the anterior rhinal cortex. *Behav. Neurosci.* **115**, 271–284 (2001).
146. Mayes, A., Montaldi, D. & Migo, E. Associative memory and the medial temporal lobes. *Trends Cogn. Sci.* **11**, 126–135 (2007).
147. Manns, J. R., Howard, M. W. & Eichenbaum, H. Gradual changes in hippocampal activity support remembering the order of events. *Neuron* **56**, 530–540 (2007).
148. Fortin, N. J., Agster, K. L. & Eichenbaum, H. B. Critical role of the hippocampus in memory for sequences of events. *Nature Neurosci.* **5**, 458–462 (2002).
149. Kesner, R. P., Gilbert, P. E. & Barua, L. A. The role of the hippocampus in memory for the temporal order of a sequence of odors. *Behav. Neurosci.* **116**, 286–290 (2002).
150. Lisman, J. E. Relating hippocampal circuitry to function: recall of memory sequences by reciprocal dentate-CA3 interactions. *Neuron* **22**, 233–242 (1999).
151. Bussey, T. J., Saksida, L. M. & Murray, E. A. The perceptual-mnemonic/feature conjunction model of perirhinal cortex function. *Q. J. Exp. Psychol. B* **58**, 269–282 (2005).
152. Braak, H. & Braak, E. Neuropathological staging of Alzheimer-related changes. *Acta Neuropathol.* **82**, 239–259 (1991).
153. McCormick, D. A. & Contreras, D. On the cellular and network bases of epileptic seizures. *Annu. Rev. Physiol.* **63**, 815–846 (2001).
154. Honea, R., Crow, T. J., Passingham, D. & Mackay, C. E. Regional deficits in brain volume in schizophrenia: a meta-analysis of voxel-based morphometry studies. *Am. J. Psychiatry* **162**, 2235–2245 (2005).
155. Campbell, S. & MacQueen, G. The role of the hippocampus in the pathophysiology of major depression. *J. Psychiatry Neurosci.* **29**, 417–426 (2004).
156. Zaborszky, L., Wouterlood, F. G. & Lanciego, J. L. *Neuroanatomical Tract-Tracing: Molecules, Neurons, and Systems* (Springer, 2006). **This book provides excellent guidance on tract-tracing methods.**
157. Wickersham, I. R., Finke, S., Conzelmann, K. K. & Callaway, E. M. Retrograde neuronal tracing with a deletion-mutant rabies virus. *Nature Methods* **4**, 47–49 (2007).
158. Luo, L., Callaway, E. M. & Svoboda, K. Genetic dissection of neural circuits. *Neuron* **57**, 634–660 (2008). **This paper showed that a genetic approach can be an additional tool, next to anatomical and physiological methods, for constructing circuit diagrams.**

Acknowledgements

The authors would like to thank E. Moser and L. Colgin for providing helpful comments on an earlier version of this article. N.L.M.C. acknowledges a personal grant from the Netherlands Organization for scientific research (NWO) — grant number 903-47-074.

FURTHER INFORMATION

Authors' homepage: www.temportal-lobe.com

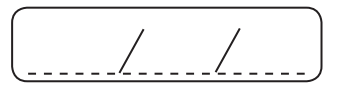
SUPPLEMENTARY INFORMATION

See online article: S1 (figure) | S2 (box) | S3 (table) | S4 (box)

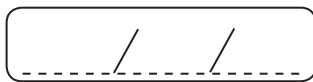
ALL LINKS ARE ACTIVE IN THE ONLINE PDF



A series of horizontal lines for handwriting practice, consisting of 20 evenly spaced lines extending across the width of the page.



A series of horizontal lines for writing, consisting of 20 evenly spaced lines.



Architecture of the Entorhinal Cortex A Review of Entorhinal Anatomy in Rodents with Some Comparative Notes

Menno P. Witter^{1*}, Thanh P. Doan¹, Bente Jacobsen¹, Eirik S. Nilssen¹ and Shinya Ohara²

¹Functional Neuroanatomy, Kavli Institute for Systems Neuroscience, Center for Computational Neuroscience, Egil and Pauline Braathen and Fred Kavli Center for Cortical Microcircuits, NTNU Norwegian University of Science and Technology, Trondheim, Norway, ²Division of Systems Neuroscience, Tohoku University Graduate School of Life Science, Sendai, Japan

OPEN ACCESS

Edited by:

Sachin S. Deshmukh,
Indian Institute of Science, India

Reviewed by:

Francisco Clasca,
Universidad Autonoma de Madrid,
Spain

Diano F. Marrone,
Wilfrid Laurier University, Canada

*Correspondence:

Menno P. Witter
menno.witter@ntnu.no

Received: 25 April 2017

Accepted: 07 June 2017

Published: 28 June 2017

Citation:

Witter MP, Doan TP, Jacobsen B,
Nilssen ES and Ohara S
(2017) Architecture of the Entorhinal
Cortex: A Review of Entorhinal
Anatomy in Rodents with Some
Comparative Notes.
Front. Syst. Neurosci. 11:46.
doi: 10.3389/fnsys.2017.00046

The entorhinal cortex (EC) is the major input and output structure of the hippocampal formation, forming the nodal point in cortico-hippocampal circuits. Different division schemes including two or many more subdivisions have been proposed, but here we will argue that subdividing EC into two components, the lateral EC (LEC) and medial EC (MEC) might suffice to describe the functional architecture of EC. This subdivision then leads to an anatomical interpretation of the different phenotypes of LEC and MEC. First, we will briefly summarize the cytoarchitectonic differences and differences in hippocampal projection patterns on which the subdivision between LEC and MEC traditionally is based and provide a short comparative perspective. Second, we focus on main differences in cortical connectivity, leading to the conclusion that the apparent differences may well correlate with the functional differences. Cortical connectivity of MEC is features interactions with areas such as the presubiculum, parasubiculum, retrosplenial cortex (RSC) and postrhinal cortex, all areas that are considered to belong to the “spatial processing domain” of the cortex. In contrast, LEC is strongly connected with olfactory areas, insular, medial- and orbitofrontal areas and perirhinal cortex. These areas are likely more involved in processing of object information, attention and motivation. Third, we will compare the intrinsic networks involving principal- and inter-neurons in LEC and MEC. Together, these observations suggest that the different phenotypes of both EC subdivisions likely depend on the combination of intrinsic organization and specific sets of inputs. We further suggest a reappraisal of the notion of EC as a layered input-output structure for the hippocampal formation.

Keywords: parahippocampal region, hippocampus, connectivity, primate, rodent

INTRODUCTION

The denomination “entorhinal cortex (EC)” (Brodman’s area 28) is based on the fact that it is (partially) enclosed by the rhinal (olfactory) sulcus. Interest in the EC arose around the turn of the 20th century when Ramón y Cajal, described a peculiar part of the posterior temporal cortex that was strongly connected to the hippocampus by way of the temporo-ammonic tract (Ramón Y Cajal, 1902; Witter et al., in press). Cajal was struck by this massive connection

and he therefore suggested that the functional significance of the hippocampus had to be related to that of EC or the sphenoidal cortex/angular ganglion, as he called it at that time. Today, EC is conceived as the nodal point between the hippocampal formation on the one hand and a variety of cortical areas on the other hand. Multimodal, as well as highly processed unimodal sensory inputs converge at the level of neurons in the superficial layers of the EC. This input is conveyed by the neurons in layers II and III of EC to all subdivisions of the hippocampal formation (Insausti et al., 2004; van Strien et al., 2009; Cappaert et al., 2014; Strange et al., 2014). The hippocampal fields CA1 and subiculum are the main source of projections that return to layer V of EC, with a less dense projection to layers II and III. Layer V neurons in turn are the main origin of EC projections to widespread cortical and subcortical domains in the forebrain (Rosene and Van Hoesen, 1977; Kosel et al., 1982; Cappaert et al., 2014).

EC comprises different subdivisions, characterized by connectivity with functionally different sets of cortical and subcortical areas in the brain. This has led to the now quite widely accepted concept of parallel input/output channels, mediated by way of perirhinal and postrhinal (rodents) or parahippocampal cortex (primates; Witter et al., 1989a, 2000; Naber et al., 1997; Eichenbaum et al., 2012; Ranganath and Ritchey, 2012). Recent electrophysiological recordings in the lateral and medial EC (LEC and MEC respectively; see below for definitions) of rodents show that cells in MEC are predominantly spatially modulated. In contrast, in LEC such modulation is essentially absent, with neuron-firing correlating to objects in context (Fyhn et al., 2004; Deshmukh and Knierim, 2011; Knierim et al., 2013; Tsao et al., 2013; Moser et al., 2014). Does this phenotypical difference between the two EC components reflect input differences, or differences in local circuits and cell types, or could this phenotypical separation be the result of interactions between these two parameters. In this review, we aim to address specifically this question by providing a comprehensive description of EC, its intrinsic organization in relation to input and output organizations. We mainly focus on data from studies in rodents, although occasional comparative remarks are inserted when considered relevant for the narrative of the article.

DEFINITION OF THE ENTORHINAL CORTEX, SUBDIVISIONS AND OVERALL ARCHITECTURE

There are different ways to define a cortical area, using different criteria, such as location, connectivity, cyto- and chemoarchitecture. Applying all of these approaches has resulted in a variety of borders, subdivisions and description of layers. Architectural parcellation schemes are useful tools to relate experimental data to standard locations in the brain (Bjaalie, 2002; van Strien et al., 2009; Zilles and Amunts, 2010; Kjonigsen et al., 2011, 2015; Boccara et al., 2015). Connection-based subdivision schemes may relate closer to our understanding of functional differences between areas

(see below). In view of the strong implications of the human EC in a variety of brain diseases (Braak and Braak, 1992), the development of adequate animal models for such diseases depends strongly on our capabilities to extrapolate the definition of the EC from rodents to non-human and human primates. Therefore, combinations of the different approaches mentioned above will likely provide the most reliable concept for subdividing EC.

An apparently good lead, since it has withstood over a century of arguments, is the definition of EC based on hippocampal connectivity, as originally suggested by Ramón Y Cajal (1902, 1911). In view of increasing insights into the connectivity of the hippocampal formation and its subdivisions, we follow the well-established practice in rodents to take the differential distribution of EC projections to the dentate gyrus as a good defining criterion for two main subdivisions of EC. These are nowadays referred to as LEC and MEC (Steward, 1976; Witter, 2007). Unfortunately, in the monkey, the terminal distribution of the entorhinal-to-dentate projection does not provide such a clear criterion to functionally subdivide EC (Witter et al., 1989b). Potentially in line with this, cytoarchitectural division schemes tend to differentiate more than two subdivisions (Amaral et al., 1987; Rosene and Van Hoesen, 1987). However, the second entorhinal-hippocampal projection, connecting the two entorhinal domains to area CA1 and the subiculum in all mammalian species studied, including primates, shows a strikingly preserved topology along the transverse axis of both hippocampal fields. Projections emerging from a posteromedial location in EC target the proximal CA1, i.e., close to DG, and distal subiculum, whereas an anterolateral origin in EC maps onto the distal CA1 and adjacent proximal subiculum (human: Witter et al., 2000; Maass et al., 2015; monkey: Witter and Amaral, 1991; rat: Naber et al., 2001; van Strien et al., 2009).

Other connectivity patterns have been proposed to functionally subdivide EC as well, one being the input from the presubiculum. In all non-primate mammalian species studied so far, including rat, guinea pig and cat, the innervation of EC by presubicular fibers is restricted to a more caudal and dorsal portion that coincides with a cyto- and chemoarchitecturally well defined area, now called MEC (Shiple, 1975; Köhler, 1984; Room and Groenewegen, 1986). Also in the monkey, inputs from the presubiculum distribute to only a restricted posterior portion of EC (Amaral et al., 1984; Saunders and Rosene, 1988; Witter and Amaral, unpublished observations), and this area may thus represent the homolog of MEC as defined in non-primates. Recent connectional MRI studies in humans have pointed to a comparable connectional bipartite system separating anterolateral from posteromedial EC, showing clear differences with respect to connectivity measures with perirhinal and parahippocampal cortex, resembling those reported in rodents (Naber et al., 1997; Maass et al., 2015; Navarro Schröder et al., 2015).

Cytoarchitectural data reveal that in all species studied, two entorhinal areas can be differentiated and that these share cytoarchitectonic features with the two entorhinal areas

defined by Brodmann as areas 28a and b (Brodmann, 1909). One can easily recognize a posteromedial area characterized by a very regular six-layered structure and a homogenous distribution of neurons in all layers, typical for area 28b or MEC. Layer II of MEC comprises a mixture of excitatory medium-sized pyramidal neurons and large multipolar neurons that have become known as stellate cells (SCs). On the opposite, anterolateral side, the laminar structure is comparable, but much less regular, resembling the cytoarchitecture of area 28a or LEC. In the latter portion, layer II comprises a mixture of large multipolar neurons, nowadays in rodents referred to as fan cells, pyramidal and medium-sized multipolar neurons. At some locations, these cell types seem to cluster into sublayers (referred to as Iia and Iib, or II and IIIa; Kobro-Flatmoen and Witter, 2017). Depending on the species, one or several additional subdivisions have been described, similar to what was mentioned above for the monkey (Lorente de Nó, 1933; Insausti et al., 1997). Note that the terms LEC and MEC do not simply reflect a particular position in anatomical or stereotaxic space. In many species, the two areas, defined by their combined architectural and hodological features occupy a more rostralateral (LEC) vs. a more caudomedial position (MEC).

CONNECTIVITY OF THE TWO ENTORHINAL SUBDIVISIONS

Both LEC and MEC project to the hippocampus, and the axons form synapses on neurons in all hippocampal subfields. Neurons in layer II are the main source of the entorhinal projections to the dentate gyrus and fields CA2 and CA3, and neurons in layer III give rise to the entorhinal projections to CA1 and subiculum (note that a small number of neurons in deeper entorhinal layers contribute to both projections). In view of a confusing nomenclature that has developed over the years to describe these different projection systems (for a recent description and discussion, see Witter et al., in press), in the present article, we differentiate between the EC-layer II projection and the EC-layer III projection. Regarding the EC-layer II projection, we know that single layer II cells project to both the dentate gyrus and CA2/CA3 (Tamamaki and Nojyo, 1993). Whether such a collateral organization is true for the layer III projection to CA1 and subiculum is unclear. In view of this striking layer-separation in the origin of the EC to hippocampus projections, we feel that a description of intrinsic and extrinsic connectivity of LEC and MEC might benefit from a layered approach. In the following, we focus on the main cell layers II, III and V (for a description of layers I and VI, the reader is referred to Canto et al., 2008; Cappaert et al., 2014).

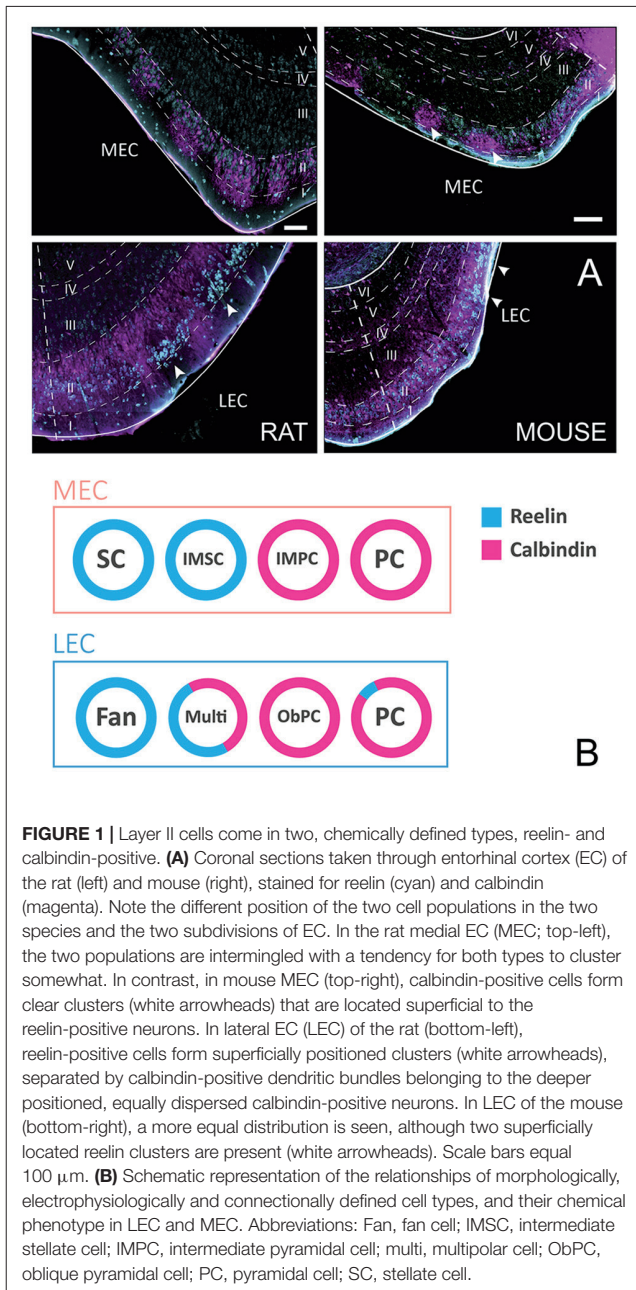
Extrinsic Connections

The two entorhinal divisions differ with respect to their major extrinsic cortical and subcortical connections (for recent detailed overviews in the rat, see Kerr et al., 2007; Cappaert et al., 2014; for broader comparative overviews of cortical connectivity in a functional context, see Eichenbaum et al.,

2012; Ranganath and Ritchey, 2012). Here we focus on a description of the distribution of main cortical inputs and their laminar preference of termination. Superficial layers of EC receive a substantial input from olfactory structures including the olfactory bulb, the anterior olfactory nucleus, and the piriform cortex (Haberly and Price, 1978; Kosel et al., 1981). Olfactory axons preferentially terminate laterally and centrally in LEC and in MEC, avoiding the most caudodorsal portion of MEC (Kerr et al., 2007). Olfactory fibers mainly distribute to layer I, where they make synaptic contacts with dendrites of neurons in layers II and III (Wouterlood and Nederlof, 1983). Other superficially terminating inputs to dorsolateral parts of LEC originate from insular cortex (Mathiasen et al., 2015), perirhinal cortex (Naber et al., 1999; Pinto et al., 2006) and orbitofrontal cortex (Hoover and Vertes, 2007, 2011; Kondo and Witter, 2014). Interestingly, the orbitofrontal and insular projections to LEC mainly terminate anteriorly, and close to the rhinal fissure. Parietal cortex projects moderately to LEC and MEC, terminating close to the rhinal fissure, preferentially in layers I and V (Olsen et al., 2017). Superficial layers of MEC receive inputs from the orbitofrontal cortex, but only from the ventral part (Kondo and Witter, 2014), postrhinal cortex (Koganezawa et al., 2015) and pre- and parasubiculum (Caballero-Bleda and Witter, 1993). The latter two inputs not only terminate on dendrites of neurons in layers II and III, but also influence neurons in layer V (Canto et al., 2012), and such a connective scheme might hold true for all superficially terminating inputs. This however remains to be established, but the possibility points to a potentially relevant role for layer V neurons as integrators of entorhinal inputs, since they also are the recipients of other major cortical inputs distributing to layer V. These include inputs from infralimbic and prelimbic cortex, apparently innervating LEC and MEC almost equally dense. LEC layer V receives a denser input from anterior cingulate cortex, whereas the retrosplenial innervation almost exclusively distributes to MEC layer V (Wyss and Van Groen, 1992; Vertes, 2004; Jones and Witter, 2007), which also receives a weak to moderate input from visual cortex (Kerr et al., 2007; Olsen et al., 2017).

Intrinsic Networks Layer II

Principal cells in both subdivisions of EC come in two chemical types, calbindin- and reelin-expressing cells. In MEC, calbindin-positive cells and reelin-positive cells appear to be grouped in patches, and in LEC the two cell types are more or less confined to two separate sublayers, reelin cells in layer Iia and calbindin cells in layer Iib. The reported clustering of calbindin-positive neurons is particularly striking in limited parts of MEC and is more striking in mice than in rats or other species. Only in mouse MEC the calbindin-positive neurons are located superficial to the reelin positive neurons (Figure 1A; Tunon et al., 1992; Fujimaru and Kosaka, 1996; Wouterlood, 2002; Ramos-Moreno et al., 2006; Kitamura et al., 2014; Ray et al., 2014; Leitner et al., 2016). EC in humans is known for its wart-like bumps or verrucae (Retzius, 1896; Klinger, 1948; Solodkin and Vanhoesen, 1996; Naumann et al., 2016), which in the largest part of EC, located centrally along



the anteroposterior and lateromedial axes, are composed of the large multipolar reelin positive layer II cells, described as the pre- α neurons by Braak (Braak and Braak, 1985; Tunon et al., 1992; Kobro-Flatmoen et al., 2016; Naumann et al., 2016). Moreover, the marked clustering of calbindin-positive neurons in all species studied is limited to a restricted posterior part of MEC (Naumann et al., 2016). In our view, it is therefore confusing to refer to calbindin-positive cells in layer II as island cells embedded in an ocean of reelin-positive cells (Kitamura et al., 2014), since this organization is likely opposite for the larger part of EC. Reelin-positive cells in both entorhinal areas project to the dentate gyrus

and CA3, whereas calbindin-positive neurons project to several other targets including the CA1 and the contralateral EC, the olfactory bulb and piriform cortex (Varga et al., 2010; Kitamura et al., 2014; Fuchs et al., 2016; Leitner et al., 2016; Ohara et al., 2016). The two chemically defined cell groups are composed of several morphological subgroups that can be distinguished based on somatic and dendritic features (Canto and Witter, 2012a,b; Fuchs et al., 2016; Leitner et al., 2016).

In MEC, SCs make up the largest subgroup of principal cells. They have multiple primary dendrites that radiate out from a round soma. SCs are typically reelin-positive and calbindin-negative. Medium to large pyramidal cells (PCs) make up the other main principal cell type in layer II of the MEC. PCs are typically calbindin-positive, although a few reelin-positive PC have been described (Fuchs et al., 2016; **Figure 1B**). There are at least two intermediate cell groups in between stellate and pyramidal morphologies, here referred to as intermediate SCs (IMSCs) and intermediate PCs (IMPCs). IMSCs all express reelin, but a few of them co-express calbindin, the IMPCs tend to be calbindin-positive, but are more diverse and come in both reelin-positive and reelin and calbindin co-expressing varieties. The four principal cell types in the MEC can also be distinguished from each other based on their electrophysiological profiles (Canto and Witter, 2012b; Fuchs et al., 2016).

In LEC layer II, there are also at least four subgroups of principal cells (Canto and Witter, 2012a; Leitner et al., 2016). Fan cells are similar in morphology to SCs, but lack a distinctive basal dendritic tree (Tahvildari and Alonso, 2005; Canto and Witter, 2012a). Most are reelin-positive, though some may express calbindin. PCs make up the other large group of principal cells in LEC, they are morphologically similar to those described in MEC. They are largely calbindin-positive, but some may be reelin-positive. Oblique PCs (ObPCs) and multipolar cell make up the intermediate cell types in the LEC (Canto and Witter, 2012a; Leitner et al., 2016). Oblique pyramidal cells display a morphology similar to PCs, but are tilted relative to the pial surface, and they predominantly express calbindin. Multipolar cells, on the other hand, have a more diverse morphology, and express both calbindin and reelin (**Figure 1B**). Electrophysiologically, the four cell groups in LEC are not as easily distinguishable as in MEC, however recent data suggest that there may be subtle physiological differences between the overarching reelin and calbindin classes (Tahvildari and Alonso, 2005; Canto and Witter, 2012a; Leitner et al., 2016).

Similar to what has been reported for neocortical areas, EC has been suggested to contain three main subgroups of interneurons, parvalbumin (PV), somatostatin (SOM) and 5HT3a expressing cells (Rudy et al., 2011; Fuchs et al., 2016; Leitner et al., 2016). PV-positive interneurons constitute approximately half of the interneuron population across EC, making them the largest subgroup of interneurons in the area (Wouterlood et al., 1995; Miettinen et al., 1996). Layer II of MEC has a large number of PV expressing somata and heavy neuropil staining. Layer II of LEC has comparatively weak PV staining, with

few somata and light neuropil staining. Particularly layer IIa appears to lack PV-positive cells (Wouterlood et al., 1995; Fujimaru and Kosaka, 1996; Miettinen et al., 1996; Leitner et al., 2016). In both LEC and MEC, there is a clear gradient of PV staining, with portions close to the rhinal fissure expressing more than ventral portions (Wouterlood et al., 1995; Fujimaru and Kosaka, 1996; Leitner et al., 2016). A comparable, and strikingly strong gradient has been reported in relation to the collateral and rhinal sulcus in primates (human: Tunon et al., 1992; monkey: Pitkanen and Amaral, 1993; for a detailed comparative description, see Kobro-Flatmoen and Witter, 2017).

Like PV cells in other parts of the brain (Hu et al., 2014), those in layer II of MEC are known to display a fast spiking physiological profile (Couey et al., 2013; Pastoll et al., 2013; Armstrong et al., 2016; Fuchs et al., 2016; Leitner et al., 2016). The existence of PV-positive baskets surrounding principal cells in layer II is supported by both histological and electrophysiological studies (Jones and Bühl, 1993; Wouterlood et al., 1995; Varga et al., 2010; Armstrong et al., 2016; Fuchs et al., 2016). Another type of basket cell in layer II of MEC is the CCK-expressing basket cell (Varga et al., 2010; Armstrong et al., 2016). These cells are less abundant than PV-expressing cells, and constitute a subgroup of the 5HT3aR expressing interneurons (Lee et al., 2010). Whereas CCK-positive basket cells preferentially target calbindin-positive principal cells, single PV-positive basket cells innervate both reelin- and calbindin-positive neurons (Armstrong et al., 2016). Basket cells have also been described in layer II of the LEC, but no details are available about different types and abundance, nor how they are part of the LEC microcircuit.

A second, common type of GABAergic interneuron that expresses PV in layer II, also present in layer III, is the chandelier or axo-axonic cell. Chandelier cells are characterized by vertical aggregations of axonal boutons, called candles which mainly make synapses on the initial axon segments of principal cells. In MEC, both vertical and horizontal chandelier cells are present, and in LEC the horizontal subtype is dominant. The local axon branches of these neurons are largely confined to layers II and III (Soriano et al., 1993).

Immunohistochemical studies describing the distribution of somatostatin expressing somata in EC are conflicting, particularly with regards to distribution in superficial layers. However, no major differences between entorhinal subdivisions have been described (Köhler and Chan-Palay, 1983; Wouterlood and Pothuizen, 2000). Somatostatin cells in MEC are generally multipolar low threshold spiking neurons (Couey et al., 2013; Fuchs et al., 2016). Available data indicate that only a small percentage of somatostatin neurons in EC are GABAergic (Wouterlood and Pothuizen, 2000), but our own data in mice show that most somatostatin neurons in EC are GABAergic (**Figure 2**). The last major interneuron group in EC, the 5HT3aR cells, consist of several subgroups, including calretinin-, VIP- and CCK-expressing cells (Lee et al., 2010; Fuchs et al., 2016; Leitner et al., 2016). 5HT3aR cells in layer II of MEC have diverse morphological and physiological profiles (Canto et al., 2008; Fuchs et al., 2016).

The regular grid pattern, typically seen in layer II of MEC has been hypothesized to emerge from the structure of microcircuits within layer II (Fuhs and Touretzky, 2006; McNaughton et al., 2006; Burak and Fiete, 2009; Bonnevie et al., 2013;

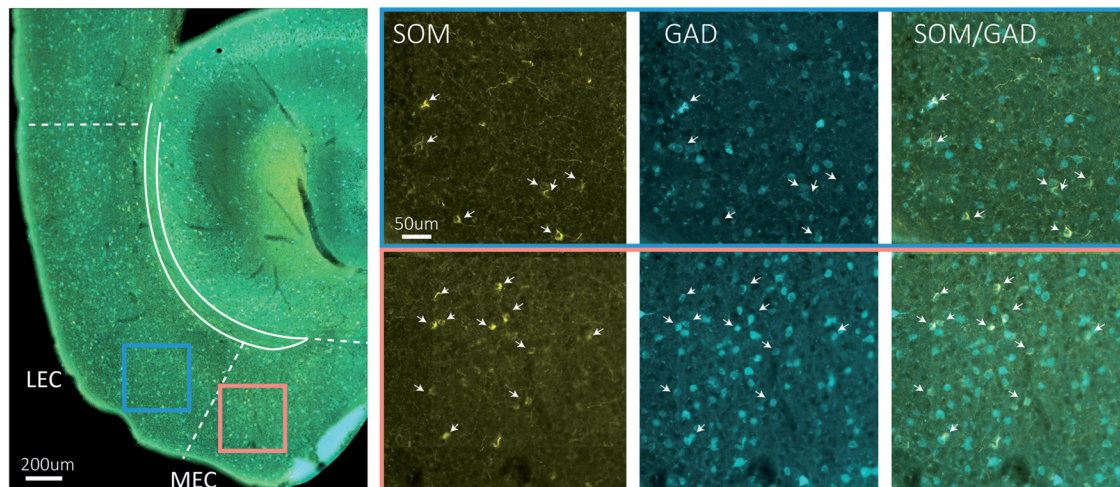
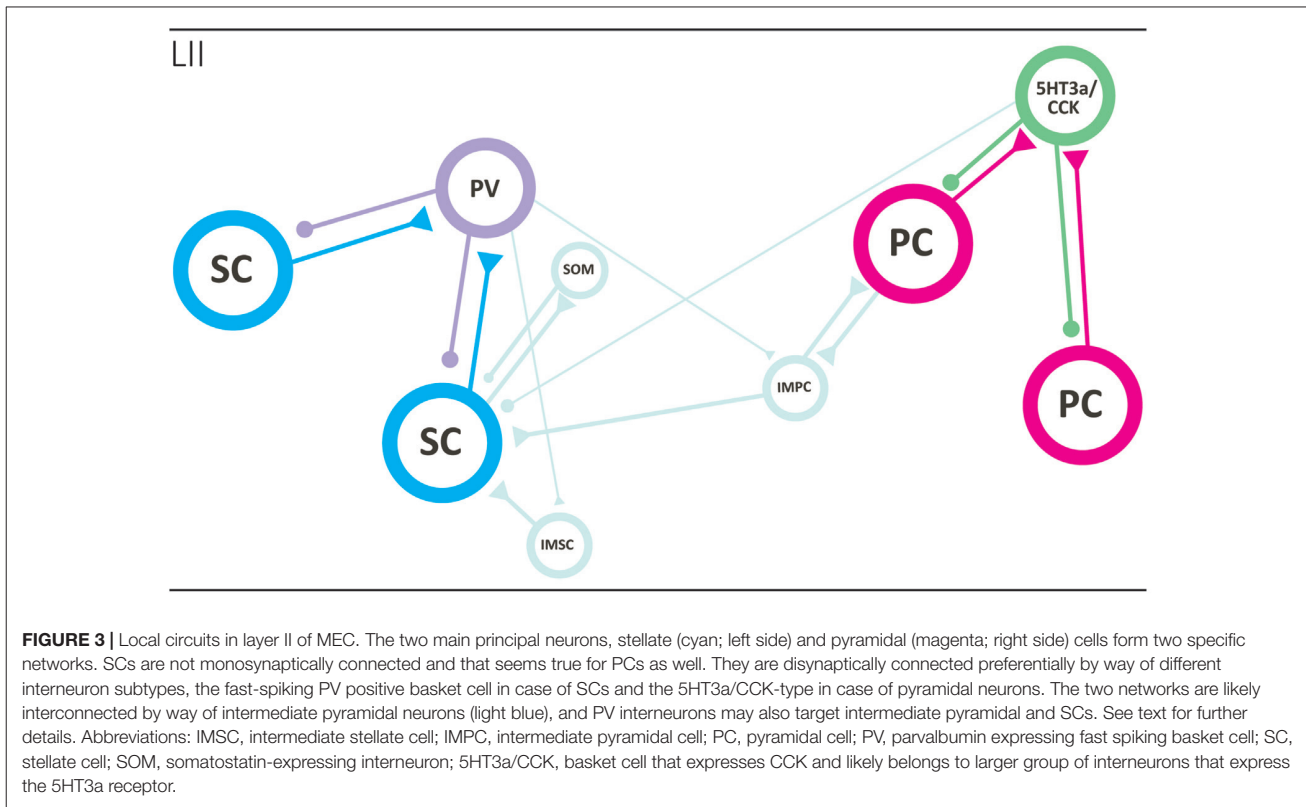


FIGURE 2 | Somatostatin neurons are GAD67 positive. The left hand side main panel shows a low power image of a horizontal section obtained from a GAD67 transgenic line expressing GFP (Tanaka et al., 2003), stained for the expression of somatostatin. The colored squares indicate the position of the high power images shown on the right. Blue square is LEC, red square is MEC. The solid blueish staining at the edge of EC is an artifact due to overlying cerebellar tissue. On the right hand side, high power images show the indicated areas in LEC and MEC in three different fluorescent channels from left to right: somatostatin (yellow), GFP (cyan) and overlay of somatostatin and GFP. Scale bars equal 200 μm in the left main panel and 50 μm for the six panels on the right-hand side.



Couey et al., 2013). The majority of grid cells in MEC are observed in layer II (Hafting et al., 2005; Sargolini et al., 2006), and the anatomical correlates of grid cells likely comprise both stellate-like and pyramidal-like cells (Domnisoru et al., 2013; Schmidt-Hieber and Häusser, 2013; Tang et al., 2014). The local circuit of SCs has been probed in several studies using *in vitro* patch clamp recordings, and it is now well established that individual SCs do not form monosynaptic connections with other SCs. Communication between SCs occurs through an intermediate inhibitory interneuron, in a mechanism by which activation of one or more SCs evokes disynaptic inhibitory currents in neighboring SCs. Paired recordings have revealed strong connectivity in both directions between SCs and fast-spiking cells and, to a much lesser extent, between SCs and low-threshold spiking interneurons (Couey et al., 2013; Pastoll et al., 2013; Fuchs et al., 2016). The functional disynaptic link that illustrates the core principle of the stellate microcircuit is mediated by a single type of inhibitory neuron, the PV positive fast spiking cell (Figure 3; Buettfering et al., 2014; Armstrong et al., 2016).

The local network of PCs has been explored using similar methods, and like the SC network, very sparse monosynaptic connectivity was detected between PCs. These results suggest that the general principle of disynaptic connectivity as described for the SC network also applies to the layer II PCs. An important distinction however is that PCs seem to communicate through different subsets of interneurons. In contrast to SCs, PCs are not

connected, in either direction, to PV positive fast-spiking cells or somatostatin positive low threshold spiking cells, but instead form synaptic connections solely with the heterogeneous 5HT_{3A} expressing population of interneurons (Figure 3; Fuchs et al., 2016).

Synaptic interaction between the pyramidal and SC networks is limited, as available data points to little monosynaptic connectivity between stellate and PCs (Couey et al., 2013; Fuchs et al., 2016). This suggests the existence of two isolated subcircuits within layer II of MEC, where information relayed to the dentate gyrus by reelin positive SCs is processed separately from information relayed by calbindin positive PCs to other downstream areas. However, it should be kept in mind that the networks may be coordinated through one of the intermediate cell types, e.g., the IMPCs, which have been shown to form synaptic connections with both pyramidal and SCs (Figure 3; Fuchs et al., 2016).

If the local microcircuit design of layer II MEC excitatory cells is crucial for generating grid cell firing, the absence of grid cells in LEC predicts a different organization of the layer II principal cell microcircuit. Given the observation that inhibition dominates microcircuits of both pyramidal and SCs in MEC, albeit provided by different types of interneurons, comparable cell types in the LEC, e.g., the fan and PC, may have a circuit structure where monosynaptic connectivity prevails. Our preliminary data from paired recordings of fan cells indicates that direct communication between cells of this type is present, but not prevalent (Nilssen et al., 2015). Potential microcircuit

differences between layer II of MEC and LEC might also reflect different contributions from the local interneuron population. In LEC, 5HT3aR expressing interneurons constitute the largest interneuron group in layer II, unlike in the MEC, where PV cells are thought to be the predominant interneuron group (Leitner et al., 2016). This finding indicates that the inhibitory systems in MEC and LEC layer II are dominated by different subtypes of interneurons.

Layer III

Compared with what is known about neurons and connectivity in layers II and V, Layer III is still largely terra incognita. Layer III in both LEC and MEC comprises a homogenous population of spiny excitatory pyramidal neurons that project to CA1 and subiculum (Tahvildari and Alonso, 2005; Canto and Witter, 2012a,b; Tang et al., 2015). Layer III neurons also project contralaterally to the hippocampus and EC (Steward and Scoville, 1976). About 40% of the layer III hippocampal projecting cells in MEC send collaterals to the contralateral MEC (Tang et al., 2015). The axons of the commissural projecting cells in MEC apparently distribute mainly to layer III, thus contrasting to the small percentage of commissural calbindin-positive neurons in layer II, of which the axons preferentially distribute in layer I of the contralateral MEC (Fuchs et al., 2016). In addition, layer III also contains a population of non-spiny PCs, sending axons towards the angular bundle. Collaterals originate from the main axon close to the cell body and those traveling towards the superficial layers distribute over the own dendritic extent (Gloveli et al., 1997). The third principal neuron type in layer III is formed by multipolar neurons. These contribute to the hippocampal projections (Germroth et al., 1989). Layer III contains a variety of interneurons, exhibiting various morphologies, including multipolar, pyramidal and bipolar neurons. Chemical characterization of layer III interneurons in the MEC shows that they express several markers including somatostatin, calbindin, vasoactive intestinal peptide and substance-P (Köhler and Chan-Palay, 1983; Köhler et al., 1985; Gloveli et al., 1997; Wouterlood and Pothuizen, 2000; Wouterlood et al., 2000; Kumar and Buckmaster, 2006).

The microcircuits of layer III are only sparsely known, but seem to be markedly different from those seen in layer II, showing a much stronger monosynaptic principal to principal neuron connectivity (van der Linden and Lopes da Silva, 1998; Dhillon and Jones, 2000; Kloosterman et al., 2003; Tang et al., 2015). Neurons in layer III are the main recipients of the local deep-to-superficial projections, which apparently predominantly originate from neurons in layer Vb (see below; Kloosterman et al., 2003; van Haften et al., 2003). Currently, no correlations have been reported between morphology, connectional profile and electrophysiological *in vitro* and *in vivo* properties (Canto and Witter, 2012a,b; Tang et al., 2015).

Layer V

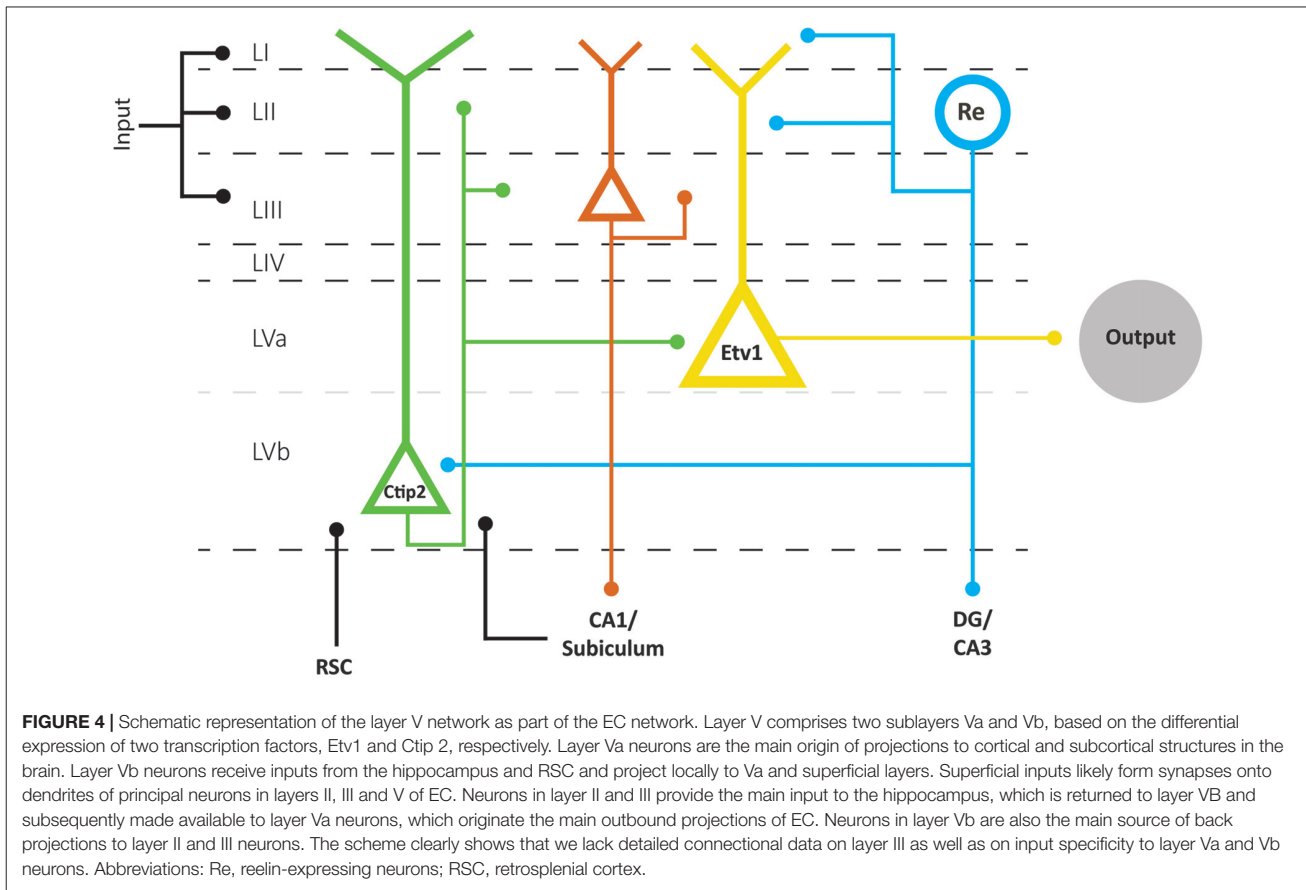
As described above, layer V is commonly subdivided into a layer Va and Vb. The superficial layer Va, adjacent to layer IV (lamina dissecans), comprises mainly large pyramidal

neurons that are unequally distributed along the extent of both MEC and LEC. Cells in layer Vb appear smaller, more uniform in soma size and are more densely packed than their counterparts in layer Va (Canto and Witter, 2012a,b; Boccara et al., 2015).

In mice, the expression pattern of the transcription factors *Etv1* and *Ctip2* provide for the differentiation between two molecularly distinct sublayers Va and Vb, respectively. This organization prevails across the whole mediolateral and dorsoventral extent of EC (Ramsden et al., 2015; Surmeli et al., 2015; Onodera et al., 2016). In both MEC and LEC, layer Va cells are the major output neurons projecting to diverse cortical and subcortical structures. Surprisingly, layer Vb cells are selectively targeted by the outputs from the hippocampus, originating in layer II of EC (**Figure 4**; Surmeli et al., 2015; Onodera et al., 2016). In MEC, these layer II inputs apparently arise specifically from reelin positive MEC II SCs and not from the calbindin positive MEC II PCs (Surmeli et al., 2015). The latter report of axon collaterals from layer II SCs in layer V in mice conflicts with previous reports in rats and monkeys, that layer II SCs issue a well-developed axonal plexus in layers I and II, but that collaterals in layer V are sparse (Tamamaki and Nojyo, 1993; Klink and Alonso, 1997; Buckmaster et al., 2004; Canto and Witter, 2012b). Whether this points to species differences or a lack of sensitivity in the older studies is not known. Irrespective of the details of this circuit, MEC layer Vb neurons could be ideally suited to integrate inputs from superficial MEC and hippocampus. Own preliminary data show these network features to be true in LEC as well, and show that layer Vb neurons in both LEC and MEC innervate layer Va as well as layers II and III (Onodera et al., 2016), which is in line with sparse data indicating that neurons in layer Vb issue superficially directed axon collaterals (Hamam et al., 2000, 2002; Canto and Witter, 2012a,b). This indicates that at least a subpopulation of layer Vb neurons form a major component of the intrinsic deep to superficial circuit.

Layer V is also innervated by additional cortical projections from frontal and cingular domains (see above). Whereas information about the postsynaptic targets of these cortical inputs is sparse, projections from the retrosplenial cortex (RSC) to MEC layer V target, among others, spiny pyramidal neurons that issue axons to superficial layers (Czajkowski et al., 2013). If the assertion is correct that in particular layer Vb neurons are the main elements mediating this deep to superficial connection, it is logical to conclude that retrosplenial inputs terminate onto a subpopulation of Vb neurons (**Figure 4**). These data are thus in line with own preliminary observations that neurons in layer V receive convergent inputs from subiculum and RSC (Simonsen et al., 2012).

Layer Vb of both MEC and LEC also contains multipolar neurons (Hamam et al., 2000; Canto and Witter, 2012b) and a population of GABA-negative/calretinin positive neurons (Miettinen et al., 1997) providing additional markers for principal cell types in the layer V network. Electrophysiologically, PCs in layer V show regular spiking, strongly adapting



physiological profiles, whereas multipolar neurons respond to a depolarization with delayed firing and slow little adaptation (Egorov et al., 2002b). It is currently not known if any of these layer V cell types correlate with the electrophysiologically defined persistent firing neurons, which can be found in EC when muscarinic acetylcholine receptors are activated (Egorov et al., 2002a). Finally, we currently lack a detailed comparison of the organization of layer V in LEC and MEC. For example, what would be the functional implication that MEC layer Va hosts pyramidal neurons with extensive basal dendritic trees restricted to the somatic layer, whereas such a neuron type has not been reported in LEC (Hamam et al., 2000, 2002; Canto and Witter, 2012a,b; Surmeli et al., 2015).

CONCLUDING REMARKS

The comparison of main trends in extrinsic and intrinsic connectivity patterns of MEC and LEC suggests that the different phenotypes of both EC subdivisions likely depend on the combinatorial effects of small differences in intrinsic organization and substantial differences in extrinsic inputs. Although this conclusion and the following details are mainly based on studies in rodents, the more sparse data in non-human and human primates seem to support a comparable organization.

To understand the functional relevance of the subtle intrinsic differences, more data are needed, for which we likely will depend on the emergence of even more specific genetic tools to identify and manipulate the activity of single classes of neurons. Eventually, detailed imaging studies in humans are expected to contribute to an increased understanding of the functional diversification within EC. The extrinsic input differences as summarized above are still in overall support with the notion that two functionally different input streams to the hippocampus are mediated by two entorhinal domains. MEC provides connective routes with extensive posterior parts of the cortex, including posterior parahippocampal, retrosplenial, parietal and occipital networks, allowing the representation of intrinsically generated signals about perceived and/or planned movements in stable contexts. In contrast, LEC mediates routes to and from the hippocampus with more anterior parahippocampal, sensory and pre- and orbitofrontal domains, providing access to evaluated information about the ever-changing external world. From a functional anatomical perspective, the above provides a suitable framework to keep adding the details needed to mechanistically understand the role(s) of EC. The connective scheme as presented here (Figure 4) assumes that the functionally different parts of EC share the network structure to mediate cortical-hippocampal interactions in a comparable matter. Neurons in layers II and III provide various combinations of information

to the hippocampal circuit, and a copy of that input is made available to neurons in layer V. The latter step might either be monosynaptic through inputs targeting the extensive apical tufts of some of the layer V pyramidal neurons or disynaptic through intrinsic projections from layer II (and layer III) to layer Vb. In view of the strict topology of the reciprocal connectivity between EC and CA1/subiculum, it is likely that at least some of these layer Vb neurons receive a hippocampally processed copy of that original input information. Layer Vb neurons are in a position to integrate those inputs with additional sets of information, and to send the resulting representations back to layers II and III. In case of layer Va neurons, which apparently are the origin of the main output pathway of EC, the hippocampally processed copy might be disynaptic, mediated through Vb neurons, and it is currently not known whether other inputs integrate at the level of these Va neurons. In view of their apical dendrites reaching the superficial layers of EC, it is likely that they, like layer Vb neurons, do receive superficially terminating inputs.

If correct, the connectional data strongly argue that differences in cortical inputs form a main feature underlying the phenotypic differences between LEC and MEC. However, we have not yet included the potential differences between LEC and MEC in local inhibitory architecture, as suggested by the yet sparse data on layer II. One additional feature of the proposed scheme needs to be discussed. The overarching strict reciprocal topology of the entorhinal-CA1-subicular network predicts that inbound information will be reciprocated with outbound information. It is exactly this last prediction, which is not supported by data. Admittedly, the available data are sparse, but the data obtained in the few studies in which this input-output dogma was addressed point to another direction. In one study in the cat, EEG recordings in freely behaving animals indicated a functional separation between LEC and MEC, where LEC is coupled to the olfactory domain, whereas MEC is coupled to the hippocampus (Boeijinga and Lopes da Silva, 1988). In more elaborate studies using the isolated guinea pig *ex vivo* brain preparation, olfactory stimulation resulted in a

sequential activation in LEC, hippocampus and MEC, followed by LEC (Biella and de Curtis, 2000). These sparse data seem to indicate that hippocampal output, resulting from olfactory input, is preferentially distributed back to MEC, not to LEC. To our knowledge, this output pathway specificity has not been explored and thus presents us with a, yet underexplored, challenge, which might very well be open to imaging studies in the human.

AUTHOR CONTRIBUTIONS

All authors contributed to the discussions that formed the foundation of the manuscript and contributed to the writing of the manuscript and to figures. All figures with exception of 1A were made by BJ. MPW supervised the process and wrote the final version of the manuscript. All authors approved this final version.

FUNDING

This work has been supported by the Kavli Foundation, the Centre of Excellence scheme—Centre for Neural Computation and research grant # 191929 and 227769 of the Research Council of Norway, The Egil and Pauline Braathen and Fred Kavli Centre for Cortical Microcircuits, and the National Infrastructure scheme of the Research Council of Norway—NORBRAIN. This work has also been supported by Grants-in-Aid for Scientific Research on Innovative Areas (#26119502), and by Grant-in-Aid for Scientific Research (KAKENHI) #15K18358 from the Ministry of Education, Culture, Sports, Science and Technology (MEXT) of Japan.

ACKNOWLEDGMENTS

We thank Michele Gianatti for providing us with the images for **Figure 1A** and Bruno Monterotti for help with the histological preparations for **Figure 2**.

REFERENCES

- Amaral, D. G., Insausti, R., and Cowan, W. M. (1984). The commissural connections of the monkey hippocampal formation. *J. Comp. Neurol.* 224, 307–336. doi: 10.1002/cne.902240302
- Amaral, D. G., Insausti, R., and Cowan, W. M. (1987). The entorhinal cortex of the monkey: I. Cytoarchitectonic organization. *J. Comp. Neurol.* 264, 326–355. doi: 10.1002/cne.902640305
- Armstrong, C., Wang, J., Yeun Lee, S., Broderick, J., Bezaire, M. J., Lee, S. H., et al. (2016). Target-selectivity of parvalbumin-positive interneurons in layer II of medial entorhinal cortex in normal and epileptic animals. *Hippocampus* 26, 779–793. doi: 10.1002/hipo.22559
- Biella, G., and de Curtis, M. (2000). Olfactory inputs activate the medial entorhinal cortex via the hippocampus. *J. Neurophysiol.* 83, 1924–1931.
- Bjaalie, J. G. (2002). Opinion: localization in the brain: new solutions emerging. *Nat. Rev. Neurosci.* 3, 322–325. doi: 10.1038/nrn790
- Boccarda, C. N., Kjonigsen, L. J., Hammer, I. M., Bjaalie, J. G., Leergaard, T. B., and Witter, M. P. (2015). A three-plane architectonic atlas of the rat hippocampal region. *Hippocampus* 25, 838–857. doi: 10.1002/hipo.22407
- Boeijinga, P. H., and Lopes da Silva, F. H. (1988). Differential distribution of β and θ EEG activity in the entorhinal cortex of the cat. *Brain Res.* 448, 272–286. doi: 10.1016/0006-8993(88)91264-4
- Bonnevie, T., Dunn, B., Fyhn, M., Hafting, T., Derdikman, D., Kubic, J. L., et al. (2013). Grid cells require excitatory drive from the hippocampus. *Nat. Neurosci.* 16, 309–317. doi: 10.1038/nn.3311
- Braak, H., and Braak, E. (1985). On areas of transition between entorhinal allocortex and temporal isocortex in the human brain. Normal morphology and lamina-specific pathology in Alzheimer's disease. *Acta Neuropathol.* 68, 325–332. doi: 10.1007/bf00690836
- Braak, H., and Braak, E. (1992). The human entorhinal cortex: normal morphology and lamina-specific pathology in various diseases. *Neurosci. Res.* 15, 6–31. doi: 10.1016/0168-0102(92)90014-4
- Brodman, K. (1909). *Vergleichende Lokalisationslehre der Grosshirnrinde in ihren Prinzipien dargestellt auf Grund des Zellenbaues*. Hirzel, Leipzig: Barth.
- Buckmaster, P. S., Alonso, A., Canfield, D. R., and Amaral, D. G. (2004). Dendritic morphology, local circuitry and intrinsic electrophysiology of principal neurons in the entorhinal cortex of macaque monkeys. *J. Comp. Neurol.* 470, 317–329. doi: 10.1002/cne.20014

- Buetfering, C., Allen, K., and Monyer, H. (2014). Parvalbumin interneurons provide grid cell-driven recurrent inhibition in the medial entorhinal cortex. *Nat. Neurosci.* 17, 710–718. doi: 10.1038/nn.3696
- Burak, Y., and Fiete, I. R. (2009). Accurate path integration in continuous attractor network models of grid cells. *PLoS Comput. Biol.* 5:e1000291. doi: 10.1371/journal.pcbi.1000291
- Caballero-Bleda, M., and Witter, M. P. (1993). Regional and laminar organization of projections from the presubiculum and parasubiculum to the entorhinal cortex: an anterograde tracing study in the rat. *J. Comp. Neurol.* 328, 115–129. doi: 10.1002/cne.903280109
- Canto, C. B., Koganezawa, N., Beed, P., Moser, E. I., and Witter, M. P. (2012). All layers of medial entorhinal cortex receive presubicular and parasubicular inputs. *J. Neurosci.* 32, 17620–17631. doi: 10.1523/JNEUROSCI.3526-12.2012
- Canto, C. B., and Witter, M. P. (2012a). Cellular properties of principal neurons in the rat entorhinal cortex. I. The lateral entorhinal cortex. *Hippocampus* 22, 1256–1276. doi: 10.1002/hipo.20997
- Canto, C. B., and Witter, M. P. (2012b). Cellular properties of principal neurons in the rat entorhinal cortex. II. The medial entorhinal cortex. *Hippocampus* 22, 1277–1299. doi: 10.1002/hipo.20993
- Canto, C. B., Wouterlood, F. G., and Witter, M. P. (2008). What does the anatomical organization of the entorhinal cortex tell us? *Neural Plast.* 2008:381243. doi: 10.1155/2008/381243
- Cappaert, N. L. M., Van Strien, N. M., and Witter, M. P. (2014). “Hippocampal formation,” in *The Rat Nervous System* 4th Edn., ed. G. Paxinos (San Diego, CA: Academic Press), 511–574.
- Couey, J. J., Witoelar, A., Zhang, S. J., Zheng, K., Ye, J., Dunn, B., et al. (2013). Recurrent inhibitory circuitry as a mechanism for grid formation. *Nat. Neurosci.* 16, 318–324. doi: 10.1038/nn.3310
- Czajkowski, R., Sugar, J., Zhang, S. J., Couey, J. J., Ye, J., and Witter, M. P. (2013). Superficially projecting principal neurons in layer V of medial entorhinal cortex in the rat receive excitatory retrosplenial input. *J. Neurosci.* 33, 15779–15792. doi: 10.1523/JNEUROSCI.2646-13.2013
- Deshmukh, S. S., and Knierim, J. J. (2011). Representation of non-spatial and spatial information in the lateral entorhinal cortex. *Front. Behav. Neurosci.* 5:69. doi: 10.3389/fnbeh.2011.00069
- Dhillon, A., and Jones, R. S. (2000). Laminar differences in recurrent excitatory transmission in the rat entorhinal cortex *in vitro*. *Neuroscience* 99, 413–422. doi: 10.1016/s0306-4522(00)00225-6
- Domnisoru, C., Kinkhabwala, A. A., and Tank, D. W. (2013). Membrane potential dynamics of grid cells. *Nature* 495, 199–204. doi: 10.1038/nature11973
- Egorov, A. V., Hamam, B. N., Fransén, E., Hasselmo, M. E., and Alonso, A. A. (2002a). Graded persistent activity in entorhinal cortex neurons. *Nature* 420, 173–178. doi: 10.1038/nature01171
- Egorov, A. V., Heinemann, U., and Müller, W. (2002b). Differential excitability and voltage-dependent Ca²⁺ signalling in two types of medial entorhinal cortex layer V neurons. *Eur. J. Neurosci.* 16, 1305–1312. doi: 10.1046/j.1460-9568.2002.02197.x
- Eichenbaum, H., Sauvage, M., Fortin, N., Komorowski, R., and Lipton, P. (2012). Towards a functional organization of episodic memory in the medial temporal lobe. *Neurosci. Biobehav. Rev.* 36, 1597–1608. doi: 10.1016/j.neubiorev.2011.07.006
- Fuchs, E. C., Neitz, A., Pinna, R., Melzer, S., Caputi, A., and Monyer, H. (2016). Local and distant input controlling excitation in layer II of the medial entorhinal cortex. *Neuron* 89, 194–208. doi: 10.1016/j.neuron.2015.11.029
- Fuhs, M. C., and Touretzky, D. S. (2006). A spin glass model of path integration in rat medial entorhinal cortex. *J. Neurosci.* 26, 4266–4276. doi: 10.1523/JNEUROSCI.4353-05.2006
- Fujimaru, Y., and Kosaka, T. (1996). The distribution of two calcium binding proteins, calbindin D-28K and parvalbumin, in the entorhinal cortex of the adult mouse. *Neurosci. Res.* 24, 329–343. doi: 10.1016/0168-0102(95)01008-4
- Fyhn, M., Molden, S., Witter, M. P., Moser, E. I., and Moser, M. B. (2004). Spatial representation in the entorhinal cortex. *Science* 305, 1258–1264. doi: 10.1126/science.1099901
- Germroth, P., Schwerdtfeger, W. K., and Buhl, E. H. (1989). Morphology of identified entorhinal neurons projecting to the hippocampus. A light microscopical study combining retrograde tracing and intracellular injection. *Neuroscience* 30, 683–691. doi: 10.1016/0306-4522(89)90161-9
- Gloveli, T., Schmitz, D., Empson, R. M., Dugladze, T., and Heinemann, U. (1997). Morphological and electrophysiological characterization of layer III cells of the medial entorhinal cortex of the rat. *Neuroscience* 77, 629–648. doi: 10.1016/s0306-4522(96)00494-0
- Haberly, L. B., and Price, J. L. (1978). Association and commissural fiber systems of the olfactory cortex of the rat. *J. Comp. Neurol.* 181, 781–807. doi: 10.1002/cne.901810407
- Hafting, T., Fyhn, M., Molden, S., Moser, M.-B., and Moser, E. I. (2005). Microstructure of a spatial map in the entorhinal cortex. *Nature* 436, 801–806. doi: 10.1038/nature03721
- Hamam, B. N., Amaral, D. G., and Alonso, A. A. (2002). Morphological and electrophysiological characteristics of layer V neurons of the rat lateral entorhinal cortex. *J. Comp. Neurol.* 451, 45–61. doi: 10.1002/cne.10335
- Hamam, B. N., Kennedy, T. E., Alonso, A., and Amaral, D. G. (2000). Morphological and electrophysiological characteristics of layer V neurons of the rat medial entorhinal cortex. *J. Comp. Neurol.* 418, 457–472. doi: 10.1002/(SICI)1096-9861(20000320)418:4<457::AID-CNE7>3.0.CO;2-L
- Hoover, W. B., and Vertes, R. P. (2007). Anatomical analysis of afferent projections to the medial prefrontal cortex in the rat. *Brain Struct. Funct.* 212, 149–179. doi: 10.1007/s00429-007-0150-4
- Hoover, W. B., and Vertes, R. P. (2011). Projections of the medial orbital and ventral orbital cortex in the rat. *J. Comp. Neurol.* 519, 3766–3801. doi: 10.1002/cne.22733
- Hu, H., Gan, J., and Jonas, P. (2014). Interneurons. Fast-spiking, parvalbumin⁺ GABAergic interneurons: from cellular design to microcircuit function. *Science* 345:1255263. doi: 10.1126/science.1255263
- Insausti, R., Amaral, D. G., and Paxinos, G. (2004). “Hippocampal formation,” in *The Human Nervous System*, ed. G. Paxinos (San Diego, CA: Elsevier Academic Press), 871–914.
- Insausti, R., Herrero, M. T., and Witter, M. P. (1997). Entorhinal cortex of the rat: cytoarchitectonic subdivisions and the origin and distribution of cortical efferents. *Hippocampus* 7, 146–183. doi: 10.1002/(SICI)1098-1063(1997)7:2<146::AID-HIPO4>3.0.CO;2-L
- Jones, R. S., and Bühl, E. H. (1993). Basket-like interneurons in layer II of the entorhinal cortex exhibit a powerful NMDA-mediated synaptic excitation. *Neurosci. Lett.* 149, 35–39. doi: 10.1016/0304-3940(93)90341-h
- Jones, B. F., and Witter, M. P. (2007). Cingulate cortex projections to the parahippocampal region and hippocampal formation in the rat. *Hippocampus* 17, 957–976. doi: 10.1002/hipo.20330
- Kerr, K. M., Agster, K. L., Furtak, S. C., and Burwell, R. D. (2007). Functional neuroanatomy of the parahippocampal region: the lateral and medial entorhinal areas. *Hippocampus* 17, 697–708. doi: 10.1002/hipo.20315
- Kitamura, T., Pignatelli, M., Suh, J., Kohara, K., Yoshiki, A., Abe, K., et al. (2014). Island cells control temporal association memory. *Science* 343, 896–901. doi: 10.1126/science.1244634
- Kjønigsen, L. J., Leergaard, T. B., Witter, M. P., and Bjaalie, J. G. (2011). Digital atlas of anatomical subdivisions and boundaries of the rat hippocampal region. *Front. Neuroinform.* 5:2. doi: 10.3389/fninf.2011.00002
- Kjønigsen, L. J., Lillehaug, S., Bjaalie, J. G., Witter, M. P., and Leergaard, T. B. (2015). Waxholm Space atlas of the rat brain hippocampal region: three-dimensional delineations based on magnetic resonance and diffusion tensor imaging. *Neuroimage* 108, 441–449. doi: 10.1016/j.neuroimage.2014.12.080
- Klinger, J. (1948). *Die makroskopische Anatomie der Ammons-formation. Denkschriften der Schweizerischen Naturforschenden Gesellschaft.* Zurich: Gebrueder Fretz.
- Klink, R., and Alonso, A. (1997). Morphological characteristics of layer II projection neurons in the rat medial entorhinal cortex. *Hippocampus* 7, 571–583. doi: 10.1002/(SICI)1098-1063(1997)7:5<571::AID-HIPO12>3.3.CO;2-W
- Kloosterman, F., Van Haeften, T., Witter, M. P., and Lopes da Silva, F. H. (2003). Electrophysiological characterization of interlaminar entorhinal connections: an essential link for re-entrance in the hippocampal-entorhinal system. *Eur. J. Neurosci.* 18, 3037–3052. doi: 10.1111/j.1460-9568.2003.03046.x
- Knierim, J. J., Neunuebel, J. P., and Deshmukh, S. S. (2013). Functional correlates of the lateral and medial entorhinal cortex: objects, path integration and local-global reference frames. *Philos. Trans. R. Soc. Lond. B Biol. Sci.* 369:20130369. doi: 10.1098/rstb.2013.0369

- Kobro-Flatmoen, A., Nagelhus, A., and Witter, M. P. (2016). Reelin-immunoreactive neurons in entorhinal cortex layer II selectively express intracellular amyloid in early Alzheimer's disease. *Neurobiol. Dis.* 93, 172–183. doi: 10.1016/j.nbd.2016.05.012
- Kobro-Flatmoen, A., and Witter, M. P. (2017). *Entorhinal Cell-Specific Changes as an Initial Cause of Alzheimer's Disease*. Trondheim: NTNU Norwegian University of Science and Technology.
- Koganezawa, N., Gisetstad, R., Husby, E., Doan, T. P., and Witter, M. P. (2015). Excitatory postthral projections to principal cells in the medial entorhinal cortex. *J. Neurosci.* 35, 15860–15874. doi: 10.1523/JNEUROSCI.0653-15.2015
- Köhler, C. (1984). Morphological details of the projection from the presubiculum to the entorhinal area as shown with the novel PHA-L immunohistochemical tracing method in the rat. *Neurosci. Lett.* 45, 285–290. doi: 10.1016/0304-3940(84)90240-4
- Köhler, C., and Chan-Palay, V. (1983). Somatostatin and vasoactive intestinal polypeptide-like immunoreactive cells and terminals in the retrohippocampal region of the rat brain. *Anat. Embryol.* 167, 151–172. doi: 10.1007/bf00298508
- Köhler, C., Wu, J. Y., and Chan-Palay, V. (1985). Neurons and terminals in the retrohippocampal region in the rat's brain identified by anti- γ -aminobutyric acid and anti-glutamic acid decarboxylase immunocytochemistry. *Anat. Embryol.* 173, 35–44. doi: 10.1007/bf00707302
- Kondo, H., and Witter, M. P. (2014). Topographic organization of orbitofrontal projections to the parahippocampal region in rats. *J. Comp. Neurol.* 522, 772–793. doi: 10.1002/cne.23442
- Kosel, K. C., Van Hoesen, G. W., and Rosene, D. L. (1982). Non-hippocampal cortical projections from the entorhinal cortex in the rat and rhesus monkey. *Brain Res.* 244, 201–213. doi: 10.1016/0006-8993(82)90079-8
- Kosel, K. C., Van Hoesen, G. W., and West, J. R. (1981). Olfactory bulb projections to the parahippocampal area of the rat. *J. Comp. Neurol.* 198, 467–482. doi: 10.1002/cne.901980307
- Kumar, S. S., and Buckmaster, P. S. (2006). Hyperexcitability, interneurons, and loss of GABAergic synapses in entorhinal cortex in a model of temporal lobe epilepsy. *J. Neurosci.* 26, 4613–4623. doi: 10.1523/JNEUROSCI.0064-06.2006
- Lee, S., Hjerling-Leffler, J., Zagha, E., Fishell, G., and Rudy, B. (2010). The largest group of superficial neocortical GABAergic interneurons expresses ionotropic serotonin receptors. *J. Neurosci.* 30, 16796–16808. doi: 10.1523/JNEUROSCI.1869-10.2010
- Leitner, F. C., Melzer, S., Lütcke, H., Pinna, R., Seeburg, P. H., Helmchen, F., et al. (2016). Spatially segregated feedforward and feedback neurons support differential odor processing in the lateral entorhinal cortex. *Nat. Neurosci.* 19, 935–944. doi: 10.1038/nn.4303
- Lorente de Nó, R. (1933). Studies on the structure of the cerebral cortex. *J. Psychol. Neurol.* 45, 381–438.
- Maass, A., Berron, D., Libby, L. A., Ranganath, C., and Duzel, E. (2015). Functional subregions of the human entorhinal cortex. *Elife* 4:e06426. doi: 10.7554/eLife.06426
- Mathiasen, M. L., Hansen, L., and Witter, M. P. (2015). Insular projections to the parahippocampal region in the rat. *J. Comp. Neurol.* 523, 1379–1398. doi: 10.1002/cne.23742
- McNaughton, B. L., Battaglia, F. P., Jensen, O., Moser, E. I., and Moser, M. B. (2006). Path integration and the neural basis of the 'cognitive map'. *Nat. Rev. Neurosci.* 7, 663–678. doi: 10.1038/nrn1932
- Miettinen, M., Koivisto, E., Riekkinen, P., and Miettinen, R. (1996). Coexistence of parvalbumin and GABA in nonpyramidal neurons of the rat entorhinal cortex. *Brain Res.* 706, 113–122. doi: 10.1016/0006-8993(95)01203-6
- Miettinen, M., Pitkanen, A., and Miettinen, R. (1997). Distribution of calretinin-immunoreactivity in the rat entorhinal cortex: coexistence with GABA. *J. Comp. Neurol.* 378, 363–378. doi: 10.1002/(SICI)1096-9861(19970217)378:3<363::AID-CNE5>3.3.CO;2-X
- Moser, E. I., Roudi, Y., Witter, M. P., Kentros, C., Bonhoeffer, T., and Moser, M. B. (2014). Grid cells and cortical representation. *Nat. Rev. Neurosci.* 15, 466–481. doi: 10.1038/nrn3766
- Naber, P. A., Caballero-Bleda, M., Jorritsma-Byham, B., and Witter, M. P. (1997). Parallel input to the hippocampal memory system through peri- and postthral cortices. *Neuroreport* 8, 2617–2621. doi: 10.1097/00001756-199707280-00039
- Naber, P. A., Lopes da Silva, F. H., and Witter, M. P. (2001). Reciprocal connections between the entorhinal cortex and hippocampal fields CA1 and the subiculum are in register with the projections from CA1 to the subiculum. *Hippocampus* 11, 99–104. doi: 10.1002/hipo.1028
- Naber, P. A., Witter, M. P., and Lopez da Silva, F. H. (1999). Perirhinal cortex input to the hippocampus in the rat: evidence for parallel pathways, both direct and indirect. A combined physiological and anatomical study. *Eur. J. Neurosci.* 11, 4119–4133. doi: 10.1046/j.1460-9568.1999.00835.x
- Naumann, R. K., Ray, S., Prokop, S., Las, L., Heppner, F. L., and Brecht, M. (2016). Conserved size and periodicity of pyramidal patches in layer 2 of medial/caudal entorhinal cortex. *J. Comp. Neurol.* 524, 783–806. doi: 10.1002/cne.23865
- Navarro Schröder, T., Haak, K. V., Zaragoza Jimenez, N. I., Beckmann, C. F., and Doeller, C. F. (2015). Functional topography of the human entorhinal cortex. *Elife* 4:e06738. doi: 10.7554/eLife.06738
- Nilssen, E. S., Fjeld, G., and Witter, M. P. (2015). Local connectivity and immunoreactivity of principal cells in layer II of lateral entorhinal cortex. *Nordic. Neurosci. Abstr.* 1:61.
- Ohara, S., Itou, K., Shiraishi, M., Gianatti, M., Sota, Y., Kabashima, S., et al. (2016). Efferent projections of the calbindin-positive entorhinal neurons in the rat: connectational differences between the medial and lateral entorhinal cortex. *SFN. Abstr.* 84.13.
- Olsen, G. M., Ohara, S., Iijima, T., and Witter, M. P. (2017). Parahippocampal and retrosplenial connections of rat posterior parietal cortex. *Hippocampus* 27, 335–358. doi: 10.1002/hipo.22701
- Onodera, M., Ohara, S., Tsutsui, K.-I., Witter, M. P., and Iijima, T. (2016). Connectational differences between the layer Va and Vb neurons in the lateral entorhinal cortex of the rat. *JNS. Abstr LBA3-023*.
- Pastoll, H., Solanka, L., van Rossum, M. C., and Nolan, M. F. (2013). Feedback inhibition enables θ -nested γ oscillations and grid firing fields. *Neuron* 77, 141–154. doi: 10.1016/j.neuron.2012.11.032
- Pinto, A., Fuentes, C., and Pare, D. (2006). Feedforward inhibition regulates perirhinal transmission of neocortical inputs to the entorhinal cortex: ultrastructural study in guinea pigs. *J. Comp. Neurol.* 495, 722–734. doi: 10.1002/cne.20905
- Pitkanen, A., and Amaral, D. G. (1993). Distribution of parvalbumin-immunoreactive cells and fibers in the monkey temporal lobe: the hippocampal formation. *J. Comp. Neurol.* 331, 37–74. doi: 10.1002/cne.903310104
- Ramón Y Cajal, S. (1902). Sobre un ganglio especial de la corteza eseno-occipital. *Trab. del Lab. de Invest. Biol. Univ. Madrid* 1, 189–206.
- Ramón Y Cajal, S. (1911). *Histologie du Systeme Nerveux de l'Homme et des Vertebres*. Paris: Maloine.
- Ramos-Moreno, T., Galazo, M. J., Porrero, C., Martínez-Cerdeño, V., and Clascá, F. (2006). Extracellular matrix molecules and synaptic plasticity: immunomapping of intracellular and secreted Reelin in the adult rat brain. *Eur. J. Neurosci.* 23, 401–422. doi: 10.1111/j.1460-9568.2005.04567.x
- Ramsden, H. L., Surmeli, G., McDonagh, S. G., and Nolan, M. F. (2015). Laminar and dorsoventral molecular organization of the medial entorhinal cortex revealed by large-scale anatomical analysis of gene expression. *PLoS Comput. Biol.* 11:e1004032. doi: 10.1371/journal.pcbi.1004032
- Ranganath, C., and Ritchey, M. (2012). Two cortical systems for memory-guided behaviour. *Nat. Rev. Neurosci.* 13, 713–726. doi: 10.1038/nrn3338
- Ray, S., Naumann, R., Burgalossi, A., Tang, Q., Schmidt, H., and Brecht, M. (2014). Grid-layout and θ -modulation of layer 2 pyramidal neurons in medial entorhinal cortex. *Science* 343, 891–896. doi: 10.1126/science.1243028
- Retzius, G. (1896). *Das Menschengehirn. Studien in der Makroskopischen Morphologie*. Stockholm: Norstedt and Sohne.
- Room, P., and Groenewegen, H. J. (1986). Connections of the parahippocampal cortex. *J. Comp. Neurol.* 251, 415–450. doi: 10.1002/cne.902510402
- Rosene, D. L., and Van Hoesen, G. W. (1977). Hippocampal efferents reach widespread areas of cerebral cortex and amygdala in the rhesus monkey. *Science* 198, 315–317. doi: 10.1126/science.410102
- Rosene, D. L., and Van Hoesen, G. W. (1987). "The hippocampal formation of the primate brain: a review of some comparative aspects of cytoarchitecture and connections," in *Cerebral Cortex: Volume 6. Further Aspects of Cortical Function, Including Hippocampus*, eds E. G. Jones and A. Peters (New York, NY: Plenum Press), 345–457.
- Rudy, B., Fishell, G., Lee, S., and Hjerling-Leffler, J. (2011). Three groups of interneurons account for nearly 100% of neocortical GABAergic neurons. *Dev. Neurobiol.* 71, 45–61. doi: 10.1002/dneu.20853

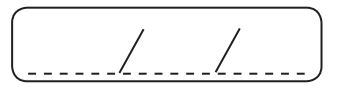
- Sargolini, F., Fyhn, M., Hafting, T., McNaughton, B. L., Witter, M. P., Moser, M.-B., et al. (2006). Conjunctive representation of position, direction, and velocity in entorhinal cortex. *Science* 312, 758–762. doi: 10.1126/science.1125572
- Saunders, R. C., and Rosene, D. L. (1988). A comparison of the efferents of the amygdala and the hippocampal formation in the rhesus monkey: I. Convergence in the entorhinal, prorhinal and perirhinal cortices. *J. Comp. Neurol.* 271, 153–184. doi: 10.1002/cne.902710202
- Schmidt-Hieber, C., and Häusser, M. (2013). Cellular mechanisms of spatial navigation in the medial entorhinal cortex. *Nat. Neurosci.* 16, 325–331. doi: 10.1038/nn.3340
- Shiple, M. T. (1975). The topographical and laminar organization of the presubiculum's projection to the ipsi- and contralateral entorhinal cortex in the guinea pig. *J. Comp. Neurol.* 160, 127–145. doi: 10.1002/cne.901600108
- Simonsen, Ø. W., Czajkowski, R., and Witter, M. P. (2012). Retrosplenial and subicular efferents converge on superficially projecting principal neurons of deep medial entorhinal cortex. *FENS Abstr.* 1412.
- Solodkin, A., and Vanhoesen, G. W. (1996). Entorhinal cortex modules of the human brain. *J. Comp. Neurol.* 365, 610–627. doi: 10.1002/(SICI)1096-9861(19960219)365:4<610::AID-CNE8>3.0.CO;2-7
- Soriano, E., Martinez, A., Farinas, I., and Frotscher, M. (1993). Chandelier cells in the hippocampal formation of the rat: the entorhinal area and subicular complex. *J. Comp. Neurol.* 337, 151–167. doi: 10.1002/cne.903370110
- Steward, O. (1976). Topographic organization of the projections from the entorhinal area to the hippocampal formation of the rat. *J. Comp. Neurol.* 167, 285–314. doi: 10.1002/cne.901670303
- Steward, O., and Scoville, S. A. (1976). Cells of origin of entorhinal cortical afferents to the hippocampus and fascia dentata of the rat. *J. Comp. Neurol.* 169, 347–370. doi: 10.1002/cne.901690306
- Strange, B. A., Witter, M. P., Lein, E. S., and Moser, E. I. (2014). Functional organization of the hippocampal longitudinal axis. *Nat. Rev. Neurosci.* 15, 655–669. doi: 10.1038/nrn3785
- Surmeli, G., Marcu, D. C., McClure, C., Garden, D. L., Pastoll, H., and Nolan, M. F. (2015). Molecularly defined circuitry reveals input-output segregation in deep layers of the medial entorhinal cortex. *Neuron* 88, 1040–1053. doi: 10.1016/j.neuron.2015.10.041
- Tahvildari, B., and Alonso, A. (2005). Morphological and electrophysiological properties of lateral entorhinal cortex layers II and III principal neurons. *J. Comp. Neurol.* 491, 123–140. doi: 10.1002/cne.20706
- Tamamaki, N., and Nojyo, Y. (1993). Projection of the entorhinal layer II neurons in the rat as revealed by intracellular pressure-injection of neurobiotin. *Hippocampus* 3, 471–480. doi: 10.1002/hipo.450030408
- Tanaka, D., Nakaya, Y., Yanagawa, Y., Obata, K., and Murakami, F. (2003). Multimodal tangential migration of neocortical GABAergic neurons independent of GPI-anchored proteins. *Development* 130, 5803–5813. doi: 10.1242/dev.00825
- Tang, Q., Burgalossi, A., Ebbesen, C. L., Ray, S., Naumann, R., Schmidt, H., et al. (2014). Pyramidal and stellate cell specificity of grid and border representations in layer 2 of medial entorhinal cortex. *Neuron* 84, 1191–1197. doi: 10.1016/j.neuron.2014.11.009
- Tang, Q., Ebbesen, C. L., Sanguinetti-Scheck, J. I., Preston-Ferrer, P., Gundlfinger, A., Winterer, J., et al. (2015). Anatomical organization and spatiotemporal firing patterns of layer 3 neurons in the rat medial entorhinal cortex. *J. Neurosci.* 35, 12346–12354. doi: 10.1523/jneurosci.0696-15.2015
- Tsao, A., Moser, M. B., and Moser, E. I. (2013). Traces of experience in the lateral entorhinal cortex. *Curr. Biol.* 23, 399–405. doi: 10.1016/j.cub.2013.01.036
- Tunon, T., Insausti, R., Ferrer, I., Sobreviela, T., and Soriano, E. (1992). Parvalbumin and calbindin D-28K in the human entorhinal cortex. An immunohistochemical study. *Brain Res.* 589, 24–32. doi: 10.1016/0006-8993(92)91157-a
- van der Linden, S., and Lopes da Silva, F. H. (1998). Comparison of the electrophysiology and morphology of layers III and II neurons of the rat medial entorhinal cortex *in vitro*. *Eur. J. Neurosci.* 10, 1479–1489. doi: 10.1046/j.1460-9568.1998.00162.x
- van Haften, T., Baks-Te Bulte, L. T., Goede, P. H., Wouterlood, F. G., and Witter, M. P. (2003). Morphological and numerical analysis of synaptic interactions between neurons in deep and superficial layers of the entorhinal cortex of the rat. *Hippocampus* 13, 943–952. doi: 10.1002/hipo.10144
- van Strien, N. M., Cappaert, N. L., and Witter, M. P. (2009). The anatomy of memory: an interactive overview of the parahippocampal-hippocampal network. *Nat. Rev. Neurosci.* 10, 272–282. doi: 10.1038/nrn2614
- Varga, C., Lee, S. Y., and Soltesz, I. (2010). Target-selective GABAergic control of entorhinal cortex output. *Nat. Neurosci.* 13, 822–824. doi: 10.1038/nn.2570
- Vertes, R. P. (2004). Differential projections of the infralimbic and prelimbic cortex in the rat. *Synapse* 51, 32–58. doi: 10.1002/syn.10279
- Witter, M. P. (2007). The perforant path: projections from the entorhinal cortex to the dentate gyrus. *Prog. Brain Res.* 163, 43–61. doi: 10.1016/s0079-6123(07)63003-9
- Witter, M. P., and Amaral, D. G. (1991). Entorhinal cortex of the monkey: V. Projections to the dentate gyrus, hippocampus and subicular complex. *J. Comp. Neurol.* 307, 437–459. doi: 10.1002/cne.903070308
- Witter, M. P., Groenewegen, H. J., Lopes da Silva, F. H., and Lohman, A. H. (1989a). Functional organization of the extrinsic and intrinsic circuitry of the parahippocampal region. *Prog. Neurobiol.* 33, 161–253. doi: 10.1016/0301-0082(89)90009-9
- Witter, M. P., Van Hoesen, G. W., and Amaral, D. G. (1989b). Topographical organization of the entorhinal projection to the dentate gyrus of the monkey. *J. Neurosci.* 9, 216–228.
- Witter, M. P., Kleven, H., and Kobro-Flatmoen, A. (in press). Comparative contemplations on the hippocampus. *Brain Behav. Evol.*
- Witter, M. P., Naber, P. A., van Haften, T., Machielsen, W. C., Rombouts, S. A., Barkhof, F., et al. (2000). Cortico-hippocampal communication by way of parallel parahippocampal-subicular pathways. *Hippocampus* 10, 398–410. doi: 10.1002/1098-1063(2000)10:4<398::AID-HIPO6>3.0.CO;2-K
- Wouterlood, F. G. (2002). “Spotlight on the neurons (I): cell types, local connectivity, microcircuits, and distribution of markers,” in *The Parahippocampal Region. Organization and Role in Cognitive Function*, eds M. P. Witter and F. G. Wouterlood (Oxford: Oxford University Press), 61–88.
- Wouterlood, F. G., Härtig, W., Bruckner, G., and Witter, M. P. (1995). Parvalbumin-immunoreactive neurons in the entorhinal cortex of the rat: localization, morphology, connectivity and ultrastructure. *J. Neurocytol.* 24, 135–153. doi: 10.1007/bf01181556
- Wouterlood, F. G., and Nederlof, J. (1983). Terminations of olfactory afferents on layer II and III neurons in the entorhinal area: degeneration-Golgi-electron microscopic study in the rat. *Neurosci. Lett.* 36, 105–110. doi: 10.1016/0304-3940(83)90250-1
- Wouterlood, F. G., and Pothuizen, H. (2000). Sparse colocalization of somatostatin- and GABA-immunoreactivity in the entorhinal cortex of the rat. *Hippocampus* 10, 77–86. doi: 10.1002/(SICI)1098-1063(2000)10:1<77::AID-HIPO8>3.0.CO;2-P
- Wouterlood, F. G., van Denderen, J. C., van Haften, T., and Witter, M. P. (2000). Calretinin in the entorhinal cortex of the rat: distribution, morphology, ultrastructure of neurons and co-localization with γ -aminobutyric acid and parvalbumin. *J. Comp. Neurol.* 425, 177–192. doi: 10.1002/1096-9861(20000918)425:2<177::aid-cne2>3.0.co;2-g
- Wyss, J. M., and Van Groen, T. (1992). Connections between the retrosplenial cortex and the hippocampal-formation in the rat: a review. *Hippocampus* 2, 1–12. doi: 10.1002/hipo.450020102
- Zilles, K., and Amunts, K. (2010). Centenary of Brodmann's map—conception and fate. *Nat. Rev. Neurosci.* 11, 139–145. doi: 10.1038/nrn2776

Conflict of Interest Statement: The authors declare that the research was conducted in the absence of any commercial or financial relationships that could be construed as a potential conflict of interest.

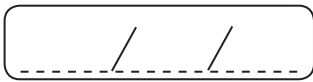
Copyright © 2017 Witter, Doan, Jacobsen, Nilssen and Ohara. This is an open-access article distributed under the terms of the Creative Commons Attribution License (CC BY). The use, distribution or reproduction in other forums is permitted, provided the original author(s) or licensor are credited and that the original publication in this journal is cited, in accordance with accepted academic practice. No use, distribution or reproduction is permitted which does not comply with these terms.



A series of horizontal lines for handwriting practice, consisting of 20 evenly spaced lines extending across the width of the page.



A series of horizontal lines for writing, consisting of 20 evenly spaced lines.



Original Paper

Brain, Behavior
and Evolution

Brain Behav Evol 2017;90:15–24
DOI: 10.1159/000475703

Published online: September 4, 2017

Comparative Contemplations on the Hippocampus

Menno P. Witter Heidi Kleven Asgeir Kobro Flatmoen

Kavli Institute for Systems Neuroscience, Center for Computational Neuroscience, Egil and Pauline Braathen and Fred Kavli Center for Cortical Microcircuits, NTNU Norwegian University of Science and Technology, Trondheim, Norway

Keywords

Hippocampal formation · Entorhinal cortex · Architecture · Neuronal networks · Comparative connectivity · Mammals · Reptiles · Birds

Abstract

The hippocampus in mammals is a morphologically well-defined structure, and so are its main subdivisions. To define the homologous structure in other vertebrate clades, using these morphological criteria has been difficult, if not impossible, since the typical mammalian morphology is absent. Although there seems to be consensus that the most medial part of the pallium represents the hippocampus in all vertebrates, there is no consensus on whether all mammalian hippocampal subdivisions are present in the derivatives of the medial pallium in all vertebrate groups. The aim of this paper is to explore the potential relevance of connections to define the hippocampus across vertebrates, with a focus on mammals, reptiles, and birds.

© 2017 S. Karger AG, Basel

aims for. In this paper, we intend to define some basic requirements that need to be met before the question as such becomes tangible. For example, in order to compare, we need to define what to compare, and at which level of biological classification. Regarding the first, we will start with a definition of what to consider as hippocampus in the context of this paper, its divisions, and the possible relevant circuitry levels. As will become clear, decisions about definitions as well as about the level of biological classification, species, family, and order are strongly dependent on the available data. We will, therefore, use a pragmatic approach, restricting ourselves to available data relevant to the narrative of this paper. In this paper, we also aim to complement an accompanying paper [Butler, 2017] by emphasizing connectivity patterns as a tool to propose potential homology in the hippocampus.

Definition of the Hippocampus and Its Subdivisions

The first mentioning of the hippocampus in the mammalian brain can likely be found in the work of a pupil of the 16th century anatomist Vesalius, named Arantius [Lewis, 1923]. The first part of the term refers to part of the formation in mammals resembling a horse's head and the second part refers to the caterpillar, or "silkworm" appearance of the tail (for further details, see Butler [2017]). One of the first detailed and comparative studies on the

Introduction

What can we learn from comparative studies of the hippocampus? An answer to this question is not straightforward since it depends, among others, on what one

KARGER

© 2017 S. Karger AG, Basel

E-Mail karger@karger.com
www.karger.com/bbe

Menno P. Witter
Kavli Institute for Systems Neuroscience
Faculty for Medical and Health Sciences, NTNU, Postboks 8905
NO-7491 Trondheim (Norway)
E-Mail menno.witter@ntnu.no

Downloaded by:
King's College London
172.16.1.12 - 6/15/2017 4:47:32 PM

structure and connectivity of the hippocampus is by Ramón y Cajal, published around the turn of the 19th century [Ramón y Cajal, 1893, 1911], followed by influential descriptions of the anatomy and connectivity of the main subdivisions of the hippocampus by his student Lorente de Nó [1933, 1934] and subsequent detailed studies from the 1960s and 1970s (for details, see Witter et al. [1989]). The typical hippocampus in mammals includes the dentate gyrus, the cornu ammonis (CA) fields CA1, CA2, and CA3, or hippocampus proper, and the subiculum. Although several authors have described an area CA4, we will not use this in the present paper and consider this part of area CA3. The hippocampus is a three-layered cortex, consisting of the molecular layer, directly deep to the pia, a cellular layer, and, deep to the latter, a polymorph layer. The superficial layer contains very few, mainly inhibitory neurons, and the polymorph layer has on average a larger number of neurons than the molecular layer. The neurons in the polymorph layer are either excitatory or inhibitory [van Strien et al., 2009].

Depending on the definition used, the entorhinal cortex (EC) is part of the hippocampus or part of the parahippocampal region. Here, we will take the perforant pathway, originating as the main cortical input from the EC to the hippocampus as belonging to the defining features of the main circuitry of the hippocampus (see also the next section). This is in line with the emphasis on the entorhinal-hippocampal connections, as mentioned by Ramón y Cajal [1902] already, based on his own work and referring to previously published data. In his seminal paper on the EC [Ramón y Cajal, 1902], he stated twice that the connections between the EC and the hippocampal formation are so conspicuous that they necessarily imply the functional solidarity of both centers. We will, however, not deal extensively with the comparative aspects of the EC in this paper (for more details, see Medina et al. [2017]).

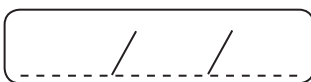
The hippocampus is a key component of an ensemble of brain structures that became known as the limbic system. The term limbic is derived from an anatomical description by Thomas Willis [1664], who referred to the brain area that surrounds the brain stem as the limbus. Subsequently, Broca referred to the cortical fringe of the hemisphere, including the subcallosal, cingulate, and parahippocampal gyri as well as the underlying hippocampal formation, as “le grand lobe limbique” [Broca, 1878]. Although this designation was purely anatomical, Broca suggested that these limbic structures might constitute a functional entity. Much later, Papez [1937] postulated the presence of a closed circuit that would play an

important role in the elaboration and the expression of emotions. This “Papez circuit” comprises a sequence of interconnected structures, i.e., the hippocampus projects by way of the fornix to the mammillary bodies which connect by way of the mammillothalamic tract to the anterior nuclei of the thalamus; from here, the cingulate cortex is reached, which through the ventral continuation of the cingulate bundle is connected with areas in the parahippocampal region, including the EC, projecting back into the hippocampus. In 1952, MacLean [1952] coined the term “limbic system” suggesting that these structures, including the amygdaloid complex, represented the “visceral brain.”

It was the seminal publication by Scoville and Milner [1957] that made the scientific community aware of the potentially important role of the hippocampus in episodic memory. In that paper, it was reported that bilateral removal of structures in the medial temporal lobe, including substantial parts of the hippocampus, the parahippocampal domain, and the amygdala, resulted in profound anterograde amnesia [Annese et al., 2014; Augustinack et al., 2014]. The implication of the hippocampus in memory processes boosted interest in its anatomical and functional organization. Major breakthrough findings, such as the discovery of long-term potentiation [Bliss and Lomo, 1973] as a potential synaptic mechanism for the formation and storage of memories, the discovery of place cells in the hippocampus [O’Keefe and Dostrovsky, 1971], and the subsequent influential theoretical description of the hippocampus as a cognitive map [O’Keefe and Nadel, 1978], strongly led the field into a focal research effort to unravel the mysteries of hippocampal circuits and functions. Interestingly, the idea of the hippocampus as part of a more elaborate network of limbic structures has started to make its comeback in recent years [Aggleton, 2014; Aggleton and Christiansen, 2015].

Standard Connectivity of the Hippocampus

The connectivity of the hippocampus known in that groundbreaking era was guided by two well-established conventions. First, the main fiber connection of the hippocampus was formed by the fornix, providing the output and input pathway of the hippocampus with subcortical structures like the septal complex and the mammillary bodies. Second, the EC provided the point of entry of cortical inputs to the hippocampus. This projection was initially referred to as the direct perforating speno- or temporo-ammonic pathway by Ramón y Cajal [1893,



1902, 1911] as one of a tripartite connection system, collectively referred to as the temporo-ammonic pathway (for more details, see Stephan [1975]). The designation “direct perforating” referred to the massive entorhinal fiber bundles perforating the subiculum on their direct course into the hippocampus. This pathway became later known as the perforant pathway [Lorente de N6, 1934]. An additional temporo-alvear tract was described as well, with fibers travelling from the EC through the alveus of the hippocampus into the CA fields. The third component, referred to as the angular pathway, carries mainly but not exclusively commissural fibers. As indicated by the name, in this early description, emphasis was on the projections to the CA fields, although projections to the dentate gyrus were included as part of the direct perforating temporo-ammonic/perforant pathway. In a detailed anterograde tracing description of the entorhinal-hippocampal connectivity in the rat in the mid-1970s [Steward, 1976], the projections to the dentate received more emphasis. The latter author referred to this projection as the temporo-dentate pathway, contrasting it with the temporo-ammonic pathway reaching the CA fields and the subiculum. Together with the knowledge about intrinsic hippocampal pathways, this led to the attractive concept of the so-called trisynaptic pathway as the blueprint circuit characterizing the hippocampus [Andersen et al., 1969; but see Amaral and Witter, 1989]. Over years, this also resulted in confusing changes in nomenclature such that the temporo-dentate pathway became erroneously referred to as the perforant pathway by many authors, since it perforated the hippocampal fissure on its way to the dentate gyrus, and the usage of temporo-ammonic pathway became restricted to the entorhinal projections to CA1. The trisynaptic circuit thus encompassed (1) the entorhinal, perforant pathway synapse on the dendrites of dentate granule cells, which in turn originate (2) the mossy fiber projection, synapsing onto the complex spines of the CA3 pyramidal cells. The latter originate not only the intrinsic auto-associative projections in CA3, but also (3) the Schaffer collateral projection, forming the third synapse on CA1 pyramidal neurons (Fig. 1a). In that concept, the projections from the EC to the CA fields became essentially ignored, and it was only in the late 1980s/early 1990s that they were “rediscovered” [Witter et al., 1988; Amaral and Witter, 1989; Yeckel and Berger, 1990] while the projections to the subiculum, also already mentioned by Ramón y Cajal, were introduced on the scene again [Witter and Groenewegen, 1990; Witter et al., 1992]. Since then, the projection to CA1 is referred to as the temporo-ammonic pathway by some, and by others

as the direct EC to CA1 projection, forming one component of the perforant pathway. Within the context of the present comparative study, this vague nomenclature becomes a problem, since searching for the perforant path in a nonmammalian animal might become an issue, depending on how this pathway is defined. It is, therefore, appropriate to redefine the entorhinal-hippocampal projections, also because we now know that neurons in layer II are the main source of the entorhinal projections to the dentate gyrus and fields CA2 and CA3, and neurons in layer III give rise to the entorhinal projections to CA1 and subiculum (note that a small number of neurons in deeper entorhinal layers contribute to both projections). For the present paper, we, therefore, propose to differentiate between the EC layer II projection and the EC layer III projection. It has been shown that single layer II cells project to the dentate gyrus and CA2/CA3 [Tamamaki and Nojyo, 1993], but whether this is true for the layer III projection to CA1 and subiculum is as yet unclear.

Considering the fornix as the main if not sole hippocampal output pathway triggered a wave of experimental studies in which fornix lesions were considered as a convenient experimental model for the more complex hippocampal lesions. Although attractive, results from these studies rapidly pointed to a serious conceptual problem in that fornix lesions did not reliably mimic the profound amnesic syndrome seen after complete hippocampal lesions. In addition, the amnesic syndrome seen in a patient was characterized as anterograde amnesia, since memories from before the surgery seemed more or less intact, indicating that the actual memory storage had to be somewhere else in the brain, most likely in the cortex [Squire and Wixted, 2011]. Since the fornix does not provide an output pathway to the cortex, an emerging challenge was to find the potential pathway mediating memory storage in the cortex. This challenge was resolved by an insightful study in the rhesus monkey, published in a series of three papers showing that the subiculum projected to deep layers of the EC, which in turn contain neurons that are the origin of direct or indirect widespread projections to higher-order cortical areas [Van Hoesen and Pandya, 1975a, b; Van Hoesen et al., 1975; Rosene and Van Hoesen, 1977]. These findings were shortly after corroborated and extended in an extensive series of publications in the cat [Witter and Groenewegen, 1986], guinea pig [Sorensen, 1985], and rat [Kosel et al., 1982; Swanson and Kohler, 1986; Insausti et al., 1997]. These and subsequent studies painted the current more complex connectional diagram of the corticohippocampal system (Fig. 1b) [van Strien et al., 2009].

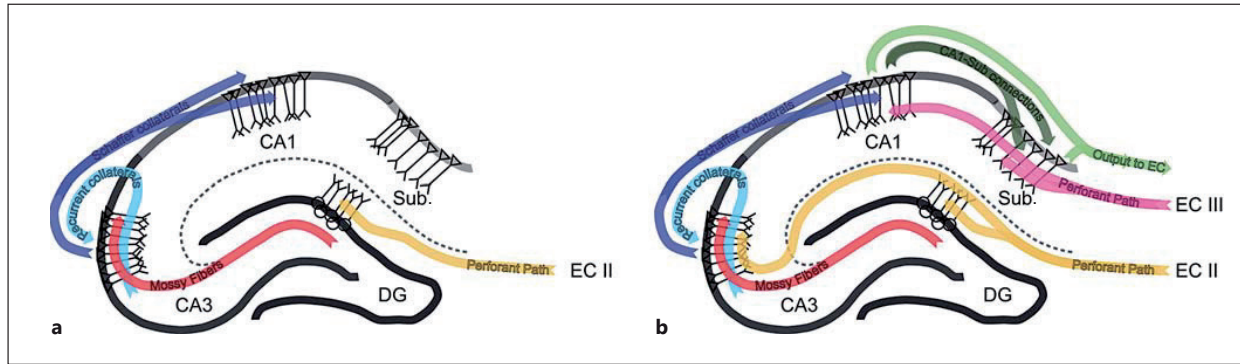


Fig. 1. Schematic representation of main hippocampal connectivity. **a** The traditional trisynaptic pathway comprising the entorhinal-dentate perforant path synapse, the dentate gyrus (DG)-cornu ammonis CA3 mossy fiber synapse, and the CA3-CA1 Schaffer synapse. Also indicated are the strong intrinsic CA3 auto-associational connections. **b** A more elaborate connective diagram including the parallel entorhinal cortex (EC) layer II and III projections, as well as incorporating the subiculum and CA1 and subicular projections to the EC.

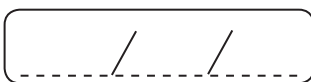
In our quest to find defining connections as arguments to establish homologies, we should, however, not ignore the massive fornix projection targeting a variety of basal forebrain and hypothalamic structures, including the lateral septum and to a lesser extent the medial septum, the nucleus accumbens, and several hypothalamic domains, with the mammillary bodies likely receiving the densest innervation [Kishi et al., 2000; Witter, 2006]. It is now well established that these pathways and the interconnected structures all play roles in higher-order cognitive functions [Aggleton et al., 2000], but manipulations result in dysfunctions dissimilar to those seen after damage to the corticohippocampal system. Clinically, the human syndrome of diencephalic amnesia is the closest to medial temporal lobe amnesia, and there is general agreement that all diencephalic patients share damage to the mammillothalamic tract [Van der Werf et al., 2003a, b; Aggleton et al., 2010]. A complete understanding of these complexities await further details about the connectivity and functional interactions of all structures involved.

Is the Characteristic Hippocampal Circuit Really Trisynaptic?

Aiming for solid features to embark on a comparative analysis, it is important to agree on what we are looking for to argue what in the nonmammalian brain might be the hippocampus. We could look for morphology, chemical or genetic identity of neurons, developmental origin,

or aspects of circuitry. Focusing on the latter, in view of the above section on connectivity, is it the trisynaptic circuit that we should be looking for in nonmammalian species? In recent years, an alternative view has been proposed, which puts emphasis on the EC layer III projection and the marked reciprocating projections from CA1 and the subiculum. Reciprocity is a common feature of cortical connectivity, and the EC layer II projection is a clear exception to that common pattern in that neither the dentate gyrus nor CA3 seems to originate reciprocating projections to EC [van Strien et al., 2009]. So, it could be argued that searching for a canonical trisynaptic pathway might not be the best comparative approach. This line of thinking is supported by the suggestion that the dentate gyrus is unique to mammals [Striedter, 2016]. In this view, the medial cortex in reptiles and amphibians represents the pyramidal hippocampal layer, i.e., the CA fields, and no dentate granular cells are present. Per this scenario, the evolutionarily preserved circuit thus includes the pyramidal cells of the hippocampus, receiving cortical inputs from more lateral parts of the cortex, in turn sending output to the lateral cortex, and, via the fornix, to septum and hypothalamus.

The morphological definition of dentate granule cells as globular cells without basal dendrites is, however, ambiguous. In some mammalian species, such as postnatal rats, but also in adult monkeys and humans, dentate granular cells come in different forms, some being less globular, occasionally having basal dendrites, such they have some resemblance to pyramidal neurons [Treves et al.,



2008]. A better criterion might be that in the commonly studied mammals, the dentate granule cells give rise to a morphologically characteristic axon, the mossy fiber, showing complex, moss-like multisynaptic terminal complexes with equally complex spine structures on the target pyramidal neurons [Treves et al., 2008]. The mossy fiber projection also expresses high levels of zinc, as traditionally stained in several species with the Timm stain [Treves et al., 2008].

If the dentate gyrus is a mammalian addition, this raises the question what to do with the two components of the entorhinal inputs, the layer II versus layer III system. Since the layer II system projects to CA2 and CA3 as well as the dentate gyrus, would we expect that a similar division is already present in nonmammals? Alternatively, is the layer II projection an addition like the dentate gyrus, which subsequently expanded to also innervate adjacent pyramidal CA fields? Assuming the latter, did this occur parallel to the dentate mossy fiber projection innervating CA3 and CA2 [Kohara et al., 2014; Haussler et al., 2016]?

Another recent hypothesis postulates that the dentate as such is not new, but that the folding of dentate, resulting in the hippocampal fissure and the discontinuity between dentate gyrus and CA fields, is the characteristic feature of the mammalian brain [Hevner, 2016]. Attractive as this may seem, this concept seems to pass over the fact that in all mammals studied, there are parts of the hippocampus that do not show these particular features. A good example can be found in the brain of marsupials, such as the opossum (Fig. 2). Whereas at more posterior levels (Fig. 2a2, 3), the hippocampus indeed comprises a folded dentate gyrus and a separated CA field emerging close to the hilar region of the dentate, at more anterior levels (Fig. 2a1), the two structures become aligned such as to show a striking similarity to what is found in some reptilian species [Striedter, 2016; Butler, 2017]. A similar arrangement has been described in monotremes, such as *Echidna* [Hassiotis et al., 2004]. However, also in placental mammals, such a nondifferentiated hippocampal-like structure is present, called the taenia tecta (Fig. 2b) and the supracallosal indusium griseum [Stephan, 1975; Treves et al., 2008].

Subdivisions and Standard Connectivity Compared

The cortex of reptiles comes in different flavors, one main group, including lizards and snakes, presenting a marked three-layered cortex, while the others come with

variable changes in that pattern from a less laminated version, generally seen in turtles to the one in crocodiles, that comes closer to the totally nonlaminated version seen in birds [Striedter, 2016]. In lizards, the medial part of the cortical sheet is commonly divided into three domains, a small-celled medial domain, a large-celled mediodorsal domain, continuing into the dorsal cortex, which is bordered in turn by the lateral cortex. The small-celled medial domain contains several morphologically different cell types, some of which give rise to a zinc-positive mossy fiber-like projection to the adjacent large-celled mediodorsal and dorsal domains, indicative for a dentate homologue. Zinc-positive terminals have also been reported on neurons in the polymorph layer of the small-celled portion. The targets are large neurons looking similar to hilar mossy cells described in the mammalian hippocampus [Treves et al., 2008]. These observations seem to indicate that, at least in some reptiles, a dentate-like structure is present, not well differentiated from the adjacent cortex which could be considered to represent an as yet not differentiated representation of the CA component described in mammals. From a morphological point of view, the resemblance between the small- and large-celled parts of the lizard cortex to what has been described for the taenia tecta and indusium griseum in rodents is striking, including a zinc-positive projection system that has been described in mice [Adamek et al., 1984; Laplante et al., 2013]. These authors conclude that the indusium griseum and potentially also the taenia tecta might be phylogenetically old representations of the hippocampus. However, studies in the Madagascan hedgehog tenrec led to the conclusion that the indusium griseum, again showing a zinc-positive projection, might be correlated with lizard medial cortex, but that it is incorrectly considered a hippocampal homologue [Kunzle, 2004]. One would hope that more detailed functional studies on the lizard brain as well as on the taenia tecta and indusium griseum in mammals might clarify the validity of these claims.

Alternative Subdivisions of the Hippocampus

Alternative ways to divide the hippocampus have been proposed, contrasting to the trisynaptic and EC layer II versus layer III partitions. Among the most prominent ones are a functional differentiation along the longitudinal axis, and a functional differentiation represented by two parallel cortical input/output systems, mediated by different components of the EC.

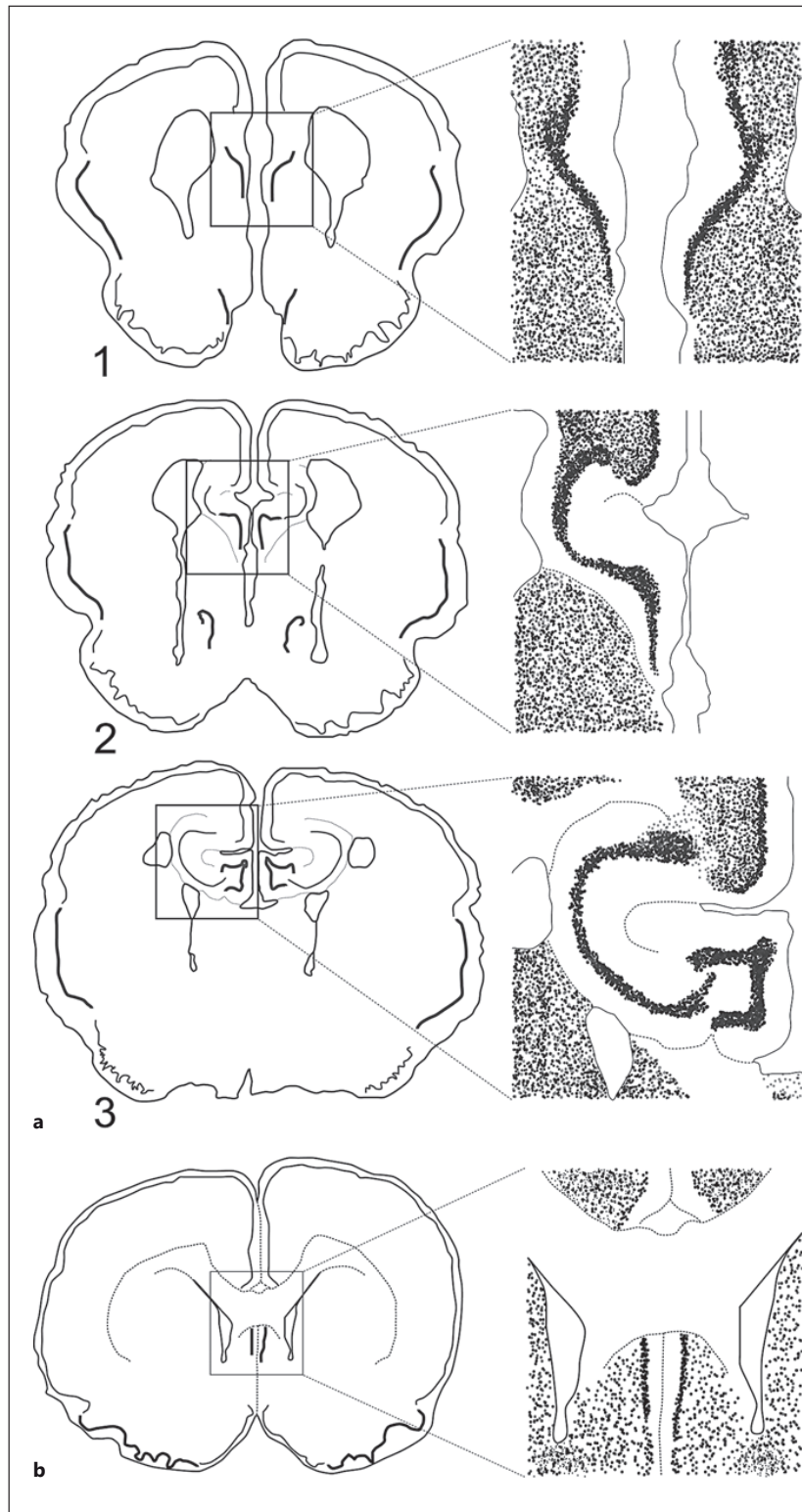
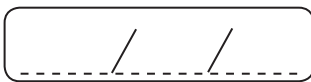


Fig. 2. Presence of an unfolded dentate gyrus in nonplacental and placental species. **a** Series of coronal sections from rostral (1) to caudal (3) through the brain of the marsupial opossum. At most anterior levels (1), the hippocampus/dentate gyrus exhibits a nonfolded appearance, comparable to the medial cortex in reptiles. **b** In rodents, such as the rat, a comparable nonfolded structure, called the taenia tecta, can be found at levels ventral to the genu of the corpus callosum.



The Hippocampal Long Axis

Based on a large body of connectional and functional data in rodents, carnivores, and primates, a dominant view has been that the dorsal (or posterior) hippocampus is implicated in memory and spatial navigation, and the ventral (or anterior) hippocampus mediates emotional, anxiety, and stress-related behaviors. Interestingly, such a functional differentiation might exist in the avian hippocampus as well [Smulders, 2017]. The border between the two domains in the mammalian hippocampus has not been well established, and some authors have suggested dividing the hippocampus into three components, inserting an intermediate domain. Gene expression studies demonstrate multiple domains along the hippocampal long axis, which often exhibit sharply demarcated borders. Together these data suggest a model in which long-axis gradients are superimposed on discrete connectionally and genetically defined domains, resulting in at least three functionally different domains [Strange et al., 2014; Maass et al., 2015; Navarro Schroder et al., 2015].

A striking example of functional differences along the long axis has been reported with respect to the representation of space through the firing properties of place cells, found in all of the CA divisions [O'Keefe and Dostrovsky, 1971; O'Keefe, 1976; Lu et al., 2015], but also to a lesser extent in dentate gyrus and the subiculum. The most detailed analysis has been carried out in CA1 and CA3, showing that the size of a place field is related to the position of the place cells along the long axis. Place cells in the dorsal hippocampus have the smallest place fields, and, at more ventral levels, the sizes increase gradually [Kjelstrup et al., 2008]. Place field size can be interpreted as a measure of spatial scale, indicating that environments might be represented at different spatial resolutions along the long axis of the hippocampal formation. Recent functional MRI findings in humans support such a difference in representational resolution along the hippocampal long axis [Evensmoen et al., 2013, 2015]. These findings, when combined with the comparative data summarized above, lead to a clear prediction about a possible spatial code in, for example, the medial and dorsal cortex of the lizard. In case place cells were to be found in this cortical domain, they will show a gradient such that spatial representation anteriorly is more fine grained than at more posterior levels. This might result in functional differences in the medial cortex, as suggested previously [Hoogland et al., 1994]. This prediction will hold irrespective of whether the lizard medial cortex comprises a dentate gyrus and an EC layer II input system or not, since place fields in rodents are independent of the EC

layer II-dentate-CA3 system [Brun et al., 2002]. Instead, they depend on the EC layer III system, more in particular the component that arises from the more posteromedial part of the EC [Brun et al., 2008]. Moreover, this input plays a role in long-term spatial memory [Rezonides and Schuman, 2004].

Parallel Cortical Pathways

The second differentiation is strongly based on observations that the more posteromedial part of the EC, generally referred to as the medial EC (MEC), has been shown to be functionally and connectionally different from the anterolateral part, the so-called lateral EC (LEC). Firing of neurons in the MEC represents spatial, directional and speed information [Fyhn et al., 2004; Sargolini et al., 2006; Solstad et al., 2008; Kropff et al., 2015]. In contrast, recordings in LEC have not indicated the presence of pure spatially modulated neurons; rather the firing of neurons in LEC seems to reflect the presence of objects in context [Tsao et al., 2013; Knierim et al., 2014]. Although the causes for these striking functional differences are as yet not fully understood, it is likely that different connectional streams into MEC and LEC, strongly involving different connectivity patterns from adjacent parts of the parahippocampal regions such as the postrhinal/parahippocampal cortex and perirhinal cortex, are key determinants of this difference [Witter et al., 2000; Eichenbaum et al., 2012; Ranganath and Ritchey, 2012]. Interestingly, the projections of the two entorhinal domains to area CA1 and the subiculum in all mammalian species studied, including nonprimates and primates, are topographically organized along the transverse axis of both fields [Witter and Amaral, 1991; Witter et al., 2000; van Strien et al., 2009]. Recent connectional MRI studies in humans have pointed to a similar connectional bipartite system separating anterolateral from posteromedial EC, showing clear differences with respect to connectivity measures in the hippocampus, resembling those reported in rodents [Maass et al., 2015]. This thus indicates that functionally different types of input may be mapped onto different hippocampal domains along the transverse axis, a prediction that was shown to be correct in CA1 in rats with respect to spatial information carried by firing properties of neurons [Henriksen et al., 2010]. It remains to be established whether comparable functional differences exist in other clades, but recent gene expression patterns during embryological development indicate that in birds and lizards, LEC and MEC might be identifiable [Abellan et al., 2014; Medina et al., 2017]. Whether these different entorhinal domains in birds and lizards show connectional

differences, comparable to those seen in mammals, is open to further study. It is of interest that in the lizard *Gekko gecko*, two connectional pathways have been described originating from lateral and medial portions, though only the lateral portion seems to project to the small- and large-celled medial cortex [Hoogland and Vermeulen-Vanderzee, 1995].

Concluding Remarks

For all mammalian species where we have connectional and functional data, it is apparent that the hippocampus receives its main cortical inputs from the EC, organized in a 2×2 matrix of origin, consisting of EC layer II and III projections on one axis, and the LEC and MEC on the other. This matrix of connections seems well conserved. With respect to reptiles, most data on the potential homologous areas in the medial and lateral cortex are restricted to a few species of lizards, and although genetically defined LEC and MEC might exist, data on the con-

nectivity of these recently identified areas are sparse if not missing. In birds, the situation is even less clear although, at least in the chicken, comparable entorhinal areas have been identified.

Acknowledgments

This work has been supported by the Kavli Foundation, the Center of Excellence scheme of the Research Council of Norway – Center for Neural Computation, The Egil and Pauline Braathen and Fred Kavli Center for Cortical Microcircuits, and the National Infrastructure Scheme of the Research Council of Norway – NORBRAIN. M.P.W. also expresses his gratitude to the staff and colleagues of the Instituto de Neurociencias in Alicante for the friendly hospitality and peace to prepare the lecture that inspired this paper, and to Karger for the support of the 28th Annual Karger Symposium in San Diego.


Disclosure Statement

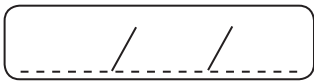
The authors report no conflict of interest.

References

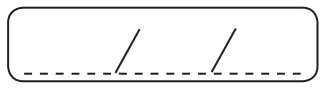
- Abellan A, Desfilis E, Medina L (2014) Combinatorial expression of *Lef1*, *Lhx2*, *Lhx5*, *Lhx9*, *Lmo3*, *Lmo4*, and *Prox1* helps to identify comparable subdivisions in the developing hippocampal formation of mouse and chicken. *Front Neuroanat* 8:59.
- Adamek GD, Shipley MT, Sanders MS (1984) The indusium griseum in the mouse: architecture, Timm's histochemistry and some afferent connections. *Brain Res Bull* 12:657–668.
- Aggleton JP (2014) Looking beyond the hippocampus: old and new neurological targets for understanding memory disorders. *Proc Biol Sci* 281:20140565.
- Aggleton JP, Christiansen K (2015) The subiculum: the heart of the extended hippocampal system. *Prog Brain Res* 219:65–82.
- Aggleton JP, McMackin D, Carpenter K, Hornak J, Kapur N, Halpin S, Wiles CM, Kamel H, Brennan P, Carton S, Gaffan D (2000) Differential cognitive effects of colloid cysts in the third ventricle that spare or compromise the fornix. *Brain* 123:800–815.
- Aggleton JP, O'Mara SM, Vann SD, Wright NF, Tsanov M, Erichsen JT (2010) Hippocampal-anterior thalamic pathways for memory: uncovering a network of direct and indirect actions. *Eur J Neurosci* 31:2292–2307.
- Amaral DG, Witter MP (1989) The three-dimensional organization of the hippocampal formation: a review of anatomical data. *Neuroscience* 31:571–591.
- Andersen P, Bliss TV, Lomo T, Olsen LI, Skrede KK (1969) Lamellar organization of hippocampal excitatory pathways. *Acta Physiol Scand* 76:4A–5A.
- Annese J, Schenker-Ahmed NM, Bartsch H, Maechler P, Sheh C, Thomas N, Kayano J, Ghatan A, Bresler N, Frosch MP, Klaming R, Corkin S (2014) Postmortem examination of patient H.M.'s brain based on histological sectioning and digital 3D reconstruction. *Nat Commun* 5:3122.
- Augustinack JC, van der Kouwe AJ, Salat DH, Benner T, Stevens AA, Annese J, Fischl B, Frosch MP, Corkin S (2014) H.M.'s contributions to neuroscience: a review and autopsy studies. *Hippocampus* 24:1267–1286.
- Bliss TV, Lomo T (1973) Long-lasting potentiation of synaptic transmission in the dentate area of the anaesthetized rabbit following stimulation of the perforant path. *J Physiol* 232:331–356.
- Broca P (1878) Anatomie comparée des circonvolutions cérébrales. Le grand lobe limbique et la scissure limbique dans la série des mammifères. *Rev Anthropol* 2:285–498.
- Brun VH, Leutgeb S, Wu HQ, Schwarcz R, Witter MP, Moser EI, Moser MB (2008) Impaired spatial representation in CA1 after lesion of direct input from entorhinal cortex. *Neuron* 57:290–302.
- Brun VH, Otnass MK, Molden S, Steffenach HA, Witter MP, Moser MB, Moser EI (2002) Place cells and place recognition maintained by direct entorhinal-hippocampal circuitry. *Science* 296:2243–2246.
- Butler A (2017) Of horse-caterpillars and homologies: evolution of the hippocampus and its name. *Brain Behav Evol* 90:7–14.
- Eichenbaum H, Sauvage M, Fortin N, Komorowski R, Lipton P (2012) Towards a functional organization of episodic memory in the medial temporal lobe. *Neurosci Biobehav Rev* 36:1597–1608.
- Evensmoen HR, Ladstein J, Hansen TI, Moller JA, Witter MP, Nadel L, Haberg AK (2015) From details to large scale: the representation of environmental positions follows a granularity gradient along the human hippocampal and entorhinal anterior-posterior axis. *Hippocampus* 25:119–135.
- Evensmoen HR, Lehn H, Xu J, Witter MP, Nadel L, Haberg AK (2013) The anterior hippocampus supports a coarse, global environmental representation and the posterior hippocampus supports fine-grained, local environmental representations. *J Cogn Neurosci* 25:1908–1925.
- Fyhne M, Molden S, Witter MP, Moser EI, Moser MB (2004) Spatial representation in the entorhinal cortex. *Science* 305:1258–1264.

- Hassiotis M, Paxinos G, Ashwell KW (2004) Cyto- and chemoarchitecture of the cerebral cortex of the Australian echidna (*Tachyglossus aculeatus*). I. Areal organization. *J Comp Neurol* 475:493–517.
- Haussler U, Rinas K, Kilias A, Egert U, Haas CA (2016) Mossy fiber sprouting and pyramidal cell dispersion in the hippocampal CA2 region in a mouse model of temporal lobe epilepsy. *Hippocampus* 26:577–588.
- Henriksen EJ, Colgin LL, Barnes CA, Witter MP, Moser MB, Moser EI (2010) Spatial representation along the proximodistal axis of CA1. *Neuron* 68:127–137.
- Hevner RF (2016) Evolution of the mammalian dentate gyrus. *J Comp Neurol* 524:578–594.
- Hoogland PV, Martinez-Garcia F, Vermeulen-Vanderzee E (1994) Are rostral and caudal parts of the hippocampus of the lizard *Gekko gecko* related to different types of behaviour? *Eur J Morphol* 32:275–278.
- Hoogland PV, Vermeulen-Vanderzee E (1995) Efferent connections of the lateral cortex of the lizard *Gekko gecko*: evidence for separate origins of medial and lateral pathways from the lateral cortex to the hypothalamus. *J Comp Neurol* 352:469–480.
- Insausti R, Herrero MT, Witter MP (1997) Entorhinal cortex of the rat: cytoarchitectonic subdivisions and the origin and distribution of cortical efferents. *Hippocampus* 7:146–183.
- Kishi T, Tsumori T, Ono K, Yokota S, Ishino H, Yasui Y (2000) Topographical organization of projections from the subiculum to the hypothalamus in the rat. *J Comp Neurol* 419:205–222.
- Kjelstrup KB, Solstad T, Brun VH, Hafting T, Leutgeb S, Witter MP, Moser EI, Moser MB (2008) Finite scale of spatial representation in the hippocampus. *Science* 321:140–143.
- Knierim JJ, Neunuebel JP, Deshmukh SS (2014) Functional correlates of the lateral and medial entorhinal cortex: objects, path integration and local-global reference frames. *Philos Trans R Soc Lond B Biol Sci* 369:20130369.
- Kohara K, Pignatelli M, Rivest AJ, Jung HY, Kitamura T, Suh J, Frank D, Kajikawa K, Mise N, Obata Y, Wickersham IR, Tonegawa S (2014) Cell type-specific genetic and optogenetic tools reveal hippocampal CA2 circuits. *Nat Neurosci* 17:269–279.
- Kosel KC, Van Hoesen GW, Rosene DL (1982) Non-hippocampal cortical projections from the entorhinal cortex in the rat and rhesus monkey. *Brain Res* 244:201–213.
- Kropff E, Carmichael JE, Moser MB, Moser EI (2015) Speed cells in the medial entorhinal cortex. *Nature* 523:419–424.
- Kunzle H (2004) The hippocampal continuation (indusium griseum): its connectivity in the hedgehog tenrec and its status within the hippocampal formation of higher vertebrates. *Anat Embryol (Berl)* 208:183–213.
- Laplanche F, Mnie-Filali O, Sullivan RM (2013) A neuroanatomical and neurochemical study of the indusium griseum and anterior hippocampal continuation: comparison with dentate gyrus. *J Chem Neuroanat* 50–51:39–47.
- Lewis FT (1923) The significance of the term hippocampus. *J Comp Neurol* 35:213–230.
- Lorente de N6 R (1933) Studies on the structure of the cerebral cortex. *J Psychol Neurol* 45:26–438.
- Lorente de N6 R (1934) Studies on the structure of the cerebral cortex. II. Continuation of the study of the ammonic system. *J Psychol Neurol* 46:113–177.
- Lu L, Igarashi KM, Witter MP, Moser EI, Moser MB (2015) Topography of place maps along the CA3-to-CA2 axis of the hippocampus. *Neuron* 87:1078–1092.
- Maass A, Berron D, Libby LA, Ranganath C, Duzel E (2015) Functional subregions of the human entorhinal cortex. *Elife* 4:e06426.
- Maclean PD (1952) Some psychiatric implications of physiological studies on fronto-temporal portion of limbic system (visceral brain). *Electroencephalogr Clin Neurophysiol* 4:407–418.
- Medina L, Abellan A, Desfilis E (2017) Contribution of genoarchitecture to understanding hippocampal evolution and development. *Brain Behav Evol* 90:25–40.
- Navarro Schroder T, Haak KV, Zaragoza Jimenez NI, Beckmann CF, Doeller CF (2015) Functional topography of the human entorhinal cortex. *Elife* 4:e06738.
- O'Keefe J (1976) Place units in the hippocampus of the freely moving rat. *Exp Neurol* 51:78–109.
- O'Keefe J, Dostrovsky J (1971) The hippocampus as a spatial map. Preliminary evidence from unit activity in the freely-moving rat. *Brain Res* 34:171–175.
- O'Keefe J, Nadel L (1978) *The Hippocampus as a cognitive map*. Oxford, Clarendon Press.
- Papez JW (1937) A proposed mechanism of emotion. *Arch Neurol Psychiatry* 38:725–743.
- Ram6n y Cajal S (1893) Estructura del asta de Ammon y fascia dentata. *Ann Soc Esp His Nat* 22:53–114.
- Ram6n y Cajal S (1902) Sobre un ganglio especial de la corteza eseno-occipital. *Trab Lab Invest Biol Univ Madrid* 1:189–206.
- Ram6n y Cajal S (1911) *Histologie du syst6me nerveux de l'homme et des vert6br6s*. Paris, Maloine.
- Ranganath C, Ritchey M (2012) Two cortical systems for memory-guided behaviour. *Nat Rev Neurosci* 13:713–726.
- Remondes M, Schuman EM (2004) Role for a cortical input to hippocampal area CA1 in the consolidation of a long-term memory. *Nature* 431:699–703.
- Rosene DL, Van Hoesen GW (1977) Hippocampal efferents reach widespread areas of cerebral cortex and amygdala in the rhesus monkey. *Science* 198:315–317.
- Sargolini F, Fyhn M, Hafting T, McNaughton BL, Witter MP, Moser MB, Moser EI (2006) Conjunctive representation of position, direction, and velocity in entorhinal cortex. *Science* 312:758–762.
- Scoville WB, Milner B (1957) Loss of recent memory after bilateral hippocampal lesions. *J Neurol Neurosurg Psychiatry* 20:11–21.
- Smulders TV (2017) The avian hippocampal formation and the stress response. *Brain Behav Evol* 90:81–91.
- Solstad T, Boccardi CN, Kropff E, Moser MB, Moser EI (2008) Representation of geometric borders in the entorhinal cortex. *Science* 322:1865–1868.
- Sorensen KE (1985) The connections of the hippocampal region. New observations on efferent connections in the guinea pig, and their functional implications. *Acta Neurol Scand* 72:550–560.
- Squire LR, Zola-Morgan M (1991) The cognitive neuroscience of human memory since H.M. *Annu Rev Neurosci* 34:259–288.
- Stephan H (1975) *Alloccortex*. Berlin, Springer.
- Steward O (1976) Topographic organization of the projections from the entorhinal area to the hippocampal formation of the rat. *J Comp Neurol* 167:285–314.
- Strange BA, Witter MP, Lein ES, Moser EI (2014) Functional organization of the hippocampal longitudinal axis. *Nat Rev Neurosci* 15:655–669.
- Striedter GF (2016) Evolution of the hippocampus in reptiles and birds. *J Comp Neurol* 524:496–517.
- Swanson LW, Kohler C (1986) Anatomical evidence for direct projections from the entorhinal area to the entire cortical mantle in the rat. *J Neurosci* 6:3010–3023.
- Tamamaki N, Nojyo Y (1993) Projection of the entorhinal layer II neurons in the rat as revealed by intracellular pressure-injection of neurobiotin. *Hippocampus* 3:471–480.
- Treves A, Tashiro A, Witter ME, Moser EI (2008) What is the mammalian dentate gyrus good for? *Neuroscience* 154:1155–1172.
- Tsao A, Moser MB, Moser EI (2013) Traces of experience in the lateral entorhinal cortex. *Curr Biol* 23:399–405.
- Van der Werf YD, Jolles J, Witter MP, Uylings HB (2003a) Contributions of thalamic nuclei to declarative memory functioning. *Cortex* 39:1047–1062.
- Van der Werf YD, Scheltens P, Lindeboom J, Witter MP, Uylings HB, Jolles J (2003b) Deficits of memory, executive functioning and attention following infarction in the thalamus; a study of 22 cases with localised lesions. *Neuropsychologia* 41:1330–1344.
- Van Hoesen G, Pandya DN (1975a) Some connections of the entorhinal (area 28) and perirhinal (area 35) cortices of the rhesus monkey. I. Temporal lobe afferents. *Brain Res* 95:1–24.
- Van Hoesen GW, Pandya DN (1975b) Some connections of the entorhinal (area 28) and perirhinal (area 35) cortices of the rhesus monkey. III. Efferent connections. *Brain Res* 95:39–59.
- Van Hoesen G, Pandya DN, Butters N (1975) Some connections of the entorhinal (area 28) and perirhinal (area 35) cortices of the rhesus monkey. II. Frontal lobe afferents. *Brain Res* 95:25–38.

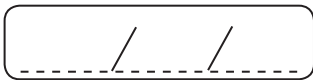
- 
- van Strien NM, Cappaert NL, Witter MP (2009) The anatomy of memory: an interactive overview of the parahippocampal-hippocampal network. *Nat Rev Neurosci* 10:272–282.
- Willis T (1664) *Cerebri anatome, cui accessit nervorum descriptio et usus*. Londini, typis Ja. Flesher, impensis Jo. Martyn & Ja. Allestry apud insigne Campanae in Coemeterio D. Pauli, p 538.
- Witter MP (2006) Connections of the subiculum of the rat: topography in relation to columnar and laminar organization. *Behav Brain Res* 174:251–264.
- Witter MP, Amaral DG (1991) Entorhinal cortex of the monkey: V. Projections to the dentate gyrus, hippocampus, and subicular complex. *J Comp Neurol* 307:437–459.
- Witter MP, Griffioen AW, Jorritsma-Byham B, Krijnen JL (1988) Entorhinal projections to the hippocampal CA1 region in the rat: an underestimated pathway. *Neurosci Lett* 85:193–198.
- Witter MP, Groenewegen HJ (1986) Connections of the parahippocampal cortex in the cat. III. Cortical and thalamic efferents. *J Comp Neurol* 252:1–31.
- Witter MP, Groenewegen HJ (1990) The subiculum: cytoarchitecturally a simple structure, but hodologically complex. *Prog Brain Res* 83:47–58.
- Witter MP, Groenewegen HJ, Lopes da Silva FH, Lohman AH (1989) Functional organization of the extrinsic and intrinsic circuitry of the parahippocampal region. *Prog Neurobiol* 33:161–253.
- Witter MP, Jorritsma-Byham B, Wouterlood FG (1992) Perforant pathway projections to the ammons horn and the subiculum in the rat. An electron microscopical PHAL study. *Soc Neurosci Abstr* 1:323.
- Witter MP, Naber PA, van Haefen T, Machielsen WC, Rombouts SA, Barkhof F, Scheltens P, Lopes da Silva FH (2000) Cortico-hippocampal communication by way of parallel parahippocampal-subicular pathways. *Hippocampus* 10:398–410.
- Yeckel MF, Berger TW (1990) Feedforward excitation of the hippocampus by afferents from the entorhinal cortex: redefinition of the role of the trisynaptic pathway. *Proc Natl Acad Sci USA* 87:5832–5836.



A series of horizontal lines for handwriting practice, consisting of 20 evenly spaced lines.



A series of horizontal lines for writing, consisting of 20 evenly spaced lines.



MENNO WITTER (NORWAY)

PARAHIPPOCAMPAL-HIPPOCAMPAL NETWORKS IN THE HEALTHY AND DISEASED BRAIN

UC Irvine

UC Irvine Previously Published Works

Title

Spatial representation in the hippocampal formation: a history

Permalink

<https://escholarship.org/uc/item/4w36z6rj>

Journal

NATURE NEUROSCIENCE, 20(11)

ISSN

1097-6256

Authors

Moser, EI
Moser, M-B
McNaughton, BL

Publication Date

2017-11-01

Peer reviewed

Spatial representation in the hippocampal formation: a history

Edvard I Moser, May-Britt Moser & Bruce L McNaughton

Since the first place cell was recorded and the cognitive-map theory was subsequently formulated, investigation of spatial representation in the hippocampal formation has evolved in stages. Early studies sought to verify the spatial nature of place cell activity and determine its sensory origin. A new epoch started with the discovery of head direction cells and the realization of the importance of angular and linear movement-integration in generating spatial maps. A third epoch began when investigators turned their attention to the entorhinal cortex, which led to the discovery of grid cells and border cells. This review will show how ideas about integration of self-motion cues have shaped our understanding of spatial representation in hippocampal–entorhinal systems from the 1970s until today. It is now possible to investigate how specialized cell types of these systems work together, and spatial mapping may become one of the first cognitive functions to be understood in mechanistic detail.

Although the study of the cellular and circuit mechanisms of spatial representation in the brain today is centered on the hippocampal and parahippocampal formation, the study of spatial coding did not begin there, but rather began with the parietal cortex, in the form of early observations on patients with parietal damage^{1,2}; in many respects, one takes a risk in attempting to limit the discussion to the hippocampal formation³. Nevertheless, in studies of spatial coding, some of the most ‘paradigm-shifting’ discoveries and ideas have come from recordings within the greater network of the hippocampal formation, particularly the dorsal parts of hippocampus, entorhinal cortex, presubiculum, and parasubiculum, where cells exhibit place-dependent activity independently of the animal’s behavior or the task that it is performing (Fig. 1). Key among these insights were the discoveries of place cells (Fig. 2)⁴, head direction cells (Fig. 3)^{5–7}, and grid cells^{8,9}, each of which

represent quantum jumps in our understanding that there is a system in the brain that has evolved to produce a representation manifold that can be linked to position (grid cells), an inertial compass (head direction cells), and a system for mapping external features and events onto internal and, at least locally, metric coordinates (place cells). In broad terms, these components and their interactions were predicted by O’Keefe in 1976 (ref. 10).

Also key to the emergence of a model for spatial representation was a gradual understanding of the role played by different spatial reference frames and their interactions. Space can be represented in three reference frames: egocentric (defined in relation to a body part axis), allocentric (based on spatial relationships to or among external features), and inertial or idiothetic (relative location and orientation based on direction and distance moved from an arbitrary reference point). Navigation in an idiothetic reference frame is often referred to as ‘path integration’, a process by which animals use self-motion cues (such as motor efference, optical flow, and vestibular information) to keep track of their own location relative to a starting point^{11–14}. Decades of investigation have shown that egocentric space is not represented primarily in the hippocampal formation but rather in parietal cortex and associated regions^{15–17}. O’Keefe’s studies showed from the outset that, instead, place cells encode an animal’s location in an

orientation-independent reference frame¹⁰. Although the term allocentric was applied to place cell representations, O’Keefe recognized early on that these representations may rely “on the fact that information about changes in position and direction in space could be calculated from the animal’s movements.”¹⁰ Yet it was not until the discovery of head direction cells in the 1980s^{5–7} and the realization that these cells were indeed performing integration of head angular velocity¹⁸ that the concept emerged, in the 1990s, that the entire hippocampal formation might be using an idiothetic reference frame—or path integration—as a basis for its coordinate system¹⁹. The possibility of a path-integration mechanism outside the hippocampus proper^{3,20,21} was reinforced at this time by studies showing that, unlike place cells, spatially modulated cells in the entorhinal cortex and subiculum had environment-independent spatial firing patterns^{22,23}. Today it is generally recognized that path integration plays a fundamental role in spatial coding in the hippocampal formation, although there continues to be controversy as to whether path integration is the primary determinant of place cell and grid cell firing or whether it plays an equal or subordinate role to the integration of information from external stimuli^{24–26}.

Finally, a discussion of model shifts would not be complete without some realization of the role that technology has played (Fig. 4).

Edvard I. Moser and May-Britt Moser are at the Kavli Institute for Systems Neuroscience, Norwegian University of Science and Technology, Trondheim, Norway, and Bruce McNaughton is at the Center for the Neurobiology of Learning and Memory, University of California at Irvine, Irvine California, USA, and the Canadian Centre for Behavioural Neuroscience, University of Lethbridge, Lethbridge, Alberta, Canada. email: edvard.moser@ntnu.no

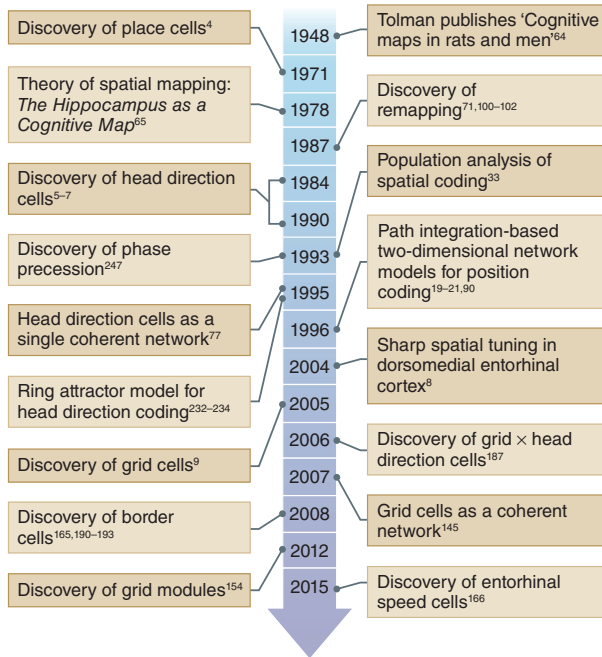


Figure 1 Selection of historical milestones in the study of spatial coding in the hippocampal formation.

Key technical advances have been the shift from recording single cells in restrained, usually anesthetized, animals to recording in freely behaving ones^{4,27-29}; the development of quantitative video-tracking methods for rodents during hippocampal recording experiments^{30,31}; the invention of stereo (tetra) recording³² (Fig. 4a) and its extension to large neuronal ensembles³³ (Fig. 4b-d); the development of micromachined silicon electrode arrays³⁴; new cell-type-specific optical and chemical methods for stimulation³⁵⁻³⁷; and, most recently, the development of large-scale Ca²⁺ cellular imaging in both freely moving animals³⁸ and in restrained animals locomoting in virtual reality environments^{39,40}. The importance of recording from substantial numbers of cells in interpreting coding dynamics for the hippocampus or any other neural system cannot be overemphasized. Apart from the obvious computational and statistical analysis power enabled by collecting data from large numbers of simultaneously active neurons, it is clear that many results that we now understand as across-trial variations in population dynamics may have been attributed to differences in single neuron classes in early single-neuron recording studies.

We have taken on the task of trying to present, in a relatively small space, an historical overview of some of the paradigm-shifting developments that led to our current

understanding of spatial coding in the hippocampal formation. This task is daunting for several reasons, not the least of which is that the number of important experimental and theoretical contributions has risen (and continues to rise) almost exponentially since 1971, when O'Keefe and Dostrovsky, after recording in freely behaving rats from what today would be considered a very small sample of CA1 units, made the bold claim that the hippocampus might construct a spatial map⁴ (Fig. 2). Length restrictions have forced us to focus the review on one particular set of ideas that has inspired the investigation of hippocampal representations of space almost since the beginning of studies of place cells, namely that spatially localized firing to a large extent reflects the dynamic integration of self-motion—or path integration—as animals move around in the environment. We shall demonstrate how the idea of a path-integration input explains many fundamental properties of place cells and how this, in turn, led investigators in the single-cell recording field to identify a path-integration-dependent neural system consisting of multiple functionally specialized cell types in the parahippocampal cortices.

We shall demonstrate that path integration appears as a leitmotif that follows the history of spatial representation in the hippocampal formation across generations of investigators. Yet by directing our spotlight

to path integration, we are forced to leave out contributions and research directions that have contributed critically to the broader understanding of place cells and hippocampal systems function, beyond the representation of self-location. First of all, the more than four decades of hippocampal spatial mapping studies have developed alongside an equally productive line of investigations, using a variety of methodological approaches, into the basis of memory in the same brain system^{3,41-47}. The focus of this review is on the coding of space, but, as we will acknowledge, this does not rule out a broader participation of hippocampal neurons and place cells in representation of experience⁴⁸⁻⁵⁰. In shying away from the memory functions of the hippocampus, we shall also pass over the vast and growing literature on how replay and preplay of firing sequences may enable consolidation and storage of hippocampal memory through interactions with neocortical neural networks⁵¹⁻⁵⁴, and we shall not discuss the important but separate question of whether or how place cells are used for goal-directed navigation and route planning⁵⁵⁻⁵⁹. We have also left out dozens of pioneering studies of temporal coding and network oscillations, including theta rhythms, that have shaped our current understanding of hippocampal function beyond the representation of space^{49,60-62}. Finally, this review is dominated by work in rats and mice, reflecting the use of freely moving rodents as subjects in nearly all studies of spatially modulated cells in the hippocampal formation (see Box 1 for extensions to the primate brain).

The origin of the spatial signal

In 1971, O'Keefe and Dostrovsky observed that neurons in the rat hippocampus had what appeared to be spatial receptive fields⁴ (Fig. 2a,b). In their 1971 paper, the number of place cells and evidence for localized firing was limited, but much more substantial data were presented by O'Keefe in 1976 (ref. 10). By this time, after thorough study of hippocampal activity in unrestrained rats²⁹, Ranck had also seen place cells⁶³. The O'Keefe paper showed that place cells fired whenever the rat was in a certain location in the local environment. Different cells had different place fields, such that at all locations investigated in the hippocampus, the animal's location could, in principle, be inferred from the joint activity of a fairly small sample of neurons¹⁰ (for direct demonstration, see ref. 33 and Fig. 4c,d). Based on this observation and inspired by Tolman's proposal that navigation is guided by internal cognitive maps⁶⁴, O'Keefe and Nadel⁶⁵ suggested that place cells are the basic element

of a distributed allocentric cognitive map of the animal's environment (Fig. 2c). The spatial relations between landmarks provided by this map were thought to enable animals to find their way independently of local view or movement trajectories, using what O'Keefe and Nadel called a locale strategy. This contrasted with route strategies, which do not take into account the relationship between landmarks. The latter strategies included a spectrum of routines from simple beacon navigation to more complex action sequences. O'Keefe and Nadel's proposal represented a major landmark in the conceptualization of hippocampal function. Their book, *The Hippocampus as a Cognitive Map*, synthesized and reinterpreted decades of discordant experimental studies using a range of experimental approaches, particularly lesions, and put these studies into a coherent theoretical framework organized around the concept of place cells as the cellular basis for representation of space as well as events and experiences associated with space. The book proposed a neural implementation of Tolman's concept of the cognitive map, with visionary perspectives on how such a map might enable a breadth of cognitive functions in higher species, including humans. Today, 40 years after its publication, *The Hippocampus as a Cognitive Map* remains the theoretical pillar on which nearly all subsequent study of spatial coding in the hippocampal formation rests.

The early years of research on place cells, in the late 1970s and 1980s, were dominated by attempts to prove that the place signal was indeed spatial and, given this, to understand what caused place cells to fire where they did, based on the idea that it was some constellation of external sensory cues, rather than a single cue or some other cause (for example, ref. 66). Two salient observations in this period that both advanced knowledge and increased perplexity were the findings that place cells appeared to be completely direction-dependent when animals ran repeatedly on restricted paths³⁰ but were unaffected by head direction during free foraging in a large cylinder⁶⁷. Perplexity about the mechanism of place cells was further increased by the fact that place cells had a sort of 'memory': they rotated their fields when external cues were rotated but continued to fire in relation to the last-seen cue location when the cues were removed^{68,69}. Indeed, early studies indicated not only that place cells continued to fire in the 'correct' location in total darkness but also that fields could be formed when animals were introduced to an environment in darkness and were minimally affected when the lights were subsequently turned on⁷⁰. Nevertheless, place fields became linked to

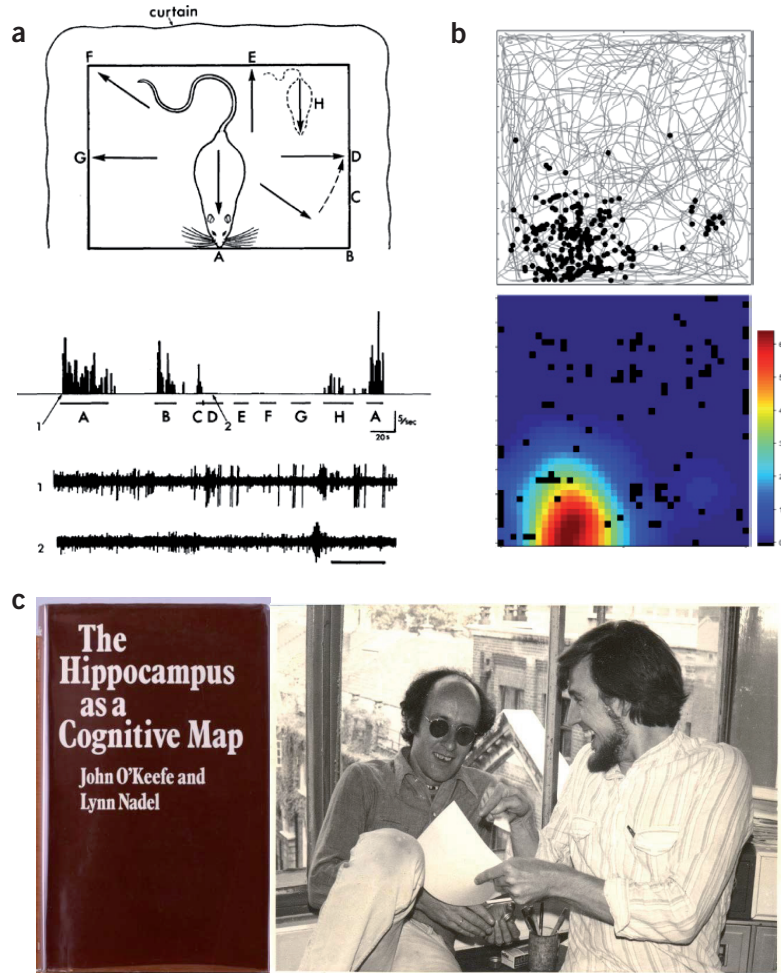


Figure 2 Place cells. (a) First place cell described⁴. Arrows and letters mark positions at which the animal was restrained as it was pushed or coaxed around the test platform. Firing rate of the unit is illustrated by the frequency histograms in the middle of the figure. Letters correspond to positions, and lines indicate periods of restraint. Bottom lines show spikes at the onset of the unit response at A (1) and during the absence of a response at D (2). Calibration bar, 400 ms. Note that the cell responds selectively at only a few positions. O'Keefe and Dostrovsky reported 8 units of 76 recorded hippocampal cells that responded solely or maximally when the rat was situated in a particular part of the testing platform and facing in a particular direction. Note that the single-electrode technology available to the authors at the time likely precluded regular good isolation of cells, which may have limited the number of clear 'place' responses observed. (b) A place field as typically displayed today. Top: rat's trajectory in gray; spike locations superimposed as black dots. Bottom: color-coded rate map; dark red is maximum rate; blue is silence. Regions not visited in black. (c) Left: the book by John O'Keefe and Lynn Nadel was long a 'bible' in the study of spatial coding in the hippocampal formation. Right: Nadel (left) and O'Keefe (right) during preparation of the book. Photo taken by Dulcie Conway around 1975, reproduced here courtesy of John O'Keefe²⁶⁴. Panel a reproduced with permission from ref. 4, Elsevier.

external cues and rotated to maintain registration with them when the cues were rotated between sessions^{68,71}.

The foregoing studies were soon followed by a number of observations that cast further doubt on the external sensory origin of place fields: most place fields had asymmetric firing fields in an environment with a symmetric cue configuration⁷²; place fields could dynamically shift between a reference

frame defined by a reward box that moved relative to the laboratory reference frame and the lab reference frame itself^{73,74}; the location and orientation of place fields followed the rat when the rat was rotated independently of the environment^{75,76}; place cells and head direction cells exhibited coordinated drift error in a cylindrical environment^{77,78}; the size of place fields was almost completely independent of local cue density, spatial frequency, or

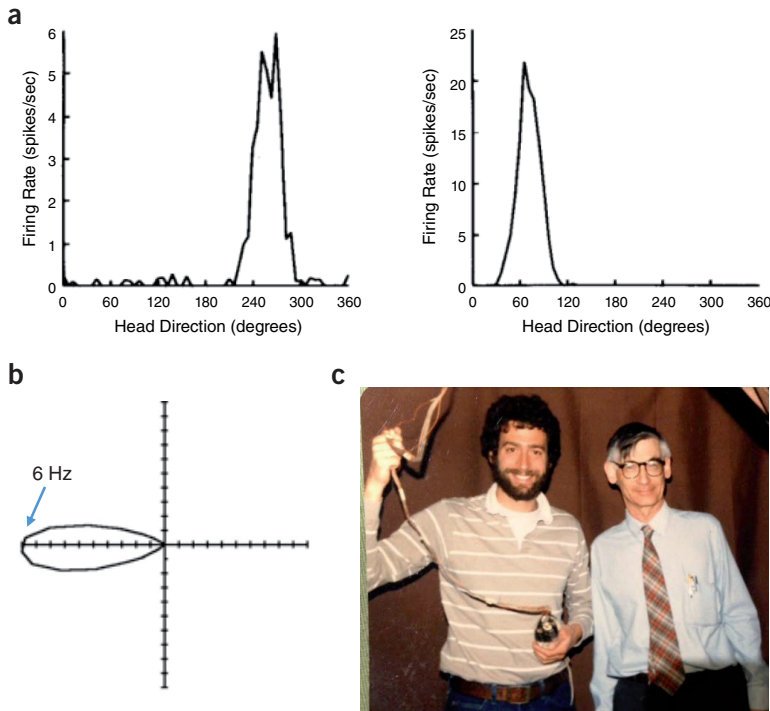


Figure 3 Head direction cells⁶. (a) Firing rate as a function of head direction for two representative cells from two different animals. (b) A head direction cell firing rate in polar coordinates. Peak firing rate, in the left orientation, is 6 Hz. (c) Jeffrey Taube (left) and James B. Ranck Jr. (right), at SUNY Downstate Medical Center in Brooklyn, N.Y., in 1987. Photo courtesy of Jeffrey Taube. Panel a reproduced with permission from ref. 6, “Head-direction cells recorded from the postsubiculum in freely moving rats. I. Description and quantitative analysis,” J.S. Taube, R.U. Muller & J.B. Ranck Jr., 1990, in *Journal of Neuroscience*, Vol. 10, pages 420–435.

salience⁷⁹ but varied systematically along the septotemporal axis of the hippocampus^{80,81}; in rats with age-related memory impairment⁸² or with NMDA receptors blocked⁸³, place fields appeared perfectly normal in a novel environment but could be completely rearranged when the animals were returned to the same environment after even a short delay; the place field map as a whole dynamically expanded when motor and vestibular information about movement speed was disrupted, in the absence of changes in landmark inputs⁸⁴; place cells shut off completely when animals were restrained from locomotion⁸⁵; and finally, the variation in scale of place fields along the hippocampal septotemporal axis was strongly correlated with the gain of physiological speed signals⁸⁶.

In spite of gradually accumulating evidence for an, in many ways, nonsensory origin of spatial receptive fields in the hippocampus, the lack of proper quantification prevented a general acceptance of this idea, and much of the initial effort was thus spent on proving that the signal was indeed spatial. As this skepticism was gradually overcome, investigators

began to focus on how place cells might be synthesized as higher-order integrators of sensory data, perhaps endowed with memory properties. However, this sensory-integration approach changed, literally overnight, when James Ranck brought a video of a recorded head direction cell to the 1984 Society for Neuroscience meeting⁸⁷ (Fig. 3). Head direction cells are cells that fire specifically when the animal faces a certain direction^{5–7} (Fig. 3a,b). Ranck first encountered these cells in the dorsal presubiculum—almost by accident, in an experiment in which electrodes targeted to the subiculum went astray⁸⁷—but they were later observed across a wide network of cortical and subcortical regions^{88,89}. In the same way that place cells covered all locations of an environment, the preferred firing directions of head direction cells were distributed evenly around angular space, enabling precise read-out of head direction in neural networks downstream of head direction cells. If the brain was endowed so clearly with an internal compass, as suggested by Ranck’s 1984 movie, the idea that it also had a map became much more palatable. However, the first full publication on

the basic properties of head direction cells did not appear until 1990, in joint work by Ranck, Taube, and Muller^{6,7}. By that time, it was already recognized that the basis of the head direction signal was likely integration of head angular velocity, and the outline of a model for how this integration was performed using conjunctive head direction \times head angular velocity cells (observed in dorsal presubiculum and parietal cortex) was proposed¹⁸.

To many investigators, the foregoing observations collectively pointed almost inescapably to the hypothesis that the primary determinant of the cognitive map is some form of coordinate system in which head angular velocity and linear velocity are integrated over time to express displacement and orientation from a starting point (path integration)^{19–21,90,91} (Fig. 5). According to this view, the path-integration mechanism assigns place fields based on motion integration. In the absence of external stationary input, errors from noise in the self-motion integration process accumulate, and place fields (and head direction tuning curves) would start to drift. However, in environments with salient cues, rapidly formed associations between cues and place cells enable stabilization of the firing fields, and previously formed maps can be recalled from session to session^{10,19–21,90}, possibly cued by landmark information conveyed through the dorsal presubiculum⁹². Nevertheless, there is also some support for the idea that place cells are formed by integration of salient sensory inputs, independently of movement. One of the main observations presented in favor of this concept is that place fields could be seen to expand⁷¹ or stretch⁹³ in response to corresponding distortions of the enclosure in which recordings took place. However, such distortions do not occur when the animal is introduced *ab initio* into the distorted environment, only when the animal has first experienced the undistorted version. Stretching or expanding can thus be seen as a result of the external inputs attempting to correct the path integrator based on prior associations⁹⁰.

During the past decade, virtual environments have enabled investigators to dissociate with increased rigor the relative contributions of self-motion inputs and stationary landmarks. Typically, head-fixed mice or rats run on an air-cushioned ball or a circular treadmill while visual flow is projected onto an immersive screen at a rate that directly reflects the animal’s running speed and direction, emulating the sensory-motor coupling of the real world^{39,40}. When the virtual environment is linear, as on a treadmill, hippocampal place cells exhibit firing fields that depend on distance moved^{94,95} or

stationary cues on the screen⁹⁴, with some variation between cells⁹⁴. Reducing the gain of ball-to-virtual-scene movement causes place fields to move toward the start of the virtual track, as expected if firing locations are determined by self-motion, but the shift is generally smaller than expected from movement distance alone, pointing to an additional role for visual inputs⁹⁴. The dual dependence on self-motion cues and external cues confirms earlier studies in which these sets of inputs were disentangled in real environments^{73,74,93}. However, when the virtual environment is made two-dimensional and movement of the head remains restricted, localized firing breaks down, although a small influence of distance traveled is detectable⁹⁶. In contrast, when body and head rotation is unconstrained, stable position coding persists⁹⁷. Together these studies point to vestibular signals (which are impoverished during head fixation) as a critical source for integrating velocity and direction signals into a coherent two-dimensional representation, in agreement with earlier work showing that place fields are disrupted following inactivation or lesions of the vestibular system^{98,99}.

Remapping: global, partial, local, and rate

In the late 1980s, Muller and Kubie began a series of investigations on the effects of changing the most salient visual cues in a cylindrical environment and introducing various local cues^{71,72,100–102} (Fig. 6). As alluded to above, cue-card rotations, changes in the size or color of the cue card, or even removal of the cue card altogether rarely changed the radial coordinate of the field but could change the angular coordinate, completely unpredictably in the case of complete removal of the cue card when the rat was not present (Fig. 6b). They coined the term ‘remapping’ to describe any manipulation-induced changes in the firing of place cells. These could include mild changes in the firing characteristics in a few cells, such as when new objects or walls were placed in a cell’s place field, up to radical changes in the location of firing, including the disappearance of a field altogether, which was sometimes observed when the environmental shape was changed or visual cues substantially altered.

Whether sets of place cells remapped completely or only partially depended on the experimental conditions. The terms ‘global’, ‘partial’, and ‘local’ remapping were introduced by Knierim and McNaughton¹⁰³ in an attempt to distinguish situations in which only fields near a specific, manipulated cue changed from situations in which there was a general (partial or complete) rearrangement of fields throughout the environment. Such limited remapping

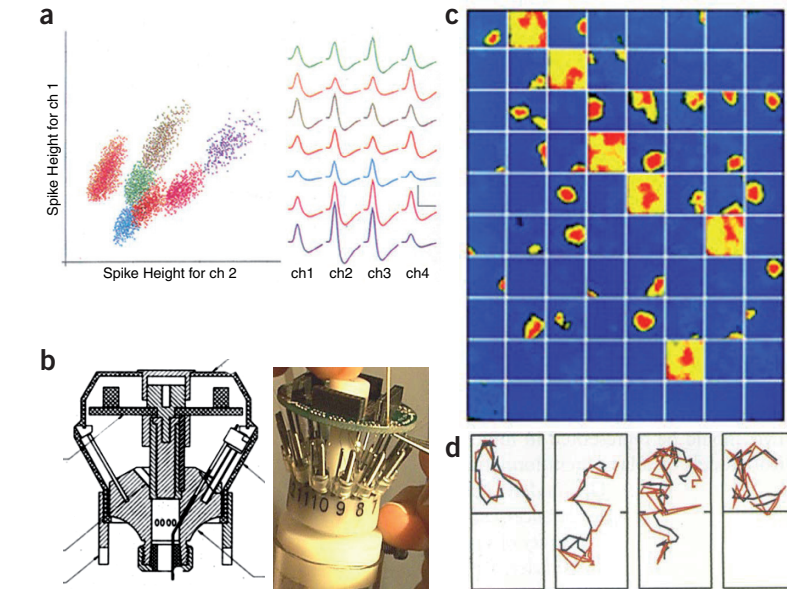


Figure 4 Ensemble recording technology. (a) The principle of tetrode recording proposed by McNaughton *et al.*³² exploits the variation in extracellular spike height as a function of distance to the recording site to resolve multiple single units in structures such as hippocampus, where the neurons are fairly tightly packed. Example of spike amplitude clusters from a tetrode recording showing two of the four spike-amplitude dimensions. The corresponding spike waveforms are shown on the right. (b) A 48-channel, 12-tetrode probe array (hyperdrive) from ca. 1995. This system exploited the flexibility of wire tetrodes, which allowed researchers to advance them by pushing them through gently curving tubes (like a mosquito proboscis). (c) Multitetrode recording made it possible to record from more than 100 hippocampal neurons simultaneously. Here we show 80 firing rate maps from simultaneously recorded CA1 cells as the rat ran in a 70 × 70-cm arena³³. Firing rate is color-coded from blue (silent) to red (maximum rate). Note that many CA1 cells were virtually silent in this particular arena, whereas about 40% had place fields. Six of the recorded cells correspond to fast-spiking cells (interneurons), which have much less spatial selectivity. (d) Examples of the actual (blue) spatial trajectory of the rat and the trajectory reconstructed from the population firing-rate vector (red). Panel a reproduced with permission from ref. 80, “Comparison of spatial firing characteristics of units in dorsal and ventral hippocampus of the rat,” M.W. Jung, S.I. Wiener & B.L. McNaughton, 1994, in *Journal of Neuroscience*, Vol. 14, page 7347–7356. Panels c and d reproduced with permission from ref. 33, AAAS.

is often seen when the animal is placed in nonuniform environments^{104,105} or in cases of deficient plasticity as discussed above^{82,83}. The concept of remapping was clarified considerably by several experiments that followed. In 2005, Leutgeb *et al.* showed that, when the cues in the recording chamber or its shape were radically changed between sessions that took place in the same physical location, CA1 and CA3 place cells underwent substantial changes in their firing rates, without changing their firing locations¹⁰⁶ (Fig. 6c). These changes could be sufficient to make a field appear to be present in only one condition, unless the rate map graphs were rescaled. In contrast, when the recordings took place in identical apparatus located in two separate rooms, the place field distributions became completely uncorrelated. Leutgeb *et al.* made the distinction between ‘rate remapping’ for the former situation and ‘global remapping’ for the latter. Thus, it appears that, under conditions in which the

path-integrator coordinates likely remain consistent, changes in external input or, indeed, internal variables such as motivation, working memory, or action plans, can result in dramatic changes in firing rate while firing location remains unaltered^{107–110}. Leutgeb *et al.* suggested that rate remapping might be the cause of apparent partial remapping or direction dependency on linear tracks. The role of the path-integrator coordinates in governing rate versus global remapping was fairly decisively demonstrated by Colgin *et al.*¹¹¹, who showed that when environmental shape was gradually morphed between a circle and a square, abrupt, global remapping only occurred if the rats had previously been allowed to locomote between a circle and a square via a connecting tunnel. When rats were pretrained on the two shapes in the same location, only rate remapping was observed. Thus, it was the path integrator that determined whether global or rate remapping was observed.

The presence of a nonspatial code on top of the place code (rate remapping) is consistent with dozens of studies, starting in the 1980s, showing that place cells encode more than space. Cells with clear place fields in one task were shown in other tasks to respond in a time-locked manner to various nonspatial features of the environment or the experience, such as odors^{112–114}, textures¹¹⁵, conditioned tones^{28,116,117}, or temporal stages of the experiment¹¹⁸. However, in combination with the remapping studies, these observations suggest that hippocampal cells respond conjunctively to spatial and nonspatial variables, with the latter represented as changes in the rate distribution. Experience-related changes in rate distribution can also account for moment-to-moment variability of firing rates within place fields (overdispersion)¹¹⁹. The conjunctive nature of spatial and event-related firing is demonstrated elegantly in a more recent study of hippocampal activity after systematic variation of location, food cups (objects), and color or pattern of the recording box (context)¹²⁰. The majority of cells in this study fired at specific locations but with rates depending on context and objects. Thus, when location is clamped, unique constellations of cues give rise to unique rate patterns, implying that each experience is characterized by its own hippocampal–neocortical output, even when those experiences occur at a fixed location. This uniqueness is a necessary condition for the widely held view that hippocampus may provide an index that links memory attributes distributed widely over neocortex^{121–123}. The wide range of stimulus configurations that activate hippocampal firing, over and above space, has been taken as evidence for a broad involvement of the hippocampus in episodic memory, where space is just one of several attributes of the encoded representation⁴⁸.

Lest one conclude from the foregoing that the phenomenon of remapping or the necessity or dominance of path integration is now fully understood, it is necessary to consider some remaining flies in the ointment. First, Tanila, Shapiro, and Eichenbaum^{124,125}, and later Knierim¹²⁶, have shown that, when an animal is highly familiar with the local and distal cues in an environment, rotating these cue sets relative to each other can cause some CA1 cells to follow the local set while others simultaneously follow the distal set (still others may remap). Such discordant responses are stronger in CA1 than CA3 (ref. 127). These effects are not inconsistent with a path-integration-based origin of the place fields, if one assumes that the subsequent, plasticity-dependent association between cues and

place cells that leads to robust rate-remapping is also strong enough in some cases to move the fields independently, depending on which type of inputs dominate the synaptic input vector of a given cell. The fact that this effect occurs predominantly in CA1, which lacks the potential stabilizing effects of reciprocal excitatory connections present in CA3, tends to support such a view¹²⁷. A second possible challenge is the fact that place fields can be expressed in CA1 under conditions in which the medial entorhinal cortex (MEC) is completely lesioned¹²⁸. This suggests that localized firing may itself be generated from alternative inputs, such as from weakly spatially modulated neurons in the lateral entorhinal cortex (LEC)¹²⁹, which may provide hippocampal cells with path-integration-independent sensory inputs necessary for efficient rate coding¹³⁰. However, even under conditions in which MEC inactivation does not impair hippocampal place selectivity, the intervention causes instant remapping^{131,132}, suggesting that MEC is obligatory for activating the correct place map. This does not preclude, of course, that place maps are also stored in the CA3 network (for example, the ‘charts’ of Samsonovich and McNaughton⁹⁰), or that, in the absence of a strong MEC input, CA3 attractor dynamics may result in the recall of some previously constructed chart in the novel context.

Moving from hippocampus to entorhinal cortex

Until the 1990s, for primarily technical reasons, most recording studies had been confined to CA1 of the dorsal hippocampus, in spite of the fact that hippocampal subfields may have distinct computational functions. David Marr had, in the early 1970s, already pointed to the unique properties of area CA3 as a recurrent network capable of auto-association, pattern formation, and pattern completion¹³³. His work was followed by theoretical investigations pointing to the possible role of the dentate gyrus in pattern-separation processes needed to counteract memory interference at subsequent stages of the hippocampal circuit^{134–136}. An additional, striking property that was discovered to differentiate between hippocampal subfields was coding sparsity. Contrary to some expectations, in the successive transformations from CA3 to CA1 to subiculum, mean firing rates increased, and coding became less sparse and less spatially selective^{137,138}. This observation led Barnes *et al.* to conclude that “discrete spatial representations are constructed within early stages of the process, for some purpose intrinsic to the hippocampus itself, possibly that of rapid

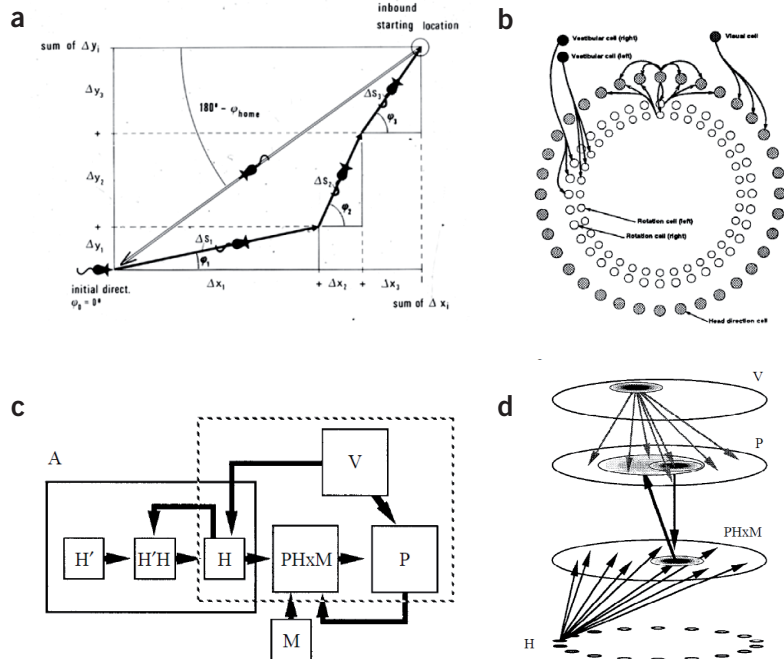
information storage” and that “the information leaving the hippocampus through the subiculum seems to consist of much more highly distributed representations, constructed perhaps through the convergence and disjunction of a number of unrelated hippocampal place cells”¹³⁷. For a long time, however, these ideas did not fully catch the attention of the place cell community, which, with few exceptions, retained its focus on the readily accessible CA1 area.

In a similar manner, until the 1990s, there was minimal focus on computational operations outside the hippocampus and computations underlying place-field formation were at risk of being erroneously attributed to the hippocampus itself. The focus on a hippocampal origin of the place cell signal was further influenced by the observations of a relatively small set of tetrode studies in the entorhinal cortex, the major cortical input to the hippocampus. These studies showed that entorhinal cells were spatially modulated but that their firing fields were broad and dispersed, with little spatial selectivity in standard laboratory environments, and the fields seemed not to remap between environments^{22,137,139}. This, together with the observation that CA1 place fields persisted following large lesions of the dentate gyrus¹⁴⁰, pointed to the remaining associative networks of CA3 as one possible origin for the formation or learning of the sharply localized place signals seen in CA1. The validity of this interpretation was questioned, however, by the fact that partial inactivation of CA3 cells, following inhibition of septal inputs, failed to remove spatial firing in CA1¹⁴¹.

Given the uncertainty about how CA3 contributed to the CA1 place signal, Brun and colleagues¹⁴² decided to record place cells in CA1 after the CA3 input to these cells had been entirely removed by excitotoxins or by knife cuts that completely separated CA1 from CA3 as well as from dentate gyrus and subcortical afferent regions. Retrograde tracer injections in CA1 verified that no input was spared. Confirming the interpretation of the septal-inactivation work¹⁴¹, the study found, in 2002, that CA1 place cells do not require input from CA3 to maintain reasonably selective spatial firing. This suggested either that place fields were generated within the limited circuitry of the CA1 itself or that place cells in CA1 received spatial input from the entorhinal cortex via temporoammonic projections that survived the CA3–CA1 transection. These observations were made only a few years after theoretical studies^{3,21,90,143} proposed that the path integrator might located outside the hippocampus—in the

COMMENTARY

Figure 5 Path integration. (a) Illustration of the Mittlestaedt & Mittlestaedt 1980 experiment¹². This experiment showed that rodents can perform angular and linear path integration. A female mouse returns directly to her nest after finding a lost pup in total darkness but makes a heading error if she is rotated below vestibular threshold before starting the inbound journey. (b) The Skaggs *et al.* continuous-attractor model from 1995 proposed to explain how head direction cells arise through integration of head angular velocity signals from the vestibular system^{18,232}. Updates in the head direction (attractor) layer were performed by a hidden layer of cells conjunctive for head angular velocity and starting head direction, whose return projections to the head direction layer are offset according to the sign of rotation. Such conjunctive cells have been found in several regions of the brain. (c,d) The continuous-attractor model for path integration in two dimensions, as proposed by McNaughton *et al.* in 1996 (ref. 19) and simulated by Samsonovich and McNaughton in 1997 (ref. 90). H', head angular velocity; H'H, conjunctive cells; H, head direction; P, place cells; M, speed cells; PHxM, cells conjunctive for place and head direction and modulated by speed; V, external sensory inputs that were assumed to associatively bind to both H cells and P cells to enable correction of drift error in the path integrator and to enable resetting of the integrator upon entry to a familiar environment. Panel a reproduced with permission from ref. 91, Nature Publishing Group. Panel b reproduced with permission from ref. 232, MIT Press. Panels c and d reproduced with permission from ref. 90, "Path integration and cognitive mapping in a continuous attractor neural network model," A. Samsonovich & B.L. McNaughton, 1997, in *Journal of Neuroscience*, Vol. 17, page 5900–5920.



most extensively to the dorsal hippocampus, where the most sharply tuned place cells of the hippocampus are located^{80,81}. This led us, eventually, after the turn of the millennium, to target tetrodes to the dorsal MEC, the origin of the majority of inputs to the dorsal hippocampus^{8,144}, a region of MEC so far not touched by electrodes *in vivo*.

Grid cells: a metric for space?

Recordings in dorsal MEC soon showed that cells in this region have sharply defined firing fields, much like those in CA1 of the dorsal hippocampus, except that each cell had multiple firing fields, distributed all over the environment⁸. These findings, reported in 2004, pointed to the MEC as a key element of a circuit for space, but the nature of the entorhinal representation remained elusive.

A striking characteristic of many spatially modulated MEC cells was that the distribution of the multiple firing fields of each cell was more regular than expected by chance⁸. When the data from MEC were presented at the 2004 Society for Neuroscience meeting, they created considerable excitement. Among those who were most excited was Bill Skaggs, who thought he saw hexagonal symmetry, inspiring the Mosers and their students, Hafting, Fyhn, and Molden, to increase the size of the recording arena and visualize the firing pattern once and for all. Using a newly constructed 2-m-wide circular recording cylinder, these authors found, in a substantial fraction of MEC superficial-layer

cells, that the firing fields of individual cells created a grid-like periodic hexagonal pattern tiling the entire space available to the animal⁹ (Fig. 7a). These cells were designated as grid cells. For each cell, the grid could be assigned a phase (the x,y locations of the grid vertices), a wavelength or spacing (the distance between the vertices), and an orientation (how much the axes through the vertices were tilted compared to an external reference line). In addition, the peak firing rates varied between fields^{9,145}. The spatial periodicity of the pattern was so striking that the authors were concerned, initially, that it was some sort of artifact. However, the grid pattern was soon found by other labs too^{129,146}.

One of the most striking aspects of the grid cell finding was that the spatial periodicity was maintained despite constant changes in the animal's running speed and running direction. The cells fired at the same vertices regardless of how much time and space the rat had traveled between each crossing, implying that grid cells had continuous access to information about distance and direction moved. The persistence of grid fields⁹ and place fields⁷⁰ when rats run in darkness is consistent with the primary role that such self-motion information might have in determining firing locations, as is the fact that grid patterns unfold immediately in new environments⁹ and are expressed with similar phase relationships between cell pairs in all environments tested¹⁴⁵. It should be added, for the sake of balance, that stable

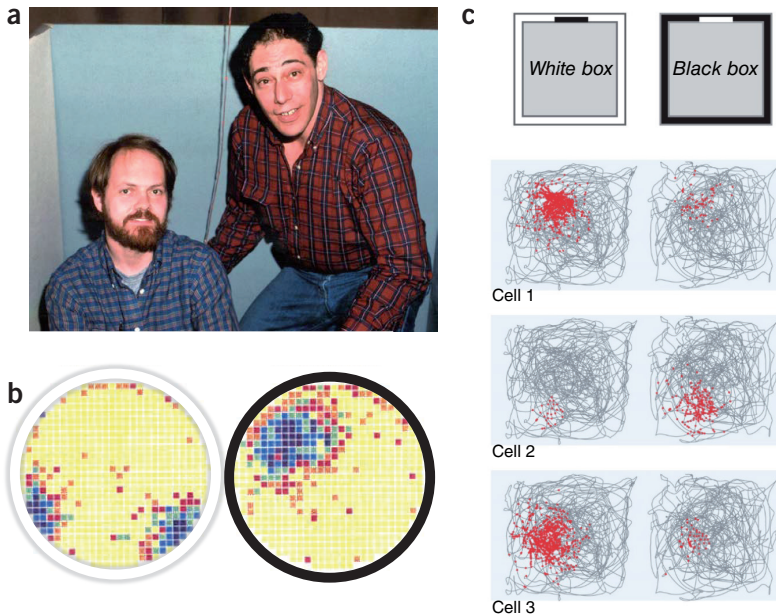


Figure 6 Remapping. (a) John Kubie and Robert Muller from SUNY Downstate Medical Center, NY. Picture courtesy of John Kubie. (b) Global remapping apparently induced by changing only the color of the recording environment¹⁰⁰. Rate maps are shown for the same place cell recorded in a white cylinder (left) and a black cylinder (right). Firing rate is color-coded from yellow (no firing) to dark blue or black (high rate). The cell fires in different regions of the cylinder (some cells are active in only one cylinder) despite changing only the color of the box. We note that the authors later confirmed, anecdotally, that they had pretrained the animals in the white and black cylinder in two different rooms, which would have allowed differences in path-integrator coordinates to control the global remapping, as later shown by Colgin *et al.*¹¹¹. (c) Rate remapping induced by changing the color of the recording environment while keeping its location constant¹⁰⁶. The rat's trajectory in a white box and a black box is shown for three cells, with spikes superimposed as red dots. Note that changing only the color of the box causes substantial change in the distribution of firing rates across cells, but firing locations are retained. Rate maps in a adapted with permission from ref. 100, Wiley. Panel c adapted with permission from ref. 265, Elsevier.

grid fields have not yet been identified in darkness in mice^{147,148}. The reason for the possible species difference is not known. Associations between path-integration coordinates and stationary cues may be weaker in mice¹⁴⁹, or grid fields of mice may simply be harder to visualize at times of increased jitter, given their smaller field size and shorter grid spacing compared to rats¹⁵⁰.

Based on the possible role of self-motion information in the formation of grid patterns, the three of us suggested, in 2006, that grid cells are part of an intrinsic path-integration-based metric for space⁹¹. A similar proposal was made the same year by a different group of investigators¹⁵¹. Both concepts bore similarities to the mechanism proposed a decade earlier from studies of place cells^{19,90}. In fact, by implementing their attractor map model for path integration on a torus, Samsonovich and McNaughton⁹⁰ indirectly predicted periodic place fields, although, at the time, the idea seemed to them too preposterous to publish, and an attempt to discover such periodicity in CA1 by running rats down a long hallway

concluded that “place field distributions can best be described by a random selection with replacement”¹⁵². A decade later, with the new data from the entorhinal cortex, it was clear that grid cells may supply the brain's spatial map with a coordinate system not available from place cells in the hippocampus, given the apparently random allocation of place fields to position¹⁵³ and the related extreme remapping across environments.

It soon turned out that if grid cells supply a metric, this metric is not always constant over time or locations. Experiments showed that when environments were stretched or rescaled, the spacing of the grid increased in the extended direction^{146,154}, in concert with either scaling or remapping in hippocampal place cells¹⁵⁵. However, these distortions of the grid pattern were recorded when the environment was changed after the animal was already familiar with it, suggesting that grid maps might be formed by path integration but linked to external cues in such a way that the latter can override the path-integration dynamics⁹⁰. Yet under

some conditions, grid cells appear to be fragmented or distorted even after extended training in a constantly shaped environment. When rats are tested in environments with discrete compartments¹⁵⁶ or irregular geometric shapes¹⁵⁷, the strict periodicity of the grid pattern is often gone. In particular, it has been shown that walls exert strong local influences on the grid pattern^{157,158}, causing distortions and rotations that can be described effectively as a shearing process¹⁵⁸. The common presence of fragmented and distorted grids has raised questions about whether grid cells are useful as a source of metric information¹⁵⁷. Countering these doubts, theoretical analyses have shown that precise symmetry may not be necessary for accurate population-based decoding of position, distance, and direction if the grid cells are all distorted in the same way¹⁵⁹. Direct behavioral evidence is needed, however, to establish how well spatial metrics can be decoded from distorted grid patterns.

Network properties of grid cells

Grid cells differ from place cells in more than one way. Not only do they have periodic firing fields but the relationship between the firing fields of different cells also follows a different rule. Whereas place cells often remap completely between environments and multiple fields can appear in large environments, with no more overlap in the subset of active cells than expected by chance^{106,153,160–162}, the ensemble activity of grid cells is normally maintained coherently from one environment to the next, without changing phase or orientation relationships between cells^{145,163}, much like in early recordings from MEC cells before grid cells were discovered²². The coherence of the grid map is particularly strong within ensembles, or modules, of similarly scaled grid cells¹⁵⁴. A similar degree of coherence is present among head direction cells^{6,7,77,78,164}, as well as in the more recently discovered populations of entorhinal border cells and speed cells^{165,166}. The coherence of grid cells and head direction cells is state-independent and persists during sleep^{167–169}. Collectively, these findings point to a fundamental difference between hippocampal and entorhinal spatial maps: hippocampal circuits are high-dimensional and capable of storing a very large number of patterns, while MEC maps are low-dimensional and rigid, expressing the same intrinsic structure in all behavioral contexts, as would be expected for a path-integration-based map that keeps metric properties constant across contexts and environments.

It was clear from the outset that grid cells come in different varieties—with different

phases, wavelengths, orientations, and field amplitudes—and that the network of grid cells is anatomically organized according to some but not all of these variables^{8,9}. While the phase of the grid pattern appeared to be distributed randomly among cells on the same tetrode, the scale of the grid showed a striking increase from dorsal to ventral recording locations in the MEC (**Fig. 7b**). In both respects, the organization of grid cells was reminiscent of that of place cells, which also appear to have random spatial relationships^{160,170,171} but show an increase in scale from dorsal to ventral^{80,81}. In the hippocampus, the scale increase is strongly coupled with decreasing gain of self-motion parameters^{84,86}. A similar gain-change may underlie the scale change in MEC, consistent with the hypothesis that the overall system parameters are dominated by path-integration mechanisms.

One question that was not settled by the earliest grid cell recordings was whether the scale gradients were smooth and gradual or instead consisted of multiple discrete maps with distinguishable scale and self-motion gain, the latter being a necessary prediction of attractor-map-based models^{91,172}. In 2007, Barry and colleagues showed, with a small cell sample, that values of grid spacing were not evenly distributed¹⁴⁶. In 2012, Stensola and colleagues were able to record activity from up to 180 grid cells in the same animal: enough to determine once and for all whether grid cells clustered in groups with similar properties¹⁵⁴. Stensola *et al.* found that grid cells were organized in at least four modules, each with their own scale, orientation, and asymmetric distortions (**Fig. 7c**). The scale change across successive grid modules could be described as a geometric progression with a constant scale factor¹⁵⁴, confirming the prior predictions^{91,172}, as well as theoretical analyses pointing to nested and modular organizations as the most efficient code for representing space at the highest-possible resolution with the lowest-possible cell number^{173,174}.

The discovery of grid cells cast new light on the mechanisms underlying formation of place cells, the very question that motivated the search for spatially modulated cells in the entorhinal cortex. The periodicity of the firing pattern and the variability of the grid scale suggested early on that place cells may emerge by a Fourier-like linear summation of output from grid cells with similar phase throughout the environment over a range of spatial scales^{91,175}. This summation mechanism might be facilitated further by coordinated gamma-frequency oscillations

in MEC and CA1 cells¹⁷⁶. Alternatively, and more in line with the sensory-integration ideas of the 1980s, place fields might be generated from any weak spatial input, so long as the hippocampal circuit contains mechanisms for amplifying a subset of these inputs, either through Hebbian plasticity or through local recurrent networks^{177–180}. The merits of these two classes of models remain to be determined. Experimental studies have shown that MEC grid cells are not necessary for the emergence of spatially tuned firing in place cells. Place fields have been reported to persist when the spatially periodic firing pattern of MEC grid cells is compromised by inactivation of septal inputs^{181,182}, and in young animals, place cells acquire stable firing fields before sharp periodic firing patterns emerge in grid cells^{183,184}. Inactivation or damage of the MEC is not sufficient to disrupt place cell firing in the hippocampus^{128,131,132,185}. However, neither of these observations rules out grid cells as a key determinant of spatially selective firing in the hippocampus. The hippocampus receives input from multiple spatially tuned entorhinal cell types, including not only grid cells but also border cells and spatially modulated cells with nonperiodic firing patterns¹⁸⁶, as well as weakly place-tuned cells in the LEC¹²⁹. Place fields may be formed from any of these inputs, by more than a single mechanism. Even pure rate changes among the MEC inputs are sufficient to completely alter the activity distribution among place cells in the hippocampus¹⁸⁵. The mechanism for grid cell to place cell or place cell to grid cell transformation may have many faces, and understanding it may require that circuitry is disentangled at a higher level of detail, possibly in terms of inputs and outputs of individual cells.

A zoo of cell types

Grid cells are abundant, especially in the superficial layers of the MEC, but not all cells are grid cells. As early as 2006, it was clear that in layers III–VI of the rat MEC, a number of cells respond to head direction¹⁸⁷ (**Fig. 7d**), very much like the head direction cells reported in the neighboring presubiculum and parasubiculum years before^{5–7,188}. The directional tuning curves of many entorhinal head direction cells were found to be broader than in presubiculum and parasubiculum, and many head direction cells responded conjunctively to location, expressing grid-like firing fields but discharging within each grid field only when the rat's face pointed in a certain direction¹⁸⁷. Head direction cells intermingled with grid cells and conjunctive grid × head

direction cells (**Fig. 7e**) throughout MEC layers III–VI, as well as in presubiculum and parasubiculum¹⁸⁹, pointing to a computational mechanism for imposing the angular component of path integration on grid cells^{19,91}.

Shortly after head direction cells were observed in recordings from the MEC, another cell type appeared on the entorhinal stage. These cells, named border cells, fired exclusively along geometric borders of the local environment: along one or sometimes several walls of the recording enclosure or along the edges of a platform^{165,190} (**Fig. 7f**). Border cells were distinct from grid cells—a border cell could never be transformed to a grid cell or vice versa—but there was overlap between border cells and head direction cells, i.e., some (conjunctive) border cells fired within their border fields only when the animal was running in one direction¹⁶⁵. Border cells intermingled with grid cells and head direction cells, particularly in layers II and III of MEC¹⁶⁵, suggesting that the three types of cells interact. However, while grid cells and head direction cells seemed to be confined to parahippocampal—and not hippocampal—regions, cells with border-like firing fields were also observed in the hippocampus¹⁹¹ and the subiculum^{192,193}, raising the possibility that firing patterns of entorhinal border cells are inherited by at least subsets of neurons in the hippocampus and subiculum^{93,194}, or vice versa.

Border cells are sparser than grid cells and head direction modulated cells, and they may comprise less than 10% of the local principal cell population¹⁶⁵, but this does not negate a significant role in shaping hippocampal–entorhinal representations. The discovery of border-like properties in several regions of the hippocampal formation confirmed, to some extent, predictions from computational models dating back to the observation that the location and shape of place fields are determined by local boundaries of the recording environment⁹³. Based on this observation, O'Keefe, Burgess, and colleagues proposed a model in which place fields are formed by summation of tuning curves from upstream 'boundary vector cells', cells with firing fields tuned to the animal's distance from a particular wall or boundary in the environment^{93,192,194}. Boundary-vector-like cells, with distance-dependent tuning curves, were reported in the subiculum¹⁹³, but, given the unidirectional wiring of the hippocampal circuit, these cells are unlikely to provide major input to hippocampal place cells. Such inputs might instead come from border cells in the MEC. On the other hand, border cells in MEC lack distance tuning, firing only along the bor-

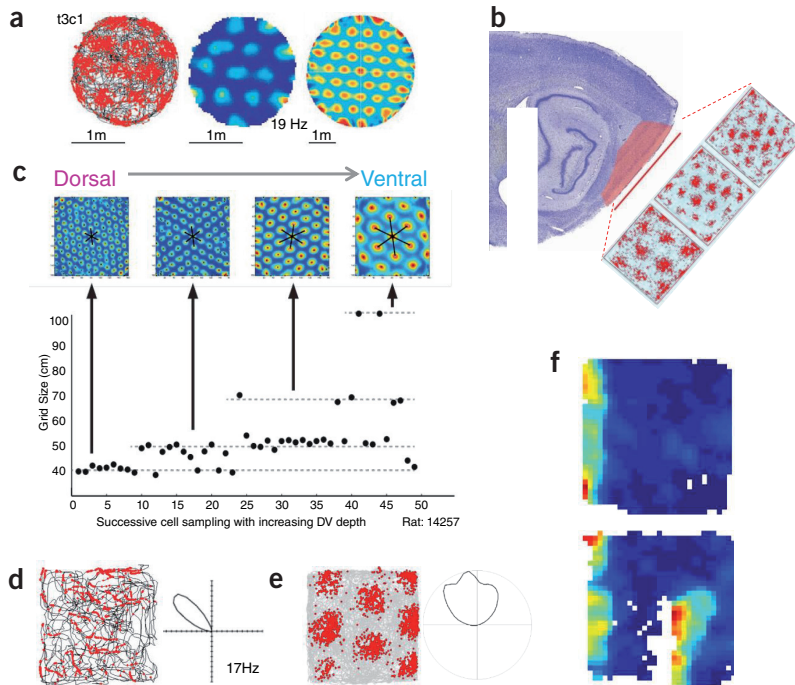


Figure 7 Grid cells and other functional cell types of the MEC. (a) Firing fields of one of the first grid cells reported in 2005 (ref. 9). Left: trajectory of the rat (black) with superimposed spike locations (red). Middle: color-coded rate map with peak rate indicated (red, peak rate; dark blue, no firing). Right: spatial autocorrelogram, color-coded from blue ($r = -1$) through green ($r = 0$) to red ($r = 1$). (b) Sagittal section of the rat brain showing the hippocampus and the MEC (red) and grid cells of different scales recorded at three locations on the dorsoventral axis (trajectories with spike locations as in a). Note the expansion of grid scale from dorsal to ventral MEC. (c) Grid cell modules¹⁵⁴. Top: autocorrelation plots showing grid patterns at successive positions along the dorsoventral axis of MEC. Bottom: grid size, defined as the distance between grid vertices, as a function of position along the dorsoventral MEC axis (positions rank-ordered). Note that the increase in grid size is not linear but discretized, following a geometric order with a factor of approximately $\sqrt{2}$. Mean grid size for each module is indicated by stippled lines. Such modularization is an essential prediction of the attractor map theory if it is to account for variable spatial scaling⁹¹. (d) Head direction cell in layer V of MEC. (e) Conjunctive grid \times head direction cell in layer III of MEC. (f) Border cell¹⁶⁵. Color-coded rate maps showing a cell with selective firing along one of the walls of the recording environment. Top: open environment. Bottom: rate map following the insertion of a wall. Note that the border cell responds to the same side of the wall insert as the main wall in the environment. Panel a reproduced with permission from ref. 9, Nature Publishing Group. Panel b adapted with permission from ref. 91, Nature Publishing Group. Panel c adapted with permission from ref. 154, Nature Publishing Group. Panels d and e adapted with permission from ref. 187, AAAS. Panel f adapted with permission from ref. 165, AAAS.

ders and not away from them. If border cells provide input to place cells, their influence might be limited to cells with firing fields in the periphery of the recording enclosure, near boundaries and not in open spaces. There is some indirect evidence for this possibility as, in juvenile rats, place cells with fields in the center of an open recording environment mature at the same slow rate as grid cells¹⁹⁵, which acquire adult-like hexagonal symmetry only late in juvenile development^{183,184}. Place cells near the borders of the recording box appear at an earlier age, similarly to entorhinal border cells¹⁹⁶. Regardless of whether border cells fulfill criteria for boundary vector cells or not, the existence of border cells,

as well as the strong asymmetries in grid patterns caused by environmental boundaries^{157,158}, point to a significant role for boundaries in defining the location of firing in place cells and grid cells, consistent with behavioral studies identifying geometry of the environment as a determinant of the animal's perception of self-location^{13,197,198}. However, these observations are not at variance with a path-integration-based account of spatial firing of grid cells. Boundaries may serve as references for path-integration-based position estimates, with resetting of the path integrator and subsequent reduction of error taking place regularly near major boundaries or landmarks^{19–21,90}. The increased variability of

grid field locations in open spaces compared to locations near the walls¹⁹⁹, as well as the instability of place fields in open spaces when spatially stable information is available only from border cells¹⁹⁵, speak in favor of a reference function for environmental boundaries, where grid and place representations are reset and corrected from drift each time the animal encounters a salient boundary.

With the identification of head direction cells and border cells, it became clear that grid cells have local access to directional information, needed for the angular component of path integration, as well as to information about the geometry of the environment needed to prevent drift in the path-integrator coordinates. Head velocity signals upstream of head direction cells, in the lateral mammillary nuclei²⁰⁰ and further upstream in the dorsal tegmental nuclei^{201,202}, might enable head direction cells to infer direction at the timescale of behavior. However, if grid cells express path integration, they must also have access to information about moment-to-moment changes in the animal's speed. Such information was known early on to be present in the hippocampus, where both place cells and fast-spiking interneurons exhibit speed tuning^{30,86,203}. Speed-responsive cells have similarly been observed in subcortical areas directly or indirectly connected with hippocampal and parahippocampal regions^{204–207}. These cells might feed into the brain's path-integration system. Speed tuning of hippocampal theta rhythm amplitude is sufficient to enable accurate reconstruction of distance traveled²⁰⁸, and distance traveled might be decoded by integrating the net discharge rate of a population of hippocampal cells or afferents of the hippocampus.

The observation of speed coding in the hippocampus and subcortical areas motivated the search for speed information locally within the MEC circuit. By 2006 it was observed that some information about speed is present in a subset of grid cells, especially in layer III and deeper¹⁸⁷, but the correlations between firing rate and speed in these cells were weak and would require decoding from large cell numbers to yield a reliable momentary speed signal¹⁶⁶. We now know that the entorhinal cortex has a distinct population of cells whose firing rates increase linearly with speed^{166,209}. In the large majority of speed-tuned MEC cells¹⁶⁶, firing rates increase linearly as a function of speed, up to 30–40 cm per s in rats. A small but significant number of cells have negative speed–rate relationships¹⁶⁶. As in the hippocampus, many of these are fast-spiking cells²¹⁰. The rates of these cells are tuned so

strongly to running speed that speed can be decoded with extreme accuracy from just half a dozen cells¹⁶⁶. Tuning profiles (slope and y -intercept of the speed–rate relationship) vary between speed cells but remain constant across environments and persist in the absence of visual cues, pointing to speed cells as yet another component of a low-dimensional path-integration-based position map in the MEC¹⁶⁶. In CA1, the gain of speed tuning varies systematically along the septo-temporal axis in register with the change in spatial scale⁸⁶. This has yet to be confirmed in MEC, but if verified it would strongly support the idea that speed cells convey the necessary information to set the grid scale.

Taken together, these observations point to a network of entorhinal and hippocampal neurons in which position, direction, and distance are encoded with sufficient accuracy to enable dynamic representation of the animal's location in an empty enclosure. However, most real-world environments differ from experimental settings, in that the available space is cluttered with objects. Salient objects may serve as references for navigation, but little is known about whether and how objects are included in the representation of self-position in the MEC. It has been shown that a subset of neurons in the LEC respond specifically at the locations of discrete objects in the recording enclosure^{211,212}. These neurons increase firing whenever the animal encounters an object at a certain location, regardless of the exact identity of the object. In a subset of these object cells, firing even persists for minutes, days, or weeks after the object is removed²¹². Whether and how these cells contribute to representation of the animal's own location has remained elusive. Theoretical models from the 1990s postulated the existence of cells with place fields, defined by the animal's vectorial relationship to salient landmarks in allocentric coordinates²¹³, and such cells are indeed found in small numbers in the hippocampus²¹⁴. These cells encode direction and distance from one or a small number of discrete objects placed at different locations in the recording arena. Now new data suggest that a class of MEC cells has more general vectorial properties. These 'object vector cells' have firing fields defined by distance and direction from an object, regardless of the object's location in the environment and regardless of what the object is²¹⁵. Thus, one main difference between object vector cells in MEC and in CA1 appears to lie in their object specificity. Perhaps, like rate remapping of hippocampal place cells, the coordinate information in CA1 is inherited from MEC, whereas the

identity information is added after the fact, possibly from LEC^{129,130,211,212}. Like rate remapping in place cells²¹⁶, at least some of the CA1 object vector cells appear to require extended experience²¹⁴.

Finally, investigators have identified a population of hippocampal cells with activity defined by the animal's egocentric orientation to a goal location. Sarel *et al.*²¹⁷ recorded from the CA1 region of flying bats, which have hippocampal–parahippocampal spatial representations similar to that of rodents^{218–220}. The investigators identified a set of cells that responded as a function of the animal's orientation toward a salient goal positioned centrally in the environment. Although the preferred orientation of the cells spanned the full 360° range relative to the direction to the goal, a large proportion of the cells in this category fired when the animal was heading directly toward the goal, ramping up their firing as the bat approached the goal. A little more than half of the cells were also place cells, but a substantial fraction did not have any significant tuning to place. Cells with essentially the same characteristics were recently reported in posterior parietal cortex¹⁷. Goal-vector cells are reminiscent of cells reported in rats in earlier hippocampal studies, in which neural firing increased in the proximity of a goal^{73,221–225}, and the finding of goal-orientation cells in both parietal cortex and hippocampus begs the question of which region is 'copying' which. Future research may determine whether similar cells are also present in the MEC circuit and whether they remap between goals and environments, like place cells, or maintain intrinsic spatial and directional relationships, like all medial entorhinal functional cell types characterized so far.

The multitude of functionally specialized cell types in the entorhinal–hippocampal space circuit is striking; however, equally striking is that many cells still express more than one type of information, particularly in the intermediate and deep layers of MEC, where many grid cells fire conjunctively for position and head direction, or position and speed, and many border cells are direction-selective^{165,166,187,226}. Conjunctive cells are recognized as essential ingredients of the 'hidden layer' for almost any type of coordinate transformation or conditional association network^{18,227–229}. A challenge for future work will be to determine how this variety and mixture of differently tuned cell types enable a dynamic representation of self-position that can be read out to guide navigation and memory for a wide variety of environments.

The role of theory: mechanisms of place cells, head direction cells, and grid cells

The abundance of functionally dedicated cell types in the entorhinal–hippocampal system has prompted investigators to look for the neural mechanisms that enable their characteristic firing patterns. Mechanisms have been sought in the properties of single cells as well as in neural networks. While details remain elusive, the preceding sections of this review have already emphasized how circumstantial evidence points to path-integration-based attractor-network properties as a key contributor to pattern formation in the entorhinal–hippocampal space system.

Attractor networks have provided starting points for models of localized firing since the earliest studies of hippocampal function. In 1949, Hebb proposed that activity may self-sustain in networks of recurrently connected neurons²³⁰. In 1977, Amari took a giant step by showing that localized firing can be maintained in networks of neurons arranged conceptually on a ring with Mexican-hat connectivity²³¹. In such architecture, each neuron has strong excitatory connections to its nearest neighbors, with excitation decreasing with distance along the ring, in contrast to inhibition, which is maintained at longer distances. Almost 20 years later, Skaggs and McNaughton and colleagues²³²; Zhang²³³; and Redish, Touretzky, and colleagues²³⁴ showed, independently, how the concept of a ring attractor with local (Gaussian) connectivity and global recurrent inhibition could be used to explain the emergence of directionally specific firing in head direction cells (Fig. 5b). The connectivity created a self-maintained activity bump, which could be induced to move around the ring in accordance with external angular velocity signals that were transmitted through a hidden layer of conjunctive head direction \times angular velocity cells¹⁸. The model explained a number of features of head direction cells, including the persistence of directional phase relationships across conditions and environments. Today, more than 20 years after its proposal, the key concepts of the ring-attractor model for head direction cells remain unchallenged, which is remarkable for theoretical models in systems neuroscience, and no competing models have surfaced. In mammals, the reciprocally connected network of the dorsal tegmental nucleus and lateral mammillary area has been proposed as a location for the ring attractor²³⁵, and in *Drosophila*, the concept of a ring attractor for directional tuning has received its first experimental support in studies of central body neurons, where a circular anatomical arrangement has been shown to

Box 1 Questions for the future

We have listed some outstanding problems in entorhinal–hippocampal space circuits that we believe can be addressed with state-of-the-art systems neuroscience tools.

1. Path-integration networks and mechanisms of grid cells and head direction cells

The performance of attractor network models for space relies on a unique and testable connectivity between functionally similar cells. With state-of-the-art tools for neural imaging, genetic tagging, and structural analysis, it may soon be possible to examine directly, in large MEC populations, the probability of connections between functionally identified neurons with various degrees of feature similarity and dissimilarity. On a longer time scale, one may hope for a direct visualization, with *in vivo* microscopy, of activity flow between connected mammalian neurons in a way that matches the animal's movement in space (similar to refs. 236,237 in flies).

2. Development of spatial network architectures

How is the specificity of the hippocampal–entorhinal spatial neural network architectures achieved during development of the nervous system? Excitatory neurons from the same radial glial progenitor are known to have stronger interconnections than other cells^{266,267}. Might such connectivity between clonally related cells underlie a possible preferential coupling between MEC cells with similar spatial or directional tuning, in the same way that cells from the same clone exhibit similarities in orientation preferences (and possibly preferential coupling) in the visual cortex^{268,269}? Does the young MEC have a topographically arranged teaching layer, with connections between clonally related cells, that during early postnatal development gives way to the largely nontopographical^{9,270} grid cell network of the adult MEC (Fig. 8 of ref. 91)? Tools have been developed for targeted analysis of the functional identity and connectivity of discrete developmental cell populations, allowing these questions to be resolved in the near future²⁷¹.

3. Including the entire entorhinal–hippocampal circuit

A key objective for a more complete understanding of entorhinal–hippocampal function will be to determine how cell types with different functional correlates map onto the variety of morphological or neurochemical cell types and their unique connectivity patterns. Recent data suggest that, in layer II of MEC, both stellate and pyramidal cells can be grid cells, although stellate cells may comprise the majority of them^{256,257,272–275}. If so, are grid patterns created independently in these two cell classes, or does one of them inherit the grid from the other?

4. Read-out

Position can be decoded from grid cells and place cells, with greater accuracy in grid cells than place cells if the population is multimodular and scaled in particular ways^{159,173,174,276}. Whether neural circuits decode information in the same way remains to be determined, however. Do neurons have access to grid cells with different phase relationships or different spacing; do they integrate information from grid cells with information from border cells or head direction cells? If so, where are these neurons and how do they communicate with neocortical regions involved in strategy formation and decision-making? Most research on the mechanisms of spatial coding in hippocampus has focused on the nature of the inputs that contribute to it, and less is known about the impact of hippocampal output on coding dynamics in the widespread regions of neocortex and other areas to which the hippocampal formation projects. The impact of outputs from the entorhinal–hippocampal circuit will perhaps constitute a new frontier in the study of this system.

5. Moving toward naturalistic environments

Natural environments are large, three-dimensional, compartmentalized, nested, and full of objects. Ultimately, studies of the hippocampal–entorhinal circuit should explore how cells map environments of shapes, sizes, and content more comparable to the animal's natural habitat²⁷⁷. Are grid cells, head direction cells, and place cells used only for local mapping, in the range of a few meters, or is the entorhinal–hippocampal network used also for extended spaces, and if so, how? Is there a single continuous map, or are there different maps for different local spaces, as proposed by theoretical studies²⁷⁸, as well as observations in compartmentalized laboratory environments¹⁵⁶? If the latter is true, how are the map fragments connected? And how is space coded in large and three-dimensional environments²⁷⁷? In flying bats, place cells have spherical firing fields²⁷⁹ and head direction cells are tuned to all three axes of orientation²²⁰. Whether such volumetric coding extends to terrestrial animals remains unsettled, although experimental data suggest that, in rats, head direction is encoded not only by classical azimuth-sensitive head direction cells but also by cells in the lateral mammillary bodies that respond to head pitch²⁰⁰. Observations in rats also suggest that the tilt of a surface is factored into hippocampal and entorhinal representations of space^{280,281}.

6. Representation of time

Understanding space and memory requires understanding time. Direct representation of the passage of time was not observed in hippocampal neurons until the Buzsáki and Eichenbaum groups showed that, when animals run for a known interval at a steady location, in a running wheel²⁸² or on a treadmill²⁸³, hippocampal neurons fire successively at distinct times during the interval, following the same order on each trial. Cells with similar properties are present in the MEC²⁸⁴. Most of these 'time cells' have discrete place or grid fields in standard spatial foraging tasks. Different assemblies and sequences of hippocampal time cells are active in different task configurations²⁸³, suggesting that hippocampal ensembles encode temporally organized information much the same way they represent space. The observation of time cells is a provocative finding that may share properties with mechanisms underlying path-integration-based representation of location, but the temporally confined firing fields of time cells do not disappear when time and distance are decoupled by restraining

(continued)

Box 1 (continued)

the animal²⁸⁵ or changing the speed of the treadmill²⁸⁶, suggesting that sequences do not exclusively reflect the number of steps at the task location. Certainly the relationship between representations of space and time and the role of time cells in perception and recall of time require further study. While time cells have firing fields in the order of a few seconds, and assemblies of time cells can represent events at the scale of tens of seconds, encoding of longer temporal distances may require different mechanisms. One may speculate that the spontaneous drift over hours and days in the firing properties of place cells in CA2 and (to a lesser extent) CA1 (refs. 287–289), as well as cell populations in LEC²⁹⁰, may possess the power to encode temporally distant events as distinguishable memories.

7. Beyond physical space

Do grid cells and other spatially modulated cells encode information beyond physical space, as suggested by O'Keefe and Nadel⁶⁵? Evidence for such an extension of functions was reported recently in a task in which rats press a lever to alter the frequency of a sound on a continuous scale; in this experiment, hippocampal and entorhinal cells display frequency fields resembling place fields during navigation of physical space²⁹¹. Further functional expansion might be expected in primates. Indeed, in monkeys, hippocampal and entorhinal cells fire in patterns defined not by the animal's location in space but by where it moves its eyes on a visual scene^{255,292,293}. This observation raises the possibility that place and grid cells create a map of visual space using eye movement signals instead of locomotor information to support coordinate transformation, without having to change any other computational elements of the circuit. In humans^{294,295}, grid cells may take on functions in conceptual mapping²⁹⁶. The possible adoption of grid cells as a metric for navigating abstract spaces would be consistent with the idea that hippocampal circuits first evolved for representation of space and later acquired the capacity for imaginary navigation^{49,65,297,298}. This expansion of functions would be reminiscent of the way cortices originally involved in object recognition formed the basis for a visual word form area during the evolution of written language processing in the human cortex²⁹⁹.

underlie firing in neurons that represent orientation relative to landmarks^{236,237}.

Only a year after the introduction of velocity-driven ring attractors to models of head direction cells, it was acknowledged that a similar integration mechanism might apply for position mapping in two dimensions, as expressed in hippocampal place cells^{19,90,233,238,239} (Fig. 5c,d). In the position version of the model, neurons were arranged conceptually according to their location of firing in two-dimensional space. A matrix of recurrent connections was generated, in which excitation decreased with the distance between neurons on the sheet. In combination with global inhibition, self-excitation between similarly tuned cells maintained localized firing. A path-integration mechanism moved the activity bump across the network in accordance with the animal's position in the environment, using conjunctive head direction \times place cells, in the same way that angular velocity inputs moved the bump in the ring attractor for head direction cells. The model was proposed to apply for any neural architecture of the hippocampal system, but with the knowledge that existed in the 1990s, the implementation was focused on area CA3 of the hippocampus. This explained a number of properties of place cells but faced one major challenge: the subset of active hippocampal neurons remaps across environments and circumstances^{71,100–102}. For position to be computed in place cells, some sort of independent architecture for each environment would then be required. This is computationally possible^{90,240} but nonetheless raises the question of whether a single network matrix, expressed in all environments, would not

be more efficient^{21,239}. A few years later it became apparent that such low-dimensional architecture exists in the entorhinal cortex.

When grid cells entered the research arena in 2005 (ref. 9), it was quite obvious that the dynamics proposed for localized firing in place cells might take place also in parahippocampal regions^{91,151,239}, as alluded to already by Samsonovitch and McNaughton⁹⁰. In the first models proposed after the discovery of grid cells^{91,151}, cells were arranged on a matrix according to the phase of the grid. A bump of activity was formed when cells with similar phases were connected through excitatory connections, in the presence of global inhibition. Competitive network interactions led to multiple activity bumps¹⁵¹, or toroidal connectivity caused a single bump that returned periodically to the same location⁹¹. Under certain conditions, in the presence of tonic excitatory input, a radius of inhibitory connectivity was sufficient to generate hexagonally patterned firing, without intrinsic excitatory connections^{241–244}.

Whether a path-integration-based attractor-network architecture exists in MEC remains to be determined, but there is indirect evidence for this possibility. First, correspondence between movement and displacement on the neural sheet can only be maintained so long as the participating grid cells have a common scale and orientation. Grid cells exist at a range of scales, suggesting that, to maintain the correspondence, grid cells must be organized in functionally independent grid modules, all with their own spacing and orientation^{91,172}. Experimental evidence suggests that such a modular functional organization is indeed present^{146,154}.

A second observation consistent with a path-integration-dependent attractor architecture is the maintenance of a single grid-phase structure across environments, tasks and brain states^{145,163,168,169}, which would be expected if MEC neurons are organized as strongly interconnected networks in which external inputs recruit the same subset of neurons under a wide range of starting conditions. The strongest prediction of the attractor models, however, is perhaps that grid cells with similar grid phases have enhanced connectivity. Statistical analysis of firing patterns in simultaneously recorded grid cells confirm this prediction^{245,246}, but direct measurements of connections between functionally verified cell types are still missing.

Attractor models do not provide the only possible explanation of how grid patterns might be created. For several years, a competing class of models, based on properties of the hippocampal theta-frequency network rhythm^{60–62}, suggested that grid patterns were generated as a result of wave interference between a constant global theta oscillation and a velocity-controlled cell-specific theta oscillation^{247–250}. The model can be traced back to O'Keefe and Recce's observation, in the early 1990s, that, as animals move through the place field of a place cell on a linear track, the spike times of the cell move forward across the cycle of background theta oscillations²⁵¹. As the animal moves through the field, the theta phase of the spikes moves progressively forward also in space, and is in fact more strongly correlated with location than with time^{251,252}. This observation suggested to O'Keefe and colleagues that position could be calculated from the interference pattern between the global

theta rhythm and a velocity-dependent oscillator specific to the cell. If position reflected peaks of the interference pattern, however, the firing positions should be periodic, which, for place cells, they were not. With the discovery of grid cells, the model was instantly revised and grid patterns were suggested to emerge from interference with velocity-controlled oscillators controlled by the projection of velocity in three directions separated by 60° intervals onto three separate dendrites^{247–249}. Interference with the global oscillator led to a band-like spatial-activity pattern along each orientation, and the combination of bands led to a hexagonal pattern. The oscillatory interference models guided some of the most influential studies of grid formation, but in the end, accumulating evidence, such as the biophysical implausibility of independent dendritic oscillations²⁵³, the sensitivity to period irregularity²⁵⁴, the persistence of grid patterns in the absence of theta oscillations^{219,255}, the presence of a ramping depolarization, and the absence of a theta interference oscillation, in intracellular recordings from MEC cells^{256,257}, suggested that oscillatory interference is not the mechanism of the grid pattern. Yet phase precession is a reliable observation. Although it may not explain periodicity in grid cells, phase precession causes sequences of place cell activation to be replicated, in compressed format, within individual theta cycles, an effect that may be used by hippocampal circuits to store temporal sequences in addition to mere locations²⁵². Indeed, as recognized by several investigators soon after phase precession was discovered^{252,258,259}, theta rhythm and phase precession may exist precisely to enable memory for spatial and temporal sequences.

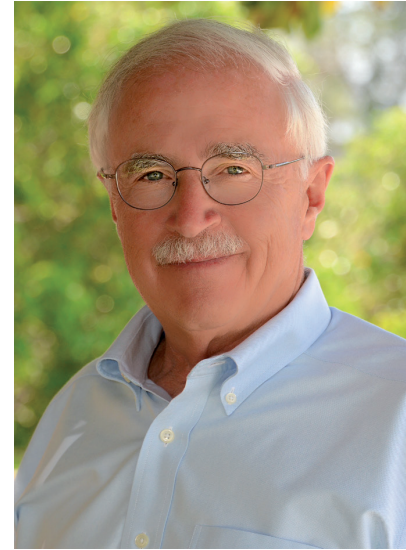
The evidence against the oscillatory-interference model did not, however, rule out single-cell properties as determinants of the grid pattern. Kropff and Treves²⁴ showed how hexagonally patterned firing may arise through competitive Hebbian plasticity in a path-integration-independent manner in feedforward networks in which neurons undergo neuronal fatigue or adaptation. Because the emergence of grids in this model required many iterations, it was proposed that the adaptation mechanism contributed particularly to development of the network in young animals and that the coherence of phase and orientation relationships across environments was the result of recurrent connections that were added as the cortex matured²⁶⁰. Thus, competitive Hebbian plasticity offers an alternative mechanism for grid formation, although this mechanism may coexist with attractor-network architectures²⁶¹. Regardless of mechanism, accounts of grid formation must consider not only

intrinsic MEC dynamics but also how external inputs from the hippocampus²⁴², the medial septum^{181,182}, and locomotor^{204–207,262} and head direction circuits²⁶³ contribute to the emergence of grid patterns (Box 1).

Perspective

The search for a hippocampal positioning system began with the discovery of place cells in 1971. We have illustrated how the next few decades were characterized by attempts to find the determinants of spatially localized firing, with a focus on the sensory sources. As we entered the 1990s, the discovery of head direction cells and the turn to population dynamics prepared the field for more-targeted investigation of the circuit operations underlying place field formation and spatial mapping. The 1990s showed how ensembles of simultaneously recorded hippocampal neurons encoded functions that could not be read out from the activity of individual neurons. From around 2000, with increasing awareness that these ensembles likely extended beyond the hippocampus, investigators entered the entorhinal cortex, and an intricate circuit of grid cells and other specialized cell types was discovered there. The investigation of space has been brought to a new level, where it is possible to ask questions about how functions emerge through interactions within extended networks of heterogeneously connected cell types and subsystems.

While we will certainly learn more about the neural origins of spatial cognition during the years to come (Box 1), studies of spatial representation and navigation are informative about cortical functions in a wider sense. The ease with which spatial functions can be examined in the hippocampal formations of a number of mammals has made the study of the positioning system an area in which investigators pioneer the development and testing of sophisticated computational neural-network models. Few other areas of systems neuroscience have benefited so strongly from the interplay between computational and experimental neuroscience. Place cells and their entorhinal counterparts have helped open the cortex to studies of neural computation, allowing researchers to identify generic circuit motifs that may be expressed not only in the spatial circuits of the hippocampus and entorhinal cortex but across widespread regions of the brain. Almost 50 years after place cells were discovered, place cells and their parahippocampal counterparts have become one of the most powerful tools we have for understanding cortical computation and spatial mapping, and navigation may become one of the first cognitive functions to be understood in mechanistic terms.



Howard Eichenbaum (1947–2017). Few individuals have contributed more to the modern understanding of hippocampal memory function, with place cells as a key component, than Howard Eichenbaum, who sadly passed away, far too early, before the publication of this article. Photo credit: photographer Dan Kirksey, KDKC Photos, Escondido, CA.

IN MEMORIAM

In memoriam, Howard B. Eichenbaum (1947–2017). The field of hippocampal and memory research mourns the loss of our friend and colleague Howard, who passed away unexpectedly recently. Howard's contributions to the field were immense, both scientifically and in service. His research was mostly focused on one of the major aspects that we have explicitly not covered in this review: the role of the hippocampus in memory. Over the years, his position evolved from that of an unafraid and much-needed devil's advocate against the pure spatial map hypothesis towards what is now the general consensus view that spatial coding provides a foundation on top of which sensory and event-specific memory is superimposed, and he became a pioneer in the study of how time and temporal order also play a role. His thinking on hippocampal–cortical interactions in memory organization and control is beautifully summarized in his 2017 *Annual Review of Psychology* article⁴⁷.

ACKNOWLEDGMENTS

The work was supported by two Advanced Investigator Grants from the European Research Council (GRIDCODE – grant no. 338865 to E.I.M.; 'ENSEMBLE'; Grant Agreement no. 268598, to M.-B.M.), and by the Centre of Excellence scheme of the Research Council of Norway (Centre for Neural Computation, grant number 223262 to M.-B.M. and E.I.M.), the Kavli Foundation (M.-B.M. and E.I.M.), and National Science Foundation Grant 1631465 to B.L.M.

COMMENTARY

COMPETING FINANCIAL INTERESTS

The authors declare no competing financial interests.

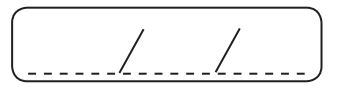
- Balint, R. *Monatsschr. Psychiatr. Neurol.* **25**, 5–81 (1909).
- Holmes, G. *BMJ* **2**, 230–233 (1919).
- Redish, A.D. *Beyond the Cognitive Map: From Place Cells to Episodic Memory* (MIT Press, 1999).
- O'Keefe, J. & Dostrovsky, J. *Brain Res.* **34**, 171–175 (1971).
- Ranck, J.B. Jr. in *Electrical Activity of the Archicortex*, (eds. Buzsáki, G. & Vanderwolf, C.H.) pp. 217–20 (Akademiai Kiado, 1985).
- Taube, J.S., Muller, R.U. & Ranck, J.B. Jr. *J. Neurosci.* **10**, 420–435 (1990).
- Taube, J.S., Muller, R.U. & Ranck, J.B. Jr. *J. Neurosci.* **10**, 436–447 (1990).
- Fyhn, M., Molden, S., Witter, M.P., Moser, E.I. & Moser, M.B. *Science* **305**, 1258–1264 (2004).
- Hafting, T., Fyhn, M., Molden, S., Moser, M.-B. & Moser, E.I. *Nature* **436**, 801–806 (2005).
- O'Keefe, J. *Exp. Neurol.* **51**, 78–109 (1976).
- Barlow, J.S. *J. Theor. Biol.* **6**, 76–117 (1964).
- Mittelstaedt, M.-L. & Mittelstaedt, H. *Naturwissenschaften* **67**, 566–567 (1980).
- Gallistel, C.R. *The Organization of Learning* (MIT Press, 1990).
- Etienne, A.S. & Jeffery, K.J. *Hippocampus* **14**, 180–192 (2004).
- Stein, J.F. Q. *J. Exp. Physiol.* **74**, 583–606 (1989).
- Snyder, L.H., Grieve, K.L., Brotchie, P. & Andersen, R.A. *Nature* **394**, 887–891 (1998).
- Wilber, A.A., Clark, B.J., Forster, T.C., Tatsuno, M. & McNaughton, B.L. *J. Neurosci.* **34**, 5431–5446 (2014).
- McNaughton, B.L., Chen, L.L. & Markus, E.J. *J. Cogn. Neurosci.* **3**, 190–202 (1991).
- McNaughton, B.L. *et al. J. Exp. Biol.* **199**, 173–185 (1996).
- Touretzky, D.S. & Redish, A.D. *Hippocampus* **6**, 247–270 (1996).
- Redish, A.D. & Touretzky, D.S. *Hippocampus* **7**, 15–35 (1997).
- Quirk, G.J., Muller, R.U., Kubie, J.L. & Ranck, J.B. Jr. *J. Neurosci.* **12**, 1945–1963 (1992).
- Sharp, P.E. *Behav. Brain Res.* **85**, 71–92 (1997).
- Kropff, E. & Treves, A. *Hippocampus* **18**, 1256–1269 (2008).
- Hayman, R. & Burgess, N. *Neuron* **82**, 721–722 (2014).
- Evans, T., Bicanski, A., Bush, D. & Burgess, N. *J. Physiol. (Lond.)* **594**, 6535–6546 (2016).
- Ainsworth, A., Gaffan, G.D., O'Keefe, J. & Sampson, R. *J. Physiol. (Lond.)* **202**, 80P–82P (1969).
- Segal, M. & Olds, J. *J. Neurophysiol.* **35**, 680–690 (1972).
- Ranck, J.B. Jr. *Exp. Neurol.* **41**, 461–531 (1973).
- McNaughton, B.L., Barnes, C.A. & O'Keefe, J. *Exp. Brain Res.* **52**, 41–49 (1983).
- Muller, R.U., Kubie, J.L. & Ranck, J.B. Jr. *J. Neurosci.* **7**, 1935–1950 (1987).
- McNaughton, B.L., O'Keefe, J. & Barnes, C.A. *J. Neurosci. Methods* **8**, 391–397 (1983).
- Wilson, M.A. & McNaughton, B.L. *Science* **261**, 1055–1058 (1993).
- Buzsáki, G. *Nat. Neurosci.* **7**, 446–451 (2004).
- Boyden, E.S., Zhang, F., Bamberg, E., Nagel, G. & Deisseroth, K. *Nat. Neurosci.* **8**, 1263–1268 (2005).
- Armbruster, B.N., Li, X., Pausch, M.H., Herlitze, S. & Roth, B.L. *Proc. Natl. Acad. Sci. USA* **104**, 5163–5168 (2007).
- Deisseroth, K. *Nat. Neurosci.* **18**, 1213–1225 (2015).
- Ziv, Y. *et al. Nat. Neurosci.* **16**, 264–266 (2013).
- Dombeck, D.A., Khabbazi, A.N., Collman, F., Adelman, T.L. & Tank, D.W. *Neuron* **56**, 43–57 (2007).
- Dombeck, D.A., Harvey, C.D., Tian, L., Looger, L.L. & Tank, D.W. *Nat. Neurosci.* **13**, 1433–1440 (2010).
- Scoville, W.B. & Milner, B. *J. Neurol. Neurosurg. Psychiatry* **20**, 11–21 (1957).
- Milner, B. *Neuropsychologia* **6**, 215–234 (1968).
- Squire, L.R. *Psychol. Rev.* **99**, 195–231 (1992).
- Cohen, N.J. & Eichenbaum, H. *Memory, Amnesia, and the Hippocampal System* (MIT Press, 1993).
- Tulving, E. & Markowitsch, H.J. *Hippocampus* **8**, 198–204 (1998).
- Martin, S.J., Grimwood, P.D. & Morris, R.G. *Annu. Rev. Neurosci.* **23**, 649–711 (2000).
- Eichenbaum, H. *Annu. Rev. Psychol.* **68**, 19–45 (2017).
- Eichenbaum, H., Dudchenko, P., Wood, E., Shapiro, M. & Tanila, H. *Neuron* **23**, 209–226 (1999).
- Buzsáki, G. & Moser, E.I. *Nat. Neurosci.* **16**, 130–138 (2013).
- Moser, M.-B., Rowland, D.C. & Moser, E.I. *Cold Spring Harb. Perspect. Biol.* **7**, a021808 (2015).
- Buzsáki, G. *Neuroscience* **31**, 551–570 (1989).
- Wilson, M.A. & McNaughton, B.L. *Science* **265**, 676–679 (1994).
- McClelland, J.L., McNaughton, B.L. & O'Reilly, R.C. *Psychol. Rev.* **102**, 419–457 (1995).
- Dragoi, G. & Tonegawa, S. *Nature* **469**, 397–401 (2011).
- Poucet, B. *et al. Rev. Neurosci.* **15**, 89–107 (2004).
- Shapiro, M.L., Kennedy, P.J. & Ferbinteanu, J. *Curr. Opin. Neurobiol.* **16**, 701–709 (2006).
- Johnson, A. & Redish, A.D. *J. Neurosci.* **27**, 12176–12189 (2007).
- Johnson, A., van der Meer, M.A. & Redish, A.D. *Curr. Opin. Neurobiol.* **17**, 692–697 (2007).
- Pfeiffer, B.E. & Foster, D.J. *Nature* **497**, 74–79 (2013).
- Buzsáki, G., Leung, L.W. & Vanderwolf, C.H. *Brain Res.* **287**, 139–171 (1983).
- Buzsáki, G. *Neuron* **33**, 325–340 (2002).
- Colgin, L.L. *Nat. Rev. Neurosci.* **17**, 239–249 (2016).
- Best, P.J. & Ranck, J.B. Jr. *Soc. Neurosci. Abstr* **1**, 837 (1975).
- Tolman, E.C. *Psychol. Rev.* **55**, 189–208 (1948).
- O'Keefe, J. & Nadel, L. *The Hippocampus as a Cognitive Map* (Clarendon Press, Oxford, 1978).
- O'Keefe, J. & Black, A.H. in *Functions of the Septo-Hippocampal System* (CIBA Foundation Symposium No. 58) pp. 179–198 (Elsevier, 1977).
- Muller, R.U., Bostock, E., Taube, J.S. & Kubie, J.L. *J. Neurosci.* **14**, 7235–7251 (1994).
- O'Keefe, J. & Conway, D.H. *Exp. Brain Res.* **31**, 573–590 (1978).
- O'Keefe, J. & Speakman, A. *Exp. Brain Res.* **68**, 1–27 (1987).
- Quirk, G.J., Muller, R.U. & Kubie, J.L. *J. Neurosci.* **10**, 2008–2017 (1990).
- Muller, R.U. & Kubie, J.L. *J. Neurosci.* **7**, 1951–1968 (1987).
- Sharp, P.E., Kubie, J.L. & Muller, R.U. *J. Neurosci.* **10**, 3093–3105 (1990).
- Gothard, K.M., Skaggs, W.E., Moore, K.M. & McNaughton, B.L. *J. Neurosci.* **16**, 823–835 (1996).
- Gothard, K.M., Skaggs, W.E. & McNaughton, B.L. *J. Neurosci.* **16**, 8027–8040 (1996).
- Jeffery, K.J., Donnett, J.G., Burgess, N. & O'Keefe, J.M. *Exp. Brain Res.* **117**, 131–142 (1997).
- Jeffery, K.J. & O'Keefe, J.M. *Exp. Brain Res.* **127**, 151–161 (1999).
- Knierim, J.J., Kudrimoti, H.S. & McNaughton, B.L. *J. Neurosci.* **15**, 1648–1659 (1995).
- Knierim, J.J., Kudrimoti, H.S. & McNaughton, B.L. *J. Neurophysiol.* **80**, 425–446 (1998).
- Battaglia, F.P., Sutherland, G.R. & McNaughton, B.L. *J. Neurosci.* **24**, 4541–4550 (2004).
- Jung, M.W., Wiener, S.I. & McNaughton, B.L. *J. Neurosci.* **14**, 7347–7356 (1994).
- Kjelstrup, K.B. *et al. Science* **321**, 140–143 (2008).
- Barnes, C.A., Suster, M.S., Shen, J. & McNaughton, B.L. *Nature* **388**, 272–275 (1997).
- Kentros, C. *et al. J. Neurosci.* **20**, 2121–2126 (1998).
- Terrazas, A. *et al. J. Neurosci.* **25**, 8085–8096 (2005).
- Foster, T.C., Castro, C.A. & McNaughton, B.L. *Science* **244**, 1580–1582 (1989).
- Maurer, A.P., Vanrhoads, S.R., Sutherland, G.R., Lipa, P. & McNaughton, B.L. *Hippocampus* **15**, 841–852 (2005).
- Ranck, J.B. Jr. Foreword: history of the discovery of head direction cells. in *Head Direction Cells and the Neural Mechanisms of Spatial Orientation*. (eds. Wiener, S.I. & Taube, J.S.) xi–xiii (MIT Press, 2005).
- Chen, L.L., Lin, L.H., Barnes, C.A. & McNaughton, B.L. *Exp. Brain Res.* **101**, 24–34 (1994).
- Taube, J.S. *Annu. Rev. Neurosci.* **30**, 181–207 (2007).
- Samsonovich, A. & McNaughton, B.L. *J. Neurosci.* **17**, 5900–5920 (1997).
- McNaughton, B.L., Battaglia, F.P., Jensen, O., Moser, E.I. & Moser, M.B. *Nat. Rev. Neurosci.* **7**, 663–678 (2006).
- Yoder, R.M., Clark, B.J. & Taube, J.S. *Trends Neurosci.* **34**, 561–571 (2011).
- O'Keefe, J. & Burgess, N. *Nature* **381**, 425–428 (1996).
- Chen, G., King, J.A., Burgess, N. & O'Keefe, J. *Proc. Natl. Acad. Sci. USA* **110**, 378–383 (2013).
- Ravassard, P. *et al. Science* **340**, 1342–1346 (2013).
- Aghajian, Z.M. *et al. Nat. Neurosci.* **18**, 121–128 (2015).
- Aronov, D. & Tank, D.W. *Neuron* **84**, 442–456 (2014).
- Stackman, R.W., Clark, A.S. & Taube, J.S. *Hippocampus* **12**, 291–303 (2002).
- Russell, N.A., Horii, A., Smith, P.F., Darlington, C.L. & Bilkey, D.K. *J. Neurosci.* **23**, 6490–6498 (2003).
- Bostock, E., Muller, R.U. & Kubie, J.L. *Hippocampus* **1**, 193–205 (1991).
- Kubie, J.L. & Muller, R.U. *Hippocampus* **1**, 240–242 (1991).
- Muller, R.U., Kubie, J.L., Bostock, E.M., Taube, J.S. & Quirk, G.J. in *Brain and Space* (ed. Paillard, J.) 296–333 (Oxford University Press, 1991).
- Knierim, J.J. & McNaughton, B.L. *J. Neurophysiol.* **85**, 105–116 (2001).
- Paz-Villagrán, V., Save, E. & Poucet, B. *Eur. J. Neurosci.* **20**, 1379–1390 (2004).
- Spiers, H.J., Hayman, R.M., Jovalekic, A., Marozzi, E. & Jeffery, K.J. *Cereb. Cortex* **25**, 10–25 (2015).
- Leutgeb, S. *et al. Science* **309**, 619–623 (2005).
- Markus, E.J. *et al. J. Neurosci.* **15**, 7079–7094 (1995).
- Wood, E.R., Dudchenko, P.A., Robitsek, R.J. & Eichenbaum, H. *Neuron* **27**, 623–633 (2000).
- Anderson, M.I. & Jeffery, K.J. *J. Neurosci.* **23**, 8827–8835 (2003).
- Bower, M.R., Euston, D.R. & McNaughton, B.L. *J. Neurosci.* **25**, 1313–1323 (2005).
- Colgin, L.L. *et al. J. Neurophysiol.* **104**, 35–50 (2010).
- Wiener, S.I., Paul, C.A. & Eichenbaum, H. *J. Neurosci.* **9**, 2737–2763 (1989).
- Wood, E.R., Dudchenko, P.A. & Eichenbaum, H. *Nature* **397**, 613–616 (1999).
- Igarashi, K.M., Lu, L., Colgin, L.L., Moser, M.-B. & Moser, E.I. *Nature* **510**, 143–147 (2014).
- Young, B.J., Fox, G.D. & Eichenbaum, H. *J. Neurosci.* **14**, 6553–6563 (1994).
- Segal, M., Disterhoft, J.F. & Olds, J. *Science* **175**, 792–794 (1972).
- Berger, T.W., Alger, B. & Thompson, R.F. *Science* **192**, 483–485 (1976).
- Hampson, R.E., Heysler, C.J. & Deadwyler, S.A. *Behav. Neurosci.* **107**, 715–739 (1993).
- Olypher, A.V., Lansky, P. & Fenton, A.A. *Neuroscience* **111**, 553–566 (2002).
- Komorowski, R.W., Manns, J.R. & Eichenbaum, H. *J. Neurosci.* **29**, 9918–9929 (2009).
- Teyler, T.J. & DiScenna, P. *Behav. Neurosci.* **100**, 147–154 (1986).
- Teyler, T.J. & Rudy, J.W. *Hippocampus* **17**, 1158–1169 (2007).
- McNaughton, B.L. *Artif. Intell.* **174**, 205–214 (2010).
- Tanila, H., Shapiro, M.L. & Eichenbaum, H. *Hippocampus* **7**, 613–623 (1997).
- Shapiro, M.L., Tanila, H. & Eichenbaum, H. *Hippocampus* **7**, 624–642 (1997).
- Knierim, J.J. *J. Neurosci.* **22**, 6254–6264 (2002).
- Lee, I., Yoganarasimha, D., Rao, G. & Knierim, J.J. *Nature* **430**, 456–459 (2004).

128. Hales, J.B. *et al.* *Cell Reports* **9**, 893–901 (2014).
129. Hargreaves, E.L., Rao, G., Lee, I. & Knierim, J.J. *Science* **308**, 1792–1794 (2005).
130. Lu, L. *et al.* *Nat. Neurosci.* **16**, 1085–1093 (2013).
131. Miao, C. *et al.* *Neuron* **88**, 590–603 (2015).
132. Ormond, J. & McNaughton, B.L. *Proc. Natl. Acad. Sci. USA* **112**, 4116–4121 (2015).
133. Marr, D. *Phil. Trans. R. Soc. Lond. B* **262**, 23–81 (1971).
134. McNaughton, B.L. & Morris, R.G. *Trends Neurosci.* **10**, 408–415 (1987).
135. McNaughton, B.L. & Nadel, L. in *Neuroscience and Connectionist Theory* (eds. Gluck, M.A. & Rumelhart, D.E.) 1–63 (Lawrence Erlbaum, 1990).
136. Treves, A. & Rolls, E.T. *Hippocampus* **2**, 189–199 (1992).
137. Barnes, C.A., McNaughton, B.L., Mizumori, S.J., Leonard, B.W. & Lin, L.H. *Prog. Brain Res.* **83**, 287–300 (1990).
138. Sharp, P.E. & Green, C. *J. Neurosci.* **14**, 2339–2356 (1994).
139. Frank, L.M., Brown, E.N. & Wilson, M. *Neuron* **27**, 169–178 (2000).
140. McNaughton, B.L., Barnes, C.A., Meltzer, J. & Sutherland, R.J. *Exp. Brain Res.* **76**, 485–496 (1989).
141. Mizumori, S.J., McNaughton, B.L., Barnes, C.A. & Fox, K.B. *J. Neurosci.* **9**, 3915–3928 (1989).
142. Brun, V.H. *et al.* *Science* **296**, 2243–2246 (2002).
143. Sharp, P.E. *Hippocampus* **9**, 432–443 (1999).
144. Witter, M.P., Groenewegen, H.J., Lopes da Silva, F.H. & Lohman, A.H. *Prog. Neurobiol.* **33**, 161–253 (1989).
145. Fyhn, M., Hafting, T., Treves, A., Moser, M.B. & Moser, E.I. *Nature* **446**, 190–194 (2007).
146. Barry, C., Hayman, R., Burgess, N. & Jeffery, K.J. *Nat. Neurosci.* **10**, 682–684 (2007).
147. Chen, G., Manson, D., Cacucci, F. & Wills, T.J. *Curr. Biol.* **26**, 2335–2342 (2016).
148. Pérez-Escobar, J.A., Kornienko, O., Latuske, P., Kohler, L. & Allen, K. *Elife* **5**, e16937 (2016).
149. Kentros, C.G., Agnihotri, N.T., Streater, S., Hawkins, R.D. & Kandel, E.R. *Neuron* **42**, 283–295 (2004).
150. Fyhn, M., Hafting, T., Witter, M.P., Moser, E.I. & Moser, M.-B. *Hippocampus* **18**, 1230–1238 (2008).
151. Fuhs, M.C. & Touretzky, D.S. *J. Neurosci.* **26**, 4266–4276 (2006).
152. Gerrard, J.L., *et al.* *Soc. Neurosci. Abstr.* 643.12 (2001).
153. Rich, P.D., Liaw, H.P. & Lee, A.K. *Science* **345**, 814–817 (2014).
154. Stensola, H. *et al.* *Nature* **492**, 72–78 (2012).
155. Barry, C., Ginzberg, L.L., O’Keefe, J. & Burgess, N. *Proc. Natl. Acad. Sci. USA* **109**, 17687–17692 (2012).
156. Derdikman, D. *et al.* *Nat. Neurosci.* **12**, 1325–1332 (2009).
157. Krupic, J., Bauza, M., Burton, S., Barry, C. & O’Keefe, J. *Nature* **518**, 232–235 (2015).
158. Stensola, T., Stensola, H., Moser, M.-B. & Moser, E.I. *Nature* **518**, 207–212 (2015).
159. Stemmler, M., Mathis, A. & Herz, A.V. *Sci. Adv.* **1**, e1500816 (2015).
160. Redish, A.D. *et al.* *J. Neurosci.* **21**, RC134 (2001).
161. Leutgeb, S., Leutgeb, J.K., Treves, A., Moser, M.B. & Moser, E.I. *Science* **305**, 1295–1298 (2004).
162. Alme, C.B. *et al.* *Proc. Natl. Acad. Sci. USA* **111**, 18428–18435 (2014).
163. Yoon, K. *et al.* *Nat. Neurosci.* **16**, 1077–1084 (2013).
164. Yoganarasimha, D., Yu, X. & Knierim, J.J. *J. Neurosci.* **26**, 622–631 (2006).
165. Solstad, T., Boccara, C.N., Kropff, E., Moser, M.-B. & Moser, E.I. *Science* **322**, 1865–1868 (2008).
166. Kropff, E., Carmichael, J.E., Moser, M.-B. & Moser, E.I. *Nature* **523**, 419–424 (2015).
167. Peyrache, A., Lacroix, M.M., Petersen, P.C. & Buzsáki, G. *Nat. Neurosci.* **18**, 569–575 (2015).
168. Trettel, S.G., Trimmer, J.B., Hwaun, E., Fiete, I.R. & Colgin, L.L. Preprint at <https://dx.doi.org/10.1101/198671> (2017).
169. Gardner, R.J., Lu, L., Wernle, T., Moser, M.-B. & Moser, E.I. Preprint at <https://dx.doi.org/10.1101/198499> (2017).
170. O’Keefe, J., Burgess, N., Donnett, J.G., Jeffery, K.J. & Maguire, E.A. *Phil. Trans. R. Soc. Lond. B* **353**, 1333–1340 (1998).
171. Hirase, H., Leinekugel, X., Csicsvari, J., Czúrkó, A. & Buzsáki, G. *J. Neurosci.* **21**, RC145 (2001).
172. Welinder, P.E., Burak, Y. & Fiete, I.R. *Hippocampus* **18**, 1283–1300 (2008).
173. Mathis, A., Herz, A.V. & Stemmler, M.B. *Phys. Rev. Lett.* **109**, 018103 (2012).
174. Mathis, A., Herz, A.V. & Stemmler, M. *Neural Comput.* **24**, 2280–2317 (2012).
175. Solstad, T., Moser, E.I. & Einevoll, G.T. *Hippocampus* **16**, 1026–1031 (2006).
176. Colgin, L.L. *et al.* *Nature* **462**, 353–357 (2009).
177. Rolls, E.T., Stringer, S.M. & Elliot, T. *Network* **17**, 447–465 (2006).
178. Savelli, F. & Knierim, J.J. *J. Neurophysiol.* **103**, 3167–3183 (2010).
179. de Almeida, L., Idiart, M. & Lisman, J.E. *J. Neurosci.* **29**, 7504–7512 (2009).
180. Monaco, J.D. & Abbott, L.F. *J. Neurosci.* **31**, 9414–9425 (2011).
181. Brandon, M.P. *et al.* *Science* **332**, 595–599 (2011).
182. Koenig, J., Linder, A.N., Leutgeb, J.K. & Leutgeb, S. *Science* **332**, 592–595 (2011).
183. Langston, R.F. *et al.* *Science* **328**, 1576–1580 (2010).
184. Wills, T.J., Cacucci, F., Burgess, N. & O’Keefe, J. *Science* **328**, 1573–1576 (2010).
185. Kanter, B.R. *et al.* *Neuron* **93**, 1480–1492.e6 (2017).
186. Zhang, S.J. *et al.* *Science* **340**, 1232627 (2013).
187. Sargolini, F. *et al.* *Science* **312**, 758–762 (2006).
188. Taube, J.S. *Hippocampus* **5**, 569–583 (1995).
189. Boccara, C.N. *et al.* *Nat. Neurosci.* **13**, 987–994 (2010).
190. Savelli, F., Yoganarasimha, D. & Knierim, J.J. *Hippocampus* **18**, 1270–1282 (2008).
191. Rivard, B., Li, Y., Lenck-Santini, P.P., Poucet, B. & Muller, R.U. *J. Gen. Physiol.* **124**, 9–25 (2004).
192. Barry, C. *et al.* *Rev. Neurosci.* **17**, 71–97 (2006).
193. Lever, C., Burton, S., Jeewajee, A., O’Keefe, J. & Burgess, N. *J. Neurosci.* **29**, 9771–9777 (2009).
194. Hartley, T., Burgess, N., Lever, C., Cacucci, F. & O’Keefe, J. *Hippocampus* **10**, 369–379 (2000).
195. Muessig, L., Hauser, J., Wills, T.J. & Cacucci, F. *Neuron* **86**, 1167–1173 (2015).
196. Bjerknes, T.L., Moser, E.I. & Moser, M.-B. *Neuron* **82**, 71–78 (2014).
197. Cheng, K. & Gallistel, C.R. in *Animal Cognition* (eds. Roitblat, H.L., Bever, T.G. & Terrace, H.S.) 409–423 (Lawrence Erlbaum Associates, 1984).
198. Cheng, K. *Cognition* **23**, 149–178 (1986).
199. Hardcastle, K., Ganguli, S. & Giocomo, L.M. *Neuron* **86**, 827–839 (2015).
200. Stackman, R.W. & Taube, J.S. *J. Neurosci.* **18**, 9020–9037 (1998).
201. Bassett, J.P. & Taube, J.S. *J. Neurosci.* **21**, 5740–5751 (2001).
202. Sharp, P.E., Tinkelman, A. & Cho, J. *Behav. Neurosci.* **115**, 571–588 (2001).
203. Czúrkó, A., Hirase, H., Csicsvari, J. & Buzsáki, G. *Eur. J. Neurosci.* **11**, 344–352 (1999).
204. King, C., Recce, M. & O’Keefe, J. *Eur. J. Neurosci.* **10**, 464–477 (1998).
205. Sharp, P.E., Turner-Williams, S. & Tuttle, S. *Behav. Brain Res.* **166**, 55–70 (2006).
206. Justus, D. *et al.* *Nat. Neurosci.* **20**, 16–19 (2017).
207. Carvalho, M.M. *et al.* *Soc. Neurosci. Abstr.* 183.10 (2016).
208. Terrazas, A. *Influences of self-motion signals on the hippocampal neural code for space*. Ph.D. thesis, The University of Arizona <http://hdl.handle.net/10150/280390> (2003).
209. Hinman, J.R., Brandon, M.P., Climer, J.R., Chapman, G.W. & Hasselmo, M.E. *Neuron* **91**, 666–679 (2016).
210. Ye, J. *et al.* *Soc. Neurosci. Abstr.* 183.11 (2016).
211. Deshmukh, S.S. & Knierim, J.J. *Front. Behav. Neurosci.* **5**, 69 (2011).
212. Tsao, A., Moser, M.-B. & Moser, E.I. *Curr. Biol.* **23**, 399–405 (2013).
213. McNaughton, B.L., Knierim, J.J. & Wilson, M.A. in *The Cognitive Neurosciences*, (ed. Gazzaniga, M.S.) ch. 37, pp. 585–595 (MIT Press, 1995).
214. Deshmukh, S.S. & Knierim, J.J. *Hippocampus* **23**, 253–267 (2013).
215. Høydal, Ø.A., Skytøen, E.R., Moser, M.-B. & Moser, E.I. *Soc. Neurosci. Abstr.* 084.17 (2017).
216. Navratilova, Z., Hoang, L.T., Schwindel, C.D., Tatsuno, M. & McNaughton, B.L. *Front. Neural Circuits* **6**, 6 (2012).
217. Sarel, A., Finkelstein, A., Las, L. & Ulanovsky, N. *Science* **355**, 176–180 (2017).
218. Ulanovsky, N. & Moss, C.F. *Nat. Neurosci.* **10**, 224–233 (2007).
219. Yartsev, M.M., Witter, M.P. & Ulanovsky, N. *Nature* **479**, 103–107 (2011).
220. Finkelstein, A. *et al.* *Nature* **517**, 159–164 (2015).
221. Eichenbaum, H., Kuperstein, M., Fagan, A. & Nagode, J. *J. Neurosci.* **7**, 716–732 (1987).
222. Breese, C.R., Hampson, R.E. & Deadwyler, S.A. *J. Neurosci.* **9**, 1097–1111 (1989).
223. Hollup, S.A., Molden, S., Donnett, J.G., Moser, M.-B. & Moser, E.I. *J. Neurosci.* **21**, 1635–1644 (2001).
224. Fyhn, M., Molden, S., Hollup, S., Moser, M.-B. & Moser, E.I. *Neuron* **35**, 555–566 (2002).
225. Hok, V. *et al.* *J. Neurosci.* **27**, 472–482 (2007).
226. Hardcastle, K., Maheswaranathan, N., Ganguli, S. & Giocomo, L.M. *Neuron* **94**, 375–387.e7 (2017).
227. Zipser, D. & Andersen, R.A. *Nature* **331**, 679–684 (1988).
228. Andersen, R.A. *Phil. Trans. R. Soc. Lond. B* **352**, 1421–1428 (1997).
229. Brozović, M., Gail, A. & Andersen, R.A. *J. Neurosci.* **27**, 10588–10596 (2007).
230. Hebb, D.O. *The Organization of Behavior* (Wiley, 1949).
231. Amari, S. *Biol. Cybern.* **27**, 77–87 (1977).
232. Skaggs, W.E., Knierim, J.J., Kudrimoti, H.S. & McNaughton, B.L. *Adv. Neural Inf. Process. Syst.* **7**, 173–180 (1995).
233. Zhang, K. *J. Neurosci.* **16**, 2112–2126 (1996).
234. Redish, A.D., Elga, A.N. & Touretzky, D.S. *Network* **7**, 671–685 (1996).
235. Clark, B.J. & Taube, J.S. *Front. Neural Circuits* **6**, 7 (2012).
236. Green, J. *et al.* *Nature* **546**, 101–106 (2017).
237. Seelig, J.D. & Jayaraman, V. *Nature* **521**, 186–191 (2015).
238. Tsodyks, M. & Sejnowski, T. *Int. J. Neural Syst.* **6** (Suppl) 81–86 (1995).
239. Conklin, J. & Eliasmith, C. *J. Comput. Neurosci.* **18**, 183–203 (2005).
240. Battaglia, F.P. & Treves, A. *Neural Comput.* **10**, 431–450 (1998).
241. Burak, Y. & Fiete, I.R. *PLoS Comput. Biol.* **5**, e1000291 (2009).
242. Bonnevie, T. *et al.* *Nat. Neurosci.* **16**, 309–317 (2013).
243. Couey, J.J. *et al.* *Nat. Neurosci.* **16**, 318–324 (2013).
244. Pastoll, H., Solanka, L., van Rossum, M.C. & Nolan, M.F. *Neuron* **77**, 141–154 (2013).
245. Dunn, B., Mørreunet, M. & Roudi, Y. *PLOS Comput. Biol.* **11**, e1004052 (2015).
246. Tocker, G., Barak, O. & Derdikman, D. *Hippocampus* **25**, 1599–1613 (2015).
247. O’Keefe, J. & Burgess, N. *Hippocampus* **15**, 853–866 (2005).
248. Burgess, N., Barry, C. & O’Keefe, J. *Hippocampus* **17**, 801–812 (2007).
249. Hasselmo, M.E., Giocomo, L.M. & Zilli, E.A. *Hippocampus* **17**, 1252–1271 (2007).
250. Blair, H.T., Weldon, A.C. & Zhang, K. *J. Neurosci.* **27**, 3211–3229 (2007).
251. O’Keefe, J. & Recce, M.L. *Hippocampus* **3**, 317–330 (1993).
252. Skaggs, W.E., McNaughton, B.L., Wilson, M.A. & Barnes, C.A. *Hippocampus* **6**, 149–172 (1996).
253. Remme, M.W., Lengyel, M. & Gutkin, B.S. *Neuron* **66**, 429–437 (2010).
254. Fiete, I.R. *Neuron* **66**, 331–334 (2010).
255. Killian, N.J., Jutras, M.J. & Buffalo, E.A. *Nature* **491**, 761–764 (2012).

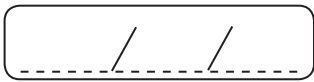
256. Domnisoru, C., Kinkhabwala, A.A. & Tank, D.W. *Nature* **495**, 199–204 (2013).
257. Schmidt-Hieber, C. & Häusser, M. *Nat. Neurosci.* **16**, 325–331 (2013).
258. Tsodyks, M.V., Skaggs, W.E., Sejnowski, T.J. & McNaughton, B.L. *Hippocampus* **6**, 271–280 (1996).
259. Jensen, O. & Lisman, J.E. *Learn. Mem.* **3**, 279–287 (1996).
260. Si, B., Kropff, E. & Treves, A. *Biol. Cybern.* **106**, 483–506 (2012).
261. Moser, E.I. *et al. Nat. Rev. Neurosci.* **15**, 466–481 (2014).
262. Winter, S.S., Mehlman, M.L., Clark, B.J. & Taube, J.S. *Curr. Biol.* **25**, 2493–2502 (2015).
263. Winter, S.S., Clark, B.J. & Taube, J.S. *Science* **347**, 870–874 (2015).
264. O'Keefe, J. Nobel Lecture: spatial cells in the hippocampal formation. *Nobelprize.org*. http://www.nobel-prize.org/nobel_prizes/medicine/laureates/2014/okeefe-lecture.html (2014).
265. Leutgeb, S., Leutgeb, J.K., Moser, M.B. & Moser, E.I. *Curr. Opin. Neurobiol.* **15**, 738–746 (2005).
266. Yu, Y.C., Bultje, R.S., Wang, X. & Shi, S.H. *Nature* **458**, 501–504 (2009).
267. Yu, Y.C. *et al. Nature* **486**, 113–117 (2012).
268. Li, Y. *et al. Nature* **486**, 118–121 (2012).
269. Ko, H. *et al. Nature* **473**, 87–91 (2011).
270. Heys, J.G., Rangarajan, K.V. & Dombeck, D.A. *Neuron* **84**, 1079–1090 (2014).
271. Donato, F., Jacobsen, R.I., Moser, M.-B. & Moser, E.I. *Science* **355**, eaai8178 (2017).
272. Sun, C. *et al. Proc. Natl. Acad. Sci. USA* **112**, 9466–9471 (2015).
273. Rowland, D.C. *et al. Soc. Neurosci. Abstr.* **85.15** (2015).
274. Tang, Q. *et al. Neuron* **84**, 1191–1197 (2014).
275. Latuske, P., Toader, O. & Allen, K. *J. Neurosci.* **35**, 10963–10976 (2015).
276. Fiete, I.R., Burak, Y. & Brookings, T. *J. Neurosci.* **28**, 6858–6871 (2008).
277. Geva-Sagiv, M., Las, L., Yovel, Y. & Ulanovsky, N. *Nat. Rev. Neurosci.* **16**, 94–108 (2015).
278. Worden, R. *Hippocampus* **2**, 165–187 (1992).
279. Yartsev, M.M. & Ulanovsky, N. *Science* **340**, 367–372 (2013).
280. Hayman, R., Verriotti, M.A., Jovalekic, A., Fenton, A.A. & Jeffery, K.J. *Nat. Neurosci.* **14**, 1182–1188 (2011).
281. Hayman, R.M., Casali, G., Wilson, J.J. & Jeffery, K.J. *Front. Psychol.* **6**, 925 (2015).
282. Pastalkova, E., Itskov, V., Amarasingham, A. & Buzsáki, G. *Science* **321**, 1322–1327 (2008).
283. MacDonald, C.J., Lepage, K.Q., Eden, U.T. & Eichenbaum, H. *Neuron* **71**, 737–749 (2011).
284. Kraus, B.J. *et al. Neuron* **88**, 578–589 (2015).
285. MacDonald, C.J., Carrow, S., Place, R. & Eichenbaum, H. *J. Neurosci.* **33**, 14607–14616 (2013).
286. Kraus, B.J., Robinson, R.J., II, White, J.A., Eichenbaum, H. & Hasselmo, M.E. *Neuron* **78**, 1090–1101 (2013).
287. Mankin, E.A. *et al. Proc. Natl. Acad. Sci. USA* **109**, 19462–19467 (2012).
288. Mankin, E.A., Diehl, G.W., Sparks, F.T., Leutgeb, S. & Leutgeb, J.K. *Neuron* **85**, 190–201 (2015).
289. Lu, L., Igarashi, K.M., Witter, M.P., Moser, E.I. & Moser, M.-B. *Neuron* **87**, 1078–1092 (2015).
290. Tsao, A. *et al. Soc. Neurosci. Abstr.* **084.21** (2017).
291. Aronov, D., Nevers, R. & Tank, D.W. *Nature* **543**, 719–722 (2017).
292. Rolls, E.T. & O'Mara, S.M. *Hippocampus* **5**, 409–424 (1995).
293. Rolls, E.T., Robertson, R.G. & Georges-François, P. *Eur. J. Neurosci.* **9**, 1789–1794 (1997).
294. Doeller, C.F., Barry, C. & Burgess, N. *Nature* **463**, 657–661 (2010).
295. Jacobs, J. *et al. Nat. Neurosci.* **16**, 1188–1190 (2013).
296. Constantinescu, A.O., O'Reilly, J.X. & Behrens, T.E.J. *Science* **352**, 1464–1468 (2016).
297. Horner, A.J., Bisby, J.A., Zotow, E., Bush, D. & Burgess, N. *Curr. Biol.* **26**, 842–847 (2016).
298. Bellmund, J.L., Deuker, L., Navarro Schröder, T. & Doeller, C.F. *Elife* **5**, e17089 (2016).
299. Dehaene, S. *et al. Science* **330**, 1359–1364 (2010).



A series of horizontal lines for handwriting practice, consisting of 20 evenly spaced lines.



A series of horizontal lines for writing, consisting of 20 evenly spaced lines.



JEAN FABER (BRAZIL)

THE 5 CRITICAL ELEMENTS OF A CONNECTOME: NODES, LINKS, TOPOLOGY, DYNAMICS AND MULTIPLEX SCALING



ANÁLISE DE CONECTIVIDADE:
Elementos básicos

Jean Faber
Universidade Federal de São Paulo (UNIFESP)
Departamento de Neurologia e Neurocirurgia - EPM
Laboratório de Neuroengenharia e Neurocognição

UNIFESP
UNIVERSIDADE FEDERAL DE SÃO PAULO

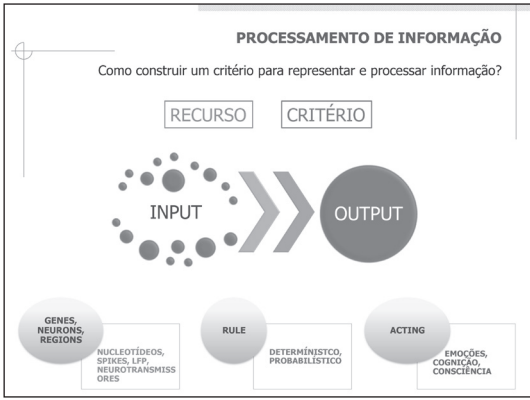
CÓDIGO NEURAL
Como a atividade neural é representada e convertida em comportamento e sensações?

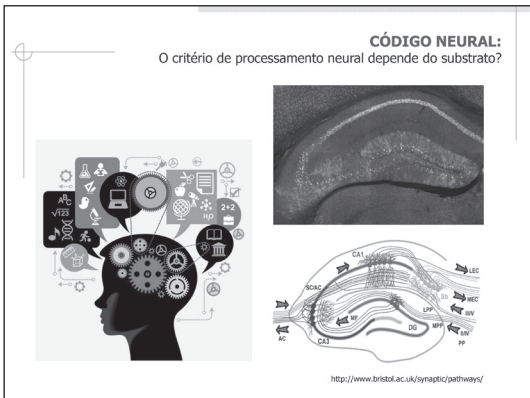
Perkel and Bullock (1968): "The problem of neural coding is to elucidate 'the representation and transformation of information in the nervous system.'"

CÓDIGO NEURAL
Qual a unidade de informação do cérebro?

Spine 1 μm Dendrite 10 μm Neuron 50 μm Circuit 100 μm Area 2 mm

Electrophysiology in the Age of Light





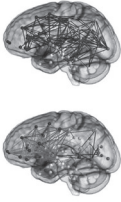






CONECTIVIDADE
Critério e representação do código neural?

Representação matemática: Teoria de Grafos

Um grafo é um par ordenado $G(V,E)$, com V : {vértices} e E : {arestas}

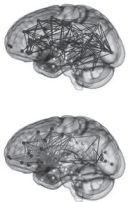
The Königsberg Bridge problem


$V = \{1, 2, 3, 4, 5, 6\}$
 $E = \{(1, 2), (1, 5), (2, 3), (2, 5), (3, 4), (4, 5), (4, 6)\}$

CONECTIVIDADE
Critério e representação do código neural?

Representação matemática: Teoria de Grafos

Um grafo é um par ordenado $G(V,E)$, com V : {vértices} e E : {arestas}




$$\begin{pmatrix} 2 & 1 & 0 & 0 & 1 & 0 \\ 1 & 0 & 1 & 0 & 1 & 0 \\ 0 & 1 & 0 & 1 & 0 & 0 \\ 0 & 0 & 1 & 0 & 1 & 1 \\ 1 & 1 & 0 & 1 & 0 & 0 \\ 0 & 0 & 0 & 1 & 0 & 0 \end{pmatrix} = \mathbf{M}$$


Matriz de Adjacência

$V = \{1, 2, 3, 4, 5, 6\}$
 $E = \{(1, 2), (1, 5), (2, 3), (2, 5), (3, 4), (4, 5), (4, 6)\}$

CONECTIVIDADE
Os 5 elementos básicos para análise de conectividade neural



CONECTIVIDADE
Os 5 elementos básicos para análise de conectividade neural

CARACTERÍSTICA

- U 
- Diapason 
- Flauta 
- Violino 
- Voz (Pietra et) 
- Clarineta 



CONECTIVIDADE
Os 5 elementos básicos para análise de conectividade neural

CARACTERÍSTICA

CONECTIVIDADE
Os 5 elementos básicos para análise de conectividade neural

CARACTERÍSTICA






CONECTIVIDADE
Os 5 elementos básicos para análise de conectividade neural

CARACTERÍSTICA

CONECTIVIDADE
Os 5 elementos básicos para análise de conectividade neural

CARACTERÍSTICA

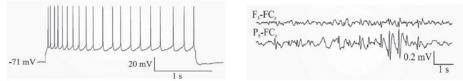
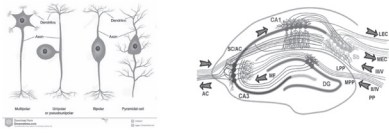
CONECTIVIDADE

FRAMEWORK OF POSSIBLE BRAIN NODES		
STRUCTURAL NODES	SIGNALIZATION : FUNCTIONAL NODES	MEASUREMENT TECHNIQUES
	GENE EXPRESSION	NORTHERN BLOT, REVERSE TRANSCRIPTION POLYMERASE CHAIN REACTION, DNA MICROARRAY, RNA-SEQUENCING
	BIOMOLECULAR CELL SIGNALING INTRACELLULAR POTENTIALS NEUROTRANSMISSIONS IONIC CONCENTRATION	FLUORESCENCE CORRELATION SPECTROSCOPY, SHARP ELECTRODE, IMMUNOFLUORESCENCE, ION SELECTIVE ELECTRODE
	BIOMOLECULAR SIGNALING MEMBRANE AND INTRA/EXTRACELLULAR POTENTIALS FLUORESCENCE CELL IMAGING	SINGLE UNITY RECORDING, PATCH CLAMP, VOLTAGE AND CURRENT CLAMP, FLUORESCENCE IMAGING
	BIOMOLECULAR SIGNALING INTRACELLULAR POTENTIALS FLUORESCENCE CELL EXPRESSION METABOLIC CELL EXPRESSION	MULTIUNITY RECORDING, MICROELECTRODES, FLUORESCENCE IMAGING, IMMUNOHISTOCHEMISTRY
	INTRA/EXTRACELLULAR POTENTIALS ELECTRIC AND MAGNETIC BIOPOTENTIALS METABOLIC EXPRESSION	MULTIUNITY RECORDING, INVASIVE PROBES, EEG, ECoG, NIRS, fMRI, PET, MEG

CONECTIVIDADE

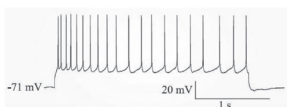
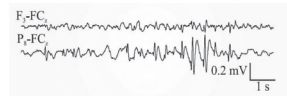
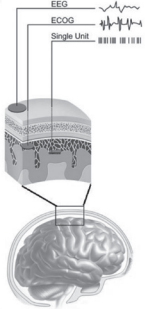
Os 5 elementos básicos para análise de conectividade neural

CARACTERÍSTICA (ANATO-ELETRFISIOLOGICA):
CANDIDATOS PARA REPRESENTAÇÃO DO CÓDIGO NEURAL



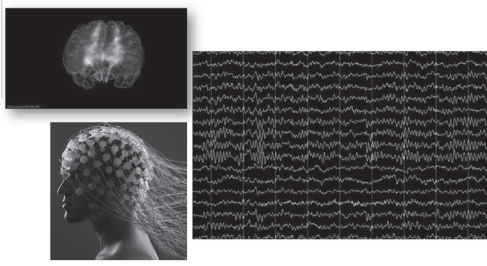
CÓDIGO NEURAL:

Existiria alguma "partitura" como ligação comum?



NEURO-ELETRFISIOLOGIA

Extracting the code!



CONECTIVIDADE
NÓS E ARESTAS...

$M = [m_{ij}] = \begin{pmatrix} x & y & z & w & x & y & z & w \\ 0 & 0 & 0 & 1 & 1 & 0 & 0 & 0 \\ 1 & 0 & 0 & 0 & 1 & 1 & 0 & 0 \\ 0 & 1 & 0 & 0 & 0 & 0 & 0 & 0 \\ 0 & 0 & 1 & 0 & 0 & 0 & 0 & 0 \end{pmatrix}$

$D = [d_{ij}] = \begin{pmatrix} x & y & z & w & x & y & z & w \\ 0 & 0 & 0 & 10 & 10 & 0 & 0 & 0 \\ 8 & 0 & 0 & 0 & 0 & 5 & 0 & 0 \\ 3 & 0 & 0 & 0 & 0 & 0 & 0 & 0 \\ 0 & 0 & 1 & 0 & 1 & 0 & 1 & 0 \end{pmatrix}$

$U = [u_{ij}] = \begin{pmatrix} x & y & z & w & x & y & z & w \\ 1 & 0 & 0 & 1 & 1 & 0 & 0 & 1 \\ 1 & 1 & 0 & 0 & 1 & 1 & 0 & 1 \\ 1 & 1 & 1 & 1 & 1 & 1 & 1 & 1 \end{pmatrix}$

A1, A2, A3, B1, B2

CONECTIVIDADE
Os 5 elementos básicos para análise de conectividade neural

TOPOLOGIA DE REDE (FUNCIONAL)

CONECTIVIDADE
Os 5 elementos básicos para análise de conectividade neural

CARACTERÍSTICA

TOPOLOGIA

INTERAÇÃO

CONECTIVIDADE
Os 5 elementos básicos para análise de conectividade neural

CARACTERÍSTICA

TOPOLOGIA

INTERAÇÃO

CONECTIVIDADE
Os 5 elementos básicos para análise de conectividade neural

TOPOLOGIA DE REDE (FUNCIONAL)

CONECTIVIDADE
Fluxo de informação

TOPOLOGIA DE REDE (FUNCIONAL)

CONECTIVIDADE
Construindo topologias

A Node **B** Edge **C** Degree

D Functional Segregation **E** Module

Modularity Triangle clustering coefficient

CONECTIVIDADE
Construindo topologias

A Node **B** Edge **C** Degree

A Functional Integration **B** Shortest path global efficiency

Hub node betweenness centrality

CONECTIVIDADE Construindo topologias

Node

A ●

Edge

B ●—●

Degree

C ●
●
●

A Triangle

B Feedback loop

C Biparallel

CONECTIVIDADE Construindo topologias

Connectivity of Cortical Networks at rest

● Node
 ■ Provincial hub
 ■ Hub
 — ConnectionEdge
 ● Hub pulse
 → Connection activation

Time: Early response → Late response

CONECTIVIDADE DISTRIBUIÇÃO DE GRAUS

RANDOM NETWORK

LATTICE NETWORK

SCALE-FREE NETWORK

SMALL-WORLD NETWORK

$P(k) \sim e^{-k}$
 $P(k) \sim \delta(k - k_0)$
 $P(k) \sim k^{-\gamma}$
 $P(k) \sim k^{-\gamma} e^{-k/k_0}$

Measure	Mathematical definition	Where:
Node degree	$k_i = \sum_j A_{ij}$	A_{ij} is the connection status between the node i and the node j (either 1 and 0 are neighbors, when the link exists, the A_{ij} value is 1 otherwise 0).
Clustering coefficient	$C_i = \frac{\Delta_i}{k_i(k_i-1)}$	Δ_i is the number of triangles in the network and k_i is the node degree.
Global clustering coefficient	$C = \frac{1}{n} \sum_i C_i$	n is the number of nodes in the network and C_i is the clustering coefficient.
Number of triangles	$\Delta = \frac{1}{6} \sum_i \sum_j \sum_k A_{ij} A_{jk} A_{ki}$	A_{ij}, A_{jk}, A_{ki} is the connection status between the nodes i and j and j and k and k and i respectively. When the nodes are connected the value is 1 otherwise 0.
Modularity	$Q = \frac{1}{n} \sum_i \sum_j A_{ij} \delta_{ij} - \frac{1}{n^2} \sum_i \sum_j A_{ij} A_{ij}$	δ_{ij} is the Kronecker delta, A_{ij} is the adjacency matrix, k_i is the degree of node i , k_j is the degree of node j , δ_{ij} is the Kronecker delta (if $i=j$ then $\delta_{ij}=1$, otherwise 0).
Shortest path length	$d_{ij} = \min_{\gamma} \sum_{k \in \gamma} A_{kk}$	A_{ij} is the connection status between nodes in the shortest path, γ is the shortest path between nodes i and j ($d_{ij}=1$, $A_{ij}=1$ if there is a connection and 0 otherwise).
Average shortest path length	$\bar{L} = \frac{1}{n(n-1)} \sum_i \sum_j d_{ij}$	n is the total number of nodes in the network.
Global efficiency	$E = \frac{1}{n(n-1)} \sum_i \sum_j \frac{1}{d_{ij}}$	d_{ij} is the shortest path length and n is the total number of nodes in the network.

Measure	Mathematical definition	Where:
Betweenness centrality	$C_i = \frac{1}{(n-1)(n-2)} \sum_j \sum_k \frac{1}{d_{ij} d_{jk} + 1}$	n is the total number of nodes in the network.
Betweenness centrality	$B_i = \frac{1}{(n-1)(n-2)} \sum_j \sum_k \frac{1}{d_{ij} d_{jk} + 1}$	A_{ij} is the number of shortest paths between i and j , and A_{jk} is the number of shortest paths between j and k that pass through i .
Assortativity	$r = \frac{\langle k_i k_j \rangle - \langle k_i \rangle \langle k_j \rangle}{\langle k_i \rangle \langle k_j \rangle}$	r is the total number of links in the network and k_i, k_j are the node degree of nodes i and j respectively.
Average neighbor degree	$\langle k_{nn} \rangle = \frac{\sum_i k_i^2}{\sum_i k_i}$	k_i is the connection status between the node i and the node j (1 if nodes are connected and 0 otherwise) and k_i is the node degree of node i .
Mean path length	$\bar{L} = \frac{1}{n(n-1)} \sum_i \sum_j d_{ij}$	d_{ij} is the number of connections of node i to all network nodes C_{ij} and A_{ij} are mean and standard deviation for the number of connections of i to all network nodes, respectively.

CONECTIVIDADE
Os 5 elementos básicos para análise de conectividade neural

DINÂMICA DE CONECTIVIDADE

CONECTIVIDADE
Os 5 elementos básicos para análise de conectividade neural

DINÂMICA DE CONECTIVIDADE

$$\rho = \frac{\text{cov}(X, Y)}{\sqrt{\text{var}(X) \cdot \text{var}(Y)}}$$

$$D_{KL}(P||Q) = \sum_{x \in X} P(x) \log \frac{P(x)}{Q(x)}$$

CONECTIVIDADE
DISTRIBUIÇÃO DE GRAUS

RANDOM NETWORK

LATTICE NETWORK

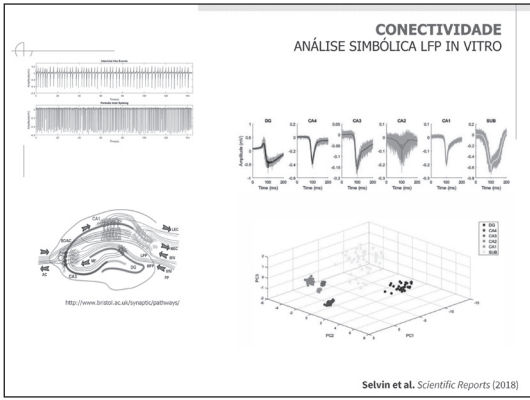
SCALE-FREE NETWORK

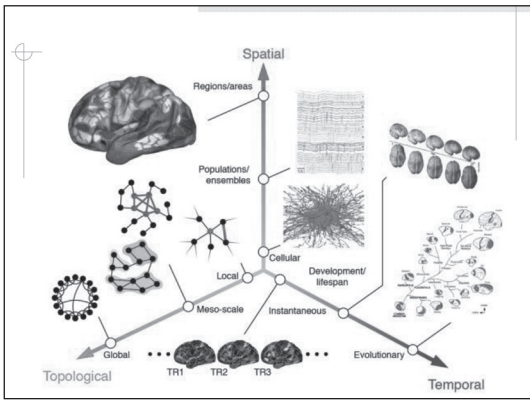
SMALL-WORLD NETWORK

INTERFERÊNCIA ⇔ COERÊNCIA
"O segredo do universo está na fase!"

Mouse ZKIV 02 Phase

Buzsáki: Annu. Rev. Neurosci. 2012.



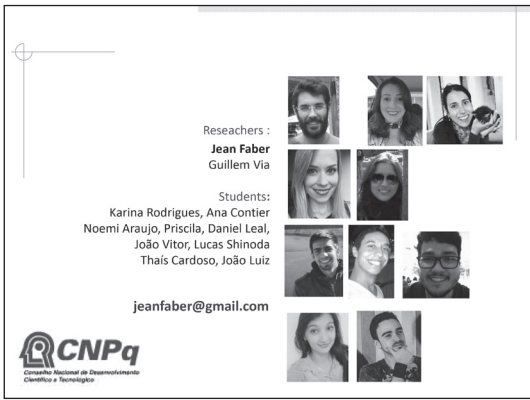


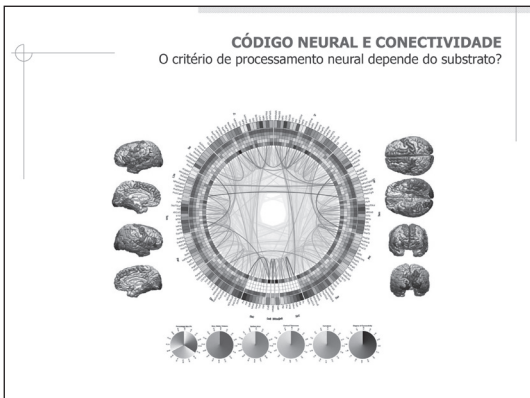
Reseachers :

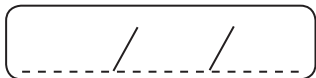
Jean Faber
Guillem Via

Students:
Karina Rodrigues, Ana Contier
Noemi Araujo, Priscila, Daniel Leal,
João Vitor, Lucas Shinoda
Thais Cardoso, João Luiz

jeanfaber@gmail.com








PHILIPPE MENDONÇA (UK)

IMAGING PRESYNAPTIC ACTIVITY

UCL

Imaging presynaptic activity in individual boutons

Philippe Mendonça

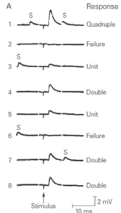


Institute of Neurology
University College London

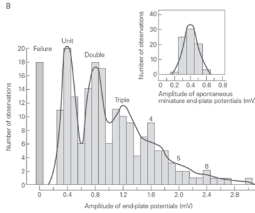
LASSE, March 2019

Principles of synaptic transmission

A




B




Kandel, E. R., Schwartz, J. H., Jessell, T. M., Siegelbaum, S. A., & Hudspeth, A. (2013). *Principles of Neural Science* (5th ed.). McGraw-Hill.

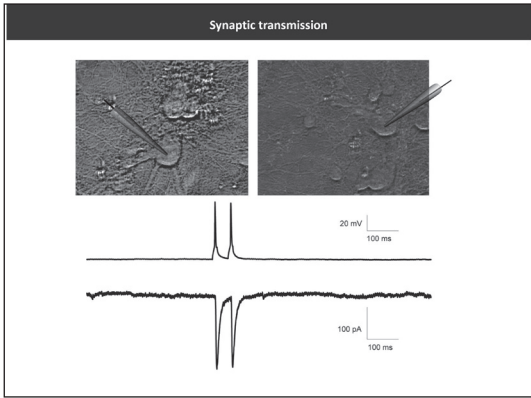
Synaptic transmission

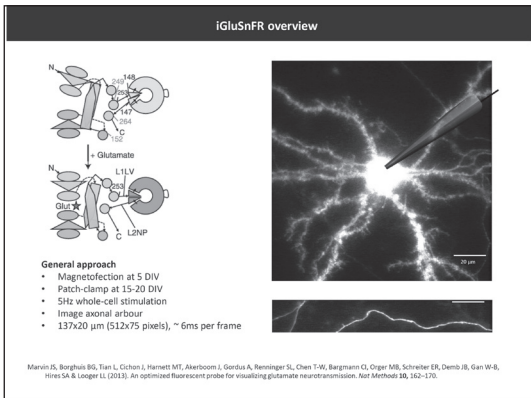


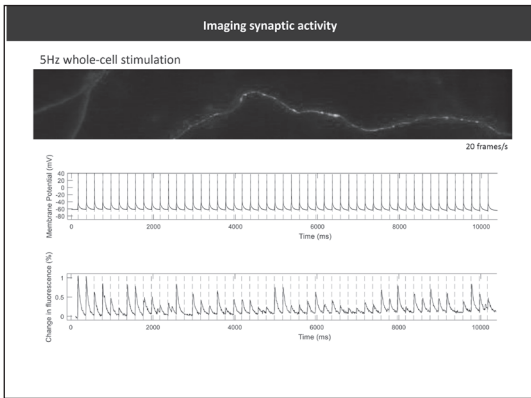
From Santiago Ramon y Cajal

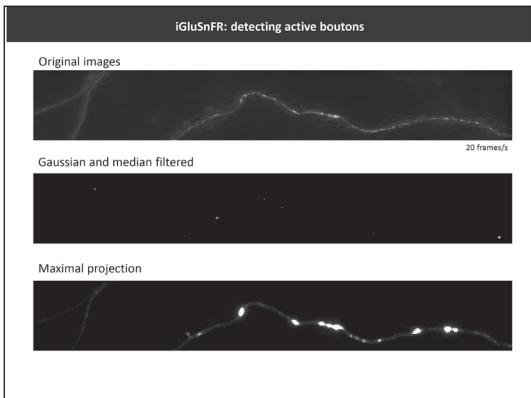


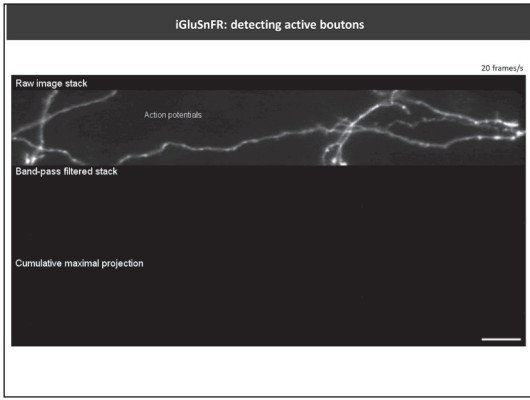
From Greg Dunn

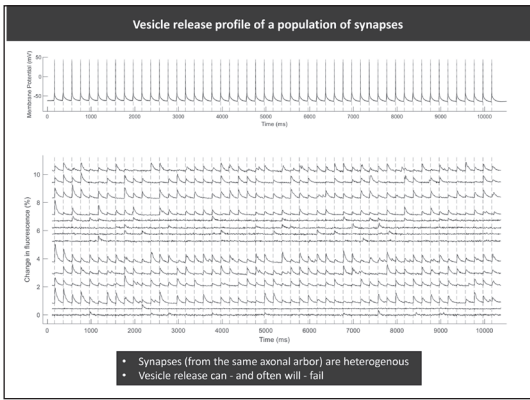


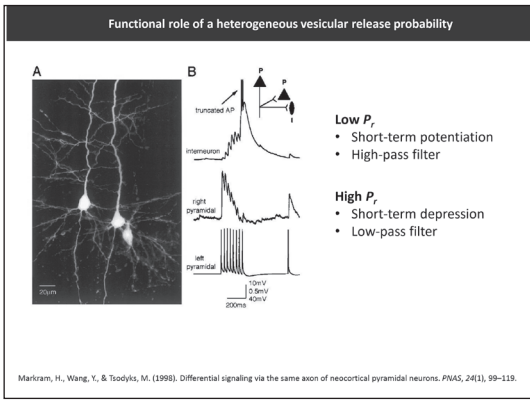


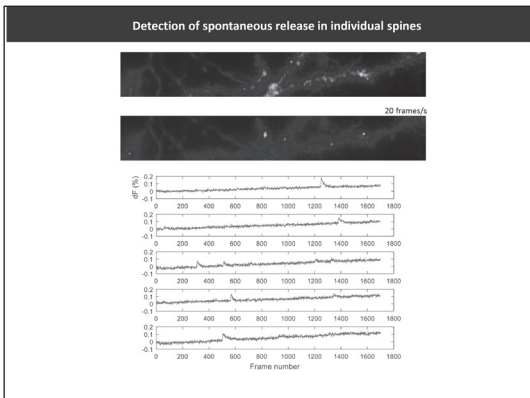


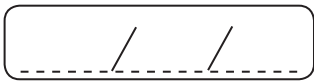












ADENAUER CASALI (BRAZIL)

INFERRING EFFECTIVE CONNECTIVITY FROM EEG RECORDINGS



XIII Latin-American Summer School On Epilepsy
7-15 Mar 2019



Inferring Effective Connectivity from EEG Recordings

Adenauer G. CASALI, PhD
Núcleo de Neuroengenharia e Computação
Instituto de Ciência e Tecnologia
Universidade Federal de São Paulo - UNIFESP



Inferring Effective Connectivity from the EEG
Adenauer G. Casali

XIII LASSE
08/03/2019

Summary

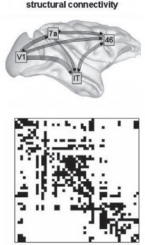
1. Structural vs Functional vs Effective Connectivity
2. Effective Connectivity, temporal resolution and the EEG
3. Source Modelling and the Inverse Problem
4. Modelling effective connectivity: Introduction to Dynamic Causal Modelling

Inferring Effective Connectivity from the EEG
Adenauer G. Casali

XIII LASSE
08/03/2019

1. Structural x Functional x Effective Connectivity

structural connectivity



Honey et al. (2007)

Inferring Effective Connectivity from the EEG
 Adenauer G. Casali XIII LASSE
08/03/2019

3. Source Modelling Forward Model

Electric Potential \vec{P}

Soma
 Dendrites
 Axons

Baillet et al. (2001)

Inferring Effective Connectivity from the EEG
 Adenauer G. Casali XIII LASSE
08/03/2019



→ 1. Cortical dipole model 3. Source Modelling:
Forward Model

Inferring Effective Connectivity from the EEG
 Adenauer G. Casali XIII LASSE
08/03/2019

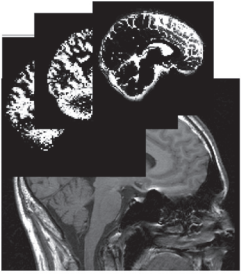
→ 1. Cortical dipole model 3. Source Modelling:
Forward Model



Inferring Effective Connectivity from the EEG
 Adenauer G. Casali XIII LASSE
08/03/2019

→ 1. Cortical dipole model 3. Source Modelling:
Forward Model

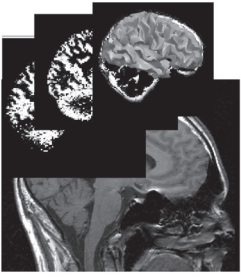

Inferring Effective Connectivity from the EEG
 Adenauer G. Casali  XIII LASSE
08/03/2019



→ 1. Cortical dipole model 3. Source Modelling:
Forward Model



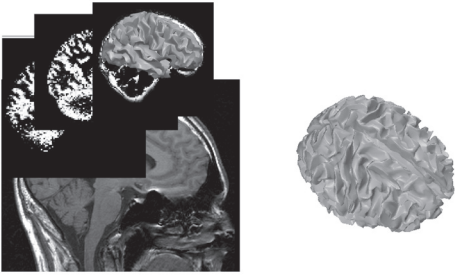

Inferring Effective Connectivity from the EEG
 Adenauer G. Casali  XIII LASSE
08/03/2019



→ 1. Cortical dipole model 3. Source Modelling:
Forward Model



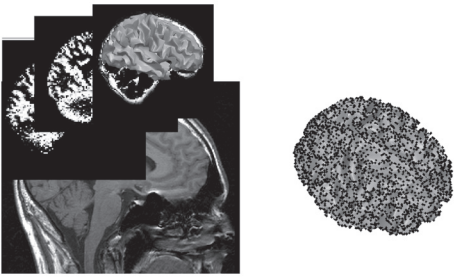

Inferring Effective Connectivity from the EEG
 Adenauer G. Casali  XIII LASSE
08/03/2019

→ 1. Cortical dipole model 3. Source Modelling:
Forward Model



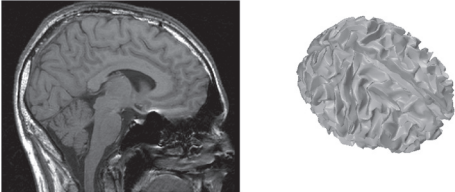

Inferring Effective Connectivity from the EEG
 Adenauer G. Casali  XIII LASSE
08/03/2019

→ 1. Cortical dipole model 3. Source Modelling:
Forward Model



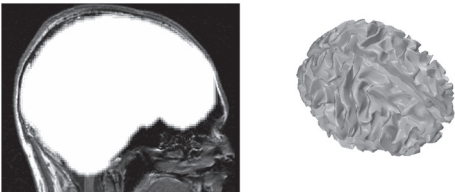
Inferring Effective Connectivity from the EEG
 Adenauer G. Casali XIII LASSE
08/03/2019

→ 1. Cortical dipole model **3. Source Modelling:**
 → 2. Head tissue conductivities **Forward Model**



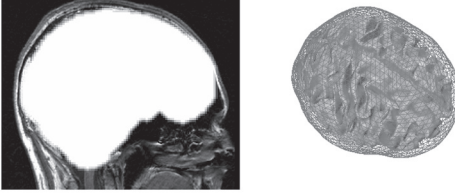
Inferring Effective Connectivity from the EEG
 Adenauer G. Casali XIII LASSE
08/03/2019

→ 1. Cortical dipole model **3. Source Modelling:**
 → 2. Head tissue conductivities **Forward Model**



Inferring Effective Connectivity from the EEG
 Adenauer G. Casali XIII LASSE
08/03/2019

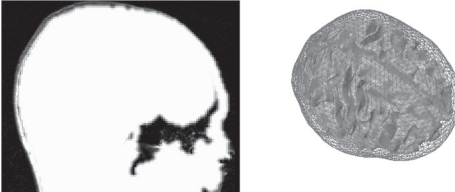
→ 1. Cortical dipole model **3. Source Modelling:**
 → 2. Head tissue conductivities **Forward Model**



Skull

Inferring Effective Connectivity from the EEG
 Adenauer G. Casali XIII LASSE
08/03/2019

→ 1. Cortical dipole model **3. Source Modelling:**
 → 2. Head tissue conductivities **Forward Model**



Inferring Effective Connectivity from the EEG
Adenauer G. Casali

XIII LASSE
08/03/2019

- ➔ 1. Cortical dipole model
- ➔ 2. Head tissue conductivities

3. Source Modelling:
Forward Model

Inferring Effective Connectivity from the EEG
Adenauer G. Casali

XIII LASSE
08/03/2019

- ➔ 1. Cortical dipole model
- ➔ 2. Head tissue conductivities
 - ➔ BEM: Real geometry + Isotropic and homogeneous conductivities

3. Source Modelling:
Forward Model

Inferring Effective Connectivity from the EEG
Adenauer G. Casali

XIII LASSE
08/03/2019

- ➔ 1. Cortical dipole model
- ➔ 2. Head tissue conductivities
 - ➔ BEM: Real geometry + Isotropic and homogeneous conductivities
- ➔ 3. Electrodes positions

3. Source Modelling:
Forward Model

Inferring Effective Connectivity from the EEG
Adenauer G. Casali

XIII LASSE
08/03/2019

3. Source Modelling

$$S = G \times J$$

$p(S | J)$ = Probability of S given J

Inferring Effective Connectivity from the EEG
Adenauer G. Casali

XIII LASSE
08/03/2019

3. Source Modelling

$$S = G \times J$$

FORWARD MODEL

$$p(S | J) = N(\mu = G \times J, \Sigma_e)$$

Normal distribution

Inferring Effective Connectivity from the EEG
Adenauer G. Casali

XIII LASSE
08/03/2019

3. Source Modelling

$$S = G \times J$$

FORWARD MODEL

$$p(S | J) = N(\mu = G \times J, \Sigma_e)$$

Expected value (average)

Inferring Effective Connectivity from the EEG
Adenauer G. Casali

XIII LASSE
08/03/2019

3. Source Modelling

$$S = G \times J$$

FORWARD MODEL

$$p(S | J) = N(\mu = G \times J, \Sigma_e)$$

Noise Covariance

Inferring Effective Connectivity from the EEG
Adenauer G. Casali

XIII LASSE
08/03/2019

3. Source Modelling

"Inverse Problem"

~100 electrodes ~10000 sources

$$S = G \times J$$

FORWARD MODEL

$$p(S | J) = N(\mu = G \times J, \Sigma_e)$$

Inferring Effective Connectivity from the EEG
Adenauer G. Casali XIII LASSE 08/03/2019

3. Source Modelling

"Inverse Problem"

~100 electrodes ~10000 sources

$$S = G \times J$$

FORWARD MODEL

$$p(S|J) = N(\mu = G \times J, \Sigma_e)$$

$$p(J|S) = ?$$

Inferring Effective Connectivity from the EEG
Adenauer G. Casali XIII LASSE 08/03/2019

3. Source Modelling: Inverse Solution

Bayesian Approach

Symptoms

Prior probability $p(\text{disease})$

Likelihood $p(\text{symptoms}|\text{disease})$

Bayes' Rule

Posterior probability $p(\text{disease}|\text{symptoms})$

$$p(\text{disease} | \text{symptoms}) \propto p(\text{symptoms} | \text{disease}) p(\text{disease})$$

Inferring Effective Connectivity from the EEG
Adenauer G. Casali XIII LASSE 08/03/2019

3. Source Modelling: Inverse Solution

Bayesian Approach

J S

Forward model

Priors

$$p(J|S) \propto p(S|J)p(J)$$

Inferring Effective Connectivity from the EEG
Adenauer G. Casali XIII LASSE 08/03/2019

3. Source Modelling: Inverse Solution

Bayesian Approach

J S

Forward model

Priors

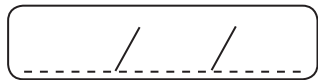
Source Covariance

$$p(J|S) \propto p(S|J)p(J)$$

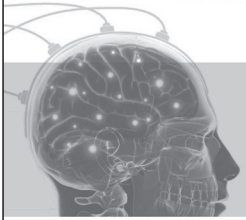
$$N(G \times J, \Sigma_e) \quad N(0, Q)$$

ADENAUER CASALI (BRAZIL)

CONSCIOUSNESS AND BRAIN COMPLEXITY: PERTURB-AND-MEASURE APPROACHES




XIII Latin-American Summer School On Epilepsy
7-15 Mar 2019



Consciousness and Brain Complexity: perturb-and-measure approaches

Adenauer G. CASALI, PhD
Núcleo de Neuroengenharia e Computação
Instituto de Ciência e Tecnologia
Universidade Federal de São Paulo - UNIFESP



Consciousness and Brain Complexity
Adenauer G. Casali

XIII LASSE
08/03/2019


Summary

1. Consciousness
2. Functional differentiation, functional integration and brain complexity
3. Effective connectivity: perturb-and-measure approaches
4. The Perturbational Complexity Index (PCI)
5. Current and future work

Consciousness and Brain Complexity
Adenauer G. Casali

XIII LASSE
08/03/2019

1. Consciousness



JAIME CARRIZOSA (COLOMBIA)

EPILEPSY REVEALED: THE HISTORY OF EPILEPSY THROUGH PAINTINGS

Epilepsy revealed: the history of epilepsy through paintings and sculpture

Jaime Carrizosa Moog
University of Antioquia
Child and Adolescent Neurology Service
Pediatric Department
Medellin, Colombia



Hammurabi, VI king of Babylon from 1792 BC to 1750 BC
Hammurabi's Code was one of the first written codes of law in history.



The epileptic seizure and the myth of Hyacinthos
Michael W. Mann

Hôpital St Anne, Department of Neurosurgery (Dr. FR. Bacc), 7 rue Cabanis, F-75014 Paris, France

Special Article
History of Epilepsy

The Epilepsy of Emperor Michael IV, Paphlagon (1034–1041
A.D.): Accounts of Byzantine Historians and Physicians

*J. Lascaratos and †P. V. Zis

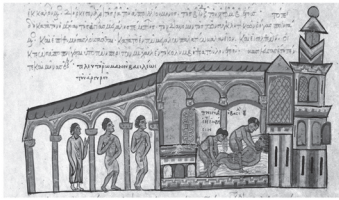
Departments of *History of Medicine and †Neurology, Medical School, National Athens University, Athens, Greece



Emperor Romanos III Argyros (968-1034 AD) + Empress Zoe the Porphyrogenitus (978 – 1050 AD)



Emperor Michael IV, Paphlagon (1010 – 1041 AD)



Numismatic Museum of Athens. Mosaics at the Hagia Sophia, Istanbul.
The murder of Romanos III Argyros in a bath, from the Chronicle of John Skylitzes.



FIG 1. Emperor Michael IV, Paphlagon, as presented on a gold coin during his reign (Numismatic Museum of Athens).

Historical Article

Epilepsy and Its Treatment in the Ancient Cultures of America

Jan G. R. Eiferink

Department of Molecular Cell Biology, University of Leiden, Leiden, The Netherlands



FIG. 1. Illustration from the work of Poma de Ayala (14), representing the wife of Inca Capac Yupanqui during an epileptic seizure.

TABLE 1. Indigenous names for epilepsy

Inca names	Description	Reference
Aya huayra	Wind (air) of the dead	5
Chayapak oncy		6
Huany oncy	Disease of the dead	12
Huan kochra	Disease of the dead	12
Llaqui oncy	Disease of sadness	12
Sanku nanay	Disease of the heart	12
Tuacu	Owl, night bird; attack	33
Urmachiscan	'He is thrown on the ground'	10
Aztec names		
Comic aquilztl		13
Cuexochmiquiztli		13
Tlacolmiquiztli	Disease due to love and desire	21
Tlacolmiquiztli	Disease due to love and desire	21
Tlayauallil		13
tegam mnomana		13
Yolcocolauiztli		13
Yollo mimiquiztli	Disease of the heart	13
Yolpazmiquiztli		13



Fig. 10. Shall preparation scene of the pre-Inca period. Painted in 1997. Technique: oil/canvas. Location: Lima Institute of Neurosciences. Artist: Juan Bravo Viegara [7].

L.D. Ladino et al. / Epilepsia 6: Behavior 29 (2013) 82-89



Fig. 9. Trepanning in ancient Peru. Painted in 1959. Technique: oil painting on masonite. From Parke, Davis Great Moments in Medicine. Collection: Michigan Medical School. Artist: Robert Thom [30].

L.D. Lodiño et al. / *Epilepsy & Behavior* 29 (2013) 82–89



L.D. Lodiño et al. / *Epilepsy & Behavior* 57 (2016) 255–264

Fig. 8. "Inca skull surgery in Machu Picchu", mural by Alton Stanley Tobey. At the National Museum of Natural History, Smithsonian Institution, Washington DC.

Tumi: Peruvian ceremonial knife of Chimu, Moche and Lambayeque cultures





Ñaylamp: after founding the Lambayeque culture, he grew wings and flew into the sky.
Tumi use: Trepanations, ceremonial rituals, prisoners' cutthroats

Associated Press 2006:11-21. Retrieved 2008:11-24.
Scott, John F. (1999). *Latin American Art: Ancient to Modern*. Gainesville: University Press of Florida, p. 128.



Review

Tlazolteotl, the Aztec goddess of epilepsy

Lady Diana Ladino ^a, José Francisco Téllez-Zenteno ^{b,*}



Fig. 2. *Beheben* index. The goddess squats in the birth-giving position, wearing the central Mexican hat with quills, similar to the Spanish one seen here. She wears black and red, decorated with ceramic stones [26]. This drawing shows Tlazolteotl carrying a child. She holds a child who wears a black/white garment, and another just the one (middle). White modelling like that of the Tlazolteotl shows the figure also of the sacrificial victim (the although she always appears this, but it is very obvious here with the extra hands hanging from the sides of the figure) [26].

Between all the Aztec deities, Tlazolteotl played an important role. She was also called *Ixcino* or *Tlazquimil*. Her name is derived from the Nahuatl word for garbage: *tlazolli*, which was used to connote filth [5]. The second part: *teotl*, signifies deity. According to Mesoamerican mythology, Tlazolteotl was the mother of Centeotl, the maize god, and of Xochiquetzal, goddess of fertility. As the goddess of fertility and sexuality, she was often depicted giving birth. Therefore, this divinity has

Tlazolteotl was the goddess of medicines, herbal remedies, fortune-tellers, surgeons, blood-letters, midwives, clairvoyants, and other healers [6]. All these people met once a year not only to perform a cele-

According to Aztecs, *yolpatzmiqilicli*, an epileptic fit, was ultimately caused by the rain god, but the proximate cause could be either possession by one of the god's helpers or a rapid accumulation of phlegm in the chest. States of health were related to equilibrium. The

generalized tonic-clonic, myoclonic, and auras, "Hupohualitmi" were epileptic disorders characterized by stillness and convulsions followed by stillness. They describe it as "the fit left the patient with a death body" (*grand mal*) and "Hicoyotl" that were epileptic episodes characterized exclusively by tremor (myoclonic seizures) [7].

the term "Tlazolli" (*dung*) means dirt, both material (physical) and moral (ethically). Seizures and epilepsy have historically been considered as a disease of impurities, and the goddess has the ability to clean the dirt/cure the disease [22].



Fig. 1. Famous depiction of Tlazolteotl in the German epilepsy museum showing the goddess giving the flower [25]. It is in the logo of the Mexican Chapter of the International League Against Epilepsy.



Fig. 3. This is a depiction of Tlazolteotl from the codex Bergia manuscript, sheet 55. In this depiction, the goddess is wearing the crescent-shaped nose ring, which refers clearly to the moon. Tlazolteotl was the lunar deity par excellence. She has small moons as decoration on her garments. According to the Aztecs, "the moon is the first death, disappears from the sky for three nights, but then reappears, returns, comes back to life, and therefore ensures the dead a new way of existence" [18].

Tlazolteotl represented sexual impurity and sinful behavior. When Tlazolteotl was a young woman, she was a carefree temptress. In her second form, she was the destructive goddess of gambling and uncertainty. In her middle age, she was the great goddess able to absorb human sin. In her final manifestation, she was a destructive and terrifying hag praying upon youths. Tlazolteotl was thought to provoke both lust and lustful behavior, but she also could grant absolution to those who had sinned. She became best known for her capacity to cleanse such sins during confessionals conducted by her priest. Although she could in one form inspire debauched behavior, she could also forgive sinners and remove corruption from the world [18].



Fig. 8. My birth by Frida Kahlo. In this painting, the head of Frida is leaning from the mother's womb. There is a puddle of blood under the mother's body, which might be a hint of the artist's own experience with a recent miscarriage. A sheet covers the mother's face. Above the birth bed, a picture of the weeping "Virgin of sorrows" hangs. The Virgin looks on in tears with sorrow and sympathy.



Fig. 9. Mural: "The History of medicine in Mexico" by Diego Rivera, at the Hospital de la Raza in Mexico City. In the middle of the painting, there is a representation of Tlazoteotl.



Fig. 10. Tlazoteotl the Aztec goddess of epilepsy. Modern representation by the artist Eduardo Urbano Merino (www.eduardourbano.com).

7 Sociocultural History of Epilepsy

Peter Wolf

THE SAINTS OF EPILEPSY

by

EDWARD L. MURPHY

EPILEPSY, at least in its grand mal variety, presents so dramatic and, to the lay observer, so terrifying a spectacle that it is not strange that its victims readily resorted to supernatural aid for alleviation. Unlike so many other diseases it offers no external signs of its presence and the horrifying suddenness with which apparently healthy and normal people could be transformed into writhing convulsives must have gone a long way in suggesting that the syndrome resulted from visitations of God or from His temporary defeat by the powers of evil. As we know, the Greeks thought of the disease as a divine intervention in the life of man, although the critical voice of Hippocrates had announced that it was no more divine than any other ailment. In early Christian times, and

Medical History Vol 3 (4); 1959

Los Sirvientes de los Epilépticos

(Salveregina2005)



Esta iniciativa vio la luz el 18 de abril de 2013.

Se dirige a aquellas personas que sufren de epilepsia, sobre todo, cuando esta enfermedad es originada por prácticas mágicas.

Patrona la Virgen Santísima en distintas advocaciones marianas :

Nuestra Señora de Montserrat
Nuestra Señora de Einsiedeln
Nuestra Señora de Lourdes
Nuestra Señora de Fátima
Nuestra Señora de Torreciudad
Nuestra Señora de la Caridad del Cobre
Nuestra Señora Auxiliadora
Nuestra Señora de África

Protectores (entre otros) : Los Coros Celestiales, san Marcial, san Benito, santa Escolástica, san Juan Bosco, santo Domingo Savio, san José Cafasso, san Romualdo, san Maximiliano Kolbe, santa Teresa de Avila, san Pedro de Alcántara, san Guy de Pomposa, Venerable Meinrad Engster, san Mathurin, san Willibrord, santa Catalina de Siena, santo Domingo de Guzmán, san Pio de Pietrelcina, san Francisco de Asís, san Francisco Javier, san Ignacio de Loyola, san José María Escrivá, Venerable Alvaro del Portillo, santa Devota, san Juan Bautista, santa Bernardita Soubirous, Beata Mirjam Abellín, santa Teresita del Niño Jesús, santa Maravillas de Jesús, san Juan de Avila, santa Genoveva Torres, san Antonio de Padua, san Camilo de Lellis, beata Margarita Bays, san Bernardo, san Antonio el Grande, san Pablo el Ermitaño, san Macario el Grande, san Atanasio el Atónita y los santos Atónitas, santa Benedicta y santa Bibiana.

Epilepsy & Behavior 57 (2016) 255–264

Contents lists available at ScienceDirect

Epilepsy & Behavior

journal homepage: www.elsevier.com/locate/yebeh

Review

Epilepsy through the ages: An artistic point of view

Lady Diana Ladino ^{AB,1}, Syed Rizvi ², Jose Francisco Téllez-Zenteno ^{AA}



Saint Valentine



Fig. 3. "Saint Valentine" - earlier painting by the Hans-Gesing-Engelhardt, oil painting, 1675. Centre of embroidery, and collection of the Brnoctor university in Masaryk University, Czechia.



Fig. 2. "Saint Valentine patron of physicians", manuscript of 1014 - 1118 on parchment, 147x100 cm, National Gallery of Art, Washington DC.

L.D. Ladinov et al. / Epilepsy & Behavior 57 (2016) 255–264



Fig. 4. "Saint Valentine", ceiling painting, 1740, Bamberg, Unterföhrbach, Germany.

Saints and ExVotos



Der Heilige Antonius
Exvoto um 1773 aus der Kapelle St. Antonius in
Haidlfing
(Photographie Claus Hansmann, Stockdorf)

Saints and ExVotos



Heilung einer Besessenen
Exvoto um 1700. Majolika-Tafel aus der
Wallfahrtskirche Madonna dei Bagni/Umbrien
(Photographie Claus Hansmann, Stockdorf)

Saints and ExVotos



Tafelbilder der Kirche in Krummenau aus der Werkstatt des Johann Georg English
Epilepsie Museum Kork

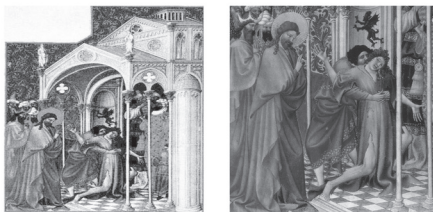
Saints and ExVotos



Jesus cures an epileptic
Anonymous



Medieval image of exorcism Diablo,
14th Century, Byzantine



Limbourg Brothers (Herman, Jean, Pol): The Exorcism in the Synagogue,
Les Très Riches Heures du Duc de Berry
Musée Condé, Château de Chantilly, 1412-16



"Jesus cures an epileptic demonic child", French School XVII Century
www.subastasisimperio.com



Verona, Basilica di San Zeno



Tratan unos hombres a una mujer endemoniada, azada con cuerdas, quien apenas vivo a la Santa rompió en gritos y se revolvió por el suelo. Catalina acercándose pidió que la soltaran en nombre de Jesucristo e inmediatamente ésta quedó libre de sus tormentos.



Monastery of Saint Catherine of Sienna, Arequipa - Peru
Painter Unknown



Aquí pinté a mi padre Wilhelm Kahlo, de origen húngaro-alemán, artista-fotógrafo de profesión, de carácter generoso, inteligente y bueno, valiente porque sufrió durante sesenta años de epilepsia pero nunca se rindió trabajando y luchó contra Hitler, con adoración, Su hija Frida Kahlo".



Fig. 5. "Die Epileptischen von Molenbeek" engraving by Hendrick Hondius the Younger (1662), after a print made after drawing by Brueghel the Elder (1564), original size: 268 cm x 414 cm, at the Middelbeker royal Albert I (Collection des Rotamper), Brussels, Belgium.



L.D. Lathin et al. / Epilepsy & Behavior 57 (2016) 295–294

299

Fig. 6. "The Pilgrimage of the Epileptics to the church at Molenbeek" also called "The dance of St. John or St. Vitus" by Pieter Bruegel, known as "Bruegel the Younger". Wood panel painting, original size: 292 cm x 622 cm, at the Royal Institute for the Study and Conservation of Belgium's Artistic Heritage, Brussels, Belgium.



The Transfiguration, Raphael Sanzio 1483 - 1520
Vatican Museum



The Transfiguration of Christ, Peter Paul Rubens (1577 – 1640)
Museum of Fine Arts of Nancy, France



Review

Art and epilepsy surgery

Lady Diana Ladino^{a,b}, Gary Hunter^a, José Francisco Téllez-Zenteno^{a,*}

^a Division of Neurology, Department of Medicine, University of Saskatchewan, Saskatoon, Saskatchewan, Canada
^b Neurology Department, College of Medicine, University of Antioquia, Medellín, Antioquia, Colombia



Image from the 14th century, a physician performs trepanation, a surgical procedure then used to treat epilepsy.

Guido da Vigevano 1280 - 1349
Reproduction of *Anathomia* (1345)



Fig. 1. Epilepsy in Istanbul (the way to cure an epileptic). From manuscript, collection of medical manuscripts, Museum painted at the end of the 13th century. Collection: British Museum, London, Accession number: 195.



Fig. 2. Epilepsy treatment from the surgical atlas Cerrahiyetif Hıfzı (Imperial surgery). Drawn in the 15th century (1465). Collection: Ataturk Institute for Modern Turkish History, Istanbul, Turkey. Artist: Selvendim Sabuncuoğlu [17].



Cutting the stoner, Pieter Jan Quast (1605 – 1647)
Kunstmuseum Sankt Gallen, Switzerland



Hieronimus van Aken, "El Bosco" (1450-1516)
Prado Museum, Madrid



A surgeon extracting "pierres de tête". Oil painting after Nicolaes
Weydmans (1570 - 1642) Wellcome Collection gallery

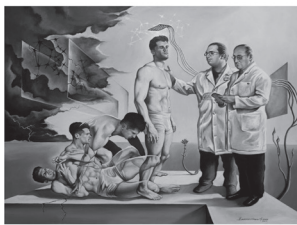


Fig. 11. Epilepsy, knowing the nightmare behind. Painted in 2013. Technique: oil/canvas. Measurements: 100 x 120 cm. Location: Royal University Hospital, Saskatoon, Saskatchewan, Canada. Artist: Eduardo Urbano Merino.



Fig. 12. "Wire", 70 x 90 aluminum and oil on canvas 2011, by Kris Hauser, Saskatoon, Saskatchewan, Canada. Reprinted with permission from the artist.



Epilepsy & Behavior 83 (2018) 151–161

Contents lists available at ScienceDirect

Epilepsy & Behavior

journal homepage: www.elsevier.com/locate/yebbeh



Review

The Montreal procedure: The legacy of the great Wilder Penfield

Lady Diana Ladino ^{*,a}, Syed Rizvi ^b, José Francisco Téllez-Zenteno ^b



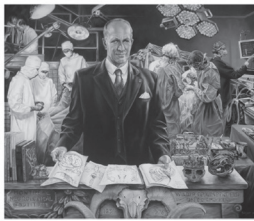


Fig. 16. The portrait by Kris Hauser. On the left is the Montreal Neurological Institute theater at Wilder Penfield's era. On the right is the current Royal University Hospital operating room at Saskatoon, Saskatchewan, Canada. The figure represents the evolution of the Montreal procedure from the past to the present, not only in Canada, but also throughout the entire world.



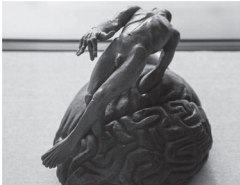
Pierre Andre Brouillet (1857-1914), "Une leçon clinique à la Salpêtrière"
Paris Descartes University, Paris



Tony Robert Fleury (1837-1912), "Philippe Pinel à la Salpêtrière"
British Museum



Bohumil Kubista (1884-1918), "Epileptic Woman"
Moravian Gallery in Brno

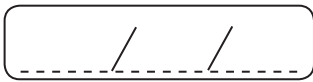


Fallsucht von Bodo Wentz
Epilepsy Museum, Kork Germany

The ceramic depicts two essential moments of the disease epilepsy, firstly the **medical aspect**: the brain as the source of the disease, and the "seizure" of the person suffering from epilepsy as the impressive symptom of the disease. Secondly it portrays the **psycho-social aspect**: the chronic disease "epilepsy" leading to exclusion, social isolation, desolation, retreating ("into one's shell").



Fig. 9. Poor Miss Fitch by unknown artist, 1872, from the book Poor Miss Fitch.
Wilkie Collins, 1824 - 1889



MATTEO MANCINI (UK)

THE DIFFUSION MRI-BASED CONNECTOME: PROMISES AND PITFALLS



UCL

The diffusion MRI-based
connectome:
promises and pitfalls

Dr. Matteo Mancini
University College London

Outline

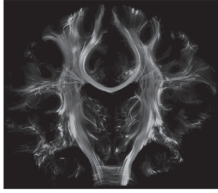
- About me;
- Network models and graph theory;
- The brain as a network;
- Diffusion MRI;
- Defining nodes;
- Defining edges;
- Network properties and graph measures;
- Current issues and pitfalls;
- Translating into clinical applications;
- Take-home message.

About me

PhD (Rome -> Utrecht -> Brighton)
Postdoc (UCL)

Diffusion MRI

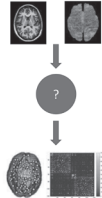
- Diffusion data can be modelled using a tensor, which is simple but unable to represent complex geometry (e.g. crossing fibers);
- More complex models, usually requiring longer protocols, can estimate a fiber orientation distribution;
- Using tractography on the modelled data, it is possible to estimate the trajectories of the white matter fibers using two classes of algorithms:
 - Deterministic: propagation of a streamline until a stop criterion is reached;
 - Probabilistic: fit of a probability distribution of the preferred direction of water diffusion;



A. Arwandic, Max Planck Institut for Human Cognitive and Brain Sciences

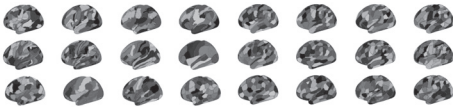
Structural networks in the brain

- In the next slides, we will go through the methodological choices to fit a network model to MRI data;
- The main steps are:
 - Definition of nodes;
 - Definition of edges;
 - Eventual definition of weights;
 - Eventual thresholding;
- Let's start by taking a look on how to define a node;
- *How hard could it be?*



Defining nodes

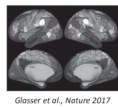
...This hard.



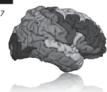
Arlon et al., NeuroImage 2018

Defining nodes: possible approaches

- Node = measurement point;
 - Pro: no assumption;
 - Con: no guarantee of any meaning behind the definition;
- Cytoarchitectonics;
 - Pro: multimodally validated;
 - Con: potential dependence on inter-individual variability;
- Macroscopic landmarks;
 - Pro: straightforward approach;
 - Con: variations in size;



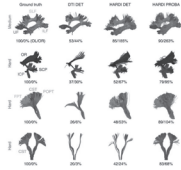
Glasser et al., Nature 2017



Desikan et al., NeuroImage 2006

Pitfalls inherited from diffusion MRI

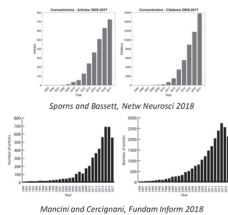
- Diffusion MRI suffers of several limitations that are inherited by the network models build on top of it:
 - Diffusion-based measures are influenced by several factors (axonal number, density, caliber, myelination);
 - Head-motion, physiological noise and imaging artifacts act as additional confounding factors;
 - Diffusion tractography has difficulty reconstructing long-range pathways;
 - Diffusion tractography cannot resolve source and target of a connection -> only undirected graphs;



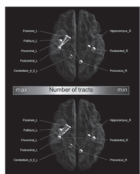
Maier-Hein et al., Nat Comm 2017

Translation into clinical applications

- The most common use of network models in neuroimaging has been first in neuroscience, in particular fundamental research;
- However, as the popularity of this approach has increased, there has been a constantly increasing number of studies in clinical populations;
- For epilepsy, the major applications in the literature so far include:
 - Getting new insights into different manifestations of epilepsy;
 - Identifying biomarkers for surgical planning;
 - Performing network-based simulations to understand seizure propagation;
 - Starting to build multimodal patient-specific models;



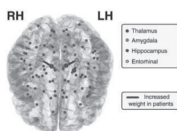
Applications: getting new insights



Caeyenberghs et al., NeuroImage Clin 2014

- Caeyenberghs and colleagues compared a group of 34 Juvenile myoclonic epilepsy (JME) patients and matched controls;
- They observed significant differences in a subnetwork involving primary motor, parietal and subcortical regions;
- They also observed significant correlation between structural connectivity and cognitive task performance;
- These findings suggest that JME-related changes extend beyond the frontal lobes;

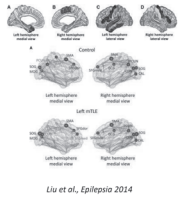
Applications: getting new insights



Taylor et al., NeuroImage 2015

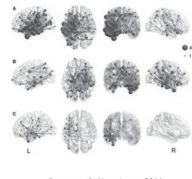
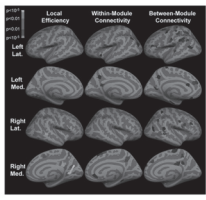
- Taylor and colleagues looked at how reduced volumes and connectivity changes are related in temporal lobe epilepsy (TLE) patients;
- Although they found several differences in terms of surface area between patients and controls, they observed more subtle changes in terms of connectivity;
- It must be noticed that the authors did use connection-wise comparisons and appropriate multiple corrections;
- Nevertheless, these results suggest that it is important to look at potential relationships between atrophy and altered connectivity;

Applications: getting new insights

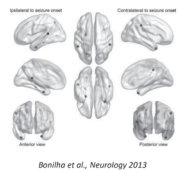


- Liu and colleagues characterized in terms of centrality the structural networks reconstructed from mesial temporal lobe epilepsy (mTLE) patients;
- They observed decreased efficiency in ipsilateral temporal, bilateral frontal and bilateral parietal areas;
- They also observed alterations in terms of hubs;
- These results seem to describe from a different perspectives the structural abnormalities previously observed in gray and white matter in mTLE;

Applications: getting new insights

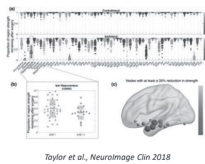


Applications: biomarkers for surgical planning



- Bonilha and colleagues retrospectively studied medial temporal lobe epilepsy (MTLE) patients who underwent temporal lobectomy;
- Using specific measures, they were able to distinguish seizure-free patients from the others;
- Non-seizure-free patients exhibited higher medial-lateral temporal and temporal-parietal connectivity;
- These results suggest the idea that structures traditionally not removed during surgery may be associated with seizure control;

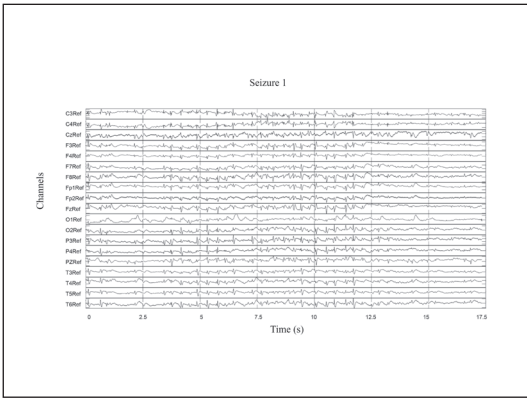
Applications: biomarkers for surgical planning

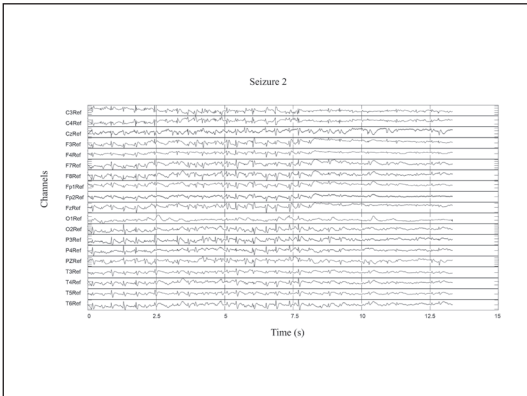


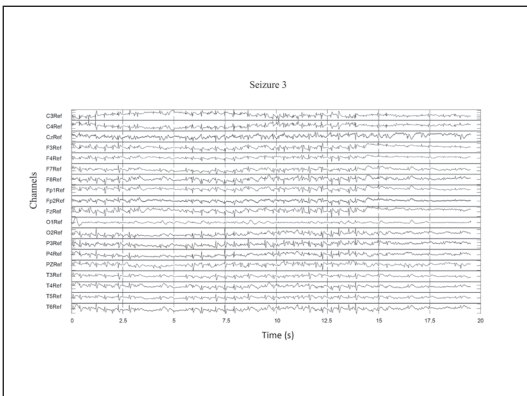
- Taylor and colleagues proposed a pipeline to estimate the structural white matter network and classify patients in seizure free or not;
- To do this, they trained their classifier using both network-based and volumetric measures;
- They observed that surgery leads to patient-specific reductions in efficiency and strength;
- This result suggest that given a resection mask it is possible to use this approach during planning;

JEAN FABER (BRAZIL)

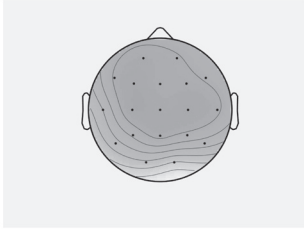
FROM ELECTROPHYSIOLOGICAL RECORDINGS TO CONNECTIVITY: HOW TO CONSTRUCT A GRAPH AND HOW TO ANALYZE IT?



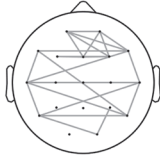




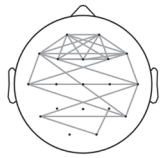
Seizure 1 Connected average power



Seizure 1 - Connected Topoplot Cross-correlation



Seizure 2 - Connected Topoplot Cross-correlation

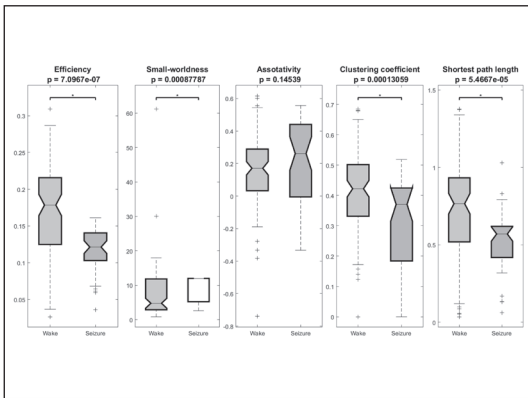


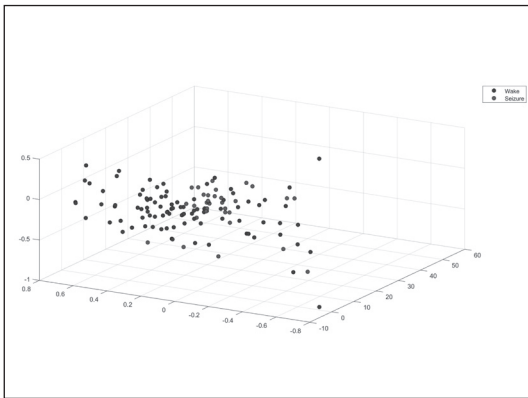
Seizure 3 - Connected Topoplot Cross-correlation

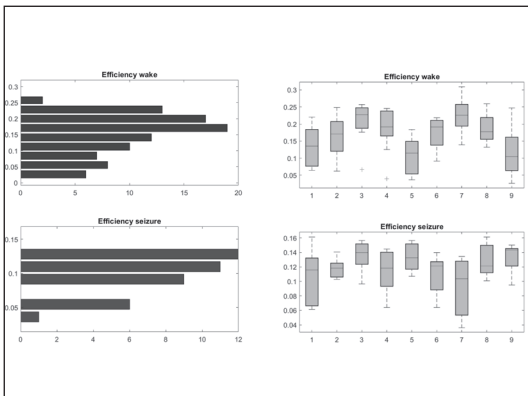


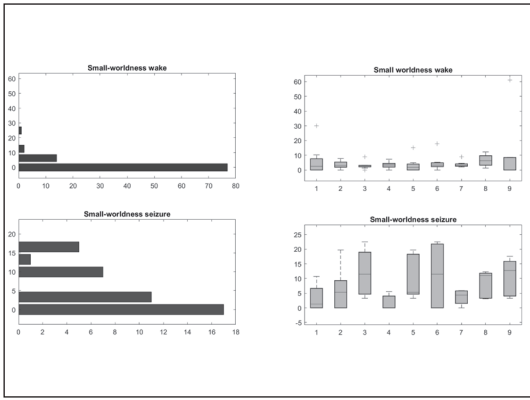
Vigil - Connected Topoplot Cross-correlation

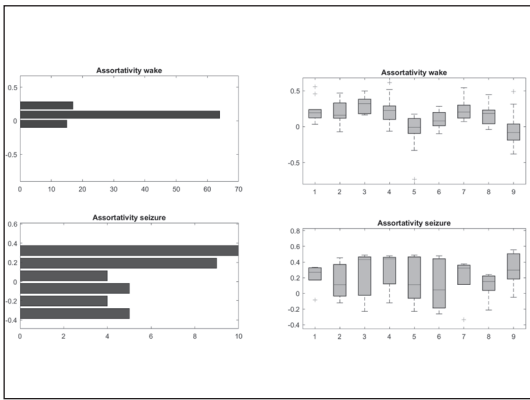


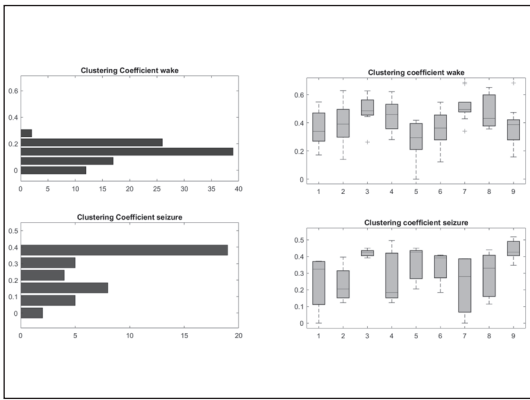


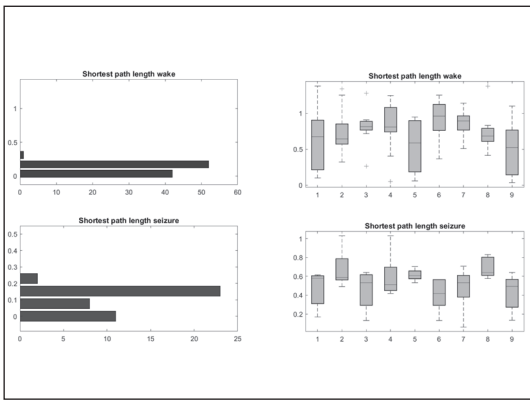


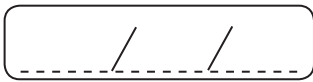








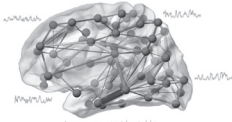





MAXIME GUYE (FRANCE)

STRUCTURE-FUNCTION RELATIONSHIPS IN EPILEPTIC NETWORKS

Structure-function relationships in epileptic brain networks



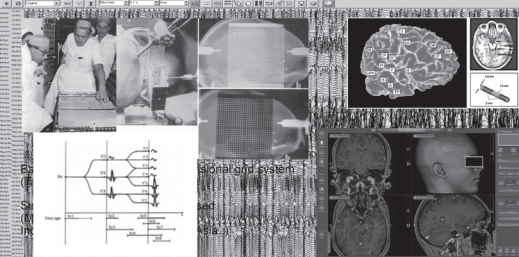
Maxime Guye
Centre for Magnetic Resonance in Biology and Medicine & Clinical Neurophysiology Department
Marseille, France



Outline

1. Epileptic and functional network organization in 'focal' epilepsy quantified by functional connectivity
2. Underpinning structural connectivity changes
3. Structure-function relationship: insights from modeling
4. Structure-function relationship: insights from multimodality

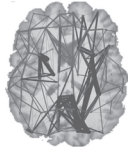
The concept of epileptogenic network defined by SEEG



Do structural alterations explain functional connectivity?

Graph analyses of structural connectivity
Alterations linked to cognitive impairments

↓ Global and local efficiency in patients with cognitive impairments only



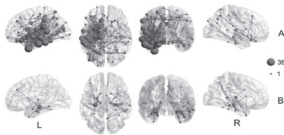
DTI
39 Patients
23 controls

Vaessen et al. *Cereb Cortex* 2011
See also: Liu et al. *Epilepsia* 2014

Fiber density / cognitive scores correlations

Do structural alterations explain functional connectivity?

Whole brain approach of pair-wise structural connectivity
Patterns of disconnection in Left and Right MTLE

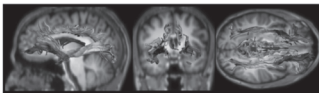


Besson et al. *Neuroimage* 2014
See also: Fang et al. *Neuroimage Clin* 2015

Does structural connectivity shape seizure organisation?

Link with propagation?

Differences among epilepsy types

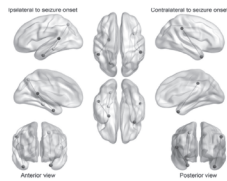


≠ patterns of 4 propagation bundles (FA, AD, RD)
In 17 TLE (-)MRI, 17 TLE (HS), 14 FLE (FCD)

Campos et al. *Epilepsia* 2015

Does structural connectivity shape seizure organisation?

Link with propagation? Predictive factor?
Patterns depending on surgical outcomes



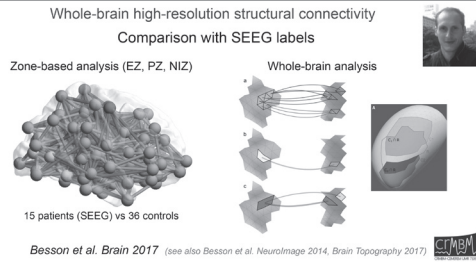
20 Patients
18 Controls

Bonilha et al.
Neurology 2013

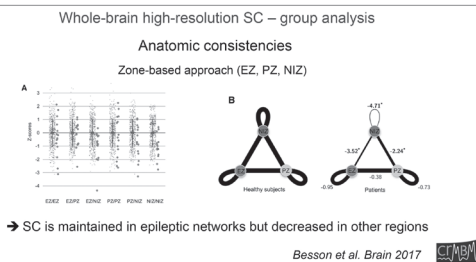
Higher fiber density in non-seizure free

See also: Dinkelacker et al. *Epilepsia* 2015

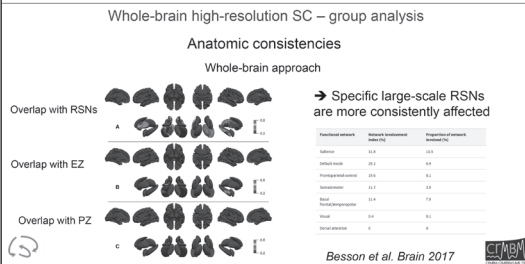
Does structural connectivity shape seizure organization?



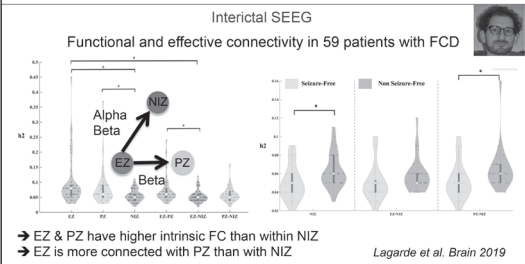
Does structural connectivity shape seizure organization?



Does structural connectivity shape seizure organization?



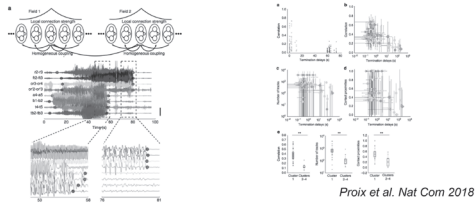
Concordant pattern of intrinsic functional connectivity



Does structural connectivity shape seizure organization?

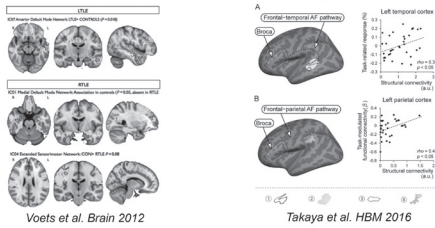
The virtual epileptic patient

Link between structural connectivity and seizure organization



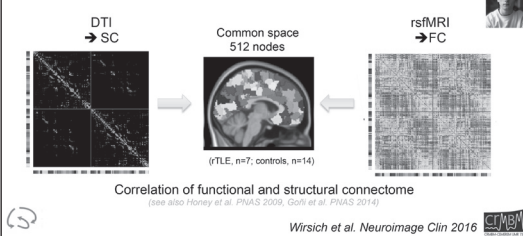
Structure-function relationship of brain connectivity

Evidences from multimodality



Structure-function relationship of brain connectivity

Whole brain network communication analyses



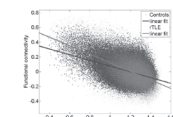
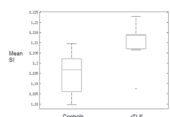
Structure-function relationship of brain connectivity

Network communication analyses

Search Information:
(Goffi et al., PNAS 2014)

Search information increased in rTLE (higher randomization of connections)

Search information is more correlated to functional connectivity in rTLE

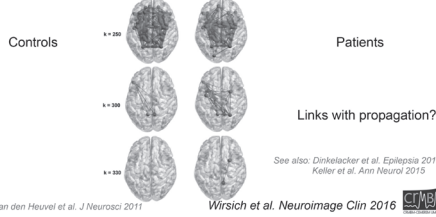


See also: Shaft et al. bioRxiv (2018)
Local SC directs seizure spread in focal epilepsy

Wirsich et al. Neuroimage Clin 2016

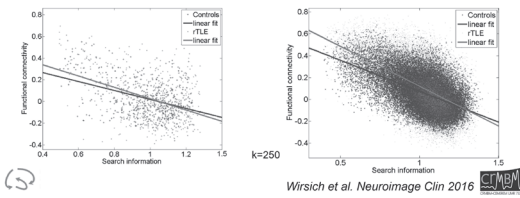
Structure-function relationship of brain connectivity

Network communication analyses
 "Rich-club" structure of hubs is preserved in rTLE



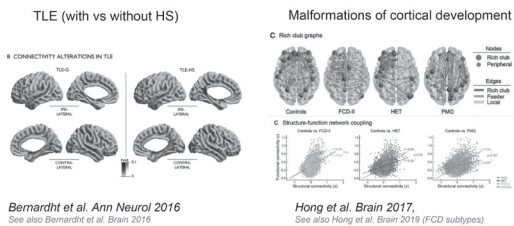
Structure-function relationship of brain connectivity

Network communication analyses
 Same structure-function correlation in rich club but not in periphery
 Rich club connections Peripheral connections



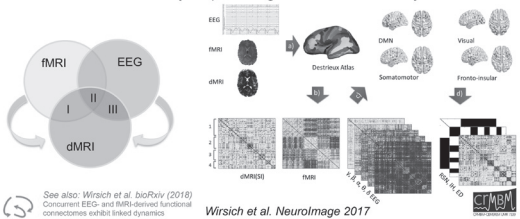
Structure-function relationship of brain connectivity

Role of the epileptogenic lesion



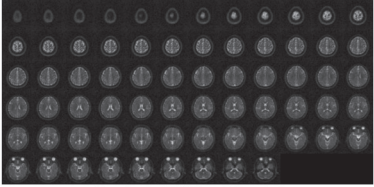
Insights from trimodal data fusion

Complementary contributions of concurrent EEG and fMRI connectivity for predicting structural connectivity




Ionic Homeostasis Alterations

Combining Sodium MRI and SEEG



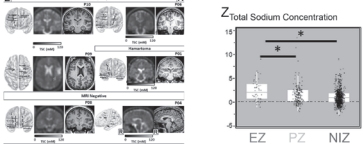
10 patients (SEEG) vs 27 controls

Ridley et al. *NeuroImage* 2017



Ionic Homeostasis Alterations


Combining Sodium MRI and SEEG



Intercal increased TSC (see also Wang et al. *Epilepsia* 1999)

Ictal decreased TSC (P04)

Ridley et al. *NeuroImage* 2017

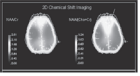


Ionic Homeostasis, Metabolism and Neurotransmission

Neuronal-glia impairment

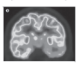
Insights from multimodal neuroimaging

Mitochondrial dysfunction (MRSI)



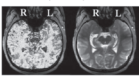
Guye et al. *NeuroImage* 2005
Guye et al. *Epilepsia* 2002

Glucose uptake (FDG-PET)



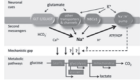
Duncan et al. *Lancet Neurol* 2016

Glutamate concentration (CEST)



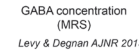
Davis et al. *Sci Transl Med* 2015

Sodium homeostasis and neuron-glia interaction / metabolism



Chatton et al. *Glia* 2016

GABA concentration (MRS)

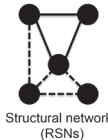


Levy & Degnan *AJNR* 2013

Conclusion – Structural Connectivity Organization

Insights from whole-brain high-resolution tractography and SEEG

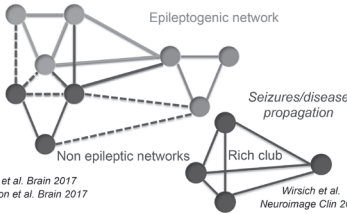
Cognitive impairments



Structural networks (RSNs)

Proix et al. *Brain* 2017
Besson et al. *Brain* 2017

Propagation networks



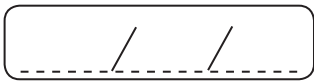
Epileptogenic network

Non epileptic networks

Rich club

Seizures/disease propagation

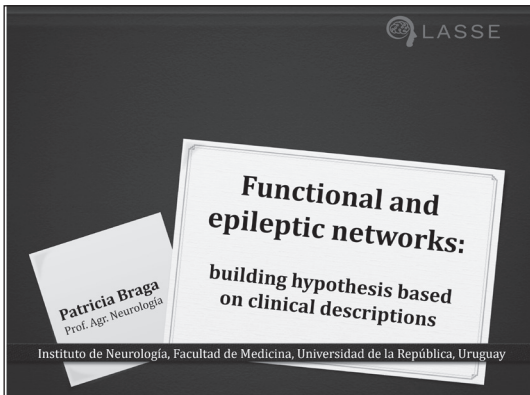
Wirisch et al. *NeuroImage Clin* 2016

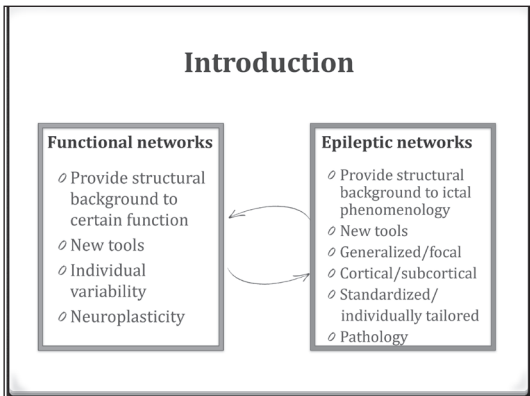


PATRICIA BRAGA (URUGUAY)

FUNCTIONAL AND EPILEPTIC NETWORKS: BUILDING HYPOTHESIS BASED ON CLINICAL DESCRIPTIONS







Building clinical hypothesis in epilepsy patients

Functional networks

- ◊ Provide structural background to certain function
- ◊ New tools
- ◊ Individual variability
- ◊ Neuroplasticity

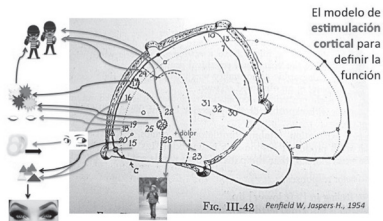
- Ictal semiology → (knowledge on functional networks) → epileptic network.
- Comprehensive evaluation → definition of epileptic network in pt. → (knowledge on functional networks) → functional risks/comorbidities.
- "Uncommon" spread patterns (ictal semiology) → "new" anatomofunctional pathways.

Epileptic networks

- ◊ Provide structural background to ictal phenomenology
- ◊ New tools
- ◊ Generalized/focal
- ◊ Cortical/subcortical
- ◊ Standardized/individually tailored
- ◊ Pathology

Building research hypothesis

◊ Epilepsy as a window to brain function



Building research hypothesis in epilepsy patients based on clinical descriptions

I. Source of data

◊ Interview

- ◊ Patient
- ◊ Witness - relative
- ◊ Video-EEG

II. Type of information: quality

III. Type of information (temporal pattern)

- | | |
|-------------------------|--|
| ◊ Ictal | ◊ Modifications after epilepsy treatment |
| ◊ Post-ictal | • Medications |
| ◊ Pre-ictal | • Surgery |
| ◊ Interictal /non-ictal | • VNS |
| • Intermittent | • DBS |
| • Permanent | |
| • Progressive | |

Interictal: progressive

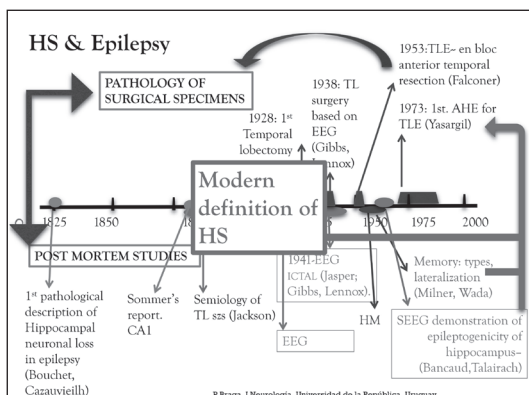
MEMORY IMPAIRMENT

Case 1

- ◊ Female, 31 years old. Righth-handed.
- ◊ No family history of seizures.
- ◊ PMH: no history of FS. Hypothyroidism. Depression.
- ◊ Spontaneous seizures starting by 18 y.o.
- ◊ Epigastric aura followed by impairment of awareness; oral automatisms and unilateral (R) hand automatisms; sometimes left hand dystonia/left face tonic. Rare bilateral TC szs.
- ◊ Recurrent, frequent seizures
- ◊ Unresponsive to pharmacotherapy with AEDs.
- ◊ Complains of progressive memory loss along the last 2 years.

DISCOVERING MEMORIES

- ◊ **Memory functional network:**
 - ◊ Until mid XX century- it was thought to be diffuse and widespread, without clear nodes or specific brain areas.
- ◊ **Memory in injured patients:**
 - ◊ Frequently affected, different clinical profiles, mostly with attention deficits.
- ◊ **Memory and epilepsy:**
 - ◊ Increasing recognition of patients with suspected TLE, complaining from memory disturbances without other symptoms of cognitive decline.
 - ◊ 1953 - Henry Molaison: severe short-term and anterograde memory impairment after bilateral mesial temporal resection, as empirical treatment for his epilepsy.



Memory and the Medial Temporal Lobe: Patient H. M.

Thomas C. Neylan, M.D., Section Editor

Loss of Recent Memory After Bilateral Hippocampal Lesions

William Beecher Scoville
Brenda Milner
The Journal of Neurology, Neurosurgery and Psychiatry
(1957; 20:11-21)



Horizontal lines for notes.

Neuropsychologia, Vol. 27, No. 1, pp. 71-81, 1989.
Printed in Great Britain.



RIGHT HIPPOCAMPAL IMPAIRMENT IN THE RECALL OF SPATIAL LOCATION: ENCODING DEFICIT OR RAPID FORGETTING?

MARY LOU SMITH* and BRENDA MILNER

Department of Psychology and the Montreal Neurological Institute, McGill University, 3801 University Street, Montreal, PQ H3A 2B4, Canada

Abstract—The recall of spatial location in patients with left or right temporal-lobe lesions was studied in two experiments, in which recall was tested either immediately after presentation of an array of objects, or after an intervening verbal task, a spatial task or an unfilled interval. Deficits were found only in patients with right temporal-lobe lesions that included extensive removal of the hippocampal region, and only when recall was tested after a delay. The presence of an intervening task in the delay interval did not accentuate the deficit. The results show that, despite a normal ability to encode location, patients with large right hippocampal lesions demonstrate an abnormally rapid forgetting of such information.

Horizontal lines for notes.

Neuropsychologia, Vol. 28, No. 4, pp. 349-359, 1990.
Printed in Great Britain.



THE ROLE OF THE LEFT HIPPOCAMPAL REGION IN THE ACQUISITION AND RETENTION OF STORY CONTENT

VIRGINIA FRISK* and BRENDA MILNER

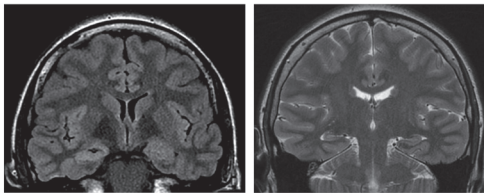
Department of Psychology and Department of Neurology and Neurosurgery, McGill University and the Montreal Neurological Institute, 3801 University, Montreal, Quebec, Canada, H3A 2B4

(Received 27 July 1989; accepted 15 October 1989)

Abstract—Thirteen normal control subjects and 62 patients who had undergone either a unilateral temporal or a unilateral frontal lobectomy learned the content of a short prose passage to a strict criterion. Compared to other subject groups, patients with left temporal-lobe excisions took longer to learn the story content and, within this group, the slowest rate noted was for patients with extensive removal from the hippocampal region. When retention of the material was tested after a 20 min delay, only the group with large excisions from the left hippocampus and/or parahippocampal gyrus was impaired. This finding of abnormally rapid forgetting of material learned to criterion highlights the role of the left hippocampal region in the long-term maintenance of verbal information presented in a context.

Horizontal lines for notes.

Case 1



- Selective amygdalo-hippocampectomy in Dec 2018.
Seizure free

Horizontal lines for notes.

MEMORY IMPAIRMENT in epilepsy

- ◊ Background
 - ◊ Building hypothesis
 - ◊ Current knowledge
 - ◊ New hypothesis?
-

Memory and epilepsy up to date

- ◊ Diagnosis of memory disturbance in epilepsy patients
 - ◊ Lateralizing value of memory disturbance in MTLE
 - ◊ Conclusions driven from available evaluation tools
 - ◊ Prognosis
 - ◊ Memory and surgical treatment
 - Memory and pharmacological treatment
 - Memory subtypes (paradigms) and epileptic networks
 - New tools
 - Other prognostic factors: complex systems
-

AREAS FOR RESEARCH

Pre-ictal phase

PRODROMES and PRODROMIC STATE

Prodromes: concept

- ◊ In **medicine**, a **prodrome** is an early sign or symptom (or set of signs and symptoms), which often indicate the onset of a disease before more diagnostically specific signs and symptoms develop.
- ◊ In **epilepsy**, it refers to premonitory symptoms preceding seizures in minutes, hours or even days.
- ◊ It is derived from the Greek word prodromos, meaning "running before".

Epilepsy & Behavior xxx (2018) xxx–xxx

Contents lists available at ScienceDirect

Epilepsy & Behavior

journal homepage: www.elsevier.com/locate/yebep

Review

Prodrome in epilepsy

Frank M.C. Besag^{a,b,c,*}, Michael J. Vasey¹

Table 2
Periodic windows.

Paper	Theoretical		For study (where applicable)	
	Start	End	Start	End
Ahning and Beniczky [9]	-	-	-	30 min
Blanchet and Frommer [14]	-	-	124 h	Not stated
Dubois et al. [19]	3 days	30 min	-	-
Hughes et al. [12]	3 days	10 min	-	30 min
Lee and Noj [14]	-	-	-	1 h
Mansfield et al. [20]	-	-	-	30 min
Peterson et al. [8]	24 h	5 min	24 h	-
Pinikahana and Dreno [16]	124 h	10 min	-	-
Rajna et al. [4]	30 h	1 h	-	-
Scaramelli et al. [7]	124 h	-	24 h	15 min
Schulze-Bohagge et al. [6]	-	-	-	30 min
Sier et al. [17]	1 week	1 h	-	-

Table 1
Paper summaries.

Study	% with prodrome
Ahning and Beniczky [9]	2.0
Cull et al. [10]	70.9
Giordano et al. [11]	8.6
Hughes et al. [12]	29.1
Janz [13]	10.0
Lee and Noj [14]	12.1
Peterson et al. [8]	68.7
Pinikahana and Dreno [16]	47.1
Pinikahana and Dreno [16]	74.4
Rajna et al. [4]	46.6
Scaramelli et al. [7]	39.0
Schulze-Bohagge et al. [6]	6.2
Sier et al. [17]	7.2
Total	21.9

Review

Prodrome in epilepsy

Frank M.C. Besag^{a,b,c,*}, Michael J. Vasey¹

Fig. 2. Prodrome frequencies.

Seizure 18 (2009) 246–250

Contents lists available at ScienceDirect

Seizure

journal homepage: www.elsevier.com/locate/yseiz

Prodromal symptoms in epileptic patients: Clinical characterization of the pre-ictal phase

Alejandro Scaramelli^{*}, Patricia Braga, Andrea Avellanal, Alicia Bogacz, Claudia Camejo, Isabel Rega, Tamara Messano, Beatriz Arciere

Instituto de Neurología, Hospital de Clínicas, Av. Italia 516, Montevideo 11600, Uruguay

ARTICLE INFO

Article history:
Received 29 July 2008
Received in revised form 17 October 2008
Accepted 23 October 2008

ABSTRACT

Although recent advances in seizure anticipation have been achieved with the development of several biomathematical electroencephalographic (EEG) methods, pre-ictal phenomena have not been extensively investigated. The aim of the study was to thoroughly analyze premonitory or prodromal symptoms (PS) in a randomly selected sample of 100 adult epileptic patients. A semi-structured protocol was used for in-person interviews to both patients and observers. PS were found in 39% of patients, the most frequent ones being behavioral, cognitive and mood changes. Both patients with focal and generalized epilepsies reported prodromes, although they were more frequently found in the former group. PS were mostly perceived preceding complex partial and generalized tonic-clonic seizures. Prodromal symptoms were reported to have an insidious onset and their duration ranged from 30 min to several hours. The potential value of prodromes in seizure anticipation would allow the use of preventive and therapeutic measures, including drugs, neurostimulation procedures and behavioral intervention.

© 2008 British Epilepsy Association. Published by Elsevier Ltd. All rights reserved.

Seizure 18 (2009) 246–250

Contents lists available at ScienceDirect

Seizure

Prodromal of the pre-ictal phase

Alejandro Scaramelli^{*}, Patricia Braga, Andrea Avellanal, Alicia Bogacz, Claudia Camejo, Isabel Rega, Tamara Messano, Beatriz Arciere

Instituto de Neurología, Hospital de Clínicas, Av. Italia 516, Montevideo 11600, Uruguay

ARTICLE INFO

Article history:
Received 29 July 2008
Received in revised form 17 October 2008
Accepted 23 October 2008

ABSTRACT

Although recent advances in seizure anticipation have been achieved with the development of several biomathematical electroencephalographic (EEG) methods, pre-ictal phenomena have not been extensively investigated. The aim of the study was to thoroughly analyze premonitory or prodromal symptoms (PS) in a randomly selected sample of 100 adult epileptic patients. A semi-structured protocol was used for in-person interviews to both patients and observers. PS were found in 39% of patients, the most frequent ones being behavioral, cognitive and mood changes. Both patients with focal and generalized epilepsies reported prodromes, although they were more frequently found in the former group. PS were mostly perceived preceding complex partial and generalized tonic-clonic seizures. Prodromal symptoms were reported to have an insidious onset and their duration ranged from 30 min to several hours. The potential value of prodromes in seizure anticipation would allow the use of preventive and therapeutic measures, including drugs, neurostimulation procedures and behavioral intervention.

© 2008 British Epilepsy Association. Published by Elsevier Ltd. All rights reserved.

Table 1
Type and frequencies of reported prodromal symptoms (PS) in the study population.

Type of PS	N
Behavioral changes	13
Cognitive disturbances	11
Anxiety and mood changes	9
Fatigue	7
Sleep disturbances	7
Dysrhythmia	6
Speech disturbances	4
Voiding changes	4
Gastrointestinal symptoms	3
Headache	2
Changes in appetite	2
Paresthesias	1
Pain (other than headache)	1
Other	5
Total	75

Case 2

- ◊ Male, 49 years old. Right-handed.
- ◊ No family history.
- ◊ No relevant PMH. Anxiety and depressive symptoms.
- ◊ Epilepsy onset: 12 yo.
- ◊ Focal seizures, starting with a perception of depersonalization ("as if he was in a movie"), followed by impaired awareness. 1-4/year
- ◊ Sometimes he refers either dysmnestic and/or epigastric auras.
- ◊ Sporadic bilateral tonic-clonic seizures.
- ◊ Normal imaging and EEG with left FT spikes.
- ◊ Non-adherence to treatment and lost to follow-up.

Case 2 His prodromes

- ◊ Before bilateral tonic-clonic seizures:
 - ◊ progressive fatigue and tiredness, during 24 hours preceding his last GTCS
 - ◊ Speech disturbance: difficulty moving the tongue, changing words, starting a few hours before the seizure and lasting up to few hours afterwards.
- ◊ Before focal seizures
 - ◊ "I have the feeling of slow thinking and I have to think everything twice; I can't remember what I have to do. It seems as if my mind were in slow motion." Starts hours, sometimes a whole day before the seizure, and may last up to a few hours after the seizure end.

Your hypothesis??

Epilepsy & Behavior 21 (2011) 184–188

Contents lists available at ScienceDirect

Epilepsy & Behavior

journal homepage: www.elsevier.com/locate/yabeh

Are prodromes preictal events? A prospective PDA-based study

Thomas Maiwald^{a,b}, Julie Blumberg^{c,d}, Jens Timmer^a, Andreas Schulze-Bonhage^{b,*}

^a Freiburg Center for Data Analysis and Modeling, Freiburg University, Freiburg, Germany
^b Systems Biology Department, Harvard Medical School, Boston MA, USA
^c Epilepsy Clinic, University Hospital Freiburg, Freiburg, Germany
^d Children's Hospital, Harvard Medical School, Boston MA, USA

ARTICLE INFO

Article history:
Received 23 November 2010
Revised 28 January 2011
Accepted 3 February 2011
Available online 22 April 2011

Keywords:
Prodrome
Seizure
Prediction
Epilepsy
Personal digital assistant
Ambulatory monitoring
Prospective

ABSTRACT

Up to 20% of patients with epilepsy report "prodromal" sensations more than 30 minutes prior to seizures. We developed and implemented an objective methodology to prospectively assess the sensitivity and specificity of these subjective experiences using personal digital assistants (PDAs). The key property, in contrast to paper-based diaries, is the internal recording of the patient's entering time of prodromes and seizures. Of 500 patients with epilepsy interviewed, 31 claimed to sense prodromal symptoms at least 30 minutes before seizure onset. Eleven of them agreed to participate in a 4-week study to objectively measure their prospective prediction performance. In 8 patients returning data, the majority of prodrome entries were not followed by seizures or were identified only retrospectively. Statistical analysis revealed that no patient could outperform a nonspecific random predictor when predicting seizures based on the occurrence of prodromes, and that the group performance matched precisely the expected result for a by-chance predictor. These results question the predictive value of "prodromes" and the specificity of their occurrence in the preictal period.

© 2011 Published by Elsevier Inc.

Are prodromes preictal events? A prospective PDA-based study
Thomas Maiwald ^{a,b}, Julie Blumberg ^{c,d}, Jens Timmer ^a, Andreas Schulze-Bonhage ^{b,*}

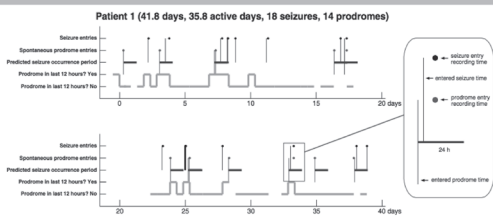


Fig. 3. Overview of events and patient compliance. Patient 1 participated for 40 days and had 18 seizures and 14 prodromes. The upper row represents the experienced seizures (black vertical lines) and their recording times (black dots). Similarly, the middle row shows the stored prodromes (red vertical lines) and their recording times (red dots). Each prodrome is followed by a 24-hour seizure SGP (blue horizontal line). If a seizure occurs within a SGP, it is classified as correctly predicted by the corresponding prodrome for a SGP of 24 hours. The lower row displays the answers of the triggered prodrome entries. Upper levels of the light blue line belong to periods in which one or more prodromes should have occurred if the patient made consistent entries. The line is interrupted if no answer is given by the patient for a triggered event.

Seizure 22 (2013) 522–527

Contents lists available at ScienceDirect
Seizure
Journal homepage: www.elsevier.com/locate/yseiz

Epileptic prodromes: Are they nonconvulsive status epilepticus?

Jørgen Alving ^{a,*}, Sándor Beniczky ^{a,b}

^aDepartment of Clinical Neurophysiology, Danish Epilepsy Centre, Dianalund, Denmark
^bDepartment of Clinical Neurophysiology, Aarhus University, Aarhus, Denmark

ABSTRACT

Purpose: The aim of this study was to assess how frequently prodromes occur in an adult patient group from a tertiary referral epilepsy centre and to investigate the EEG changes during the prodromes.

Methods: 578 consecutive patients were interviewed on subjective phenomena, experiences heralding the seizures, for at least 30 min before the start of the seizure. EEGs were recorded during the prodromes.

Results: Ten out of 400 included patients had prodromes (2.5%). We were able to record EEG during prodromes in 6 patients. Three patients had EEG changes corresponding to nonconvulsive status epilepticus. Three patients had unrevealing EEG recordings during prodromes.

Conclusion: Our results suggest that at least in a part of the patients, the prodromes are actually ictal phenomena, and should be treated as nonconvulsive status epilepticus.

© 2013 British Epilepsy Association. Published by Elsevier Ltd. All rights reserved.

Pre-ictal phase

PRECIPITATING FACTORS

PRECIPITATING FACTORS and REFLEX SEIZURES

PRECIPITATING FACTOR:
In most of the cases seizure occurs spontaneously, but there may be association with various triggers. These triggers may act as seizure precipitating factors.

REFLEX SEIZURE: Objectively and consistently demonstrated to be evoked by a specific afferent stimulus or by activity of the patient. (Blume WT et al., 2001)

- Specificity of stim/activity
- Internal /external
- Simple / Elaborated
- Time lapse
- Event (specific or non-specific sz type or trait)

Case 3

- ◊ Female, 15 yo. Right-handed.
- ◊ PMH unremarkable. No family history.
- ◊ Focal epilepsy of unknown etiology
- ◊ Onset 13 yo
- ◊ Focal aware seizures: olfactory (unpleasant, strong perception) followed by epigastric aura, eventually presenting a vertiginous sensation and impairment of awareness with automatisms.
- ◊ Sporadic bilateral TC seizures
- ◊ Precipitating factors: stress, sleep deprivation

Case 3

- ◊ After some years, she noticed that:
1. Once she perceives the strong, unpleasant and unexplained odor, she can stop the seizure progression by inhaling parfum.
 2. A certain odor (bath soap) could precipitate her seizures.
 3. When she perceives the precipitating odor, she can sometimes avoid the seizure by inhaling parfum.

Case 3

Hypothesis?

- ◊ For clinical approach
- ◊ Any research hypothesis?

Hypothesis

- ◊ **Clinical hypothesis**
 - ◊ Epileptogenic zone in a "non-lesional" patient
 - ◊ Fitting clinical hypothesis with a structural lesion
- ◊ **Research hypothesis?**
 - Network-etiology-epilepsy type specificity of PF/RS?
 - Tailored non-pharmacological treatment in patients with reflex seizures?

Post-surgical period

PERCEPTUAL CHANGES

Case 1

- Male, 30 yo
 - Epilepsy onset 19 yo. Refractory.
 - **Right MTS**
 - Atypical features: reflex seizures (cognitive task)
 - AEDs at time of surgery: CBZ + LTG
 - Surgery (2010): selective amigdalo-hippocampectomy
 - **Perceptual disturbance modality: olfactory.**
- Referred enhanced perception of odors "could not avoid perceiving even those fragrances that are usually on the background and are not consciously perceived." No changes in the perception quality or emotional reaction to it.
- Duration: 3 months
 - Simultaneous decrease in libido, during the same time window
 - Emotional instability early after surgery
 - Seizure free first year after surgery; late relapse with different seizure type.

Case 2

- Male, 39 yo
 - Epilepsy onset 18 yo. Refractory
 - **Right MTS**
 - Atypical features: early bilateral spread on ictal EEG
 - AEDs at time of surgery: PHT + VPA + CLZ
 - Surgery (2010): Anterior temporal lobectomy
 - **Perceptual disturbance modality: olfactory.**
- "All odors perceived strongly and are felt with disgust, associating rejection of food intake and sexual approach".
- Duration: 3 months
 - Simultaneous decrease in libido and erectile dysfunction, persisting with some fluctuations along the following years
 - Late depression (1 yr after surgery)
 - Seizure free since surgery

Case 3

- Female, 39 yo.
 - Epilepsy onset 15 yo
 - Left MTLE. Refractory
 - **Low grade tumor; Left amygdala**
 - AEDs at time of surgery: CBZ
 - Surgery (2013): Lesionectomy
 - **Perceptual disturbance modality: auditory**
- "Used to like music at very high volume before surgery; afterwards, she prefers it at a much lower volume"
- Duration: permanent /long lasting
- No sexual or behavioral changes
 - Mood instability (alternating euphoria, anxiety, depression, irritability) during the whole first year after surgery (improvement under SSRI and decreasing CBZ)
 - Seizure free since surgery

Perceptual disturbances after epilepsy surgery

Eraga P, Bogacz A, Scaramelli A.
Epilepsy Section, Institute of Neurology, Hospital de Clinicas, Facultad de Medicina,
Universidad de la República. Montevideo, Uruguay

CONCLUSIONS

- We propose the hypothesis that compensatory mechanisms involving changes of excitability in functional networks connected to epileptic foci (increased threshold with inhibitory effect), and their reset after surgery (decreasing threshold to normal parameters, with transient relative hyper-excitability), may underlie these postoperative perceptual changes.
- Disruption of limbic circuits by surgery allow for plastic changes in connectivity and excitability, with potential impact on emotion, behavior and perceptual processing.
- Perceptual, as well as behavioral, sexual and mood changes, should be addressed in patients after epilepsy surgery.
- Further research is needed in order to identify risk factors, outcome and underlying physiopathology.

Poster presentation, IEC 2015, Istanbul (unpublished)

Final remarks

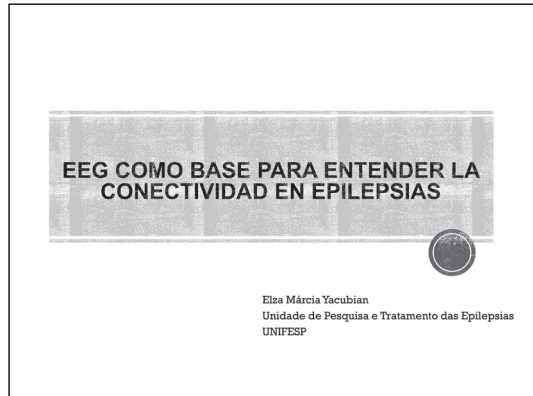
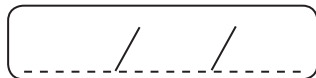
- Advanced technology is extremely helpful for analyzing and demonstrating neural connectivity.
- Clinical descriptions are still useful both to choose relevant questions in clinical practice, and to foster new answers.
- If you are a clinician, and particularly if you are or want to be an epileptologist, do never forget to use this fantastic tool

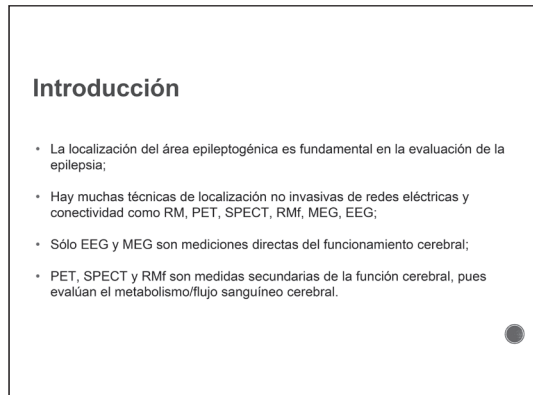


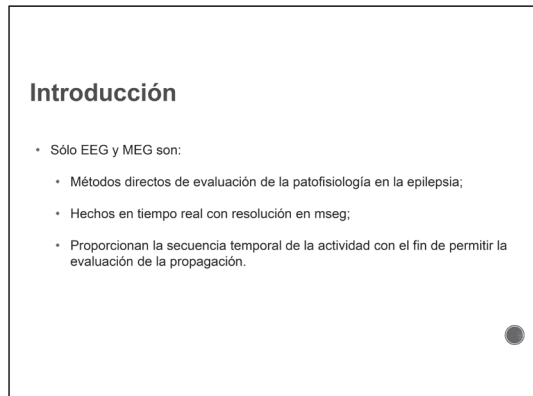
o And please remember, when questioning on our brain functioning, to ask the proper question to the adequate interlocutor: your own brain!!

Thank you for your attention!!!







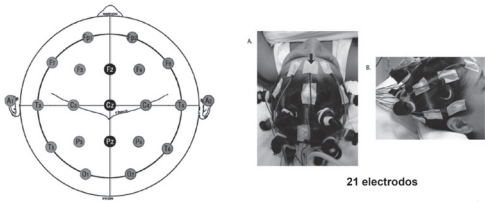


BIOFÍSICA DE LOS CAMPOS EEG Y MEG



ELECTROENCEFALOGRAMA

El sistema 10-20 de colocación de electrodos

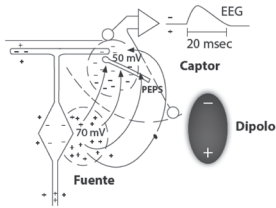


21 electrodos

Rios-Pohl & Yacubian, 2016



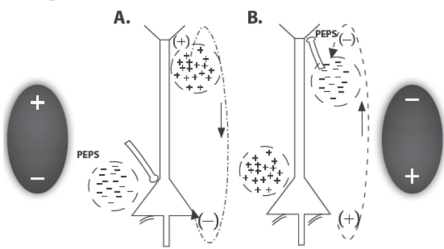
Electrogénesis



Rios-Pohl & Yacubian, 2016



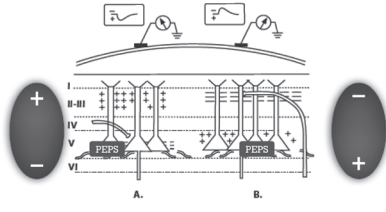
Electrogénesis



Rios-Pohl & Yacubian, 2016

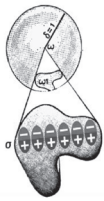


Electrogénesis



Rios-Pohl & Yacubian, 2016

Electrogénesis

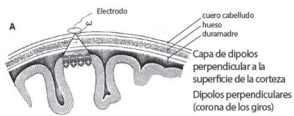


Teorema del ángulo sólido de Woodbury

Rios-Pohl & Yacubian, 2016

CAMPOS RADIALES Y TANGENCIALES

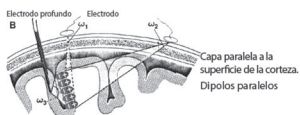
- Radiales- orientación de las células piramidales y de sus campos son ortogonal al cráneo (convexidad cortical). EEG es más sensible, MEG no es sensible;



Rios-Pohl & Yacubian, 2016

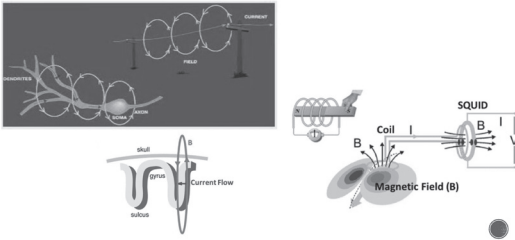
CAMPOS RADIALES Y TANGENCIALES

- Tangenciales- orientación de las células piramidales y de sus campos son paralelos al cráneo (por ejemplo, surcos o fisuras profundas). EEG es menos sensible que en la evaluación de los dipolos radiales.



Rios-Pohl & Yacubian, 2016

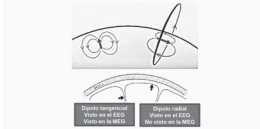
¿Por qué MEG?



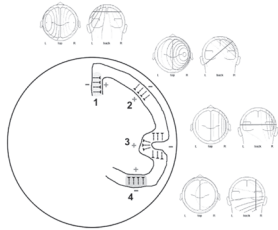
¿Por qué MEG?

Corrientes radiales no producirán campos magnéticos fuera de la cabeza

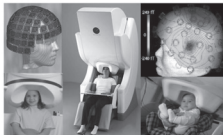
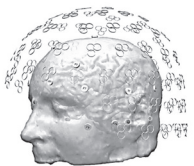
↳ MEG detecta sólo las corrientes tangenciales



CAMPOS RADIALES Y TANGENCIALES



Magnetoencefalografía 200- > 300 sensores

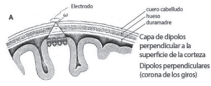


• La señal de MEG decae más rápidamente con la distancia que el del EEG-difícil el registro de estructuras profundas

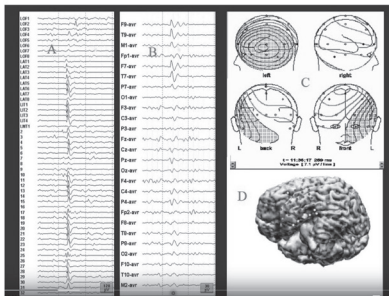
• El hueso es transparente al magnetismo y los campos magnéticos no sufren la resistencia del cráneo

Sensibilidad del EEG

- Requiere $> 6 \text{ cm}^2$ de corteza sincronizada;
- Visualiza generadores en los surcos y fisuras pero menos en generadores de los giros;
- EEG es sensible a todas las orientaciones de los generadores, pero de los radiales más que de las tangenciales.



Rios-Pohl & Yacubian, 2016



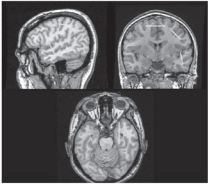
Ventajas del EEG

- Sensible a todas las orientaciones de los generadores;
- Caracteriza la extensión de la propagación;
- Permite registros prolongados, aumentando la posibilidad del registro de crisis epilépticas;
- Es parte de la evaluación de rutina en epilepsia;
- Relativamente barato.

Sensibilidad de la MEG

- MEG requiere $4-6 \text{ cm}^2$ de corteza sincronizada;
- MEG visualiza surcos grandes, fisuras y planos tangenciales, pero no la corteza de la convexidad;
- Los dipolos de la MEG reflejan de forma más precisa la ubicación del generador;
- Sensible a la orientación de los generadores tangenciales.

Ventajas de la MEG



- No es atenuada o distorsionada por el cráneo, los modelos simples de cabeza son adecuados;
- Mayor capacidad de cobertura de la cabeza: 200- >300 sensores;
- Sensibilidad superior, ve generadores más pequeños, especialmente los tangenciales a la superficie;
- Precisión superior al EEG en el generador, surcos/giros específicos;
- Sensibilidad a la frecuencia superior (DC a gama).



EEG Y MEG SON COMPLEMENTARES!

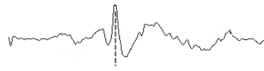


ACTIVIDADES EPILEPTIFORMES FOCALES Y GENERALIZADAS EN EL EEG



Descargas epileptiformes focales

Descarga de onda aguda ('sharp wave')



ASIMÉTRICA

Actividad de superficie negativa, de connotación anormal, epileptiforme, que perturba claramente la actividad de base y compromete dos o más electrodos, cuya duración varía de 70 a 200 mseg. Usualmente la fase ascendente es ligeramente inclinada y la fase descendente aún más inclinada, lo que confiere asimetría al grafocoleamiento. Es seguida de una onda lenta y su amplitud es variable. Sinónimo de punta lenta (del francés, pointe lente). Sin embargo, se recomienda el término onda aguda (del inglés, sharp wave).

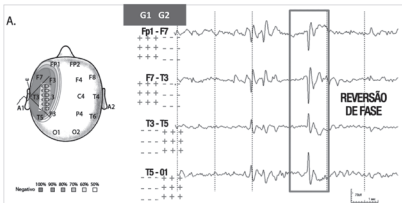
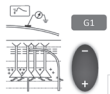


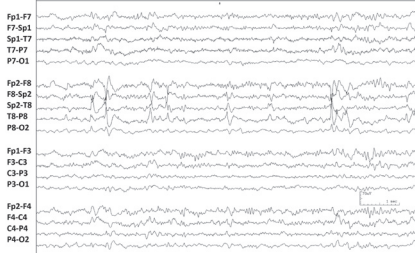
DESCARGAS EPILEPTIFORMES FOCALES

- Pueden ocurrir en cualquier lobo o lado, pero son más comunes en los lobos temporal y frontal;
- Son casi siempre de superficie negativa;
- Tiene morfología característica;
- En el montaje bipolar la negatividad máxima es representada por la reversión de fase instrumental.

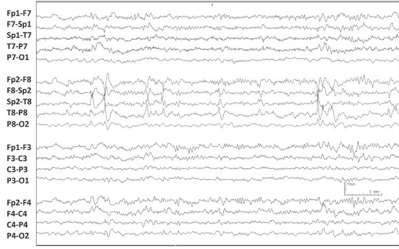


Reversión de fase instrumental Principio de amplificación diferencial

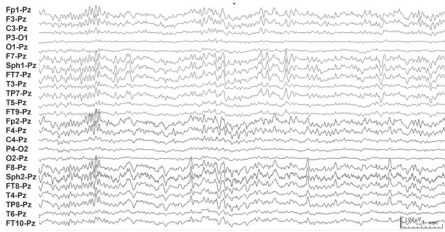




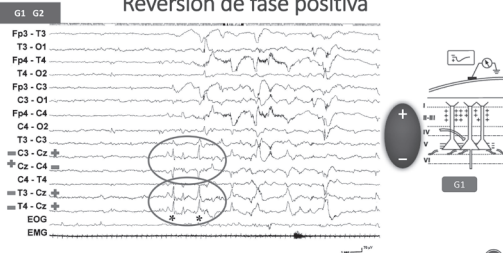
MONTAJE BIPOLAR LONGITUDINAL DOBLE BANANA



MONTAJE REFERENCIAL

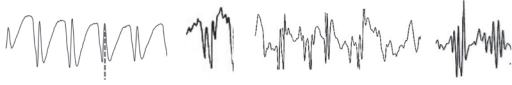


Reversión de fase positiva



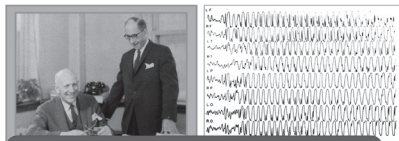
Descargas epileptiformes generalizadas

Descargas de espigas ('spikes')



SIMÉTRICA

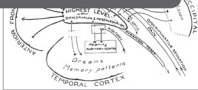
Actividad de superficie negativa, que claramente se distingue de la actividad de base, que compromete dos o más electrodos, cuya duración es de 20 a 70 mseg. Usualmente sus fases ascendente y descendente son igualmente pronunciadas. Puede o no ser seguida de una onda lenta, pero su forma es relativamente simétrica. Es sinónimo de punta, del francés pointe. Sin embargo, se recomienda el uso del término espiga, del inglés spike.



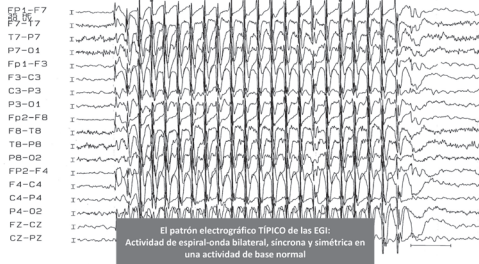
DECARGAS BILATERALES, SÍNCRONAS y SIMÉTRICAS

Crisis generalizadas
Sistema centrencefálico

Penfield W. Brain 1958;81(2):231-4.



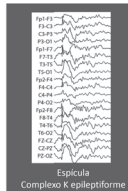
Lo que no debemos esperar



El patrón electrográfico TÍPICO de las EGI:
Actividad de espiral-onda bilateral, sincrona y simétrica en una actividad de base normal

Descargas epileptiformes generalizadas

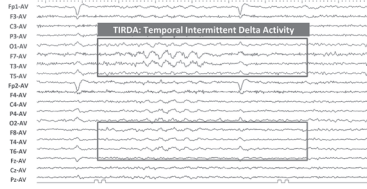
- Usualmente CEO típicos o atípicos o descargas de polispicula, polispicula-onda o ambos;
- 50% pacientes con crisis TCG en el 1º. EEG;
- 1-13% de individuos sin epilepsia, particularmente parientes en primer grado de pacientes con epilepsias generalizadas.



Espicula
Complejo K epileptiforme

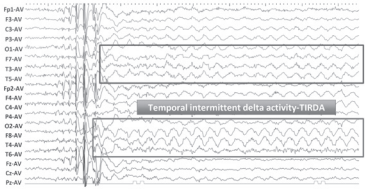
3. Morfología atípica Epilepsia ausencia juvenil

Mujer, 50 años, inicio de las crisis a los 7 años. EAU refractaria. Topiramato y fenobarbital. Valproato y etosuximida- efectos adversos. Ausencias relativamente raras. Crisis TCG controladas.



3. Morfología atípica Epilepsia ausencia juvenil

Mujer, 50 años, inicio de las crisis a los 7 años. EAU refractaria. Topiramato y fenobarbital. Valproato y etosuximida- efectos adversos. Ausencias relativamente raras. Crisis TCG controladas.



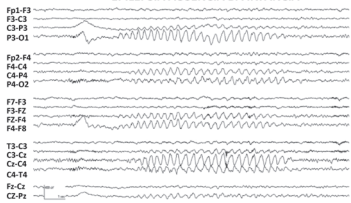
¿Qué sabemos sobre TIRDA?

Temporal intermittent rhythmic delta activity (TIRDA) in the diagnosis of complex partial epilepsy: sensitivity, specificity and predictive value.
Reiher J, Beaudry M, Leduc CP. Can J Neurol Sci 1989;16(4):398-401.

- 45/127 registros (35%);
- TIRDA fue más abundante en somnolencia y sueño;
- Cuando ocurre bilateralmente e independientemente, TIRDA varió de lado a lado;
- TIRDA es frecuentemente asociado con descargas temporales anteriores, particularmente durante el sueño;
- TIRDA debe considerarse un indicador intermedio de crisis parciales complejas.

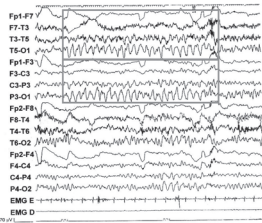
¿Cuál es la actividad delta rítmica más conocida?

ACTIVIDAD DELTA RÍTMICA OCCIPITAL INTERMITENTE
EPILEPSIA AUSENCIA DA INFANCIA

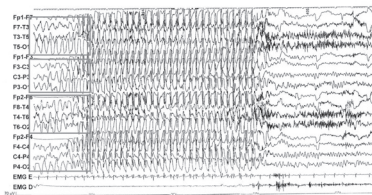


Actividad delta en regiones occipitales, atenuada por la apertura de los ojos y etapas profundas del sueño, acentuada por la hiperventilación y somnolencia- 83% relacionada a las epilepsias generalizadas.

ACTIVIDAD DELTA RÍTMICA OCCIPITAL INTERMITENTE
EPILEPSIA AUSENCIA DA INFANCIA



ACTIVIDAD DELTA RÍTMICA OCCIPITAL INTERMITENTE
HIPERVENTILACIÓN



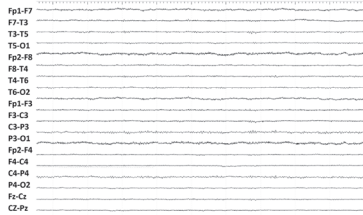
TEMPORAL INTERMITTENT RHYTHMIC DELTA ACTIVITY EN EPILEPSIA AUSENCIA JUVENIL

- Tres casos (13%) en una serie de 23 pacientes con EAJ;
- Nunca observado en 80 pacientes con epilepsia mioclónica juvenil;
- Esta actividad delta fue activada por la hiperventilación y somnolencia. Disminuía en sueño NREM y reapareció en el sueño REM. Su frecuencia era alrededor de 3 Hz;
- TIRDA es muy sugestivo de EAJ así como ondas delta rítmicas posteriores o son de la epilepsia ausencia de la infancia pero con una localización más anterior, sobre los lobos temporales;
- Este patrón EEG debe ser conocido para evitar el tratamiento de pacientes con EAJ con FAEs inapropiados.

Gélisse et al. Seizure 2011;20:38-41

4. Actividad rápida generalizada

Hombre, 30 años, estudiante universitario, crisis TCG de difícil control



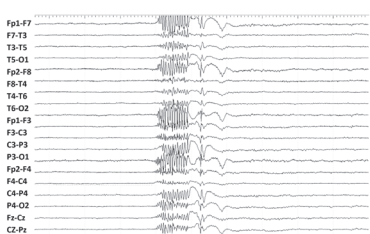
4. Actividad rápida generalizada

Hombre, 30 años, estudiante universitario, crisis TCG de difícil control

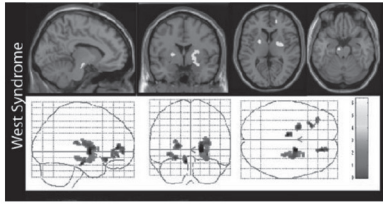


4. Actividad rápida generalizada

Hombre, 30 años, estudiante universitario, crisis TCG de difícil control

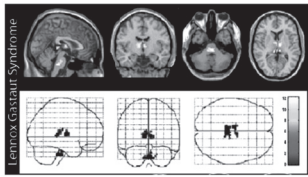


EEG- fMRI
Encefalopatías epilépticas- Síndrome de West



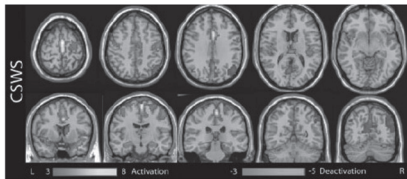
Moeller et al. Epilepsia 2013;54(6):971-82

EEG- fMRI
Encefalopatías epilépticas- Síndrome de Lennox-Gastaut



Moeller et al. Epilepsia 2013;54(6):971-82

EEG- fMRI
Encefalopatías epilépticas- Punta-onda continua en sueño

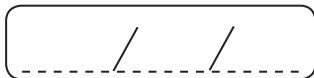


Moeller et al. Epilepsia 2013;54(6):971-82

EEG- fMRI
Síndrome de Doose



Moeller et al. Neurology 2014;82(17):1508-13



LORETO RIOS (CHILE)

NEUROPLASTICITY IN REFRACTORY EPILEPSY: IS IT A PROTECTIVE OR RISK FACTOR?

Neuroplasticity in refractory Epilepsy
¿Protective or risk factor?

Dra. Loreto Rios Pohl
 Neuróloga Infantil

www.clinicainepilepsia.cl

Neuroplasticity **Refractory Epilepsy**

Neuroplasticity
 ¿Protective factor?
 ¿Risk factor?

¿How much, when and how
 does epileptic activity
 affects neuroplasticity?

www.clinicainepilepsia.cl

What is Neuroplasticity?

- The term neuroplasticity is derived from the Greek word "plastikos" meaning "to form".
- Plasticity is an intrinsic property of the CNS, reflecting its capacity to respond with physiological changes in a dynamic manner to the environment and experience via modification of structural and functional changes of neural circuitry.
- It refers to the physiological changes in the brain that happen as the result of our interactions with our environment. From the time the brain begins to develop in utero until the day we die, the connections among the cells in our brains reorganize in response to our changing needs. This dynamic process allows us to learn from and adapt to different experiences."

www.clinicainepilepsia.cl

- Different as computers, which are built to certain specifications and receive software updates periodically, our brains can actually receive hardware updates in addition to software updates. Different pathways form and fall dormant, are created and are discarded, according to our experiences.
- When we learn something new, we create new connections between our neurons. We rewire our brains to adapt to new circumstances. This happens on a daily basis, but it's also something that we can encourage and stimulate.

www.clinicosepilepsia.cl

Neuroplasticity has 3 particular characteristics:

1. It happens at any time of life.
2. Presents a CRITICAL PERIOD of maximum efficiency and effectiveness.

"Immature Brain"

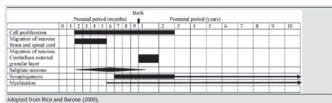


3. It implies long lasting changes of Learning and Memory.

www.clinicosepilepsia.cl

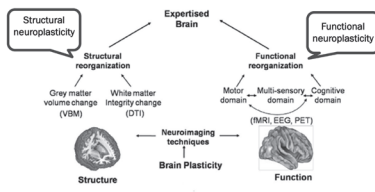
Brain maturation is not linear:

- It is punctuated by a series of developmental spurts, some additive and some regressive, consisting in stepwise processes with 'critical' or 'sensitive' periods.
- This critical periods mark phases of increased plasticity where specific brain circuits are maximally sensitive to acquiring certain kinds of information, or even need that information to be consolidated so that the system involved can establish interconnections with other system.



Adapted from Rice and Beattie (2005).
www.clinicosepilepsia.cl

Many neuroscientists use the word neuroplasticity as an umbrella term, it means different things to researchers in different subfields...



www.clinicosepilepsia.cl

Functional connectivity (Functional Neuroplasticity)



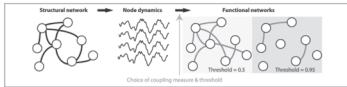
Functional refers to the interactions between activities in different brain regions that form a functional connectivity with a resulting network map.

www.clinicseplesia.ch

■ In neuroscience, "brain networks" (i.e., graphs representing the connectivity of brain components) are typically divided into two categories:

- **structural networks**
 - the edges represent physical connections between nodes (synaptic or gap junctional connections between individual neurons at microscopic spatial scale)

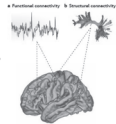
- **functional networks**



www.clinicseplesia.ch

How can we measure different types of connectivity?

- **Structural connectivity** can be measured using diffusion tractography.
- **Functional / effective connectivity** between nodes are quantified. Both functional connectivity and effective connectivity can be measured during active task performance or task-free ('resting') states using functional MRI.



www.clinicseplesia.ch

■ Neuroplasticity implies stable and permanent structural and functional changes ... but "modifiable"

For better or for worse ...

www.clinicseplesia.ch

Excessive Synaptogenic , Pruning and myelination.

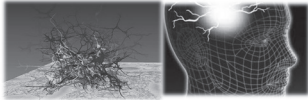
- This critical period where exists an excessive synaptogenesis and secondary pruning allows that internal and external experiences can have its peak effect on development or learning.
- But this excessive synaptogenic and prune capacity can become the brain 's Achilles heel in situations when excitatory mechanism become over stimulated resulting in maladaptive neuronal circuits resulting in an "Epileptic Brain"



www.clinicahospitaldeepilepsia.cl

- This "epileptic brain" results of a combination between:

- "Useful" neuronal loss.
- Increase in excitability.
- Formation of anomalous circuits with recruitment of peripheral circuits, revealing complex propogations, even to non-continuous areas.



www.clinicahospitaldeepilepsia.cl

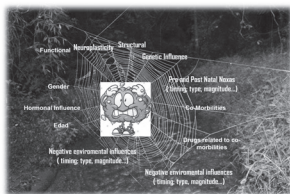


- A generic property of any network is that the dysfunction can spread easily between linked elements, leading to **pathological cascades** that can encompass large swathes of the system.
- It is also possible for focal hyper excitability pathology to disinhibit activity and cause cell death or damage in remote sites owing to excess neuronal stimulation.
- Such excitotoxicity plays a central part in the damage sustained to remote areas following focal cerebral noxas and may underlie the distributed degenerative changes seen in focal epilepsy.



www.clinicahospitaldeepilepsia.cl

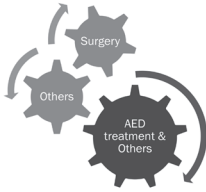
It 's not only the moment, it also matters...



www.clinicahospitaldeepilepsia.cl

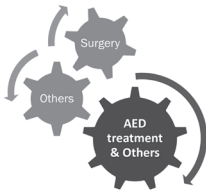


Can we do something for ameliorate this damage?



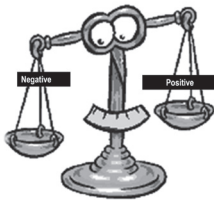
www.clinicahospitaldeepilepsia.cl

Can we do something for ameliorate this damage?



www.clinicahospitaldeepilepsia.cl

Treating and controlling the Seizures...



www.clinicahospitaldeepilepsia.cl

- Studies show that the biggest parents' problem in a child with epilepsy is focus on the neurocognitive and behavioral aspects derived from the treatment with AEDs.
- All AEDs can affect in some degree skills as cognitive function, behaviour and global learning.
- Multifactorial influences do these studies with methodological problems, complicating it interpretation.



JCH Neuro 2008;24:734-43
Rev. Neurol 2008;42 (supl. 2):S 99-70

www.clinicahospitaldeepilepsia.cl

Categorical evidences :



- AED's reduction (polytherapy to monotherapy), improves intellectual performance.
- The intake of AED of healthy volunteers induces on them a significant reduction in intellectual performance.
- Patients with recent diagnosis of Epilepsy have a lower cognitive performance after taking a single AED for one month compared to those who didn't start treatment.

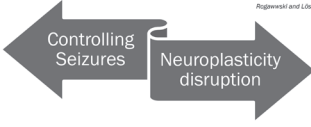
J Child Neurol 2004;19 (suppl 2): S23-S24
Rev. Neurol 2005;155(suppl 5):S21-S5
Epilepsia 2003;44:707-18

www.clinicahospitalde.com

- All AED's interact on ion channels, metabolic enzymes, neurotransmitter receptors and transporters:
 - Modifying discharge properties of neurons.
 - Decreasing synchronization.
 - Decreasing or inhibiting propagation.



Rogawski and Löscher, 2004



www.clinicahospitalde.com

This goal of re-establishing the balance "excitation-inhibition":



- It inhibits seizures but ...
- Its not a physiological normalization.
- The physiologically excitatory state in an immature Brain is indispensable for Neuroplasticity.
- Brain Neuroplasticity, defines learning and memory capacity.



www.clinicahospitalde.com

"Early" Surgery

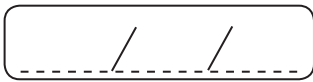
Basically studies before 1997, were focused on seizure control. However, the "current goal" is to improve the cognitive and psychosocial outcome.

- Asarnow et al. Dev Med Child Neurol. 1997
- Looddenkemper et al. Pediatrics 2007



Cognitive outcome in patients that underwent epilepsy surgery before 2 years old, is better. A better previous neurocognitive status is predictor a better outcome.

www.clinicahospitalde.com

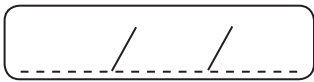


PETER WOLF (DENMARK)

GROUP B – CASE STUDY



A series of horizontal lines providing a writing area for the case study.



GUILCA CONTRERAS (VENEZUELA)


CLINICAL CORRELATION OF CONNECTIVITY ALTERATIONS IN CHILDHOOD EPILEPSY WITH CENTROTEMPORAL SPIKES





Epilepsy: from connectivity to connectome

Clinical Correlation of Connectivity Alterations in Children with Childhood Epilepsy with Centrottemporal Spikes

Guilca Contreras
LASSE XIII




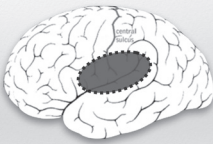
Childhood Epilepsy with Centrottemporal Spikes (CECTS)



- Accounts for 15 – 25% of epilepsy diagnosis in children younger than 15 years of age¹. Approximately 700 to 800 new cases of RE are expected each year
- Occurs in neurologically and cognitively healthy children¹
- Nocturnal focal seizures with a typical EEG that shows centrottemporal spikes (CTS)¹

1- Engel J, Peddy TA. Epilepsy: a comprehensive textbook, 2nd ed. Philadelphia, 2008.

Childhood Epilepsy with Centrottemporal Spikes (CECTS)

Childhood Epilepsy with Centrotemporal Spikes (CECTS)

- ◊ Comorbidity with a wide spectrum of neuropsychological and learning disabilities such as speech and language disorders, reading disabilities, attention impairment, visuomotor and behavior impairments, and psychiatric problems 1-4
- ◊ Attention impairments 67%; language impairments 54%; reading disability 42% 5,6

CECTS IS NOT BENIGN!!!

- 1- Damma T, Zentgraf D, Dierhoff V, Mander M, et al. *Dev Med Child Neurol* 2009;42:595-603.
- 2- Goldberg-Stern H, Gonen O, Sadeh M, et al. *Seizure* 2010;19:123-6.
- 3- Giordano B, Carrozzini AJ, Laghi L, et al. *Epilepsy Res* 2006;68:89-94.
- 4- Smith AH, Karam FM, Clarke T, et al. *Epilepsia* 2012;53:765-771.
- 5- Smith AH, Berman O, Pal DK. *Dev Med Child Neurol* 2015;57:1019-1026.
- 6- Chwielkova T, Pal DK, McGroarty CJ, et al. *Epilepsia* 2016;57:936.

Childhood Epilepsy with Centrotemporal Spikes (CECTS)

- ◊ With its typical onset between the age of 7 - 10 years, RE might critically influence the development and maturation of brain networks that are essentially involved in cognitive and psychological functioning
- ◊ Several factors such as localization, lateralization, and focality of IEDs may mediate their impact on cognitive development, moreover IEDs may have similar implications on cognition as seizures and might be coupled with the Concept of System Epilepsy¹⁻⁴
- ◊ The term "idiopathic" (traditionally implies lack of "demonstrable anatomic lesions". However, structural and functional abnormalities have been described in typical CECTS children: bilaterally increased gray matter volume in the frontal lobes and insula⁵, extensive cortical thinning in frontal, central, parietal and temporal lobes⁶. Abnormal white matter in the frontal and temporal lobes⁷

- 1- Riva D, Vago C, Francobaldi S, et al. *Epilepsy Behav* 2007;10:278-85.
- 2- Wolf AM, Winkler N, Soria E, et al. *Epilepsia* 2005;46(10):1663-7.
- 3- Nivola J, Ebra S, Bionato D, et al. *Epilepsia* 2012;53(6):1013-9.
- 4- Antonini G, Manginotti P, Miletto S, et al. *Epilepsia* 2012;53(5):771-8.
- 5- Pankov HB, Berg AT, Archer JS, et al. *Epilepsy Res* 2013;105:133-9.
- 6- Chertler CM, Bessling RMH, James HA, et al. *Neuroimage Clin* 2013;2.
- 7- Lundberg S, Eric-Olsson O, Ramstedt B, et al. *Epilepsia* 1999;40:1808-15.

Childhood Epilepsy with Centrotemporal Spikes (CECTS)

- ◊ Neurocognitive deficit in epilepsy has been considered to be a chronic consequence of repetitive spikes inhibiting the same cortical area over a period of many years, leading to delayed or incomplete maturation of the brain¹⁻³

- 1- Finucci LC, Tedrus GM, Decheto LM. *Epilepsy Behav* 2007;11:65-70.
- 2- Hommet C, Billard C, Maitte J, et al. *Epilepsy Disord* 2005;3:207-16.
- 3- Monjeaur C, Boudinet W, Boyd SG, et al. *Epilepsia* 2011;52:e79-83.

Childhood Epilepsy with Centrotemporal Spikes (CECTS)

- ◊ Studies of altered functional connectivity in pediatric epilepsy patients are becoming more common, mainly concerning the resting state brain network (rs-fMRI)
- ◊ Alterations in the RS FC patterns between specific brain areas would be correlated with cognitive impairments in CECTS
- ◊ Language disabilities and academic impairments found in RE are also common in relative of RE probands, with an incidence 5.4 times than in the general population¹
- ◊ The similarity in neurocognitive profiles between probands and siblings, suggest that these neurodevelopmental traits in RE should be genetically influenced²

- 1- Clarke T, Wang L, Murphy JL, et al. *Epilepsia* 2007;48(12):2258-65.
- 2- Oliveira EJ, Neri ML, Capelato LL, et al. *Arq Neuropsiquiatr* 2014;72(11):826-31.

Resting functional MRI connectivity studies in patients with CECTS

Authors (year)	BECTS population (mean age ± SD)	Control population (mean age ± SD)	Selected neurophysiology	Analysis	Findings
Jew et al (2010) ¹	21 BECTS with RE (11 ± 2) 22 BECTS without RE (11 ± 2)	21HC (10 ± 2)	WVC fMRI task Q2 WVC fMRI task Q2 WVC fMRI task Q2	Graph theory with regional parcellation, NBS	Decreased global and local efficiency for both BECTS with and without RE. Decreased functional connectivity for both BECTS with and without RE in left R, and PL. Interfunctional connectivity within and between networks (CPI and ITC) significantly different in left inferior to the left and right C1.
Loew et al (2010) ²	21 BECTS (11 ± 2) (9 with epilepsy)	21HC (10 ± 2) (9 with epilepsy)	WVC fMRI task Q2 WVC fMRI task Q2 WVC fMRI task Q2	Seed-based correlation; seed-based GCM	Decreased functional connectivity for four regions with increased CPN R, P, and A. Higher CPN A and P, and increased PL. Decreased functional connectivity in areas PL, right and left.
Loew et al (2010) ²	21 BECTS (11 ± 2)	21HC (10 ± 2)	WVC fMRI task Q2 WVC fMRI task Q2 WVC fMRI task Q2	Seed-based correlation	Decreased functional connectivity for four regions with increased CPN R, P, and A. Higher CPN A and P, and increased PL. Decreased functional connectivity in areas PL, right and left.
Whe et al (2010) ³	21 BECTS (11 ± 2)	21HC (10 ± 2)	WVC fMRI task Q2 WVC fMRI task Q2 WVC fMRI task Q2	Seed-based GCM	Decreased functional connectivity for four regions with increased CPN R, P, and A. Higher CPN A and P, and increased PL. Decreased functional connectivity in areas PL, right and left.
Xiao et al (2010) ⁴	21 BECTS (11 ± 2)	21HC (10 ± 2)	WVC fMRI task Q2 WVC fMRI task Q2 WVC fMRI task Q2	Graph theory with regional parcellation, NBS	Decreased global CC and efficiency. Decreased connectivity in sensorimotor regions.
Xiao et al (2010) ⁴	21 BECTS with ADHD (11 ± 2) 21 BECTS without ADHD (11 ± 2)	21HC (10 ± 2)	WVC fMRI task Q2 WVC fMRI task Q2 WVC fMRI task Q2	Seed-based correlation	BECTS with ADHD: decreased DAN connectivity. BECTS with ADHD: increased DAN connectivity.
Zeng et al (2010) ⁵	14 sensorimotor BECTS (11 ± 2) 14 sensorimotor BECTS (11 ± 2)	14HC (10 ± 2)	Annual Reading School Exam Annual Reading School Exam Annual Reading School Exam	Ratio	Non-overlapping BECTS: abnormal ratio in sensorimotor CPN, C, and P. Overlapping BECTS: abnormal ratio in sensorimotor CPN, C, and P. Non-overlapping BECTS: abnormal ratio in sensorimotor CPN, C, and P.
Reinhold et al (2014) ⁶	22 BECTS (11 ± 2)	22HC (11 ± 2)	NI	Graph theory with regional parcellation, correlation of structural-functional graphs	Decreased functional connectivity in medial part of CPN. Decreased functional connectivity in CPN, C, and P. Decreased functional connectivity in CPN, C, and P.
Tang et al (2014) ⁷	22 BECTS (11 ± 2)	22HC (11 ± 2)	WVC fMRI task Q2 WVC fMRI task Q2 WVC fMRI task Q2	Ratio	Decreased functional connectivity in CPN, C, and P. Decreased functional connectivity in CPN, C, and P. Decreased functional connectivity in CPN, C, and P.
Reinhold et al (2015) ⁸	22 BECTS (11 ± 2)	22HC (11 ± 2)	CEB-4 Core Language Score CEB-4 Core Language Score CEB-4 Core Language Score	ICA of task-related data	Decreased connectivity between I, P, and "sensorimotor network".
Reinhold et al (2015) ⁸	22 BECTS (11 ± 2)	22HC (11 ± 2)	CEB-4 Core Language Score CEB-4 Core Language Score CEB-4 Core Language Score	Seed-based correlation	Decreased connectivity between I, P, and "sensorimotor network".

Childhood Epilepsy with Centrotemporal Spikes (CECTS)



- Many researches have searched for a genetic cause of CECTS, but the common form of this epilepsy syndrome itself does not seem to have a clear mendelian inheritance
- Components of the syndrome may be linked more consistently to specific genes. Family association studies have shown that the centrotemporal spike trait is often inherited in an autosomal dominant fashion and may be associated with mutations of the elongator protein complex 4 (ELP4) gene on chromosome 11, but this association has not been consistent^{1,2}
- Additional analyses have suggested linkage of speech sound disorder in RE to 11p13 and reading disability to chromosome 7q21 y 1q42. Although RE is a common disorder, the genetics underlying it are complex and still being investigated³
- GRIN2A a gene on chromosome 16p13 that encodes a subunit of the glutamate N-methyl-D aspartate receptor, important in brain development, synaptic plasticity, memory, and sleep. A variety of mutations have been identified in families with ESES, CSWS, LKS (9-20%) and 3.6% of patients with RE⁴
- RFXO3 genes responsible for splicing of neuronal transcripts important in control of membrane excitability⁵

1- Ali B, Kuhl JL, Stray LJ, Clarke T, et al. *Epilepsia* 2007;48:2306-12
 2- Ni DJ, Li JW, Clarke T, Lohmann P, et al. *Genes Brain Behav* 2010;9:908-12
 3- Wang JJ, Adani L, Cheng C, et al. *PLoS ONE* 2012;7:e34916
 4- Linnarsson D, Buitrago M, Brannstrom N, et al. *Nat Genet* 2012;44:1003-6
 5- Corneil AC, Roguski MS, Vargha K, et al. *Nat Genet* 2013;45:1067-72
 6- Lohmann P, Li JW, Brannstrom M, Vargha K, et al. *Nat Genet* 2013;45:1067-72
 7- Li JW, Brannstrom M, Vargha K, et al. *Epilepsia* 2013;54:1067-72

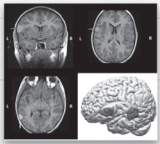
Language skills in children with benign childhood epilepsy with centrotemporal spikes: A systematic review

Study	Author(s) (Year)	Study Design	Assessment of language performance	Assess language areas	Influence of these areas related to BECTS
1	Whe et al. 2010	21 BECTS with RE (11 ± 2) 22 BECTS without RE (11 ± 2)	Annual Reading School Exam	Decreased functional connectivity in medial part of CPN	Decreased functional connectivity in CPN, C, and P
2	Loew et al. 2010	21 BECTS (11 ± 2) (9 with epilepsy)	WVC fMRI task Q2	Decreased functional connectivity for four regions with increased CPN R, P, and A	Higher CPN A and P, and increased PL
3	Whe et al. 2010	21 BECTS (11 ± 2)	WVC fMRI task Q2	Decreased functional connectivity for four regions with increased CPN R, P, and A	Higher CPN A and P, and increased PL
4	Xiao et al. 2010	21 BECTS (11 ± 2)	WVC fMRI task Q2	Decreased global CC and efficiency	Decreased connectivity in sensorimotor regions
5	Zeng et al. 2010	14 sensorimotor BECTS (11 ± 2) 14 sensorimotor BECTS (11 ± 2)	Annual Reading School Exam	Non-overlapping BECTS: abnormal ratio in sensorimotor CPN, C, and P	Overlapping BECTS: abnormal ratio in sensorimotor CPN, C, and P
6	Reinhold et al. 2014	22 BECTS (11 ± 2)	NI	Decreased functional connectivity in medial part of CPN	Decreased functional connectivity in CPN, C, and P
7	Tang et al. 2014	22 BECTS (11 ± 2)	WVC fMRI task Q2	Decreased functional connectivity in CPN, C, and P	Decreased functional connectivity in CPN, C, and P
8	Reinhold et al. 2015	22 BECTS (11 ± 2)	CEB-4 Core Language Score	Decreased connectivity between I, P, and "sensorimotor network"	Decreased connectivity between I, P, and "sensorimotor network"

Language skills in children with benign childhood epilepsy with centrotemporal spikes: A systematic review

Study	Author(s) (Year)	Study Design	Assessment of language performance	Assess language areas	Influence of these areas related to BECTS
1	Whe et al. 2010	21 BECTS with RE (11 ± 2) 22 BECTS without RE (11 ± 2)	Annual Reading School Exam	Decreased functional connectivity in medial part of CPN	Decreased functional connectivity in CPN, C, and P
2	Loew et al. 2010	21 BECTS (11 ± 2) (9 with epilepsy)	WVC fMRI task Q2	Decreased functional connectivity for four regions with increased CPN R, P, and A	Higher CPN A and P, and increased PL
3	Whe et al. 2010	21 BECTS (11 ± 2)	WVC fMRI task Q2	Decreased functional connectivity for four regions with increased CPN R, P, and A	Higher CPN A and P, and increased PL
4	Xiao et al. 2010	21 BECTS (11 ± 2)	WVC fMRI task Q2	Decreased global CC and efficiency	Decreased connectivity in sensorimotor regions
5	Zeng et al. 2010	14 sensorimotor BECTS (11 ± 2) 14 sensorimotor BECTS (11 ± 2)	Annual Reading School Exam	Non-overlapping BECTS: abnormal ratio in sensorimotor CPN, C, and P	Overlapping BECTS: abnormal ratio in sensorimotor CPN, C, and P
6	Reinhold et al. 2014	22 BECTS (11 ± 2)	NI	Decreased functional connectivity in medial part of CPN	Decreased functional connectivity in CPN, C, and P
7	Tang et al. 2014	22 BECTS (11 ± 2)	WVC fMRI task Q2	Decreased functional connectivity in CPN, C, and P	Decreased functional connectivity in CPN, C, and P
8	Reinhold et al. 2015	22 BECTS (11 ± 2)	CEB-4 Core Language Score	Decreased connectivity between I, P, and "sensorimotor network"	Decreased connectivity between I, P, and "sensorimotor network"

Review
Language skills in children with benign childhood epilepsy with centrotemporal spikes: A systematic review
 Joanna Trębicka^{1,2*}, Maria Emilia Sanches¹
¹Center for Health and Quality Improvement Studies, University of Applied Sciences, Poznań, Poland
²Center for Health and Quality Improvement Studies, Poznań, Poland



- Since epileptic discharges in this type of epilepsy occur in central or medial regions of the temporal lobe, we consider this a good model to understand the relationship between epileptic activity and language functions
- Semantic, morphosyntactic, and phonological features of the language were identified in the 18 studies
- In the domain of morphosyntax, there is no consensus regarding the altered skills
- As regard the phonological domain, there is some variability among studies, but changes in the intrasyllabic, syllabic, and phonemic levels were identified in tasks of rhyming identification and production, and syllabic and phonemic segmentation and manipulation
- The verbal memory was also identified as altered

10298-1738-0088-v01000-2020-0013 | J Child Neurol 2019;34(13):1402-17 | https://doi.org/10.1177/0885265519858200

Role of Language-Related Functional Connectivity in Patients with Benign Childhood Epilepsy with Centrotemporal Spikes

Table 1. Clinical characteristics of the BECTS patients and healthy controls

Clinical characteristics	BECTS	Controls	p
Number of subjects	18	20	
Sex (male/female)	7/11	9/11	0.382
Age at MRI study (month)	14(12.23)	12.17(2.14)	0.127
Age at onset (month)	7.07(2.21)	-	-
Duration of seizure (month)	30.88(4.63)	-	-
IQ at MRI study	-	-	-
Duration (month)	17.42(7.16)	-	-
Age (yr)	-	-	-
None	3/16(8)	-	-
Left hemisphere	2/16(12)	-	-
Right hemisphere	1/16(8)	-	-
Left CT or CP	8/16(5)	-	-
Right CT or CP	8/16(5)	-	-
Both CT or CP	0/16(0)	-	-
Structural MRI	-	-	-
None	9/16(6)	-	-
Brain (1 per child)	2/16(12)	-	-
Occipital (1 per child)	0	-	-
Temporal (1 per child)	3/16(18)	-	-
Frontal (1 per child)	3/16(18)	-	-
None	3/16(18)	-	-

Rolandic Mask and Language Area

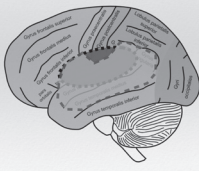


Table 2. Comparison of neuropsychological test scores between the BECTS patients and healthy controls

Neuropsychological test	BECTS (n=18)	Controls (n=20)	p
4-BECF-Q	93.2(12.58)	100.3(8.52)	<0.001*
PICT	82.7(11.52)	100.7(9.58)	<0.001*
PICT-2	86.5(12.12)	100.2(12.24)	<0.001*
Abstract V-P	11.16(3.88)	10.6(2.39)	0.796
Verbal P-P	4.74(1.58)	7.26(1.31)	<0.001*
VCI	92.16(13.6)	100.2(12.12)	<0.001*
PICT	98.8(10.82)	100.6(10.13)	<0.001*
PICT-2	99.17(10.1)	100.0(10.7)	<0.001*
Phonological	88.6(20.08)	102.7(9.16)	<0.001*
Acoustic verbal memory test	-	-	-
Immediate recall	9.17(3.17)	10.1(2.72)	0.236
Delayed recall	9.6(3.12)	10.4(2.84)	0.147
Recognition	8.87(3.01)	9.6(3.19)	0.272
Visuospatial memory test	-	-	-
OW	15.8(20.08)	10.0(9.17)	1.800
Immediate recall	15.8(14.28)	10.0(12.19)	0.622
Delayed recall	11.8(13.2)	12.3(8.17)	0.428
Executive function test	-	-	-
Trail making test part A	32.14(13.28)	30.49(8.41)	0.682
Trail making test part B	79.7(17.42)	69.6(16.54)	0.129
Stroop word	6.6(4.12)	6.6(4.12)	0.978
Stroop color word	6.3(4.45)	7.0(4.19)	0.280

Figure 1. Bar charts showing IQ scores for BECTS and Controls.

A. IQ scores

Group	IQ Score
BECTS	92.16
Controls	100.2

B. IQ scores by hemisphere

Group	Left Hemisphere IQ	Right Hemisphere IQ
BECTS	92.16	92.16
Controls	100.2	100.2

Figure 2. Scatter plot showing IQ scores for BECTS and Controls.

Figure 3. Scatter plot showing IQ scores for BECTS and Controls.

10298-1738-0088-v01000-2020-0013 | J Child Neurol 2019;34(13):1402-17 | https://doi.org/10.1177/0885265519858200

Role of Language-Related Functional Connectivity in Patients with Benign Childhood Epilepsy with Centrotemporal Spikes

Table 2. Comparison of neuropsychological test scores between the BECTS patients and healthy controls

Neuropsychological test	BECTS (n=18)	Controls (n=20)	p
4-BECF-Q	93.2(12.58)	100.3(8.52)	<0.001*
PICT	82.7(11.52)	100.7(9.58)	<0.001*
PICT-2	86.5(12.12)	100.2(12.24)	<0.001*
Abstract V-P	11.16(3.88)	10.6(2.39)	0.796
Verbal P-P	4.74(1.58)	7.26(1.31)	<0.001*
VCI	92.16(13.6)	100.2(12.12)	<0.001*
PICT	98.8(10.82)	100.6(10.13)	<0.001*
PICT-2	99.17(10.1)	100.0(10.7)	<0.001*
Phonological	88.6(20.08)	102.7(9.16)	<0.001*
Acoustic verbal memory test	-	-	-
Immediate recall	9.17(3.17)	10.1(2.72)	0.236
Delayed recall	9.6(3.12)	10.4(2.84)	0.147
Recognition	8.87(3.01)	9.6(3.19)	0.272
Visuospatial memory test	-	-	-
OW	15.8(20.08)	10.0(9.17)	1.800
Immediate recall	15.8(14.28)	10.0(12.19)	0.622
Delayed recall	11.8(13.2)	12.3(8.17)	0.428
Executive function test	-	-	-
Trail making test part A	32.14(13.28)	30.49(8.41)	0.682
Trail making test part B	79.7(17.42)	69.6(16.54)	0.129
Stroop word	6.6(4.12)	6.6(4.12)	0.978
Stroop color word	6.3(4.45)	7.0(4.19)	0.280

Figure 1. Bar charts showing IQ scores for BECTS and Controls.

A. IQ scores

Group	IQ Score
BECTS	92.16
Controls	100.2

B. IQ scores by hemisphere

Group	Left Hemisphere IQ	Right Hemisphere IQ
BECTS	92.16	92.16
Controls	100.2	100.2

Figure 2. Scatter plot showing IQ scores for BECTS and Controls.

Figure 3. Scatter plot showing IQ scores for BECTS and Controls.

10298-1738-0088-v01000-2020-0013 | J Child Neurol 2019;34(13):1402-17 | https://doi.org/10.1177/0885265519858200

Role of Language-Related Functional Connectivity in Patients with Benign Childhood Epilepsy with Centrotemporal Spikes

Table 3. Regions exhibiting differences between the patient and control groups in seed-based functional connectivity to voxels throughout the brain.

Seed region	z	p (FDR-corr)	Peak level	T value	X	Y	Z	Coordinate (mm)	Regions
Rolandic area									
IFC-AC	71	0.007*	<0.001	3.108	26	-10	-44	Left inferior temporal gyrus	
HC-PT	88	0.074	<0.001	4.425	20	12	-10	Left putamen/ventral lenticular nucleus	
IFC-AC	62	0.042	<0.001	3.275	10	-76	-26	Left cerebellar posterior lobe/sulcus	
IFC-AC	75	0.074	<0.001	3.907	80	26	14	Right inferior frontal gyrus	
IFC-AC	62	0.042	<0.001	3.848	46	-22	-22	Right middle frontal gyrus	
IFC-AC	80	0.074	<0.001	3.704	46	-60	-6	Left temporal fusiform gyrus	
IFC-AC	69	0.068	0.001	3.390	-12	-54	-7	Left inferior temporal gyrus	
Language area									
IFC-AC	74	0.007*	<0.001	5.201	-28	-13	-46	Left inferior temporal gyrus	
IFC-AC	28	0.001	<0.001	4.022	4	38	-18	Left medial frontal gyrus	
IFC-AC	11	0.117	<0.001	4.838	10	25	19	Right inferior frontal gyrus	

Figure 4. Brain maps showing functional connectivity differences.

A. Rolandic IC

B. Language IC

Role of Language-Related Functional Connectivity in Patients with Benign Childhood Epilepsy with Centrotemporal Spikes

Hyun Ju Kim, Jung Hyeon Lee, Changyong Park, Hyeon Sun Hwang, Yoon Hye Choi, Jung Hyun Yoo, Hong Inwon Lee

- CECTS patients showed significantly lower cognitive performance as measured by K-WISC-III IQ scores, in addition to different V-P patterns
- Both the Rolandic and Language areas exhibited greater FC to voxels in the left inferior temporal gyrus in CECTS patients than in healthy controls
- The K-WISC-III IQ scores of our subjects were negatively correlated either with Rolandic or language FC to voxel in the left inferior temporal gyrus, demonstrating higher seed based FC values in CECTS patients than in the healthy controls
- The negative tendency of the VCI score combined with the EDs frequency suggests that poor seizure control has a deleterious impact on cognitive function and maybe the trajectory of neurodevelopmental disruption or secondary pathology induced by the propagation of EDs

Decreased functional connectivity within a language subnetwork in benign epilepsy with centrotemporal spikes

Colin J. McGINITY, Anna B. Smith, Shi N. Yashik, Sofia Widenbach Gerdes, Ariana Gummerum, Adam L. Tyson, Tiffany K. Bell, Marwa Elmour, GCarenth J. Barker, Mark P. Richardson, and Deb K. Pal

Epilepsia Open. 2021;14: 225-2017. doi: 10.1002/epi.13911

	CECTS	Single	Healthy
	mean (SD)	mean (SD)	mean (SD)
Intelligence			
WISC-III Full Scale IQ (n = 24 (12/30))	109 (13.4, 8.4)	108 (8.6, 11)	114 (9.33)
WISC-III Verbal IQ (n = 24 (12/30))	108 (8.32, 8.3)	108 (9.75, 9.7)	111 (10.45)
WISC-III Performance IQ (n = 24 (12/30))	107 (10.85, 8.4)	107 (11.32, 9.7)	113 (10.55)
WISC-III Full Scale IQ - Performance IQ absolute difference (n = 24 (12/30))	15 (4.08, 6.2)	15 (10.95, 6.3)	18 (7.84)
Reading			
CCC General Reading Composite (n = 24 (11/19))	71 (14.8, 8.9)	80 (20.5, 9.7)	85 (10.8)
CCAGNC Copying Word (n = 24 (11/19))	93 (10.1, 5.7)	93 (10.7, 6.5)	95 (7.1)
TOWSE-3 Total Word Reading Efficiency (n = 24 (11/19))			
TOWSE-3 High Word Efficiency (n = 24 (11/19))	87 (11.88, 8.4)	87 (11.35, 9.4)	88 (10.318)
TOWSE-3 Basic Word Efficiency (n = 24 (11/19))	102 (13.85, 8.4)	101 (11.6, 9.1)	102 (10.318)
WRAT-4 Reading Composite (n = 20 (10/20))	108 (14.32, 8.4)	112 (12.75, 9.2)	114 (8.657)
WRAT-4 Word Reading (n = 20 (10/20))	107 (8.170, 8.4)	111 (12.67, 9.1)	113 (8.576)
WRAT-4 Sentence Comprehension (n = 20 (10/20))	106 (13.2, 8.4)	111 (15.92, 9.1)	113 (10.814)
WRAT-4 Spelling (n = 24 (12/30))	113 (11.92, 8.3)	113 (12.67, 9.1)	115 (8.430)
Nonverbal cognition			
Conner's Global Impairment (n = 23 (11/17))	102 (20.5), 8.7	95 (15.5), 8.3	87 (20.4)
Conner's Attention Deficit Hyperactivity Disorder Index (n = 23 (11/17))			
SDQ Total Disability (n = 25 (12/18))	10 (16.8), 6.1	5 (9.2), 5.0	5 (9.2)
SDQ Attention (n = 25 (12/18))	2 (6.5), 3.1	2 (6.0), 2.1	2 (6.2)
SDQ Conduct Problems (n = 25 (12/18))	1 (5.5), 3.2	1 (11.5), 2.1	1 (13.0)
SDQ Hyperactivity (n = 25 (12/18))	4 (5.9), 6.8	2 (6.7), 8.1	3 (8.5)
SDQ Peer Problems (n = 25 (12/18))	1 (7.0), 6.3	1 (2.1), 6.1	1 (2.0)
Communication			
DCD-Q-7 Total (n = 24 (12/19))	56 (9.1), 10.1	46 (24.3), 8.4	48 (9.7)

Decreased functional connectivity within a language subnetwork in benign epilepsy with centrotemporal spikes

Colin J. McGINITY, Anna B. Smith, Shi N. Yashik, Sofia Widenbach Gerdes, Ariana Gummerum, Adam L. Tyson, Tiffany K. Bell, Marwa Elmour, GCarenth J. Barker, Mark P. Richardson, and Deb K. Pal

Epilepsia Open. 2021;14: 225-2017. doi: 10.1002/epi.13911

- Relative to controls, patients with CECTS showed a significant decrease in connectivity ($p < 0.05$) within a language subnetwork within the left superior frontal gyrus - orbital part, the left inferior frontal gyrus - opercular part, the left supramarginal gyrus, and the right inferior parietal lobe
- A significant increase in connectivity was identified in the left and right superior medial frontal regions, the left and right olfactory regions, and the left anterior cingulate gyrus

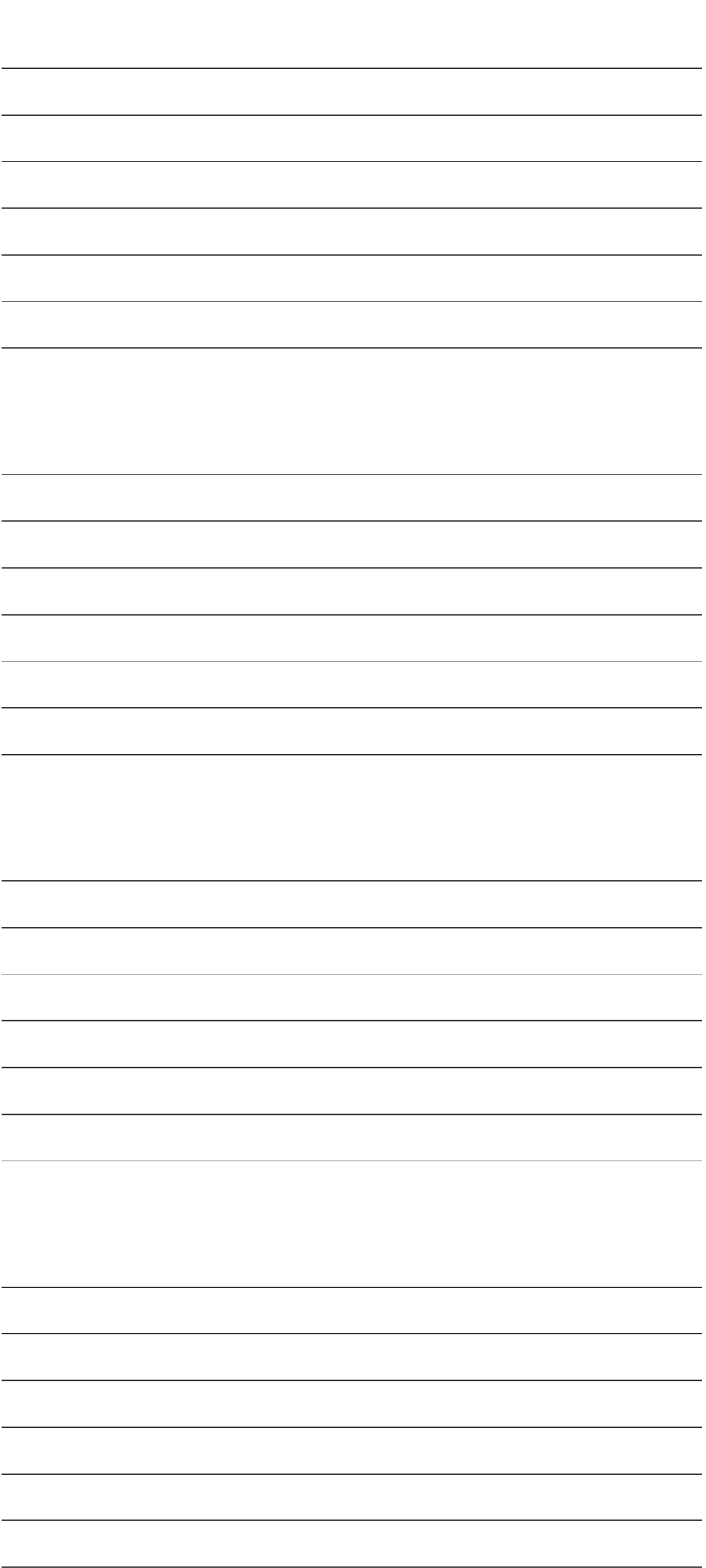
Disruption of Rolandic Gamma-Band Functional Connectivity by Seizures is Associated with Motor Impairments in Children with Epilepsy

George M. Braganza, Tommyaki Akiyama, Ayako Ochi, Hiroaki Ohnishi, Mary Lou Smith, Richard P. Taylor, Elizabeth Stoeberl, Anna T. Yashik, G. Carter Stroud, Lisa M. Saxe, M. Dwanthony...

Epilepsia June 2012 | Volume 7 | Issue 4 | 489-508

- Seizures alter the functional connectivity of eloquent cortical areas and these alterations are predictive of clinical neurological deficit
- Ictal phase desynchronization and disruption of functional connectivity within a variety of distributed brain networks may underlie the broad spectrum of impairments-affecting children with epilepsy
- The most significant frequency was the high gamma band (81-150 Hz) ($p < 0.01$), suggesting that ictal desynchronization was strongest within the gamma band, which has been reliably implicated in the formation of networks supporting cognition, perception and motor control
- Role of interictal discharges in disrupting networks beyond the ictal period, further contributing to network destabilization

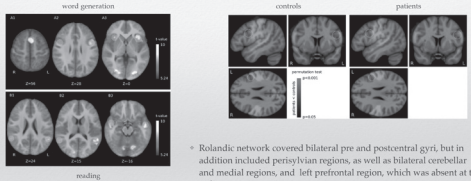
The figure includes two brain scan images (A and B) showing functional connectivity in the Rolandic region. Below them is a line graph titled 'High Gamma Band Functional Connectivity' comparing 'Normal Motor Function' (black line with circles) and 'Disrupted Motor Function' (grey line with squares) across frequency bands from 0 to 150 Hz. The y-axis is 'Mean Functional Connectivity' ranging from -0.2 to 0.2. The x-axis is 'Frequency Bands (Hz)'. The graph shows that normal motor function has a positive connectivity peak in the high gamma band (around 100 Hz), while disrupted motor function shows a significant decrease (negative connectivity) in this band.



Reduced functional integration of the sensorimotor and language network in rolandic epilepsy^{1,2}

René M.H. Besseling^{1,2,3,4,5}, Jacobus F.A. Jansen^{3,4}, Geke M. Overvliet^{1,2,3,4}, Sylvie J.M. van der Kruijs^{1,2,3,4}, Johannes S.H. Vles^{1,2,3,4}, Saskia C.M. Ebus^{1,2,3,4}, Paul A.M. Hofman^{1,2,3,4}, Antón de Louw^{1,2,3,4}, Albert P. Aldenkamp^{1,2,3,4}, Walter H. Backes^{1,2,3,4}

Neurology Clinical 2 (2013) 238-246



- Rolandic network covered bilateral pre and postcentral gyri, but in addition included perisylvian regions, as well as bilateral cerebellar and medial regions, and left prefrontal region, which was absent at right
- This region corresponded to the left inferior frontal gyrus showing activation for the word generation task, and had significantly reduced rolandic network connectivity in patients compared to controls
- This functional decoupling might be key in understanding RE typical language impairment, and is in line with the identified neuropsychological profile of anterior language dysfunction

Authors aim to link epileptiform activity / seizures originating from the rolandic cortex with language impairment in children with RE using fMRI in resting state and during task (word generation and reading)

Rolandic epilepsy and dyslexia

Epilepsia 54(10) 1838-1844

Risk factors for reading disability in rolandic epilepsy families

RD in RE is strongly associated with history of speech sound disorder (SSD), ADHD, and male sex among probands

RD in RE is very common (43% probands vs 22% siblings, and often preceded by SSD (53% probands, 28% siblings)

When ADHD is reported in probands, it is usually associated with RD (84%)

Within the context of RE, neither seizure number or early seizure onset, nor treatment factors, increase risk for RD

Patients diagnose with dyslexia had a lower performance in reading and writing and average performance in arithmetic, a condition consistent with the diagnosis of dyslexia

The six patients diagnosed with dyslexia, the worst scores found were related to verbal memory and learning, while visual memory remained within average or above average

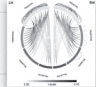
Group	Dyslexia	OD	ND
A	6 (19.4%)	23 (74.20%)	2 (6.50%)
B	0 (0.0%)	11 (35.5%)	20 (64.50%)
Total	6 (9.70%)	34 (54.80%)	22 (35.50%)

Legend: A: Patients with BECTS; B: Control group; OD: Diagnostic Dyslexia; ND: Other difficulties; ND: Without difficulties; OD-square area

Increased resting-state EEG functional connectivity in benign childhood epilepsy with centro-temporal spikes

Béla Clemens¹, Szilvia Puszkás^{1,2}, Tamás Spisák¹, Imre Lajtos¹, Gábor Opposits¹, Mónika Besenyő¹, Katalin Hollódy¹, András Fogarasi¹, Noémi Zsuzsanna Kovács¹, István Felvari¹, Miklós Emei¹

Seizure 33 (2014) 50-55



- **Abnormal EEGC in frontal areas:** Abnormally increased neuronal coupling between frontal and frontal, frontal and temporal regions. We found increased bilateral beta band connectivity. Decreased hemodynamic coupling together with increased electrical coupling (EEGC) is common finding in focal epilepsy. These abnormalities are presumably pathophysiologically related to specific language deficit, the neuropsychological endophenotype of RE
- **Abnormal EEGC in the parietal area:** Increased EEGC within the right parietal area. This abnormality was topographically limited but involved the entire investigated frequency spectrum, so it should be considered as neurophysiologically important. It topographically corresponds to the superior parietal area, an important node of the attention network. Attention deficit due to superior parietal dysfunction is part of the neuropsychological profile of RE
- **No abnormal EEGC in the central area:** It was surprising that EEGC was normal in the central region that generates spikes and seizures in CECTS. CECTS differs from the rest of focal epilepsies in this respect.

Childhood Epilepsy with Centrotemporal Spikes (CECTS)

- Prevalence of ADHD: healthy school children (3 – 5%); children with epilepsy (8-33%)¹
- Many studies have suggested various pathogenetic mechanisms of ADHD including a common genetic predisposition or biochemical factor in children with epilepsy²
- Bilateral CTSs are significantly more frequent in patients with treated ADHD
 - Perhaps, left lateralized language and auditory processing, and typically right lateralized sustained attention are both disrupted by bilateral CTSs, and these combined deficits produce more severe ADHD symptoms³
- Although the pathophysiology of attention impairment in children with CECTS is still unknown, the overlap between neural circuitry for attention and the networks involved in the generation of rolandic seizures may be the basis for this association^{4,5}

1. Dixon DW, Asatya JK, Harzidek J, Ambrosius WT. *Dev Med Child Neurol* 2003;45:50-4
 2. Parisi J, Mastroi R, Verotta A, Cavaliere P. *Brain Dev* 2010;32:310-4
 3. Egan-Boyer K, McAsa Y, Egan-Boyer K, Tan-Song E. *Epilepsia Behav* 2010;47:54-58
 4. Parvaz HR, Berg AT, Archer JS, et al. *Epilepsia Res* 2011;10:5:133-9
 5. Besseling RM, Jansen JF, Overvliet GM, et al. *PLoS One* 2013;8:e63568

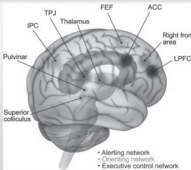
The attentional networks in benign epilepsy with centrotemporal spikes

Bin Yang^{a,b}, Xiaocui Wang^b, Liwei Shen^b, Xiaofei Ye^b, Guang-e Yang^b, Jin Fan^c, Panpan Hu^{a,b,c}, Kai Wang^{a,b}

Table 1
The clinical details of children with BECTS (N = 90).

Variables	BECTS (N = 90)	Controls (N = 90)
Gender (female)	51 (56.7)	51 (56.7)
Duration of clinical course (months)	4.55 ± 8.72	—
Age at first seizure (years)	8.67 ± 1.22	—
Age at last seizure (years)	10.8 ± 1.88	—
Family history of convulsions (yes)	12 (13.3)	—
Family history of epilepsy (yes)	4 (4.4)	—
Consciousness lost/aware?	16 (17.8)	—
Discharge type (yes)?	62 (72.2)	—
Seizure with home or generalised? (yes)?	71 (78.9)	—
Total number of seizures	—	—
1	34 (37.8)	—
2	24 (26.7)	—
3	12 (13.3)	—
Frequency of seizures (seizures per month)	—	—
None (0)	35 (38.9)	—
Medicines (1–3)	25 (27.8)	—
Duration of seizures?	—	—
<1 min	13 (14.4)	—
1–10 min	71 (78.9)	—
>10 min	4 (4.4)	—
EEG	—	—
Normal	1 (1.1)	—
Left hemisphere spikes	34 (37.8)	—
Right hemisphere spikes	34 (37.8)	—
Bilateral hemisphere spikes	21 (23.3)	—
Spike wave	—	—
Head up	5 (5.6)	—
Head down	28 (31.1)	—
Brain wave data	—	—
Normal CT findings	21 (23.3)	—
Normal MRI findings	87 (96.7)	—

Note. ACC = anterior cingulate cortex.
 * Frequency of seizures is defined as the average number of seizures per month.
 † Duration of seizures is an estimate reported by parents of patients, according to their own records.
 ‡ Refer to total seizures in BECTS.



The attentional system can be divided into three subsystems: alerting, orienting, and executive control, based on their neuroanatomical and physiological mechanisms, amid these three subsystems are coordinated to complete the entire information processing of attentional networks

The attentional networks in benign epilepsy with centrotemporal spikes

Bin Yang^{a,b}, Xiaocui Wang^b, Liwei Shen^b, Xiaofei Ye^b, Guang-e Yang^b, Jin Fan^c, Panpan Hu^{a,b,c}, Kai Wang^{a,b}

Table 2
Comparison of ANT performance between children with BECTS and controls.

Variables	BECTS (N = 90)	Controls (N = 90)	U	Z	P
Alerting effect (ms)	35.30 ± 13.75	42.58 ± 23.45	3160.50	-2.545	0.011
Orienting effect (ms)	24.19 ± 15.55	47.80 ± 27.36	1916.50	-1.805	<0.001
Conflict effect (ms)	76.20 ± 14.34	72.76 ± 14.18	3480.00	-1.005	0.318
Grand mean effect (ms)	95.22 ± 147.82	713.53 ± 108.55	959.50	-8.842	<0.001
Accuracy (%)	95.71 ± 5.65	98.27 ± 1.73	2294.00	-5.179	<0.001

Data are presented as mean ± SD. P-value represents the results of Mann-Whitney U-test.

This study found that RE mainly affected the orienting function, the grand mean effect, and the accuracy
 Various degrees of impairments related to the orienting function, such as the visuospatial coordination and the visuospatial capacities, have been reported in children with RE

The attentional networks in benign epilepsy with centrotemporal spikes

Bin Yang^{a,b}, Xiaocui Wang^b, Liwei Shen^b, Xiaofei Ye^b, Guang-e Yang^b, Jin Fan^c, Panpan Hu^{a,b,c}, Kai Wang^{a,b}

Table 3
Comparison of ANT performance in children with BECTS under and above 8 years old.

Variables	BECTS (N = 50)	Controls (N = 45)	U	Z	P
Alerting effect (ms)	36.8 ± 13.8	36.11 ± 14.38	516.00	-0.506	0.615
Orienting effect (ms)	26.36 ± 14.26	26.95 ± 19.95	697.00	-2.481	0.014
Conflict effect (ms)	76.60 ± 13.50	75.95 ± 15.64	674.00	-2.511	0.012
Grand mean effect (ms)	99.76 ± 13.00	802.72 ± 138.62	483.00	-4.178	<0.001
Accuracy (%)	94.68 ± 6.64	98.76 ± 4.80	681.00	-2.620	0.009

Data are presented as mean ± SD. P-value represents the results of Mann-Whitney U-test.

Table 4
Multiple linear regression of accuracy and the grand mean effect.

The age of onset	Accuracy		The grand mean effect	
	B	SE	B	SE
Age of onset	0.08	0.23	-0.001	-0.212
Age at first seizure	0.11	0.11	0.325	1.48
Age at last seizure	0.07	0.20	0.016	-1.41

Adjusted: gender, total number of seizures, duration of seizures

The age at onset of seizures was highly correlated with the accuracy and the grand mean effect. The younger the children with RE were, the lower the accuracy and the longer the grand mean effect
 Centrotemporal spikes were associated with widespread adverse effects on attentional networks

Interictal Activity is an Important Contributor to Abnormal Intrinsic Network Connectivity in Paediatric Focal Epilepsy

Elium A. Shamsi¹, Tim M. Tierney¹, Maria Centeno¹, Kelly St Pier¹, Ronit M. Pressler¹, David J. Sharp¹, Sujan Perani¹, Helen Cross¹, and David W. Carmichael¹

The goal of treatment in epilepsy is seizure freedom. However, the benefits of IEDs suppression are controversial as the evidence for the impact of IEDs on cognitive function is mixed
 IED prevalence is not typically used as an indication for treatment modification
 The increased rate of epileptiform discharges has been associated with lower performance on cognitive functioning and attention-sensitive tasks which is dependent on when and where the activity occurs
 Non transient effects of IEDs are less well characterised although there is some evidence that a worse cognitive outcome in the long term is related to increased frequency of epileptic discharges in focal epilepsies

Interictal Activity is an Important Contributor to Abnormal Intrinsic Network Connectivity in Paediatric Focal Epilepsy

Elham A. Shannir^{1,2}, Tim M. Tierney¹, Maria Centeno¹, Holly Se Plue¹, Ross M. Presler^{1,2}, David J. Sharp¹, Stephen Parsons^{1,2}, J. Helen Cross^{1,2} and David W. Carmichael¹

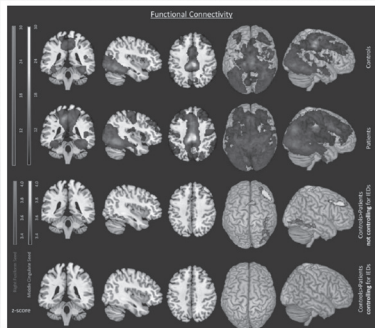
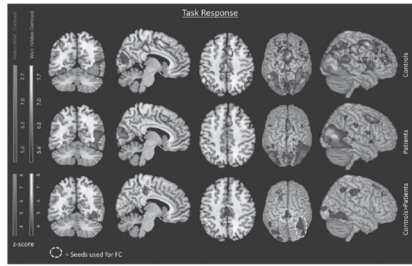
Patient	Gender	Age	Age at seizure onset (years)	Seizure type	Lesion type	Q1	Q2	Q3	Medication (mg/kg/day)
#1	Female	14	0	4	Left Frontal	None	81	CRZ 800, LVT 2000	
#2	Male	11	105	0.25	Left Temporal	Hypothalamic hamartoma	88	LVT 1425	
#3	Male	15	0	10	Left Temporal	None	108	CRZ 400	
#4	Female	11	06	1.1	Right Frontal/Temporal	None	93	LCM 100, LAM 500, CLRZ 5	
#5	Male	13	04	10	Right Frontal	None	83	CRZ 1200	
#6	Male	14	07N	0	Left Temporal/Posterior	Focal Cortical Dysplasia	84	CRZ 1200, LVT 1000	
#7	Female	14	101	2.3	Right Temporal	Cortical Abnormality Unknown aetiology	N/A	LVT 2000, TPM 150	
#8	Female	11	200	6	Right Fronto-temporal	None	66	CRZ 800, LVT 200	
#9	Female	10	220	0	Right Frontal	Focal Cortical Dysplasia	111	CRZ 1000	
#10	Female	16	21	6	Left Frontal	None	83	VPA 200, CRZ 400	
#11	Female	17	0	0.25	Left Temporal	Atypicality	82	TPM 500, CRZ 200	
#12	Female	15	100	13	Left Insulo-temp	Focal Cortical Dysplasia	N/A	TPM 50, CRZ 400	
#13	Male	17	07	0.008	Right Precentral	Focal Cortical Dysplasia	107	TPM 100, LCM 400	
#14	Male	11	204	3	Right Frontal	None	56	CRZ 100, TPM 200	
#15	Male	13	224	9	Temporal/parietal opercular	Hydrocephalus	91	LTC 175, TPM 200	
#16	Female	17	124	3	Left Temporal	None	56	LVT 1000	
#17	Female	16	0	5	Left Frontal	None	109	CRZ 1000	
#18	Male	13	100	0	Right Frontal	None	110	PMV 4	
#19	Male	12	06	3	Right Frontal	Focal Cortical Dysplasia	100	CRZ 1000, CLRZ 4	
#20	Female	16	00	0	Right Frontal	None	80	LVT 1000, CRZ 200	
#21	Male	16	008	0	Left Frontal	None	87	LVT 200, CRZ 1000, CLRZ 20	
#22	Male	16	100	8	Right Frontal	None	103	LVT 1000, VPA 400	
#23	Female	17	100	0	Right Frontal	Malformed sulcus/gyrus	103	LVT 2000, VPA 400	
#24	Female	17	0	1	Right Frontal/Parietal	cortical dysplasia	07	CRZ 1000, TPM 200, RLP 2000	
#25	Female	11	002	1	Right Frontal	Focal Cortical Dysplasia	81	CRZ 1000, CLRZ 10, VPA 1000	
#26	Female	16	140	12	Left Frontal/Midline	None	102	VPA 1000	

The aim of the study was to provide a detailed investigation on the impact of IEDs in paediatric focal epilepsy by measurements of network connectivity, known to be a possible marker of cognitive performance.

Two hypothesis: 1) epilepsy patients would have reduced functional connectivity within networks engaged by the natural stimulus task; 2) functional connectivity would increase in epilepsy patients after the removal of fMRI signal changes related to IEDs



Figure 1. Task paradigm.



Epileptic Discharge Related Functional Connectivity Within and Between Networks in Benign Epilepsy with Centrotemporal Spikes

Rong Li¹, Gong-Jun Ji¹, Yangyang Yu¹, Yang Yi¹, Mei-Ping Ding¹, Ye-Lei Tang¹, Huihui Chen² and Wei Luo^{1*}

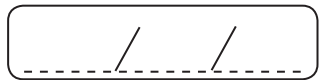
- ◊ The results support the proposed network inhibition hypothesis, which suggests that epileptiform activity arising from the epileptic focus (and subsequently propagating to subcortical structures such as medial thalamus and upper brainstem) may lead to inhibition of nonseizing cortical cortices
- ◊ The current study found that RE patients with IEDs exhibited increased positive connectivity between the AN and the SMN compared with the non IED group and HCs
- ◊ The sensorimotor cortex is thought to be the neural source of centrotemporal epileptiform activity, and sensorimotor cortex to one or more functionally interconnected areas
- ◊ The downstream effects of epileptic activity may this eventually lead to disruption of functional neural systems and normal function of other brain areas in children with RE

Conclusion

- ◊ Neurocognitive impairment in CECTS is common and related to abnormal functional connectivity that involves regions remote from sensorimotor cortices, which suggests that CECTS is a network disorder, genetically influenced

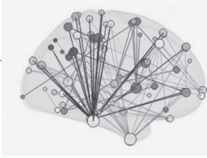


ALICIA BOGACZ (URUGUAY)



IS SEIZURE CLASSIFICATION COMPATIBLE WITH THE CONNECTOME CONCEPT?


IS SEIZURE CLASSIFICATION
COMPATIBLE WITH THE
CONNECTOME CONCEPT?



Dra. Alicia Bogacz
Sección Epilepsia Instituto de Neurología
Universidad de la República
Montevideo-Uruguay
LASSE 2019



What it is a seizure?



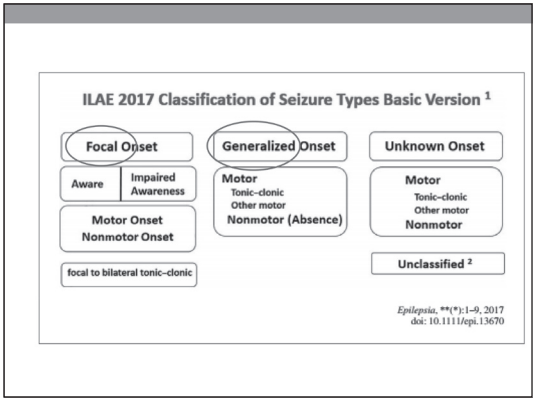
Epilepsy is a sudden excessive and rapid discharge of grey matter of some part of the brain, it is a local discharge.
(John Hughlings Jackson, 1873)

• An epileptic seizure is a transient occurrence of signs and/or symptoms due to abnormal excessive or synchronous neuronal activity in the brain.
(Fisher, R. et al., 2005)

• What are the spatial and temporal boundaries of seizure activity in brain networks?

• Network interactions give rise to abnormal activity in local circuits, more or less extend, and can involved remote brain regions.

• Are these remote network changes part of the seizure or are they "side effects" caused by the seizure but not directly involved in the seizure network?



- **“Focal epileptic seizures** are originating within networks limited to one hemisphere. They may be localized or more widely distributed. Focal seizures may originate in subcortical structures.”
- For each seizure type, ictal onset is consistent from one seizure to another, with preferential propagation patterns that can involve the contralateral hemisphere.”
- **“Generalized epileptic seizures** are originating at some point within, and rapidly engaging, bilaterally distributed networks. Such bilateral networks can include cortical and subcortical structures, but do not necessarily include the entire cortex.”

(Berg A et al. Epilepsia, 51(4):676–685, 2010)

- The terms “focal” and “generalized” express a dichotomous based on current electro-clinical evidence.
- A distinction between focal and generalized onset is a practical one , and may change with advances in ability to characterize the onset of seizures.

(Fisher RS et al. Epilepsia, 58(4):522–530, 2017)

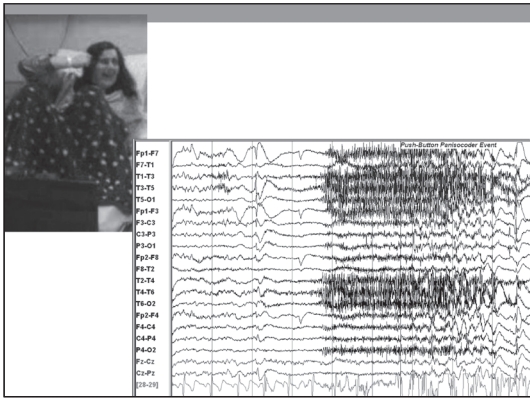
FOCAL SEIZURES

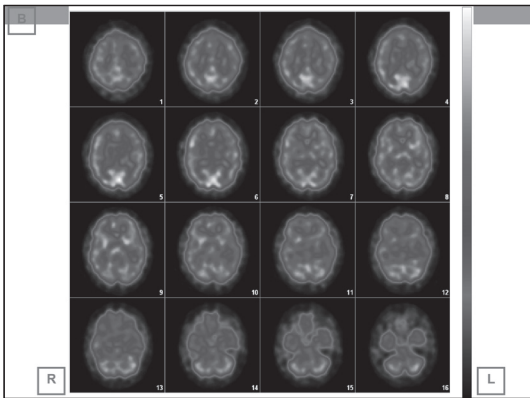
- “Focus” concept was developed with the records using scalp-EEG or subdural grids.
- With SEEG the concept of epileptogenic zone was developed as interrelated brain zones that are involved in the primary organization of the ictal discharge.
- Seizures are the expression of a sufficient number of neurons connected in a network.

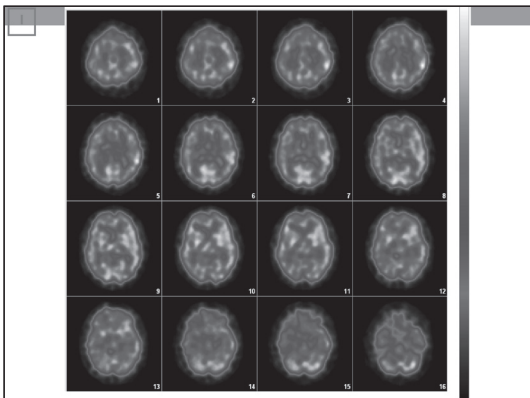
What is the evidence?

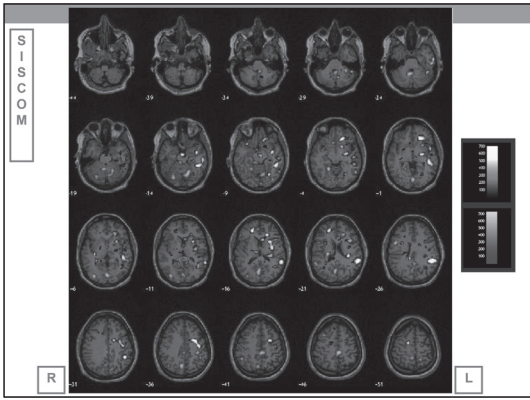
ICTAL

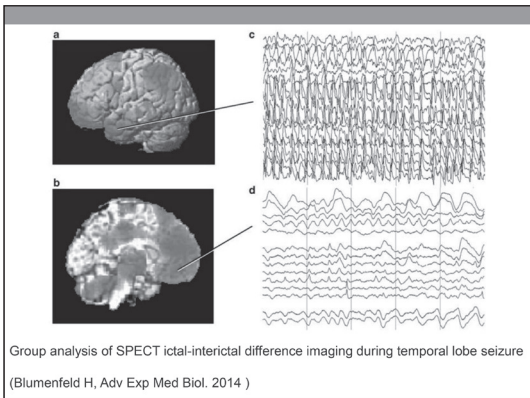
- Scalp-EEG or subdural grids
- Stereo-EEG
- Ictal-SPECT

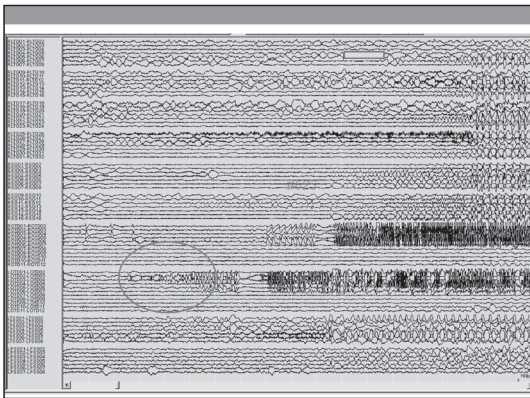


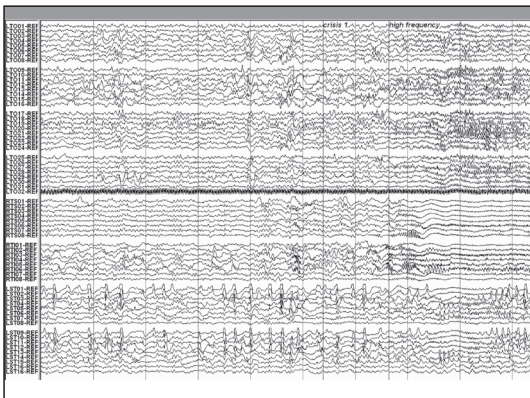












ILAE 2017 Classification of Seizure Types Expanded Version ¹

Focal Onset		Generalized Onset	Unknown Onset
Aware	Impaired Awareness	Motor tonic-clonic clonic tonic myoclonic myoclonic-tonic-clonic myoclonic-tonic atonic epileptic spasms Nonmotor (absence) typical atypical myoclonic eyelid myoclonia	Motor tonic-clonic epileptic spasms Nonmotor behavior arrest Unclassified ²
Motor Onset automatisms atonic ² clonic epileptic spasms ² hyperkinetic myoclonic tonic Nonmotor Onset autonomic behavior arrest cognitive emotional sensory			

focal to bilateral tonic-clonic

High frequency oscillations (HFOs) (100-500 Hz) and ripples (8-12 Hz) are associated with the seizure onset zone (SOZ). Propagation networks (PNs) are also shown.

Need descriptors to define the network.

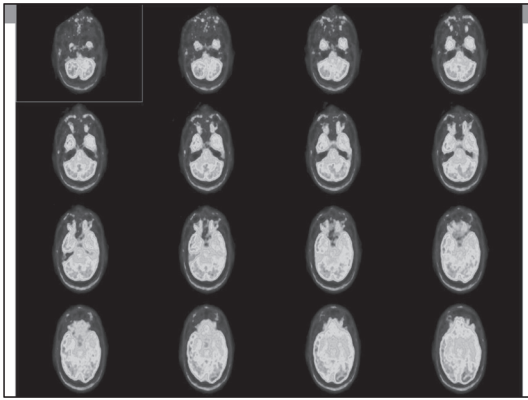
INTERICTAL

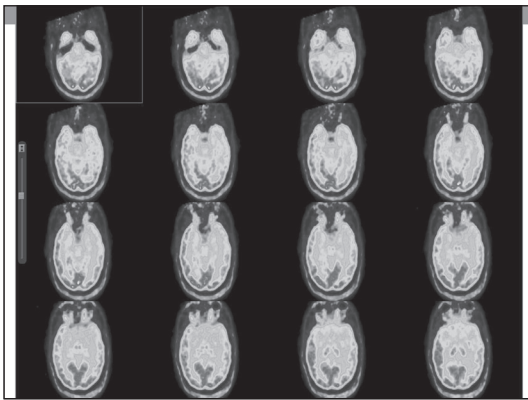
- EEG
- FDG-PET
- EEG-fMRI
- f-MRI : Resting state networks

› During the interictal state there are electro-physiologic biomarkers of the pathologic process:

- **Epileptic spikes** closely related to the epileptogenic zone ("irritative zone") but can appear in regions remote from the epileptogenic zone (propagation networks).
- **High-frequency oscillations (HFOs)** can be a biomarker for the delineation of the seizure-onset zone. (Bragin et al. 2010; Zijlmans et al. 2012)

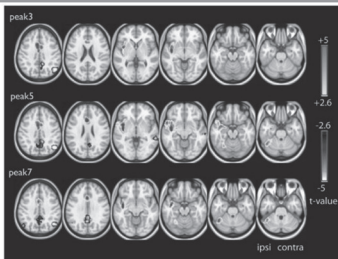






EEG-fMRI

- EEG-fMRI could explore the whole brain noninvasively at the time of a discharge.
- Focal IEDs recorded from scalp EEG may represent only a fraction of events that involve widespread brain areas despite their focal appearance.
- Studies revealed widespread activations and deactivations outside the epileptic focus.



Temporal lobe interictal discharges showing: Activation clusters in the mid-cingulate gyri bilaterally, and in the ipsilateral insula, mesial and lateral temporal regions, and cerebellum. Significant deactivations are found bilaterally in the inferior parietal lobules, posterior cingulate cortex, and precuneus and in the contralateral posterior temporal cortex.

Fahoumet F. et al. *Epilepsia*, 53(9):1618-1627, 2012

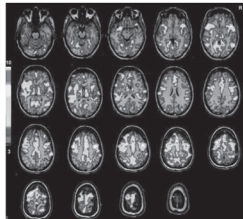
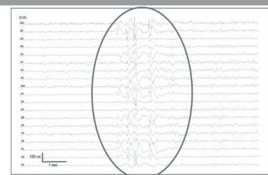
GENERALIZED SEIZURES

- Generalized seizure are events for which no side can be identified from the onset.
- They involve both cortical and subcortical circuits, in both hemispheres from the onset.
- In many instances are defined by EEG .
- Can be either symmetrical or asymmetrical.
- They consist of absences or motor seizures: tonic, atonic, clonic, tonic-clonic, myoclonic seizures; or spasms.
- Each of these seizure types involves a distinct hyperexcitable circuitry that in most instances does not comprise the whole brain.

SYSTEM EPILEPSIES

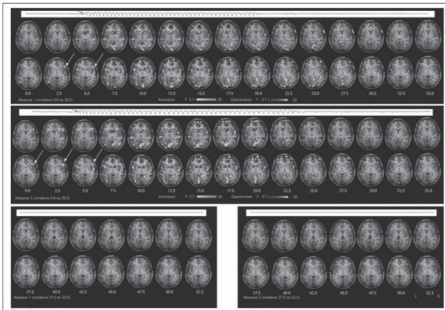
- Epilepsies where the “enduring propensity to generate seizures” is due to the **specific susceptibility of a system**, although it may be possible to identify some **trigger areas** within the system.
- EEG-fMRI studies have shown the involvement of neural networks in spike and wave discharges in generalized epilepsy, supporting the idea of a hyperexcitable cortico-subcortical network, consisting of well-defined brain regions, rather than the expression of generalized brain dysfunction.

Avanzini G. et al. *Epilepsia*,53(5):771–778,2012



- Childhood absence epilepsy:
- GSW burst recorded inside the MRI scanner.
 - fMRI results superimposed on anatomical MRI showing diffuse cortical fMRI activation, as well as thalamic activation.
 - The cortical activation involves widespread cortical areas(superior and mesial frontal regions).

Aghakhani Y *Brain*, Volume 127 (5,) 2004: 1127–1144

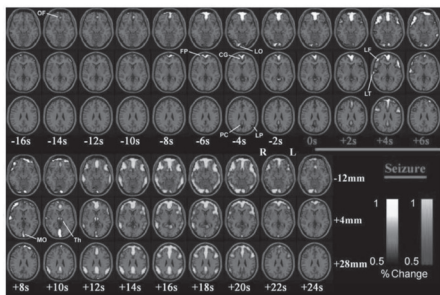


First activation was found in the right inferior frontal cortex. The thalamic activation and deactivation in default mode areas and caudate nucleus started between 5 s and 7.5 s after onset. Thalamic activation was followed by thalamic deactivation.

Moeller F. et al *Epilepsia*,51(10):2000–2010,2010

> Simultaneous EEG-fMRI studies in absence seizures have found:

- -increases in the thalamus.
- -decreases in the medial frontal, medial parietal, anterior/posterior cingulate, and lateral parietal cortex.
- -mixture of increases and decreases in the lateral frontal cortex.

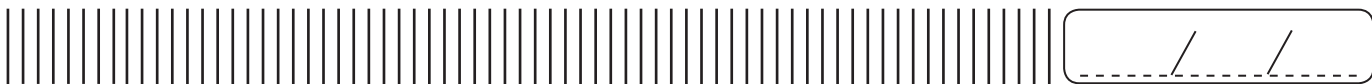


Absence seizures: early and late fMRI changes in cortical-subcortical networks (Bai X et al, 2010, Journal of Neuroscience 30:5884-5893.)

CONCLUSIONS

- The dichotomies of the seizure classification are not sufficient to include all the new information, for this reason it is necessary to include a third category, unknown.
- It is the most important category because it is an opportunity to open our mind to new knowledge.
- "The supreme goal of all theory is to make the irreducible basic elements as simple and as few as possible without having to surrender the adequate representation of a single datum of experience."

Albert Einstein
Philosophy of Science
Vol. 1, No. 2 (Apr., 1934), pp. 163-169

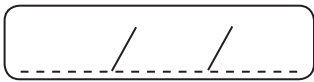


MÁRCIO FLÁVIO DUTRA DE MORAES (BRAZIL)

HYPEREXCITABLE AND HYPER SYNCHRONOUS NEURAL NETWORKS IN ANIMAL MODELS OF EPILEPSY: ASPECTS OF THE TEMPORAL DYNAMICS OF NEURAL RECRUITMENT IN EPILEPTOGENESIS



Lined area for text or notes, consisting of multiple horizontal lines.



JAIME CARRIZOSA (COLOMBIA)

TRANSITION IN EPILEPSY



Transition programs: between a successful or broken connection in epilepsy care

Jaime Carrizosa Moog
University of Antioquia
Child and Adolescent Neurology Service
Pediatric Department

Medellin, Colombia

THE HEALTH OF ADOLESCENTS AND YOUTH IN THE AMERICAS

IMPLEMENTATION OF THE REGIONAL STRATEGY AND PLAN OF ACTION ON ADOLESCENT AND YOUTH HEALTH 2010-2018

THE HEALTH OF ADOLESCENTS AND YOUTH IN THE AMERICAS

Young persons living with chronic conditions: These young persons have the same developmental issues, challenges, and needs as their peers, in addition to dealing with their chronic condition. While information is limited on the burden of chronic conditions among young persons in the Region, the available data suggest a significant burden, ranging from respiratory conditions such as asthma to diabetes, cancers, epilepsy, skin and musculoskeletal conditions, and HIV. Each

Figure II.12: Changes in causes of youth disability-adjusted life years (DALYs) lost in those 20-24 years old (both sexes), Latin America and the Caribbean, 1990-2015

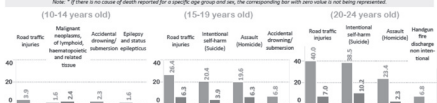


Adolescent and Youth Health - 2017 Country Profile
URUGUAY



MORTALITY RATES - Four Leading Causes of Death, by Age Group and Sex (per 100,000 Population)

Source: PAHO Regional Mortality Database, Pan American Health Organization (PAHO/WHO), 2018 Edition. Country-level mortality data available as of 2014.
Note: * If there is a change of death reporter for a sex/age group and sex, the corresponding bar with zero value is not being represented.



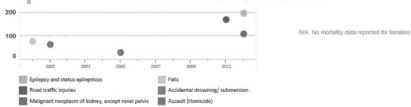
Annex II.B2: Leading causes of death in adolescents (aged 10-19 years) in the Americas in 2011 (39 countries reporting, with number of deaths and age-adjusted rates per 100,000, by sex)

Rank	Cause of death	Males		Females		Total	
		Number	Adjusted rate	Number	Adjusted rate	Number	Adjusted rate
1	Assault (homicide)	17,464	22.21	2,119	3.82	19,583	12.73
2	Road traffic injuries	10,042	12.80	9,509	4.67	19,551	8.81
3	Intentional self-harm (suicide)	4,230	5.30	1,910	2.54	6,140	4.00
4	Event of undetermined intent	3,199	4.32	587	0.83	3,786	2.42
5	Malignant neoplasm of lymphoid, hematopoietic and related tissue	1,775	2.27	1,280	1.72	3,055	2.00
6	Accidental drowning and submersion	2,336	3.04	448	0.61	2,784	1.84
7	Congenital malformations, deformations and chromosomal abnormalities	984	1.27	763	1.03	1,747	1.15
8	Influenza and pneumonia	880	1.13	706	0.94	1,586	1.05
9	Accidental poisoning	778	1.05	373	0.52	1,151	0.79
10	Diseases of the urinary system	556	0.71	454	0.6	1,010	0.65
11	Cardiovascular diseases	409	0.54	382	0.51	791	0.53
12	Pregnancy, childbirth and the puerperium	0	0.00	830	1.14	830	0.54
13	Malignant neoplasm of brain	463	0.69	320	0.44	773	0.51
14	Epilepsies	385	0.52	289	0.40	674	0.45
15	Epilepsy and status epilepticus	306	0.52	187	0.34	493	0.43
16	Others	14,468	0.190	1,130	0.15	15,598	0.10
Total		58,445	34.46	23,397	31.11	81,802	33.24

Adolescent and Youth Health - 2017 Country Profile
MONTERRAT



MORTALITY TRENDS - Reported Causes of Death, by Sex (per 100,000 Population)
Adolescent and Youth (10-24 years old), 2000-2012

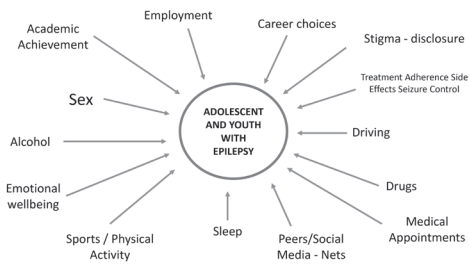


Prevalence Rate of Epilepsy in Latin America

Country	Nr. Studies	Year	Prevalence Rate / 1000
Argentina	3	1991	3,2 – 6,2
Bolivia	2	1994 - 2010	6,6 – 12,3
Brazil	5	2000 - 2006	5,4 – 20,4
Chile	2	1975 - 1988	17,7 – 31,9
Colombia	4	1993 – 2005	10,1 – 24,0
Cuba	1	?	7,5
Ecuador	5	1992 - 2015	7,14 – 28,0
Guatemala	2	1990	8,5 – 28,0
Honduras	2	1997 - 2005	11,8 – 23,4
Mexico	2	2007 - 2010	3,9 – 25,4
Peru	3	2000 – 2007	10,8 – 32,1
Panama	1	?	57
Uruguay	1	1990	9,1
TOTAL	33	MEAN	12,2 – 25,3

Estimated number of young persons (10 – 24 years) with epilepsy in Latin America
2.022.821 – 4.194.866

Rev Neurol 2018; 67: 249-62.



Dynamic mapping of human cortical development during childhood through early adulthood

Miles Gogtay^{1,2}, Jay N. Giedd¹, Lerdie Lusk¹, Khalise M. Hayashi¹, Deanna Greenstein¹, A. Catherine Vallbo^{1,3}, Frank J. Rupprecht^{1,4}, David R. Henken¹, Lisa S. Calmon¹, Arthur W. Toga^{1,5}, Judith L. Rapoport^{1,6}, and Paul M. Thompson^{1,6}

¹Child Psychology Branch, National Institute of Mental Health, National Institutes of Health, Bethesda, MD 20895 and ²Laboratory of Neuro Imaging, Department of Neurology, University of California School of Medicine, Los Angeles, CA 90095 USA

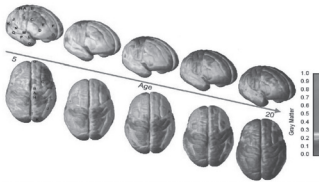
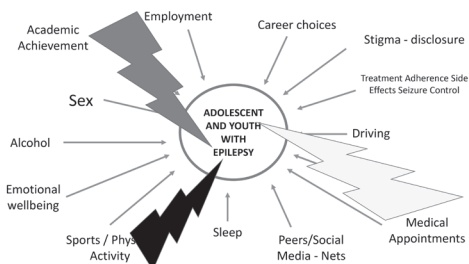


Fig. 8. Magnified and top-down view of the dynamic response of GMV maturation over the cortical surface. The color bar shows a color representation in units of millimeters. Top-down brain image depicts the lateral view of the cortex as described in Fig. 1. The color bar depicts the dynamic response.



Physical Activity in Children/Teens with Epilepsy Compared with That in Their Siblings without Epilepsy

*Judy Wong and †Elaine Wirrell

*University of Alberta, Edmonton; and †Department of Pediatrics and Neurosciences, University of Calgary, Calgary, Alberta, Canada

Summary: Purpose: To determine (a) whether children and teens with epilepsy participate in less physical activity and have higher body mass index (BMI) percentiles for age than do their siblings without epilepsy; and (b) what epilepsy-specific factors limit their participation.

Methods: Patients 5–17 years, with a ≥ 3 month history of epilepsy a development quotient ≥ 80 , no major motor or sensory impairments, and at least one sibling without epilepsy in a similar age range, were identified from the Neurology Clinic database or at the time of clinic visit. Parents completed a questionnaire regarding sedentary activities and group, individual, and total sports activities. Children aged 11–15 years also completed the physical activity portion of the Health Behavior in School Aged Children questionnaire. Clinic charts were reviewed for seizure

type, etiology, frequency, duration of epilepsy, and number of antiepileptic drugs (AEDs) ever taken.

Results: Teens with epilepsy participated in fewer group and total sports activities than did controls and were more likely to be potentially overweight or obese. Receiving three or more AEDs in the past showed a significant negative correlation with sports participation. Although a trend was noted for those with higher seizure frequency to be less active, no other epilepsy-specific factors or prior seizures or seizure-related injury during a sports event correlated with participation in physical activity.

Conclusion: Programs that promote exercise in adolescents with epilepsy should be encouraged to improve their physical, psychological, and social well-being. **Key Words:** Physical activity—Sports—Overweight.

Contents lists available at ScienceDirect

Epilepsy Research

Journal homepage: www.elsevier.com/locate/epilepsyres

Review article

The impact of epilepsy on academic achievement in children with normal intelligence and without major comorbidities: A systematic review

S.W. Wo^a, L.C. Ong^b, W.Y. Low^a, P.S.M. Lai^{a,*}

ABSTRACT

Purpose: To systematically examine published literature which assessed the prevalence of academic difficulties in children with epilepsy (CWE) of normal intelligence, and its associating factors.

Methods: A search was conducted on five databases for articles published in English from 1980 till March 2015. Included were studies who recruited children (aged 5–18 years), with a diagnosis of newly/recurrent epilepsy, an intelligent quotient (IQ) of ≥ 70 or attending regular school, with or without a control group, which measured academic achievement using a standardised objective measure, and published in English. Excluded were children with learning difficulties, intellectual disabilities (IQ < 70) and other comorbidities such as attention deficits hyperactive disorder or autism. Two pairs of reviewers extracted the data, and met to resolve any differences from the data extraction process.

Results: Twenty studies were included. The majority of the studies assessed “low achievement” whilst only two studies used the IQ-achievement discrepancy definition of “underachievement”. Fourteen studies (70%) reported that CWE had significantly lower academic achievement scores compared to healthy controls, children with autism or reported norms. The remaining six studies (30%) did not report any differences. CWE had stable academic achievement scores over time (2–4 years), even among those whose seizure frequency improved. Higher parental education and children with higher IQ, and had better attention or had a positive attitude towards epilepsy, were associated with higher academic achievement score. Older children were found to have lower academic achievement score.

Conclusion: In CWE of normal intelligence, the majority of published literature found that academic achievement was lower than controls or reported norms. The high percentages of low achievement in CWE, especially in the older age group, and the stability of scores even as seizure frequency improved, highlights the need for early screening of learning problems, and continued surveillance.

Psychiatric and Behavioural Disorders in Children with Epilepsy (ILAE Task Force Report): Epidemiology of psychiatric/behavioural disorder in children with epilepsy¹

Matti Sillanpää¹, Frank Besag², Albert Aldenkamp³, Rochelle Caplan⁴, David W. Dunn⁵, Giuseppe Gobbi⁶

High comorbidity: ADHD (30%), Cognitive disability (40%), Anxiety (15-36%), Depression (8-35%), Autism (20%), Psychosis (2%).

Epileptic Disorders (2016), Vol. 18, Supplement 1; Developmental Medicine Child Neurology(1999), 41, 473-479; Epilepsia (2014), 55(12):1910-1917.



The "Cinderella Syndrome": A narrative study of social curfews and lifestyle restrictions in juvenile myoclonic epilepsy

Teresa Leahy, Michael J. Hennessy, Timothy J. Counihan *

ABSTRACT

Several factors are thought to contribute to inadequate seizure control in patients with juvenile myoclonic epilepsy (JME), including drug resistance, neuropsychiatric comorbidity, and poor lifestyle choices. Recent evidence supports the existence of frontal lobe microstructural deficits and behavioral changes that may contribute to poor seizure control in a minority of patients. Counseling patients on the importance of adequate sleep hygiene and alcohol restriction is an important part of the management strategy for patients with JME. However, information is lacking on how these lifestyle restrictions impact on patients with JME. We conducted a qualitative descriptive analysis of the social impact of JME on 12 patients, from their own perspective. We identified four prominent themes: the importance of alcohol use as a social "norm", how JME affected relationships, decision making (risk versus consequences), and knowledge imparting control. Given that these restrictions were interpreted by patients as social "curfews", we suggest that the term "Cinderella Syndrome" encapsulates the perceived imperative to be home before midnight. Our findings underscore the importance for clinicians to recognize that in counseling patients with JME about lifestyle adjustments, there may be a significant social consequence unique to this patient group.

© 2017 Elsevier Inc. All rights reserved.

Determinants of Social Outcomes in Adults With Childhood-onset Epilepsy

Anne T. Berg, PhD,^{1,2} Christine B. Baca, MD, MSHS,^{1,2} Karen Rychlik, MS,³ Barbara G. Vickrey, MD, MPH,¹ Rochelle Caplan, MD,³ Francine M. Testa, MD,³ Susan R. Levy, MD³

To cite: Berg AT, Baca CB, Rychlik K, et al. Determinants of Social Outcomes in Adults With Childhood-onset Epilepsy. *Pediatrics* 2016;137(4):e20153844

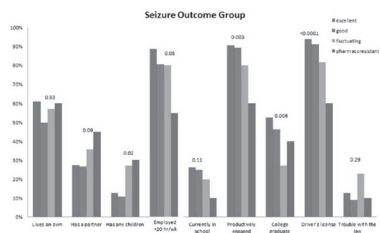


FIGURE 2 Association between seizure course and each of the benchmark social outcomes studied.



Epidemiological study of mortality in epilepsy in a Spanish population
 María Isabel Chamorro-Muñoz^{a,1}, Guillermina García-Martín^a,
 Francisco Pérez-Errazquin^a, Manuel Romero-Acebal^b, Antonio García-Rodríguez^b,
 Mario Gutiérrez-Bedmar^a

ABSTRACT

Purpose: Studies concerning mortality in epilepsy have been performed primarily in Northern-Central Europe and US. The aim of this study was to provide information about mortality in people with epilepsy in Southern European countries.

Method: We studied a Spanish prevalence and incidence cohort of 2309 patients aged ≥ 14 years with epilepsy who were treated in an outpatient epilepsy clinic between 2000 and 2013. The deceased were identified through Civil Registries. Causes of death were determined using death certificates, forensic autopsies, hospital reports, family practitioners, and care-givers' records. Standardized mortality ratios (SMRs) were calculated.

Results: In a total of 15,865 person-years of follow-up, 152 patients died, resulting in an SMR of 2.11 (95% CI 1.79–2.47), which was higher for those aged 14–24. There was also a high rate of death for symptomatic epilepsies, progressive causes (SMR=6.12, CI 3.50–9.94), and remote causes (SMR=2.02, CI 2.12–2.12). High SMRs were found for all kinds of epilepsy and for respiratory and tumoural causes. Patients who died of epilepsy itself were 12.5%. Sudden unexpected death in epilepsy incidence was 0.44/1000. Death from status epilepticus incidence was 20/100,000. SMRs for external causes were of no statistical significance.

Conclusions: This is the first epidemiological study to examine rate of mortality in epilepsy in a Southern European country. The identified mortality patterns is similar to the one provided by researchers from developed countries. The similarities between our results concerning epilepsy-related deaths and those provided by population-based studies are the result of the scarcely selected character of our study cohort.

© 2015 British Epilepsy Association. Published by Elsevier Ltd. All rights reserved.



Hospital care for mental health and substance abuse in children with epilepsy



Dylan P. Thibault ^{a,b}, Adys Mendizabal ^c, Nicholas S. Abend ^{a,d}, Kathryn A. Davis ^{a,e}, James Crispo ^{b,f}, Allison W. Willis ^{g,h,i,j}

ABSTRACT

Results: We observed 353319 weighted MHSA hospitalizations of children ages 6–20; 3280 of these involved a child with epilepsy. Depression was the most common MHSA diagnosis in the general population (39.5%) whereas bipolar disorder was the most common MHSA diagnosis among children with epilepsy (36.2%). Multivariate logistic regression models revealed that children with comorbid epilepsy had greater adjusted odds of bipolar disorder (AOR: 1.17, 1.04–1.30), psychosis (AOR: 1.78, 1.51–2.09), sleep disorder (AOR: 5.90, 1.90–18.34), and suicide attempt/ideation (AOR: 3.20, 1.46–6.99) compared to the general MHSA inpatient population. Epilepsy was associated with a greater LOS and a higher adjusted incidence rate ratio (IRR) for prolonged LOS (IRR: 1.12, 1.09–1.17), particularly for suicide attempt/ideation (IRR: 3.74, 1.68–8.34).

CRITICAL REVIEW AND INVITED COMMENTARY



Epilepsy: Transition from pediatric to adult care. Recommendations of the Ontario epilepsy implementation task force

¹Dominic W. Andrade, ²Aimee S. Bunney, ³Edward B. Berovic, ⁴Phillip Barker, ⁵Esther Bai, ⁶Peter Cantfild, ⁷Guilia Quaglia Clozza, ⁸Eyal Cohen, ⁹Timothy Coffin, ¹⁰Lisa Graves, ¹¹Jan Greenaway, ¹²Bevly Guttmann, ¹³Raj, Catherine Hagen, ¹⁴Amya Harnik, ¹⁵Regina Hinton, ¹⁶Patrick Kaufman, ¹⁷Bernard Lawford, ¹⁸Hannah Lee, ¹⁹Leslie Lindholm, ²⁰Yves Boivin Lomax, ²¹Mary Pat Macdonald, ²²Daly Pleoniz Dadi, ²³Berge A. Pelissier, ²⁴Janice Pridgen, ²⁵Rima Rabibovic, ²⁶Tracy Naim, ²⁷Mary Secora, ²⁸Lauren Sellers, ²⁹Mitchelle Shapiro, ³⁰Marie Degré, ³¹Boris Smith, ³²Peter Szatmari, ³³Loeung Tao, ³⁴Anastasia Vogt, ³⁵Sharon Whiting, and ³⁶Dr. Carter Smead III

Epilepsia, Volume 58, Number 11, November 2017
doi:10.1111/epi.13932

Transition:

Transition of care is the planned, coordinated movement of adolescents from the child – oriented family centered environment of pediatrics to the adult oriented care setting. (Process)

Transition is the integral** empowerment* of patients/families with a chronic disease in a planned, coordinated movement of adolescents from the child – oriented family centered environment of pediatrics to the adult oriented care setting. (Process)

Transition:

- * Empowerment:

Authority or power given to someone to do something. The philosophy of health promotion is to guide and support patient care through **empowerment** and collaboration.

- **Integral:

1. Diagnosis and management of seizures
2. Mental health and psychosocial issues
3. Financial, community and legal supports

Transfer:

The action of handing over a patient to an adult health care provider. (Step)

Step 1: Preparation for the adult health care system

- Introduce the concept of transition.
- Education about "your own disease".
- Need for developing knowledge and skills to be more independent.
- Search services for adults with disabilities.
- Age of discharge.

INTRODUCTORY PHASE (AGE 12 – 15 YEARS)

Step 1: Preparation for the adult health care system

- Develop an individual transition plan
- Provide specific information to individual needs/risks/interests/concerns
- Empowerment of care

PREPARATION PHASE (AGE 12 – 17 YEARS)

Step 1: Preparation for the adult health care system

- Where possible the pediatric neurologist/epileptologist and their team consult with the patient and family along with the adult neurologist/epileptologist.
- Follow – up or evaluation of the whole transition process

FINAL PHASE OF TRANSITION (AGE 17 - 18 YEARS)

Step 2. Identifying adolescents at risk for poor transition

- Inconsistent medication compliance
 - Risk of unwanted pregnancy
 - Use of recreational /illegal drugs
 - Driving and seizures
 - Comorbidity
- Identify knowledge gaps

Step 3: Epilepsy reevaluation, screening and management

- Epilepsy diagnosis reevaluation
- EEG or videoEEG monitoring
- Imaging
- Genetic testing
- Mental health needs/screening
- Treatment: neuromodulation, ketogenic diet
- Contraception and family planning
- Healthy lifestyle: nutrition, physical activity, sleep

Step 3: Epilepsy reevaluation, screening and management

- Epilepsy diagnosis reevaluation: West Syndrome → LGS → Focal epilepsy
- EEG or videoEEG monitoring:
 - Patient is not seizure free.
 - Seizure semiology has changed
 - Patient has other non epileptic events
 - Possible psychologic non epileptic events (PNES)
 - Adult service without easy availability of EEG service

Step 3: Epilepsy reevaluation, screening and management

- Imaging:

- If an MRI has never been done (?)
- Progressive etiology
- Seizure change in semiology or frequency
- Patient as possible surgery candidate

Step 3: Epilepsy reevaluation, screening and management

- Genetic Testing:

- Chromosome microarray, massive parallel sequencing, exome or genome sequencing
- Possibility that adult neurologist is (more?) unfamiliar with genetic testing

Step 3: Epilepsy reevaluation, screening and management

- Mental health needs:

- Mental health screening (Depression, anxiety, suicidal ideation, ADHD)
- Bipolar disorder and schizophrenia beginning in adolescence
- Intellectual disability reevaluation

Questionnaires for normal adolescents

- GAINS (Global Appraisal of Individual Needs Short Scener)
- MFQ (Mood and Feelings Questionnaire)
- THREADS (Transition, Home, Medication, Education, Activity, Peers, Drugs, Suicidality, Body Image)
- HEADSS (Home, Education, Employment, Activities, Drugs, Sexuality, Suicidality, Depression)
- ADOLESCENTE



FACULTAD DE MEDICINA - UNIVERSIDAD DE ANTIOQUIA
MEDICINA GENERAL
CLÍNICA ADOLESCENTE Y JUVENIL
INSTITUTO ADOLESCENTE Y JUVENIL
DEPARTAMENTO DE PSICHIATRÍA Y NEUROLOGÍA

VARIABLES / INDICADORES

A	Admisión, Atención, Actividades Incidencia, agresión, comportamiento, conducta delirante, hiperactividad, hiperactividad, ríen, autolesión, maltrato, castigo, técnica de disciplina, área física o de salud
D	Compromiso y prevención, acceso, exposición, consumo, presión de grupo, actitud en la familia, acceso y consumo
O	Organización, Ocio, Experimentación, hobby Estrés, trabajo, expectativas laborales, tiempo libre, vinculo y grupos juveniles y comunitarios
L	Salud Compromiso y prevención, acceso, exposición, consumo, presión de grupo, actitud en la familia, acceso a servicios
E	Estabilidad Compromiso y mecanismos de adaptación (emocional, percepción, valores, negación, negación, separación, desencanto, aislamiento, aceptación, internalización, compensación) adherencia terapéutica, efectos deseado y efectos secundarios, interacción farmacológica y con otros medicamentos, consumo médico, prevención
S	Salud, familia, salud Contexto médico, diagnóstico, tratamiento, calidad de vida, barreras, efectividad, adherencia, salud
C	Costo Compromiso, seguimiento, identificación de riesgos, seguros etc.
E	Eficiencia, Actividad Física Tipo, regularidad, intensidad, expectativas, ventajas, desventajas y ventajas
N	Nutrición Intake y estado nutricional
T	Tecnología y medios sociales Habilidades, riesgos, ventajas, horas/día, tipo de videoblogs, género de programas
E	Educación, Expectativas Aprendizaje, cursos, bullying expectativa laboral
S	Seguridad Conocimiento, ETS, ACO, VIH, riesgos, violencia sexual

For each of the following statements please indicate the responses that best describe you	Yes, I do	Yes, but I am having to do this	Yes, I have stopped doing this	Yes, I do not do this	Does not apply to me
90 I separate and keep track of my health information independently from my parents, relatives, etc.					
91 I can get to medical appointments on my own					
92 I spend time alone with my health care provider at each appointment					
93 I speak up for myself and tell others what I need during health care visits					
94 I have discussed sexually and reproductive health with my health care team (concurrent or sequential questions)					
95 I know how my lifestyle can impact my health, including and being able to discuss this with my health care team (e.g. use of alcohol, drugs, aggression and driving)					
96 I understand the importance of my health information on career choice and future employment					
97 I know my legal rights as a patient (e.g. who they belong to) and how to discuss medical information with my family and at work					
98 I know about my health insurance coverage, if any, and how to use it (e.g. how to get an appointment, I know the plan for an emergency) (e.g. health insurance, etc.)					
99 I know about my rights to participate in research and decision making regarding my health					
100 I know how to access the internet, I make it a habit to use the internet for information and updates					
101 I know how to access the internet, I make it a habit to use the internet for information and updates					
102 I know what to expect in adult services and how to access those services					

TRANSITION OF EPILEPSY CARE FROM CHILDREN TO ADULTS

Models for transition clinics

*Jaime Carrizosa, †Isabelle An, ‡Richard Appleton, §Peter Camfield, and ¶Arpad Von Moers

Epilepsia, 55(Suppl.3):46-51, 2014
doi:10.1111/epi.12716

Table 2. Proposed transition checklist

Transition items – date	Key notes	Observations
Name: Age: Diagnosis: Treating physician: Receiving physician:		
Complete medical history	Diagnosis and comorbidity; medication schedule(s) adherence, AED efficacy, drug interactions, adverse effects, AED withdrawal trials, plasma concentrations, seizure follow-up/diaries; neuroimaging, electrophysiologic, neuropsychological studies, liver function, blood tests	
Education information	Building up awareness and consciousness about his/her disease, drug treatment, triggering factors, status, legal rights	
Family dynamics	Quality of parent/adolescent relationship, overprotection, dependence, shame, cultural and religious background, resilience	
Individual health supervision issues	Nutritional status: weight/height/BMI; vaccinations, body image	
Sexuality, pregnancy and reproductive issues	Anticonception, irregular menses, sexual performance and desire, sexually transmitted diseases, pregnancy risks, sexual abuse, teratogens, pregnancy termination, breastfeeding	
Smoking, alcohol, drugs	Seizure risks, antiepileptic drug interaction, dependence, addiction, peer pressure	
Education and career choices	Vocational, technical, professional orientation; overnight duties	
Physical activity	Extreme sports, seizure control, SUDAP prevention	
Driver's license	Legislation, seizure control, autonomy	
Comorbidity	Physical and psychiatric comorbidity, drug treatment and interactions, quality of life	
Mortality	Higher risk of mortality, SUDAP, depression, suicide, accidents	
Insurance	Social security, family dependence, work insurance, treatment and follow-up guarantee	

Accepted Manuscript

Title: Failed transition to independence in young adults with epilepsy: The role of loneliness

Authors: R.P.J. Geerlings, L.M.C. Gotmmer-Welschen, J.E.M. Machielse, A.J.A. de Louw, A.P. Aldenkamp





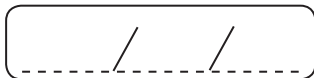
Handwritten marks: / /

RŪTA MAMENISKIENĖ (LITHUANIA)

GROUP B – CASE STUDY



Lined writing area with horizontal lines.





FERRUCCIO PANZICA (ITALY)

IDENTIFICATION OF EPILEPTIC ZONE FROM STEREOEEG: A CONNECTIVITY BASED APPROACH


Identification of epileptic zone from StereoEEG: a connectivity based approach

ferruccio.panzica@istituto-besta.it
Fondazione IRCCS Istituto Neurologico C. Besta, Milano

ferruccio.panzica@istituto-besta.it






Focal seizures





- Originate within networks limited to one hemisphere
- May be discretely localized or more widely distributed....

Scheffer ILAE 2017

Focal seizures

- Focal epilepsies represent a common neurological disorder and account for more than 50% of all epilepsies.
- Approximately 30% of patients with focal epilepsies experience seizures that are resistant to anti-epileptic drugs
- A subset of these patients can be considered candidates for epilepsy surgery
- The main issue to be solved is the precise definition of the *Epileptogenic Zone (EZ)*

Epileptogenic Zone



In 1965, Talairach and Bancaud introduced the term “epileptogenic zone” (EZ) as “the site of the beginning and of their primary organization of the epileptic seizures ”

EZ the “area of cortex that is necessary and sufficient for initiating seizures and whose removal (or disconnection) is necessary for complete abolition of seizures (Luders, 1992)

Indications for Stereo-EEG in drug-resistant focal epilepsies



- Discrepancies between:
 - ✓ anatomical and clinical data;
 - ✓ anatomical and electrical data;
 - ✓ electrical and clinical data;
- Supposed bi- or multi-lobar ictal discharges;
- Early ictal involvement of functional cortical areas (suggested by the clinical semiology);



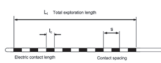
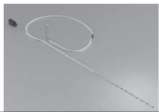
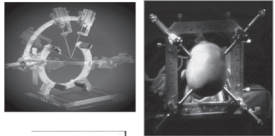
Individually tailored surgical removal

Stereo-EEG.



Diagnostic invasive technique used for pre-surgical evaluation of patients with drug-resistant partial epilepsy.

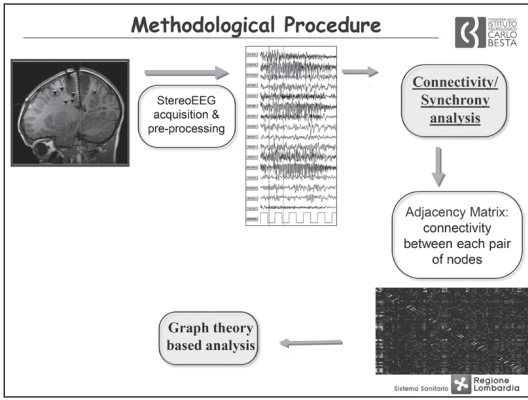
It consist in stereotactic placement of intracerebral multilead electrodes for EEG recordings. 150-200 EEG signals are recorded for 1-2 weeks, and analysed in order to correctly identify the Epileptogenic Zone

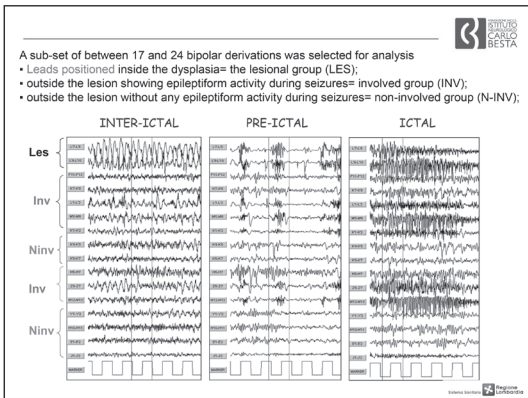


The appropriate identification of the EZ, is the fundamental step in the diagnostic work-up prior to surgery.

Its organization can be quite complex: the seizure onset may involve distant and functionally distinct brain sites almost simultaneously

The issue of defining the EZ is closely related to that of identifying ‘abnormal’ couplings among neuronal ensembles distributed over distant areas.





CONNECTIVITY

Functional Connectivity: statistic measure of temporal interaction between activities in different areas.

Effective Connectivity: influence that one neural system exerts on another (who drives whom). It describes the dynamic directional interactions (causal effects) among brain regions

Couplings are:

- ✓ transient
- ✓ dynamic (time-varying)
- ✓ frequency-specific

Sistema Sanitario Regione Lombardia

Autoregressive Models (AR)

MULTIVARIATE AR

$$\begin{bmatrix} x_1(t) \\ \vdots \\ x_Q(t) \end{bmatrix} = \sum_{k=1}^p A_k \begin{bmatrix} x_1(t-k) \\ \vdots \\ x_Q(t-k) \end{bmatrix} + \begin{bmatrix} w_1(t) \\ \vdots \\ w_Q(t) \end{bmatrix}$$

$$A_k = \begin{bmatrix} a_{1,1}(k) & a_{1,2}(k) & \dots & a_{1,Q}(k) \\ \vdots & \vdots & \ddots & \vdots \\ a_{Q,1}(k) & \dots & \dots & a_{Q,Q}(k) \end{bmatrix}$$

Partial Directed Coherence (PDC)

$$\bar{A}(f) = I - A(f) \quad A(f) = \sum_{k=1}^p A_k e^{-i2\pi f k}$$

$$Pdc_y(f) = \frac{\bar{a}_y(f)}{\sqrt{\bar{a}_j(f) \cdot \bar{a}_j(f)}}$$

$$\bar{A}(f) = \begin{bmatrix} \bar{a}_1(f) & \dots & \bar{a}_1(f) & \dots & \bar{a}_1(f) \\ \bar{a}_2(f) & \ddots & \vdots & \ddots & \vdots \\ \vdots & \vdots & \bar{a}_j(f) & \ddots & \vdots \\ \vdots & \vdots & \vdots & \ddots & \bar{a}_m(f) \\ \bar{a}_n(f) & \dots & \bar{a}_n(f) & \dots & \bar{a}_n(f) \end{bmatrix}$$

Sistema Sanitario Regione Lombardia

Comments



In patients with type II FCD, the region inside the dysplasia corresponds to the abnormal hubs of the epileptic network that originates and sustains the seizures, plays a leading role in generating and propagating ictal EEG activity, and in recruiting other distant areas to become involved in the seizure. This leading role of the dysplasia may account for the good post-surgical outcome of patients with type II FCD because the resection of dysplastic tissue removes the entire EZ responsible for seizure onset.



Comments



In all of the examined cases, we observed significant differences in the interactions between SEEGs obtained from EZ, other regions involved in the ictal activity and regions non-involved in seizure

Effective connectivity + indexes from graph theory can add new information to support clinician in localizing the EZ (EN)

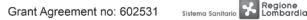


European Project (Fp7 funded project)

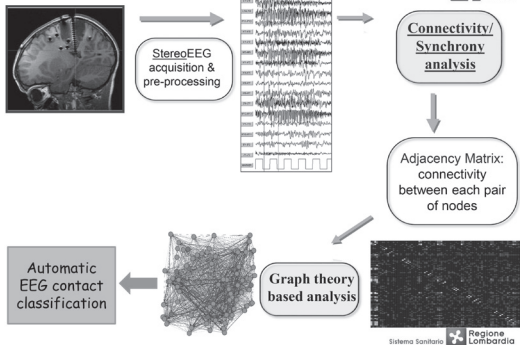


Project full title: "Development and Epilepsy - Strategies for Innovative Research to improve diagnosis, prevention and treatment in children with difficult to treat Epilepsy"
Grant agreement no: 602531

Non-invasive neurophysiologic biomarkers for the recognition of the epileptogenic zone and networks interfering with cognitive brain function in FCD patients



Methodological Procedure



Methods



- 14 patients recorded at the Epilepsy Surgery Center of Niguarda Hospital (Milano) with drug-resistant focal epilepsy, all seizure free after one year from surgery.
- Analysis was performed on the entire set of SEEG contacts using a bipolar montage
- And focused on interictal SEEG signals: 3 minutes, divided into 36 consecutive non-overlapping epochs
- For the connectivity analysis we used the h2 index (Bartolomei et al., 2001).
- Several graph theory based indexes were used to test different classification procedures. Indices characterizing the centrality of a node were better related to the ZE, namely: degree, strength and betweenness centrality
- For an automatic classification of the nodes we used the following procedure:
 - For each graph index we defined as threshold the average value among the nodes and time epochs.
 - For each graph index, we assigned a value of 1 to a node when its mean value was higher than the threshold, 0 otherwise.
 - A Node was classified as belonging to EZ if at least one of the three index had value of 1.
- The same procedure was applied on different frequency bands and the results compared.
- The accuracy of the classification was evaluated by comparing our results with the EZ defined by a clinician

Sistema Sanitario Regione Lombardia

Results



	PRE-SURGERY EZ					
	1-30Hz		30-80 Hz		1-80 Hz	
	TP (%)	FP (%)	TP (%)	FP (%)	TP (%)	FP (%)
P11	100	86	90	58	100	59
P12	100	51	44	58	60	50
P13	67	58	78	69	89	48
P14	50	60	58	63	75	62
P15	100	47	100	46	100	50
P16	86	55	86	32	85	53
P17	82	47	76	56	76	50
P18	100	69	100	50	100	64
P19	89	55	78	65	100	62
P10	83	57	67	46	75	57
P11	92	58	75	56	92	56
P12	100	58	56	55	89	61
P13	67	54	76	35	71	47
P14	59	51	59	64	71	55
Mean	82,6923	55,3846	73,3077	53,4615	83,3846	55
St. Dev.	16,98	5,85	16,54	11,32	12,98	5,86

TP=True positive, % of correctly classified leads.

	RESECTED EZ			
	1-30Hz		1-80 Hz	
	TP (%)	FP (%)	TP (%)	FP (%)
P11	100	86	100	60
P12	100	54	60	56
P13	67	58	100	69
P14	71	58	71	62
P15	100	47	100	46
P16	100	55	100	38
P17	100	53	100	58
P18	100	69	100	50
P19	89	55	78	60
P10	100	58	100	45
P11	100	59	75	57
P12	100	58	56	55
P13	85	52	92	37
P14	100	49	100	60
Mean	93,7143	57,9286	88	54
Dev.	11,51	9,62	16,49	9,45

FP=false positive, % of leads classified as belonging to EZ, but not included in the EZ identified by clinician and/or not in the region removed by surgery.

Sistema Sanitario Regione Lombardia

Comments



- ♣ Most (all?) of the studies are retrospective studies including only patients with good outcome
- ♣ Most are based on analysis of seizures or transition to seizures epochs
- ♣ Non consensus about the protocols
- ♣ Small sample size
- ♣ Different type of epilepsy
- ♣ Different Algorithms
- ♣ Mostly group studies in which inferences are made about a population BUT Neurosurgical planning requires single-subject-specific information, spatial precision, maximizing sensitivity

Sistema Sanitario Regione Lombardia

Comments



Key point: Changes in EZ connectivity can be extracted from SEEG signals analyzing short segments of interictal activity (also Bettus et al., 2008; Wilke et al., 2011)



Sistema Sanitario Regione Lombardia

Comments: What Next?



- The appropriateness of this approach in correctly identify the EZ should be validated on large group of patients, including also patients not in Engel class I
- Much work is needed to understand which measures of connectivity and topology (and protocol), work best to delineate the EZ region
- At present visual analysis of SEEG signals by clinical experts remains the "gold standard", but it can be complemented by quantitative automatic methods, which offer more objective criteria for EZ assessment

Sistema Sanitario Regione Lombardia

Thanks



R. Spreafico L. Tassi G. Varotto
S. Franceschetti



Sistema Sanitario Regione Lombardia

Graph analysis of epileptogenic networks in human partial epilepsy



*|Christopher Wilke, |Gregory Worrell, and **|Bin He

*Department of Biomedical Engineering, University of Minnesota, Minneapolis, Minnesota, U.S.A.; |Center for Neuroengineering, University of Minnesota, Minneapolis, Minnesota, U.S.A.; and |Department of Neurology, Mayo Clinic, Rochester, Minnesota, U.S.A.

SUMMARY

Purpose: The current gold standard for the localization of the cortical regions responsible for the initiation and propagation of the ictal activity is through the use of invasive electrocorticography (ECoG). This method is utilized to guide surgical intervention in cases of medically intractable epilepsy by identifying the location and extent of the epileptogenic focus. Recent studies have proposed mechanisms in which the activity of epileptogenic cortical networks, rather than discrete focal sources, contributes to the generation of the ictal state. If true, selective modulation of key network components could be employed for the prevention and termination of the ictal state.

Methods: Here, we have applied graph theory methods as a means to identify critical network nodes in cortical networks during both ictal and interictal states. ECoG recordings were obtained from a cohort of 23 patients undergoing presurgical monitoring for the treatment of

intractable epilepsy at the Mayo Clinic (Rochester, MN, U.S.A.).

Key Findings: One graph measure, the betweenness centrality, was found to correlate with the location of the resected cortical regions in patients who were seizure-free following surgical intervention. Furthermore, these network interactions were also observed during random nonictal periods as well as during interictal spike activity. These network characteristics were found to be frequency dependent, with high frequency gamma band activity most closely correlated with improved post-surgical outcome as has been reported in previous literature.

Significance: These findings could lead to improved understanding of epileptogenesis. In addition, this theoretically allows for more targeted therapeutic interventions through the selected modulation or disruption of these epileptogenic networks.

KEY WORDS: Seizure, Source localization, Graph analysis, Electroencephalography.

Epilepsia, 52(1):84-93, 2011

Sistema Sanitario Regione Lombardia

Ictal-onset localization through connectivity analysis of intracranial EEG signals in patients with refractory epilepsy



*Pieter van Mierlo, |Evelien Carrette, |Hans Hallex, |Alfred Meurs, **Stefaan Vandenbergh, |Dirk Van Roost, |Paul Boon, |Steven Staelens, and |Krist Vofsi

*Medical Image and Signal Processing Group, Department of Electronics and Information Systems, Ghent University, |Mind, Ghent, Belgium; |Laboratory for Clinical and Experimental Neurophysiology, Neurobiology and Neurobiology, Department of Neurology, Ghent University Hospital, Ghent, Belgium; |Electrical Circuit Design and Realization, Department of Industrial Sciences and Technology, College University of Brno-Czechia, Brno, Belgium; |Department of Neurosurgery, Ghent University Hospital, Ghent, Belgium; and |Molecular Imaging Center Antwerp, Faculty of Medicine, Antwerp University, Antwerp, Belgium

SUMMARY

Purpose: Fifteen percent to 25% of patients with refractory epilepsy require invasive video-electroencephalography (VEEG) monitoring (VMEG) to precisely delineate the ictal-onset zone. This delineation based on the recorded intracranial EEG (iEEG) signals occurs visually by the epileptologist and is therefore prone to human mistakes.

The purpose of this study is to investigate whether effective connectivity analysis of intracranially recorded EEG signals provides an objective method to localize the ictal-onset zone.

Methods: In this study data were analyzed from eight patients who underwent VMEG at Ghent University Hospital in Belgium. All patients had a focal ictal onset and were seizure-free following resective surgery. The effective connectivity pattern was calculated during the first 20 s of ictal rhythmic EEG activity. The out-degree, which is reflective of the number of outgoing connections, was calculated for each electrode contact for every single seizure during these 20 s. The seizure

specific out-degrees were summed per patient to obtain the total out-degree. The electrode contact with the highest total out-degree was considered indicative of localization of the ictal-onset zone. This result was compared to the conclusion of the visual analysis of the epileptologist and the resected brain region segmented from postoperative magnetic resonance imaging (MRI).

Key Findings: In all eight patients the electrode contact with the highest total out-degree was among the contacts during seizure. This electrode contact was the ictal-onset zone. This contact, that we named "the driver", always laid within the resected brain region. Furthermore, the patient-specific connectivity patterns were consistent over the majority of seizures.

Significance: In this study we demonstrated the feasibility of correctly localizing the ictal-onset zone from EEG recordings by using effective connectivity analysis during the first 20 s of ictal rhythmic EEG activity.

KEY WORDS: Ictal-onset zone localization, Intracranial EEG, Connectivity.

Epilepsia, 54(8):1409-1418, 2013

Sistema Sanitario Regione Lombardia

Graph Measures of Node Strength for Characterizing Preictal Synchrony in Partial Epilepsy

Sandra Courina¹, Bruno Colombo², Agnese Tribuchon^{1,3}, Andrea Brouillet¹, Fabrice Bartolomei^{1,2*} and Christian G. Bena^{1*}

Abstract

The reference electrophysiological pattern at seizure onset is the “rapid discharge,” as visible on intracerebral electroencephalography (EEG). This discharge typically corresponds to a decrease of synchrony across brain areas. In contrast, the preictal period can exhibit patterns of increased synchrony, which can be quantified by network measures. Our objective was to compare preictal synchrony with a quantification of the rapid discharge as provided by the epileptogenicity index (EI). We investigated 24 seizures from 12 patients recorded by stereotaxic EEG (SEEG). Seizures were classified visually as containing preictal synchrony or not. We computed pairwise nonlinear correlation (h^2) across channels in the 8 sec preceding the rapid discharge. The sum of ingoing and outgoing links (IN and OUT node strength), as well as the sum of all links (total strength, TOT) were computed for each region. We tested several filtering schemes, and quantified the capacity of each strength measure to serve as a detector of regions with high EI values using a receiver operating characteristic (ROC) analysis. We found that the best correspondence between node strength and EI was obtained for the OUT and TOT measures, for signals filtered in the 15–40 Hz band—that is, for the band corresponding to the spiky part of epileptic discharges. In agreement with these results, we also found that the ROC results were improved when considering only seizures with visible synchronous patterns in the preictal period. Our results suggest that measuring strength of preictal connectivity graphs can bring useful clinical information on the epileptogenic zone.

BRAIN CONNECTIVITY
Volume 6, Number 7, 2016

Stimema Sanborn  Regione Lombardia

Localization of epileptogenic zone based on graph analysis of stereo-EEG

Yong-Hua Li^{1*}, Xiao-Lai Ye^{1*}, Qiang-Qiang Liu¹, Jun-Wei Mao¹, Pei-Ji Liang¹, Ji-Wen Xu^{1,2,3*}, Pu-Ming Zhang^{1,2,3*}

¹School of Biomedical Engineering, Shanghai Jiao Tong University, Shanghai 200240, China
²Department of Functional Neurosurgery, Ruiji Hospital, School of Medicine, Shanghai Jiao Tong University, Shanghai 200001, China

ABSTRACT

Localization of the epileptogenic zone (EZ) is essential for the successful surgical treatment of medically intractable epilepsy. In the present study, stereo-EEG (SEEG) recordings were obtained from seven patients underwent presurgical evaluation for treatment of intractable epilepsy. Partial directed coherence (PDC) analysis was applied to construct peri-ictal effective connectivity networks. The graphic measures, in-degree, out-degree and betweenness centrality, were evaluated to localize the EZ. A receiver operating characteristic (ROC) analysis was used to quantify the localization accuracy. We found that the in-degree coincided well with the EZ identified by epileptologists' visual inspection in all seven patients who had a significant improvement in seizure outcomes, however, the other two measures were effective only in some cases. Furthermore, in all seven patients the electrode contact with the highest in-degree was always located within the EZ identified by epileptologists' visual inspection. These results indicate that the graph theory is an effective method to localize the EZ when suitable graphic measures were chosen. Furthermore, the in-degree was the most effective measure among the three graphic measures in localizing the EZ when the PDC method was used.

Epilepsy Research 128 (2016) 149–157

Stimema Sanborn  Regione Lombardia

Dynamic Network Connectivity Analysis to Identify Epileptogenic Zones Based on Stereo-Electroencephalography

Jun-Wei Mao^{1*}, Xiao-Lai Ye^{1*}, Yong-Hua Li¹, Pei-Ji Liang¹, Ji-Wen Xu^{1,2*} and Pu-Ming Zhang^{1,2,3*}

Objectives: Accurate localization of epileptogenic zones (EZs) is essential for successful surgical treatment of refractory focal epilepsy. The aim of the present study is to investigate whether a dynamic network connectivity analysis based on stereo-electroencephalography (SEEG) signals is effective in localizing EZs.

Methods: SEEG data were recorded from seven patients who underwent presurgical evaluation for the treatment of refractory focal epilepsy and for whom the subsequent resective surgery gave a good outcome. A time-variant multivariate autoregressive model was constructed using a Kalman filter, and the time-variant partial directed coherence was computed. This was then used to construct a dynamic directed network model of the epileptic brain. Three graph measures (in-degree, out-degree, and betweenness centrality) were used to analyze the characteristics of the dynamic network and to find the important nodes in it.

Results: In all seven patients, the indicative EZs localized by the in-degree and the betweenness centrality were highly consistent with the clinically diagnosed EZs. However, the out-degree did not indicate any significant differences between nodes in the network.

Conclusions: In this work, a method based on ictal SEEG signals and effective connectivity analysis localized EZs accurately. The results suggest that the in-degree and betweenness centrality may be better network characteristics to localize EZs than the out-degree.

Frontiers in Computational Neuroscience | www.frontiersin.org | October 2016 | Volume 10 | Article 11

Stimema Sanborn  Regione Lombardia

SozRank: A new approach for localizing the epileptic seizure onset zone

Yonathan Murin¹, Jeremy Kim¹, Josef Parvizi², Andrea Goldsmith^{1*}

Abstract

Epilepsy is one of the most common neurological disorders affecting about 1% of the world population. For patients with focal seizures that cannot be treated with antiepileptic drugs, the common treatment is a surgical procedure for removal of the seizure onset zone (SOZ). In this work we introduce an algorithm for automatic localization of the seizure onset zone (SOZ) in epileptic patients based on electrocorticography (ECoG) recordings. The proposed algorithm builds upon the hypothesis that the abnormal excessive (or synchronous) neuronal activity in the brain leading to seizures starts in the SOZ and then spreads to other areas in the brain. Thus, when this abnormal activity starts, signals recorded at electrodes close to the SOZ should have a relatively large causal influence on the rest of the recorded signals. The SOZ localization is executed in two steps. First, the algorithm represents the set of electrodes using a directed graph in which nodes correspond to recording electrodes and the edges' weights quantify the pair-wise causal influence between the recorded signals. Then, the algorithm infers the SOZ from the estimated graph using a variant of the PageRank algorithm followed by a novel post-processing phase. Inference results for 19 patients show a close match between the SOZ inferred by the proposed approach and the SOZ estimated by expert neurologists (success rate of 17 out of 19).

PLOS Computational Biology | <https://doi.org/10.1371/journal.pcbi.1005953> January 30, 2018

Stimema Sanborn  Regione Lombardia

Using network analysis to localize the epileptogenic zone from invasive EEG recordings in intractable focal epilepsy

Alan Li¹, Bhaskar Chennu², Srinidhi Subramanian³, Robert Yaffe⁴, Steve Gilboa⁵, William Stray⁶, Robert Naritoku⁷, Austin Jordan⁸, Kayvan A. Zaghafel⁹, Sara K. Bail¹⁰, Shadi Agrebi¹¹, Jennifer J. Huggan¹², Jennifer Hryg¹³, Charles Kurland¹⁴, Emily Johnson¹⁵, Nathan Cross¹⁶, William S. Anderson¹⁷, Zach Fitzgerald¹⁸, Juan Belmonte¹⁹, John E. Gale²⁰, Stefan V. Sarnow²¹, and Jorge Gonzalez-Martinez²²

ABSTRACT

Treatment of medically intractable focal epilepsy (MIFE) by surgical resection of the epileptogenic zone (EZ) is often effective provided the EZ can be reliably identified. Even with the use of invasive recordings, the clinical differentiation between the EZ and normal brain areas can be quite challenging, mainly in patients without MRI detectable lesions. Consequently, despite relatively large brain regions being removed, surgical success rates barely reach 60-65%. Such variable and unfavorable outcomes associated with high morbidity rates are often caused by imprecise and/or inaccurate EZ localization. We developed a localization algorithm that uses network-based data analytics to process invasive EEG recordings. This network algorithm analyzes the centrality signatures of every contact electrode within the recording network and characterizes contacts into susceptible EZ based on the centrality trends over time. The algorithm was tested in a retrospective study that included 42 patients from four epilepsy centers. Our algorithm had higher agreement with EZ regions identified by clinicians for patients with successful surgical outcomes and less agreement for patients with failed outcomes. These findings suggest that network analytics and a network systems perspective of epilepsy may be useful in assisting clinicians in more accurately localizing the EZ.

Network Neuroscience 2(2), 218-240.

Identification of the epileptogenic zone of temporal lobe epilepsy from stereo-electroencephalography signals: A phase transfer entropy and graph theory approach

Meng-yang Wang¹, Jing Wang¹, Jian Zhou¹, Yu-guang Guan², Feng Zhai¹, Chang-qing Liu¹, Fei-fei Xu¹, Yi-xian Han¹, Zhao-fen Yan¹, Guo-ming Lu^{1,3}

ABSTRACT

The aim of this research is to apply an approach based on phase transfer entropy (PTE) and graph theory to study the interactions between the stereo-electroencephalography (SEEG) activities recorded in multilobar origin, in order to evaluate their ability to detect the epileptogenic zone (EZ) of temporal lobe epilepsies (TLE). Forty-three patients were included in this retrospective study. Five to sixteen (median = 12) multilead electrodes were implanted per patient, and, for each patient, a sub-set of between 10 and 32 (median = 22) bipolar derivations was selected for analysis. The leads were classified into the onset leads (OLs), the early propagation leads (EPLs), and the rest of the leads (RLs). The results showed that a significantly different dynamic trend of the out/in ratio (more obvious in the gamma band) distinguishes the OLs from RLs in the 23 patients who were seizure-free not only during the ictal event (significant elevation), but also during the inter-, pre-, late-ictal periods, and especially in the post-ictal (sharp decline) state. However, in the 20 patients who were not-seizure-free, the differences between the OLs and RLs during the post-ictal period were not found in any frequency band. The dynamic trend was used to predict surgical outcome, and the results showed that the sensitivity was 91% and the specificity was 70%. In brief, this study indicates that our approach may add new and valuable information, providing efficient quantitative measures useful for localizing the EZ.

NeuroImage: Clinical 16 (2017) 184-195

Betweenness centrality of intracranial electroencephalography networks and surgical epilepsy outcome

Bartosz T. Grobelny¹, Dennis London², Travis C. Hill³, Emily North⁴, Patricia Dugan⁵, Werner K. Doyle^{6,7,8}

Objective: We sought to determine whether the presence or surgical removal of certain nodes in a connectivity network constructed from intracranial electroencephalography recordings determines postoperative seizure freedom in surgical epilepsy patients.

Methods: We analyzed connectivity networks constructed from peri-ictal intracranial electroencephalography of surgical epilepsy patients before a tailored resection. Thirty-six patients and 123 seizures were analyzed. Their Engel class postsurgical seizure outcome was determined at least one year after surgery. Betweenness centrality, a measure of a node's importance as a hub in the network, was used to compare nodes.

Results: The presence of larger quantities of high-betweenness nodes in interictal and postictal networks was associated with failure to achieve seizure freedom from the surgery ($p < 0.001$), as was resection of high-betweenness nodes in three successive frequency groups in mid-seizure networks ($p < 0.001$).

Conclusions: Betweenness centrality is a biomarker for postsurgical seizure outcomes. The presence of high-betweenness nodes in interictal and postictal networks can predict patient outcome independent of resection. Additionally, since their resection is associated with worse seizure outcomes, the mid-seizure network high-betweenness centrality nodes may represent hubs in self-regulatory networks that inhibit or help terminate seizures.

Significance: This is the first study to identify network nodes that are possibly protective in epilepsy.

Clinical Neurophysiology 129 (2018) 1804-1812

CRITICAL REVIEW AND INVITED COMMENTARY



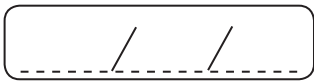
Defining epileptogenic networks: Contribution of SEEG and signal analysis

Fabrice Bartolomeo^{1,2}, Hamed Agrebi³, Fabrice Wendling⁴, Abbas McGonigal⁵, Walter Jans⁶, Mhamed Guez⁷, and Christian Binar⁸

Epilepsia, 56(11):1131-1147, 2015
doi:10.1111/epi.13170

SUMMARY

Epileptogenic networks are defined by the brain regions involved in the production and propagation of epileptic activities. In this review we describe the historical, methodologic, and conceptual bases of this model in the analysis of electrophysiologic intracerebral recordings. In the context of epilepsy surgery, the determination of cerebral regions producing seizures (i.e., the "epileptogenic zone") is a crucial objective. In contrast with a traditional focal view of focal drug-resistant epilepsies, the concept of epileptogenic networks has been progressively introduced as a model better able to describe the complexity of seizure dynamics and realistically describe the distribution of epileptogenic anomalies in the brain. The concept of epileptogenic networks is historically linked to the development of the stereoelectroencephalography (SEEG) method and subsequent introduction of means of quantifying the recorded signals. Seizures, and preictal and ictal discharges produce clear patterns on SEEG. These patterns can be analyzed utilizing signal analysis methods that quantify high-frequency oscillations or changes in functional connectivity. Dynamic changes in SEEG brain connectivity can be described during seizure genesis and propagation within cortical and subcortical regions, associated with the production of different patterns of seizure semiology. The interictal state is characterized by networks generating abnormal activities (interictal spikes) and also by modified functional properties. The introduction of novel approaches to large-scale modeling of these networks offers new methods in the goal of better predicting the effects of epilepsy surgery. The epileptogenic network concept is a key factor in identifying the anatomic distribution of the epileptogenic process, which is particularly important in the context of epilepsy surgery.



ISABELLA D'ANDREA MEIRA (BRAZIL)

**UNDERSTANDING THE VAGUS AFFERENT NETWORK AND ITS ROLE IN
TRANSLATIONAL CONNECTOMICS**



A series of horizontal lines for writing, spaced evenly down the page.

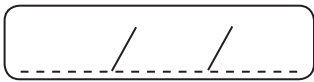


MATTHIAS KOEPP (ENGLAND)

**EFFECT OF PHARMACOLOGICAL AND SURGICAL INTERVENTIONS ON
COGNITIVE NETWORKS**



A series of horizontal lines providing a writing area for the abstract.




LILIA MORALES (CUBA)

CONNECTIVITY DERIVED FROM EEG AND NEUROIMAGING IN FOCAL EPILEPSIES

CONECTIVIDAD ESTRUCTURAL Y FUNCIONAL EN PACIENTES CON EPILEPSIA FOCAL FÁRMACO-RESISTENTE. ANÁLISIS TOPOLÓGICO DE REDES CEREBRALES

Lilia Morales Chacón, MD, PhD
marzo 2019



LA EPILEPSIA ES UNA ENFERMEDAD NEUROLÓGICA CONSIDERADA HOY COMO UNA ALTERACIÓN GLOBAL DE REDES NEURALES

What is the IMPACT of epilepsy?
50 000 000
More than 50 million people are living with epilepsy globally

Aproximadamente 30% de los pacientes se convierten en

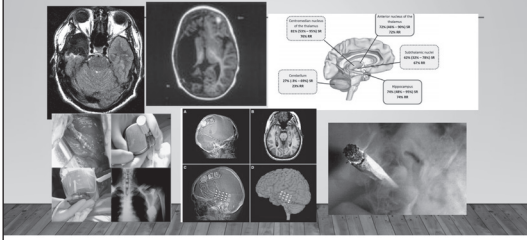
Figure 1. Antiepileptic Drug Regimens Over the Study Period

monotherapy polytherapy epilepsy surgery drug withdrawal
 monotherapy polytherapy epilepsy surgery drug withdrawal
 monotherapy polytherapy epilepsy surgery drug withdrawal

Figure 2. Cumulative Probability of Seizure Freedom by Treatment Duration and Probability of Achieving Seizure Freedom

The seizure-free rate observed was virtually unchanged over the study period, and the probability of achieving seizure freedom declined for each unsuccessful antiepileptic drug regimen prescribed.

¿¿¿QUÉ HACER? Medicar, resecar, estimular, cannabis

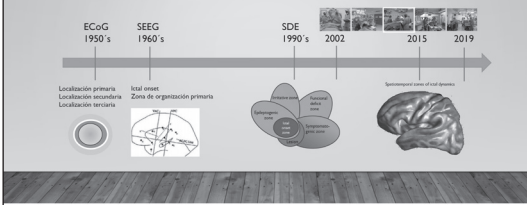


Objetivo de la cirugía epilepsia

Resección completa o desconexión de la "zona epileptogénica" o interrupción de la "red epileptogénica"

Este objetivo debe garantizarse con la preservación de la corteza elocvente.

EVOLUCIÓN HISTORICA DEL CONCEPTO DE ZONA EPILEPTOGENICA

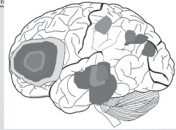


CIRUGIA DE EPILEPSIA

Localización de la zona epileptogénica ESENCIAL

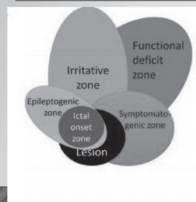
MULTIPLES ESCENARIOS

Zona Epileptogénica:
Área del cerebro que debe ser reseca para que el paciente quede //



- Lesión epileptogénica (RMN)
- Intactiva & déficit funcional (EEG, PET, SPECT, NPS)
- Zona de inicio ictal (VEEG, SPECT, etc)

SOBRELAPAMIENTO VARIABLE DE LA ZE CON LAS PRINCIPALES ÁREAS CORTICALES IMPLICACIONES



No prueba equivalente a ZE

No existe un test que permita estimar la ZE

Definir la zona de inicio ictal no es similar a definir la ZE

¿QUÉ HACER?

Very High-Frequency Oscillations: Novel Biomarkers of the Epileptogenic Zone
Mina Bissell, MD, PhD,^{1,2} Maria Paul, MD, PhD,¹ and Neville, PhD,^{1,2}
Hag Hagberg, PhD,¹ Jan Lindqvist, PhD, PhD,¹ Peter Hahn,¹
Paul D'Avella,^{1,2} Jon D'Souza, MD, PhD,¹ Eyal Seidemann, MD, PhD,¹
Sara Haber, MD, PhD,^{1,2} Gregoire D. Wilson, MD, PhD,¹ and David J. Williamson, MD, PhD,^{1,2}

Automated Online Quantification Method for ¹⁸F-FDG Positron Emission Tomography/CT Improves Detection of the Epileptogenic Zone in Patients with Pharmacoresistant Epilepsy

Victoria Cristina Morales Guadalupe,¹ Alicia E. Morales,¹ Barbara J. Bauer,¹
Cristina Garcia-Ramos,¹ Gabriel L. Nuñez,¹ André Rebeaux,¹ Anne Salazar,¹
and Francisco J. Gonzalez,¹

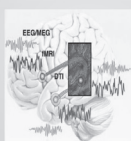
Improving Electroencephalographic Source Localization of Epileptogenic Zones With Time-Frequency Analysis

Journal of
Clinical EEG and Neuroscience
Volume 10(10)
October 2019
Epilepsy and Epileptogenesis
DOI: 10.1177/1550094418822331
journals.sagepub.com

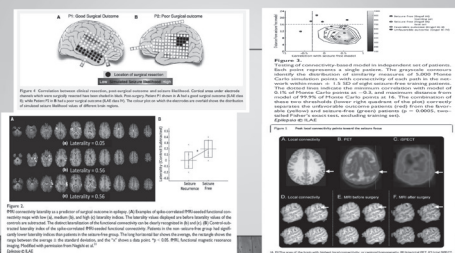
Imaging the seizure onset zone with stereo-electroencephalography

Olivier David,^{1,2,3} Thomas Blaubloom,⁴ Anne-Sophie Job,⁵ Stéphane Chabardes,^{1,2,4}
Dominique Hoffmann,⁶ Lovella Winoti,⁶ and Philippe Kahane^{1,2,3}

Las técnicas de neuroimágenes se utilizan actualmente para investigar la integración de regiones cerebrales especializadas funcionalmente



¿CONECTIVIDAD?



Las técnicas de mapeo cerebrales (como la DTI) producen patrones de conectividad más precisos, permitiendo un enfoque nuevo y multidisciplinario que permite estudiar sistemas complejos.

Rubinov M, Sporns O. Complex network measures of brain connectivity: Uses and interpretations. *Neuroimage*. 2010; 52(3): 1059-1095.

Table 1. Common modalities used to study functional connectivity in focal epilepsy

Modality	Advantage	Disadvantage
MEG	Noninvasive whole-brain coverage; high spatial resolution; high temporal resolution	Sensitive to non-neural signals; few long-term measurements; costly; requires shielding to avoid noise
fMRI	Noninvasive whole-brain coverage; whole-brain functional connectivity; high spatial resolution; whole-brain coverage	Low temporal resolution; requires shielding to avoid noise; requires a reliable neural correlate
iEEG	High spatial resolution; high temporal resolution; direct measurement of neural activity; reliable neural correlate	Invasive; limited to focal areas covered with electrodes; risk of seizures
Optical	Noninvasive; high temporal resolution; whole-brain coverage; reliable	Low spatial resolution; optical signals; limited depth of penetration

U.S. neuroepilepsy BC; neuroepilepsy PE; functional magnetic resonance imaging (fMRI); magnetoencephalography (MEG).

Englot D, Kiorad PE, Morgan VL. Regional and global connectivity disturbances in focal epilepsy related neurocognitive sequelae, and potential mechanisms underlying. *Epilepsia*. 2015;57(10):1546-1557.

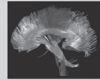
Con esta técnica no es posible determinar la direccionalidad de las fibras, además de que es imposible reconstruir de manera totalmente detallada los caminos neuronales, especialmente cuando las fibras se ramifican o se cruzan.

Cuenca I. Caracterización de la conectividad estructural cerebral basada en la teoría de redes complejas (tesis doctoral). Valencia: Escuela Técnica Superior de Ingeniería Industrial; 2017.

Conceptos básicos

- * Friston: define el término conectividad como la correlación temporal entre los datos de la activación de dos áreas cerebrales. Esta medida indica una sincronización sistemática entre áreas, modulada por diversas variables. La sincronización se considera como evidencia de conectividad funcional.

Conectividad estructural se refiere a las conexiones físicas o estructurales (sinápticas) que unen grupos de neuronas, y a sus propiedades biofísicas estructurales asociadas, como fuerza o efectividad sináptica.



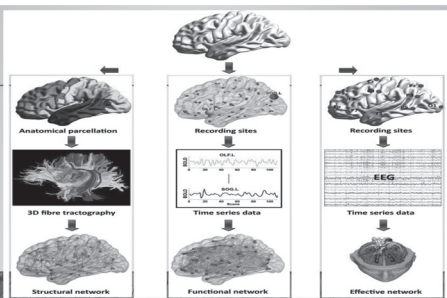
MEDIDAS DE CONECTIVIDAD ANATOMICA

medidas de conectividad entre regiones: Fuerza de Conexión Anatómica (FCA), Densidad de Conexión Anatómica (DCA) y Probabilidad de Conexión Anatómica (PCA)

FCA provee una estimación del flujo potencial de información entre cualquier par de regiones, considerando que dicho flujo es proporcional a la cantidad de fibras nerviosas compartidas por estas.

DCA es una medida de la fracción del área externa de las regiones que se encuentra conectada con respecto al área externa total de ambas, es, por tanto, una medida que intenta corregir por el tamaño de las regiones involucradas en cada conexión

ACP es una medida de la probabilidad de conexión, al menos por una fibra nerviosa, entre estas regiones. Dicha medida permite inferir si dos regiones se pueden encontrar vinculadas funcionalmente de forma directa, sin tener en cuenta las características de la conexión



Conceptos básicos

Conectividad funcional se refiere al grado con el cual la actividad en un área se correlaciona con la actividad de otra área, o la sincronización temporal de activación de dos áreas cerebrales.



Describe el conjunto de efectos causales de un sistema neuronal sobre otro.



Análisis topológico de redes cerebrales

Si tenemos las redes que representan las conexiones anatómicas cerebrales, ¿qué hacer con ellas?, ¿cómo analizar la información que contienen?, ¿qué conclusiones biológicas pueden extraerse?

Medidas topológicas, propias de la teoría de grafos, que buscan caracterizar las propiedades de la red en su forma general (como eficiencia global, índice de "mundo-pequeño", longitud del camino medio, configuración de motivos estructurales) y las de sus nodos locales (eficiencia local, centralidad, vulnerabilidad), brindando valores cuantitativos que reflejan las facultades intrínsecas para apoyar o soportar el flujo potencial de actividad neural.

Conceptos básicos

Teoría de grafos: estudia las teorías de los gráficos en conjunto no vacío utilizando términos como: vértices o nodos y selección de pares de vértices, las aristas orientados o no.

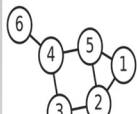


Diagrama de un grafo con 6 vértices y 7 aristas.

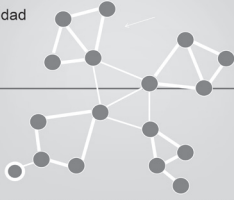


TEORÍA DE GRAFOS (REDES) - PROBLEMAS COMPLEJOS



TEORÍA DE GRAFOS (REDES) - PROBLEMAS COMPLEJOS

Conectividad Local



TEORÍA DE GRAFOS (REDES) - PROBLEMAS COMPLEJOS

Conectividad Global



TEORÍA DE GRAFOS (REDES) - PROBLEMAS COMPLEJOS

Alta Conectividad Local
Baja Conectividad Global



Regular



Small-world

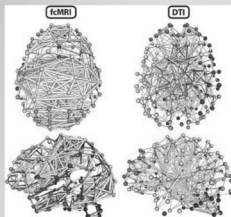
Baja Conectividad Local
Alta Conectividad Global



Random

Desorden

LAS REDES CEREBRALES SON SMALL-WORLD



Tjoms et al. *Neurobiology of Aging* (2013)



ANTECEDENTES
Conectividad - EPILEPSIA

- La epilepsia focal (EF) considerada tradicionalmente como un trastorno regional ya en la actualidad se ha demostrado como una alteración de redes neurales.
- Los cambios en la conectividad se relacionan con la duración y severidad de la enfermedad sugiriendo una reorganización progresiva de la conectividad.
- A pesar de todos los métodos y evaluaciones multidisciplinares para estimar la ZE, luego de la cirugía un 20% de los pacientes para la epilepsia del lóbulo temporal (ELT) y un 40% para la epilepsia extratemporal (EXT), recaen con crisis, lo que evidencia la necesidad de nuevos acercamientos para identificar la ZE y con ello lograr una mejor estrategia para el manejo de estos pacientes.
- Existe incremento de la conectividad en la zona epileptogénica (ZE) acompañada de una disminución distal en las redes

APLICACIONES PROMISORIAS
Conectividad - EPILEPSIA

- La conectividad cerebral funcional obtenida a partir de los registros de EEG puede ser utilizada para localizar la ZE (Carisch and Gatzert (1978), Galman (1983), Mars et al., 1985, Galeano (1987), Loh et al. (1987), Sandstone et al. 1998, 2001, 2004, 2005), Wendling et al., 2003, 2010) Potters et al. (2007), Babinski and Lehtvirta (2013) y para la predicción de las crisis (Mormann et al. (2007) and Salmus-Rottger et al. (2011).
- Los estudios de conectividad en EF pueden dar mejores estrategias para la localización de la ZE, en la predicción de la evolución quirúrgica y una mejor comprensión de las implicaciones neurofisiológicas en la recurrencia de las crisis.
- Otras aplicaciones promisorias del análisis de la conectividad funcional es la investigación de los mecanismos de acción de los tratamientos de neuromodulación, así como la identificación mas precisa de blancos para cirugía de epilepsia. En este sentido resulta importante avanzar en la comprensión de la correlación entre los cambios en la organización de la red funcional producto de la cirugía y la evolución clínica postquirúrgica

LINEAS ACTUALES
Conectividad - EPILEPSIA

- Minimizar las implicaciones de la metodología en los resultados obtenidos de conectividad en las epilepsias focales.
- Determinar cuales alteraciones de la conectividad son reversibles luego de la cirugía de epilepsia.
- Identificar la zona epileptogénica utilizando métodos cuantitativos

Predecir la evolución post quirúrgica.

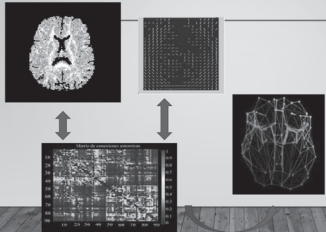
Problema: ¿Podrían las propiedades topológicas de las redes, a partir de la conectividad estructural derivada de la IRM-DTI y funcional del EEG en pacientes con epilepsia focal farmacorresistente (EFFR) del lóbulo temporal y extratemporal, ofrecer una aproximación cuantitativa a la estimación de la ZE?

DATOS DEMOGRÁFICOS EN PACIENTES CON EFFR DE LÓBULO TEMPORAL Y EXTRATEMPORAL.

Tipo de EFFR/ Condición	ELT no operados n=6	ExT no operados n=6	(p-valor)
Edad	33,3±15,7	24,6±10,8	p=0,26
Sexo/Femenino	5	6	p=0,24
Sexo/Masculino	1	-	p=0,42
Edad de inicio de las crisis	12,3±11,5	9,8±5,6	p=0,936
Duración de la enfermedad	21±15,2	13,1±14,6	p=0,47
Lateralidad/Izquierda	5	2	p=0,08
Lateralidad/Derecha	1	3	p=0,13
Línea media	-	1	p=0,42
Cantidad de FAE/1	2	1	p=0,38
FAE/2	2	2	p=1
FAE/+3	2	3	p=0,47

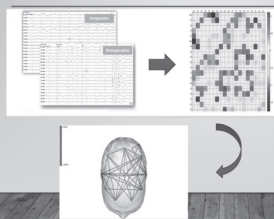
Observaciones:
EFFR, epilepsia focal farmacorresistente; ELT, epilepsia del lóbulo temporal; ExT, epilepsia extratemporal; FAE, fármacos antiepilépticos.

METODOLOGÍA DE REGISTRO Y EVALUACIÓN DE LA CONECTIVIDAD ESTRUCTURAL



- Se realizó en estado de reposo una RMI de 1.5T y DTI de 64 direcciones.
- Con la serie de DTI se estimó una imagen que es el tensor de difusión y a partir de este se obtuvieron diferentes mapas y la función ODF.
- Se realizó un análisis teórico de los datos obtenidos en programación en MatLab 7.0 2014a™.
- Se realizó teoría de grafo para describir las propiedades de las redes.

METODOLOGÍA DE REGISTRO Y EVALUACIÓN DE LA CONECTIVIDAD FUNCIONAL

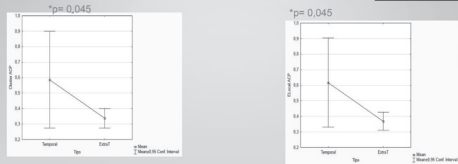


- Se registró en estado funcional de vigilia (duración mínima: 20 minutos).
- Se seleccionaron hasta 15 segmentos, libres de artefactos con ojos cerrados.
- Se realizó un análisis teórico (programación en MatLab 10 2014a™).
- Se obtuvieron las matrices de conectividad funcional por banda de frecuencia para todos los pacientes.
- Se realizó teoría de grafo para describir las propiedades de las redes.

PARA LA CUANTIFICACIÓN TOPOLÓGICA DE LA TEORÍA DE GRAFOS

- Índice de clusterización: Medida del grado en que los nodos de una red tienden a agruparse entre ellos.
- Eficiencia local: Medida basada en el número mínimo de enlaces entre cada nodo y sus vecinos, reflejo de cuán eficiente puede ser la comunicación entre los vecinos inmediatos de cada nodo.
- Longitud del camino corto: Número mínimo de enlaces que habría que recorrer para ir de un nodo al otro.
- Eficiencia global: Es la inversa del promedio del número mínimo de enlaces entre cada nodo y sus vecinos, en toda la red.

PROPIEDADES TOPOLÓGICAS DE LA RED DERIVADAS DE LAS MATRICES DE CONECTIVIDAD ESTRUCTURAL EN PACIENTES CON EFFR DEL LÓBULO TEMPORAL Y EXTRATEMPORAL



En pacientes con ELT se encontró un mayor índice de clusterización y eficiencia local para la ACP en la región del hipocampo comparados con EXT.

SHORT COMMUNICATION

Medial temporal lobe epilepsy is associated with neuronal fibre loss and paradoxical increase in structural connectivity of limbic structures
 Giovanni Striano¹, Enzo Sciacca¹, Luigi Di Marco¹, Josep Diaz², Maria V. Sanchez¹, Jonathan C. Scahill³, Al. Laxari⁴

FULL-LENGTH ORIGINAL RESEARCH

Hippocampal-thalamic wiring in medial temporal lobe epilepsy: Enhanced connectivity per hippocampal voxel
 Maria Striano¹, Giuseppe Striano², Luigi Di Marco¹, Giuseppe Striano¹, Maria V. Sanchez¹, Jonathan C. Scahill³, Al. Laxari⁴

FULL-LENGTH ORIGINAL RESEARCH

Rates and predictors of success and failure in repeat epilepsy surgery: A meta-analysis and systematic review
 Maria D. Kocarevic^{1,2}, Marina V. Cincin¹, Rebecca K. Robinson¹, Marina V. Cincin¹, Maria D. Kocarevic^{1,2}, John D. Williamson^{2,3}, Geoff D. Smith⁴, Jeff D. Williamson¹

PROPIEDADES TOPOLÓGICAS DE LA RED DERIVADAS DE LAS MATRICES DE CONECTIVIDAD FUNCIONAL EN PACIENTES CON EFFR DEL LÓBULO TEMPORAL Y EXTRATEMPORAL.

- No encontramos diferencias significativas en las variables estudiadas para la teoría de grafos, índice de clusterización, eficiencia local, longitud del camino y eficiencia global, a partir de la prueba no paramétrica U Mann–Whitney.

PROS

Functional Connectivity Estimated from Intracarotid EEG Predicts Surgical Outcome in Intractable Temporal Lobe Epilepsy
 Joseph J. Hebl¹, Benjamin V. Hasek², Joseph S. Quilley³, Joseph S. Quilley³, Joseph S. Quilley³, Joseph S. Quilley³, Joseph S. Quilley³, Joseph S. Quilley³, Joseph S. Quilley³

Neuroanatomic coherence of epileptic activity: An MEG study
 Yong-Min Kim¹, Chang-Gi Lee², Hui-Joon Jeong¹, Dong-Gook Kim¹, Dong-Gook Kim¹, Dong-Gook Kim¹, Dong-Gook Kim¹, Dong-Gook Kim¹

RELACIÓN ENTRE LAS PROPIEDADES TOPOLÓGICAS DE LA RED A PARTIR DE LA CONECTIVIDAD ESTRUCTURAL Y FUNCIONAL

Para abordar este objetivo se comprobó las diferencias entre las variables de las propiedades topológicas de la red derivadas de la IRM-DTI y el EEG, mediante un t test, donde todas las variables resultaron diferentes estadísticamente significativas.

Relación entre la conectividad funcional y estructural para la eficiencia local, en pacientes con ELT, por regiones correspondientes a la ZPE. Correlación de Spearman.

Elcc AD	Elcc AD	Elcc AD	Elcc AD	Elcc AD	Elcc AD	Elcc AD	Elcc AD	Elcc AD	Elcc AD
Region 1	Region 2	Region 3	Region 4	Region 5	Region 6	Region 7	Region 8	Region 9	Region 10
0.0007	0.0007	0.0007	0.0007	0.0007	0.0007	0.0007	0.0007	0.0007	0.0007
0.3426	0.3426	0.3426	0.3426	0.3426	0.3426	0.3426	0.3426	0.3426	0.3426
0.0007	0.0007	0.0007	0.0007	0.0007	0.0007	0.0007	0.0007	0.0007	0.0007
0.0007	0.0007	0.0007	0.0007	0.0007	0.0007	0.0007	0.0007	0.0007	0.0007

Relación entre la conectividad funcional y estructural para la longitud del camino corto, en pacientes con ELT. Correlación de Spearman.

Variables	LCC ACCP
LCC Delta	-0.2377 ± 0.2
LCC Theta	-0.600000
LCC Alfa	-0.8557 ± 0.2
LCC Beta	-0.600000

Relación entre la conectividad funcional y estructural para el índice de clusetrización, en pacientes con ELT, por regiones correspondientes a la ZPE. Correlación de Spearman.

Variables	Clustering Coef
Clustering Theta	0.172439
Clustering Alpha	0.000000
Clustering Delta	0.000000

• Se muestra una relación entre la segregación e integración de la red funcional derivada del EEG y la estructural en pacientes con EFR específica para la banda alfa.

SCIENTIFIC REPORTS

OPEN | A small change in neuronal network topology can induce explosive synchronization transition and activity propagation in the entire network



CONCLUSIONES.....

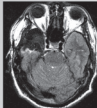
La topología de la red cerebral funcional derivada del EEG en los pacientes con EFR muestra un comportamiento similar independiente de la localización de la ZE, en tanto, los patrones de conectividad estructural son diferentes. Estos resultados pueden atribuirse a las diferencias en el sustrato neuropatológico y/o la lesión epileptogénica en ambos grupos de pacientes.

La metodología utilizada permite aportar evidencias de las diferencias en las medidas de conectividad derivadas por diferentes modalidades (IRM-DTI y EEG). Se muestra una relación entre la segregación e integración de la red funcional derivada del EEG y la estructural en pacientes con EFR específica para la banda alfa.

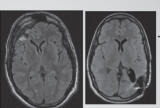
CONCLUSIONES

• Los resultados de este estudio crean las pautas para la cuantificación de la zona potencialmente epileptogénica desde la perspectiva estructura-función, y pueden contribuir a la identificación de biomarcadores cuantitativos para estimar la ZE, y predecir la evolución clínica postquirúrgica.

LAS TÉCNICAS QUIRÚRGICAS VARIAN EN DEPENDENCIA DE LA LOCALIZACIÓN Y LA PATOLOGÍA



Lobectomías temporales



Lobectomías extratemporales

MODALIDADES QUIRÚRGICAS RESECTIVAS
Resecciones focales temporales y extratemporales

Table 3. Postoperative seizure outcomes classified by patient characteristics

Group	Pre-Op (%)	Post-Op (%)	p
All demographics	34 (27.0)	41 (33.0)	0.68
Age	21 (20.0)	24 (20.0)	0.88
Sex	17 (17.0)	17 (17.0)	0.84
Age at seizure onset, yr (mean ± SD)	11.2 ± 3.4	11.2 ± 3.4	0.97
Age at surgery, yr (mean ± SD)	17.1 ± 3.3	17.1 ± 3.3	0.99
Age at seizure onset, yr (mean ± SD)	10.2 ± 2.7	10.2 ± 2.7	0.99
Resection characteristics			
Resection	35 (30)	33 (28)	<0.01
Resection of the epileptogenic zone	44 (38)	44 (38)	<0.01
Age	22 (20)	22 (20)	0.87
Sex	12 (12)	12 (12)	0.87
Age at seizure onset, yr (mean ± SD)	12.0 ± 3.0	12.0 ± 3.0	0.98
Age at surgery, yr (mean ± SD)	17.1 ± 3.3	17.1 ± 3.3	0.98
Resection type			
Resection	22 (20)	22 (20)	0.97
Resection of the epileptogenic zone	44 (38)	44 (38)	<0.01
Age	21 (20)	21 (20)	0.88
Sex	17 (17)	17 (17)	0.84
Age at seizure onset, yr (mean ± SD)	11.2 ± 3.4	11.2 ± 3.4	0.97
Age at surgery, yr (mean ± SD)	17.1 ± 3.3	17.1 ± 3.3	0.99
Resection type			
Resection	22 (20)	22 (20)	0.97
Resection of the epileptogenic zone	44 (38)	44 (38)	<0.01
Age	21 (20)	21 (20)	0.88
Sex	17 (17)	17 (17)	0.84
Age at seizure onset, yr (mean ± SD)	11.2 ± 3.4	11.2 ± 3.4	0.97
Age at surgery, yr (mean ± SD)	17.1 ± 3.3	17.1 ± 3.3	0.99

SD, standard deviation. Fisher's exact test was used for categorical variables. Fisher's exact test was used for categorical variables. Fisher's exact test was used for categorical variables.

La cirugía de epilepsia ha ofrecido una opción para el control de crisis a largo plazo en el 60-80% en epilepsia del lóbulo temporal (ELT) y del 40-60% en epilepsia del lóbulo extratemporal (ELT).

Koufouf MD, Chen AY, Howard SC, et al. Rates and predictors of success and failure in repeat epilepsy surgery: A meta-analysis. *Epilepsia* 2017; 58:217-227.

CIREN
Centro Internacional de Restauración Neurológica

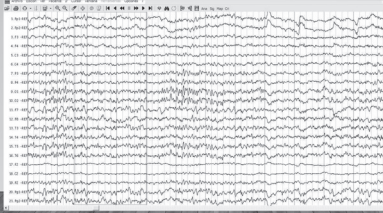
PATRONES DE CONECTIVIDAD DEL EEG EN FUNCION DE LA EVOLUCION CLINICA POSTQUIRURGICA. UN ESTUDIO EN PACIENTES CON EPILEPSIA DEL LOBULO TEMPORAL FARMACORESISTENTE

SUJETOS Y METODOS
DATOS CLINICOS

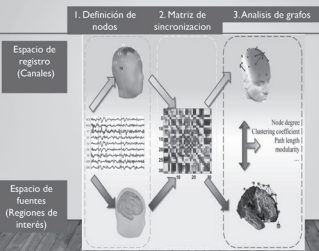
Edad	34.1±7.9 A	m:35
Sexo	F: 15	M: 15
Factores de riesgo	Febril convulsion :25% Encefalitis:20%	
Edad de inicio crisis	12.28±9.3	(8m-29 y) m: 14
No. MAE	2	(1-3)
Tiempo duración crisis	20.2±10.59	(2- 36 A) m: 21
Frecuencia Crisis/m	4-16/m	
Lateralización ZE	17 izquierdos	13 derechos
Evolución Clínica Postquirúrgica	Izquierdos Derechos	Engel I 11 Engel I 6 Engel II-IV 6 Engel II-IV 7

METODOLOGIA

- Se analizó la conectividad funcional calculada a partir de la sincronización entre los electrodos, así como las propiedades de la red derivada de la misma a partir de los datos obtenidos del Electroencefalograma postquirúrgico (2 años), en el estado funcional ojos cerrados.



EN TODOS LOS SEGMENTOS SELECCIONADOS SE CALCULÓ LA MATRIZ DE SINCRONIZACIÓN ESPACIAL (EN INGLÉS SYNCHRONIZATION LIKELIHOOD). SI ENTRE LOS ELECTRODOS SE DETERMINÓ PARA LAS CUATRO BANDAS DE FRECUENCIA. EL ANÁLISIS TEÓRICO DE GRAFOS SE REALIZÓ A PARTIR DE LA MATRIZ DE SINCRONIZACIÓN DE TODAS LAS COMBINACIONES POSIBLES DE ELECTRODOS.



Cuantificación topológica de la teoría de grafos:

- Los parámetros evaluados fueron

Clustering coefficient (local integration): proporción de conexiones entre los vecinos más cercanos relativo al máximo número de conexiones posibles.

Longitud del camino medio: mínimo número de aristas que deben transcurrir de un nodo a otro. Refleja la eficiencia de comunicación en una red.

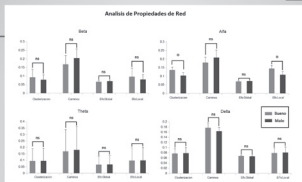
Eficiencia local: refleja cuan conectados están los nodos vecinos (sub-red local)

Eficiencia global: refleja cuan conectado está cualquier par de nodos

Estos parámetros permiten reflejar la cantidad de información neural que puede ser intercambiada y, qué tan optimizadamente pueden realizar estos procesos.



RESULTADOS

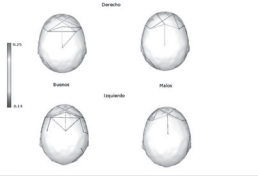


En los pacientes libres de crisis el análisis de las propiedades de la red evidenció para la banda alfa una estructura de red subyacente más organizada con una clustering significativamente mejor y una mejor eficiencia local que la de los pacientes con persistencia de crisis ($t(28) = 2.21$, $p < 0.03$, $FDR q = 0.1$; $t(28) = 2.22$, $p < 0.03$, $FDR q = 0.1$ respectivamente).

RESULTADOS



Conectividad Funcional - Sincronización Banda Alfa



La sincronización espacial dentro de esta banda de frecuencia también mostró un patrón de organización diferente en las regiones anteriores de ambos grupos de pacientes. En el resto de las bandas de frecuencias analizadas no se constataron diferencias en las medidas evaluadas.

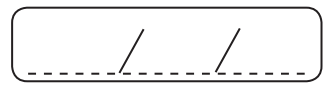
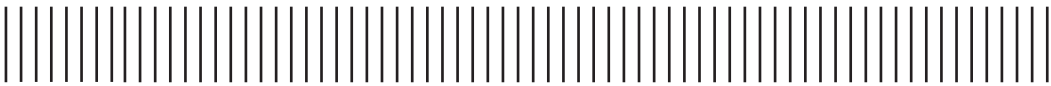
Se constataron diferencias significativas en la organización de la red en función de la evolución clínica postquirúrgica independientemente de la lateralización de la zona epileptogénica.

CONCLUSIONES

- Las características topológicas de las redes neuronales de los pacientes con ELT sometidos a cirugía que se encuentran libres de crisis se reorganizan de forma más eficiente expresada en los cambios de clusterización y de eficiencia local. Estos cambios topológicos garantizarían un mejor balance en la segregación e integración del procesamiento de información dentro de la red neuronal.
- Estos resultados aunque preliminares sugieren que el resultado postquirúrgico en pacientes con ELT se refleja en la organización funcional de la red.

AGRADECIMIENTOS

YADIRA ROMERO MORALES
KARLA BATISTA
SHEILA BERRILLO
PROYECTO CIRUGIA EPILEPSIA CIREN



MATTHIAS KOEPP (ENGLAND)

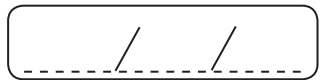
STRUCTURAL AND FUNCTIONAL CONNECTIVITY DURING EPILEPTOGENESIS

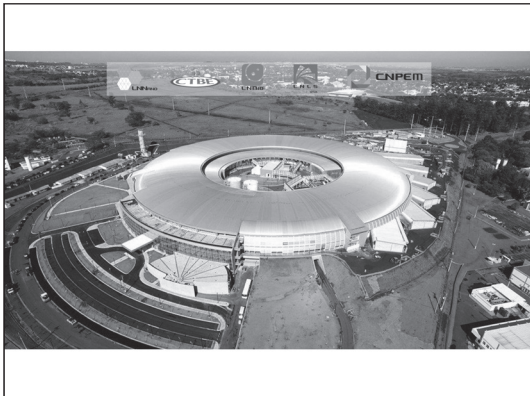


A series of horizontal lines for writing, consisting of 20 parallel lines.

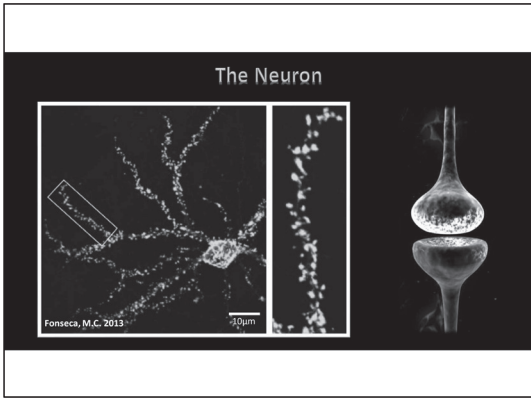
MATHEUS DE CASTRO FONSECA (BRAZIL)

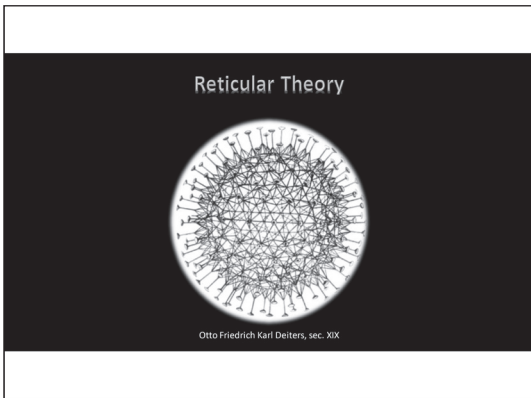
FUTURE TRENDS IN NEURONAL CIRCUITRY IMAGING

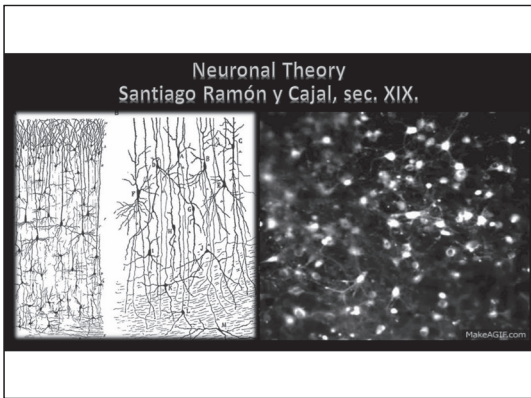


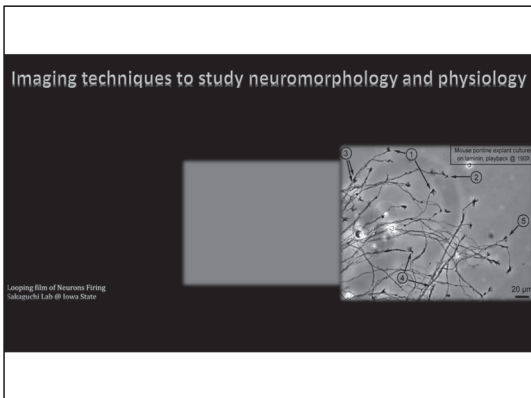










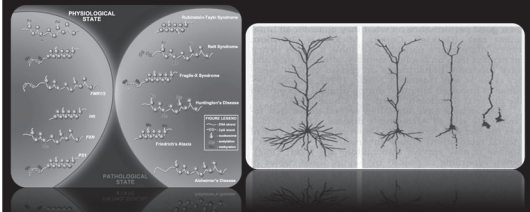


Imaging techniques to study neuromorphology and physiology

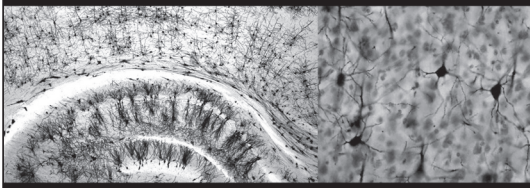


EM data from N. Kasthuri, R. Schalek, K. Hayworth, J.-C. Tapia, and J. Lichtman at Harvard University; reconstruction and rendering by D. Berger and S. Seung at MIT

Morphofunctional alteration of the neuronal cell in neurodegenerative diseases



The Golgi-Cox technique



X-ray microtomography to study the nervous system in a macro and microscopic manner

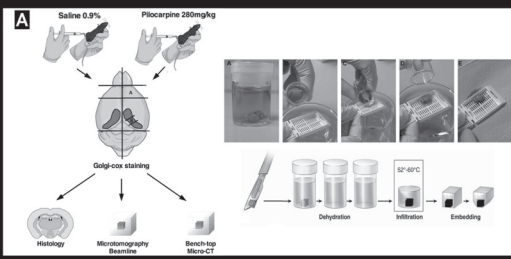


High-resolution synchrotron-based X-ray microtomography as a tool to unveil the three-dimensional neuronal architecture of the brain

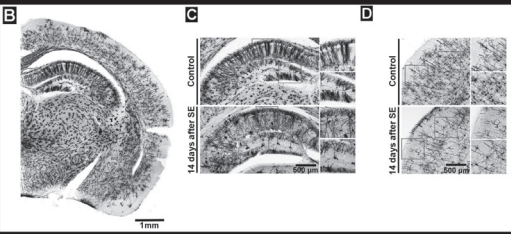
Matheus de Castro Fonseca , Bruno Henrique Silva Araujo, Carlos Sato Baraldi Dias, Nathaly Lopes Archilha, Dionísio Pedro Amorim Neto, Esper Cavalheiro, Harry Westfahl Jr, Antônio José Roque da Silva & Kláber Gomes Franchini

Scientific Reports **8**, Article number: 12074 (2018) | Download Citation &

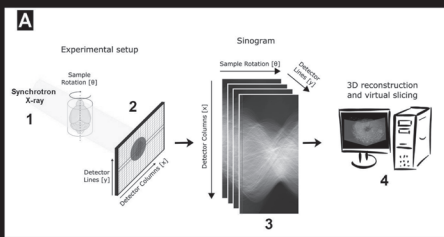
Experimental Setup

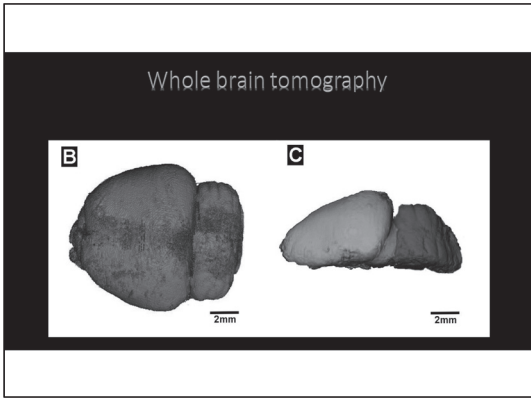


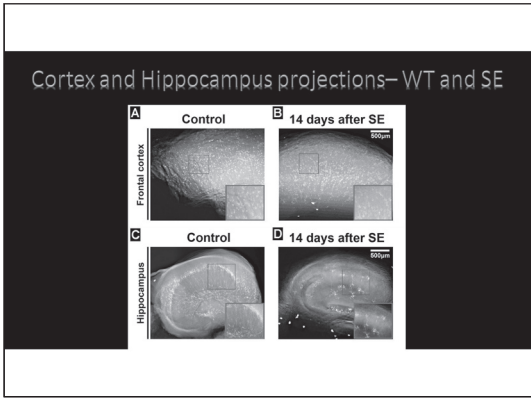
Histological evaluation

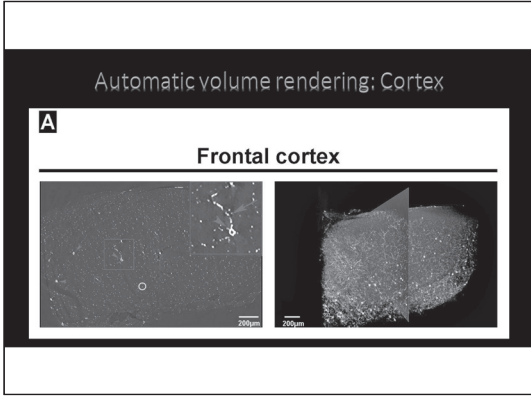


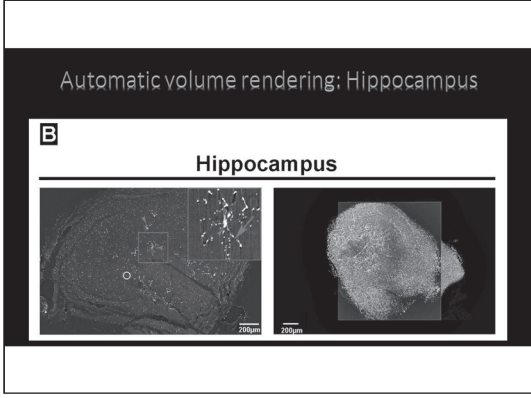
Experimental setup at the IMX beamline - UVX

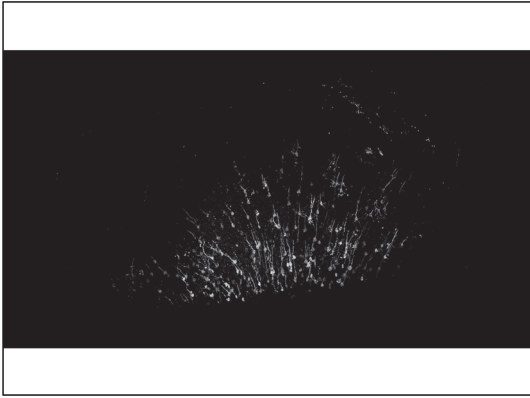


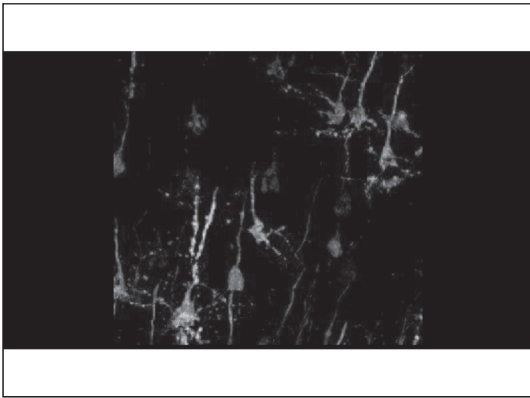


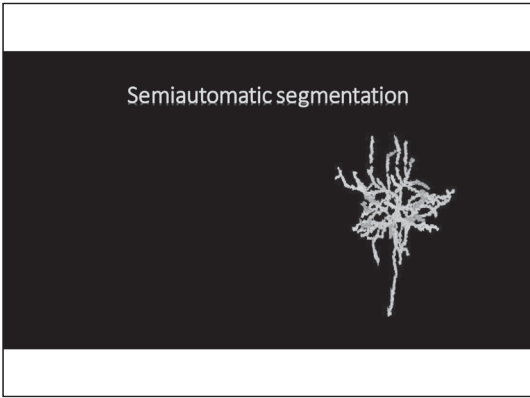


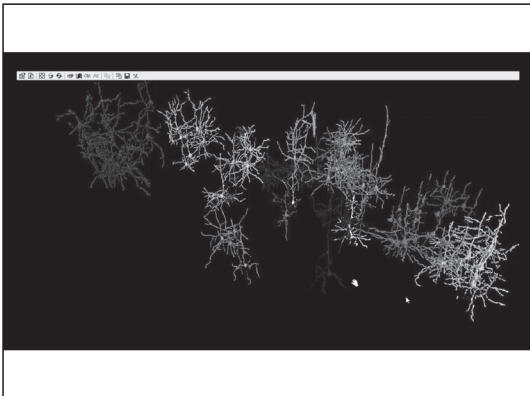


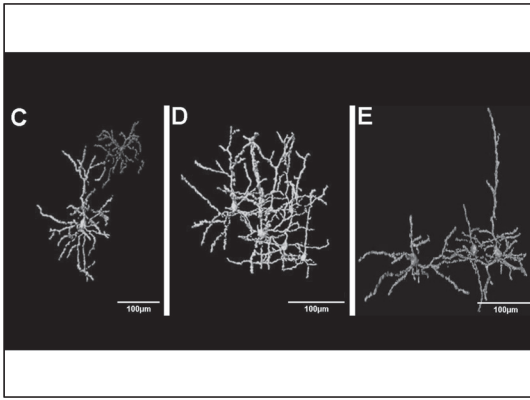


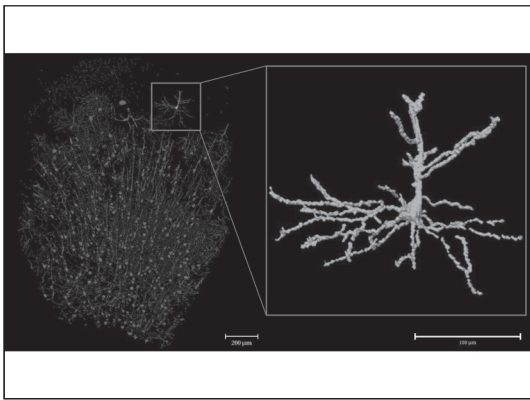


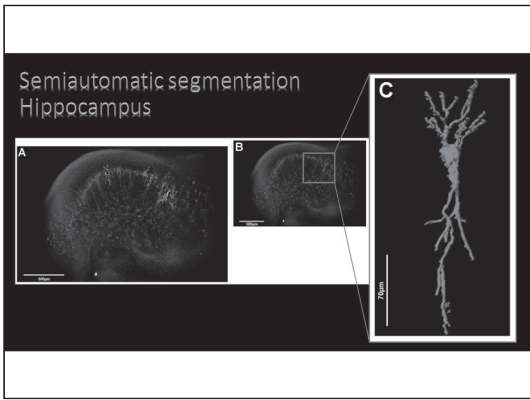


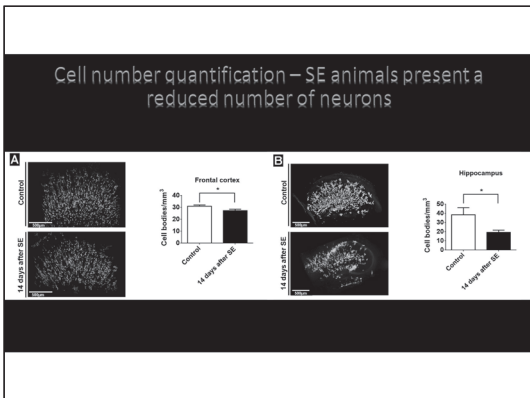




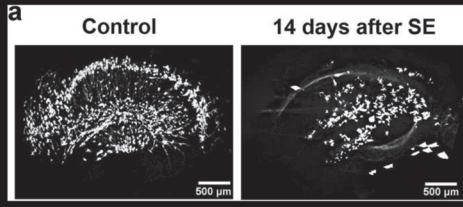




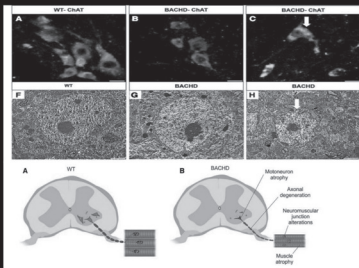


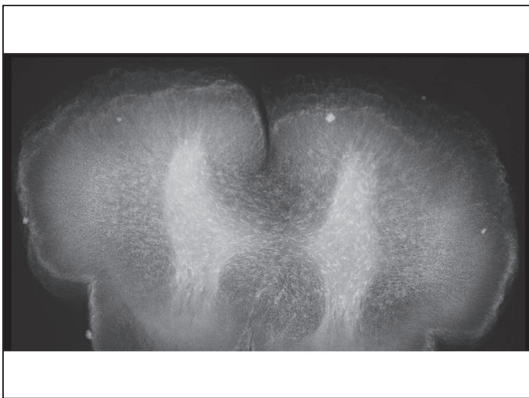


Microtomography at a bench-top μ CT



BACHD mouse model of Huntington's disease

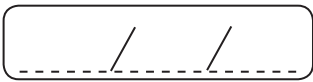




Take-home message

Synchrotron based X-ray microtomography is a powerful tool to study the nervous system at a macro and microscopic level
In health and disease.





GUILCA CONTRERAS (VENEZUELA)

NEUROSTIMULATION IN THE TREATMENT OF DRUG-RESISTANT EPILEPSY



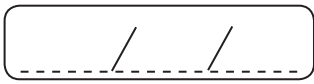
A series of horizontal lines for writing, spaced evenly down the page.



GROUPS 1, 3, 5, 7



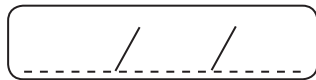
A series of horizontal lines for writing, starting with a solid line, followed by a dashed line, and then several more solid lines.



GROUPS 2, 4, 6, 8




Lined writing area with multiple horizontal lines for text entry.



O amplo espectro das
Epilepsias “Metabólicas” da Infância

Dra Maria Luiza Manreza –
Neurologista Pediátrica



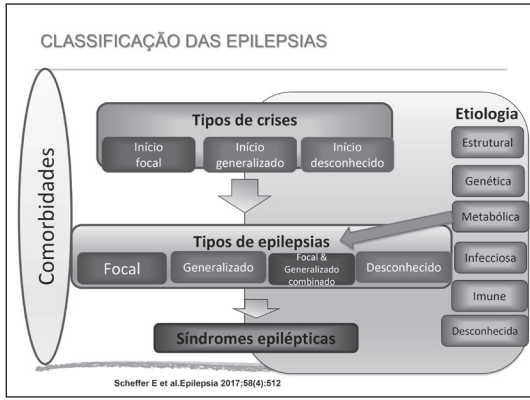
BIOMARIN

Conflito de Interesses

Pesquisadora Aché, UCB
Palestrante: BioMarin e UCB
Consultora: BioMarin e UCB

Agenda

- ✓ **Encefalopatias epilépticas de etiologia metabólica**
 1. Definição
 2. Quando pensar em doença metabólica
 3. Principais encefalopatias epilépticas metabólicas
- ✓ **Lipofuscinoses Ceroide Neuronal (LCN)**
 1. Definição e Histórico
 2. Incidência e Prevalência
- ✓ **Lipofuscinoses Ceroide Neuronal Tipo 2 (CLN2)**
 3. Fisiopatologia
 4. Diagnóstico Clínico
 5. Exames complementares
 6. Tratamento da CLN2.
- ✓ **Considerações Finais**



EPILEPSIA METABÓLICA

- ✓ Erros Inatos do Metabolismo (EIM) são uma causa rara de epilepsia, mas crises epilépticas e epilepsia são frequentemente encontradas em pacientes com EIM.
- ✓ EPILEPSIA METABÓLICA
 - idade precoce de apresentação
 - atraso / regressão do desenvolvimento
 - resistência à terapia com FAE convencionais
 - positividade em testes genéticos -> 7%
 - condições tratáveis > 4%

Mercimek-Mahmutoglu S et al. *Epilepsia*. 2015; 56 : 707-716

ERROS INATOS DO METABOLISMO E EPILEPSIA FISIOPATOLOGIA

- ✓ Interferem em funções do metabolismo cerebral
- ✓ Levam ao acúmulo de compostos que causam neurotoxicidade
- ✓ Determinam distúrbios primários ou secundários nas vias dos neurotransmissores.
- ✓ Associação à malformação do desenvolvimento cortical
- ✓ Outros mecanismos como alteração na permeabilidade da membrana neuronal, deficiência de substrato, etc

Campistol J et Plecko B. *Epileptic Disorder*. 2015; 17 : 229-242.

CLASSIFICAÇÃO NEONATAL E PRIMEIRA INFÂNCIA

- ✓ INDÍCIOS DA PRESENÇA DE EIM NO PERÍODO NEONATAL
 - Consanguinidade parental
 - História familiar de morte neonatal e/ou doenças neurológicas
 - Gravidez - síndrome HELLP* , movimentos fetais excessivos (convulsões intra-uterinas)
 - Deterioração após um período de aparente normalidade
 - Encefalopatia Rapidamente Progressiva
 - Acidose metabólica severa
 - Soluços
 - Odores incomuns de urina

*hemólise, elevação das enzimas hepáticas e plaquetas

Sharma S et Prasad AN. *Int J Mol Sci*. 2017 Jul 2;18(7)

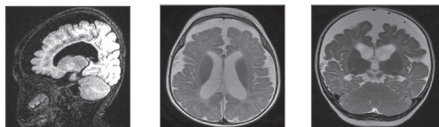
CLASSIFICAÇÃO NEONATAL E PRIMEIRA INFÂNCIA

- Epilepsia Dependente de Piridoxina
- Deficiência de piridox (am) ine 5'-fosfato oxidase (PNPO)
- Convulsões responsivas ao ácido folínico
- Deficiência de biotinidase e holocarboxilase sintetase
- Defeito do Transportador de Glicose (Síndrome de Deficiência de GLUT1)
- Transtornos da Biossíntese Serina
- Cofactor de Molibdênio e Deficiência Isolada de Sulfito Oxidase
- Doença de Menkes
- Hiperiglicemia não-cetótica
- Encefalopatia Epiléptica Responsiva à Uridina (CAD)
- Defeitos do Ciclo da Ureia, Acidemias Orgânicas e Aminoacidopatias
- Transtornos Congênitos da Glicosilação
- Transtornos Peroxissômicos
- Transtornos Congênitos da Autofagia
- Lipofuscinoses Ceróide Neuronal

Sharma S et Prasad AN. Int J Mol Sci. 2017 Jul 2;18(7).

CASO CLÍNICO 1

- ✓ Criança do sexo feminino, 11 meses de idade
- ✓ Sem relato de consanguinidade, mas **história familiar de irmã com quadro similar**, que foi a óbito aos 2 anos de idade por provável SUDEP
- ✓ Referia crises epilépticas desde o 1º dia de vida, "tremores generalizados" inicialmente controladas com fenobarbital, mas que evoluíram com diversas semiologias inclusive espasmos epilépticos, descompensações graves, EME, fármaco-resistência e regressão do DNPM
- EEG: multifocal, status, surto supressão



CASO CLÍNICO 1

- ✓ EXOMA

Exame: Sequenciamento do exoma

Resultado

Diagnóstico: Epilepsia Piridoxina-dependente (OMIM # 266100)

Gene	Posição	Variação	Consequência	Cópias
ALDH7A1	chr5:525.894.936	C > T	p.Arg335Gln ENST00000409134	Homozigose (2 cópias)

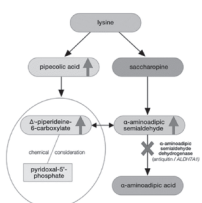
Definitivamente patogênico

Método

Captura de exons com Agilent SureSelect Clinical Research Exome V2 seguida por sequenciamento de nova geração com Illumina HiSeq. Alinhamento e identificação de variantes utilizando protocolos de bioinformática, tendo como referência a versão GRCh37 do genoma humano. Análise médica orientada pelas informações que motivaram a realização deste exame.

Epilepsia Dependente de Piridoxina

METABOLISMO DA LISINA



Mutação do gene *ALDH7A1*

- ✓ Deficiência de semi-desidrogenase α -aminoadípica (**antiquitina**), resulta no acúmulo de :

1. semialdeído α -aminoadípico (AASA)
2. Δ -1-piperidina-6-carboxilato (P6C)
3. ácido pipercolíco

Van Karnebeek CD et Jaggamantri S. Curr Treat Options Neurol 2015;17:335.

Epilepsia Dependente de Piridoxina

- ✓ Doença autossômica recessiva rara: prevalência de 1: 20.000 a 1: 600.000
- ✓ Caracterizada por convulsões recorrentes nos períodos pré-natal, neonatal e/ou pós-natal resistentes aos fármacos antiepilépticos (FAE) convencionais, mas responsiva às dosagens farmacológicas da piridoxina
- ✓ Formas típicas: as crises iniciam-se horas ou dias após ou mesmo intra-útero
- ✓ Formas atípicas:
 - início tardio
 - crianças cujas convulsões respondem inicialmente aos FAEs, mas ocorrem semanas a meses mais tarde de forma refratárias
 - pacientes cujas convulsões não são controladas por grandes doses iniciais de piridoxina, mas que respondem mais tarde a um segundo tratamento

Van Karnebeek CD et Jaggamantri S. Curr Treat Options Neurol 2015;17:335.

Epilepsia Dependente de Piridoxina Características

- ✓ **Sintomas gerais** iniciais: vômitos, distensão abdominal, insônia, irritabilidade, contratura facial paroxística e movimentos oculares anormais.
- ✓ **Epilepsia** é bastante variável e dependente da resposta a piridoxina ocorrem crises: focais motoras recorrentes, tônicas generalizadas, mioclonicas, espasmos infantis, convulsões e estado epiléptico recorrente
- ✓ **EEG** é inespecífica e pode permanecer anormal mesmo com a terapia com piridoxina
- ✓ **Retardo do desenvolvimento neuropsicomotor** varia de leve a grave. A incapacidade intelectual comumente afeta a linguagem expressiva, juntamente com um QI de desempenho / motor abaixo do normal
- ✓ **Ressonância magnética**, padrões variáveis, desde lesões da substância branca, atrofia cerebral geral, hipoplasia ou displasia do corpo caloso até um cérebro estruturalmente normal

Van Karnebeek CD et Jaggamantri S. Curr Treat Options Neurol 2015;17:335.

Epilepsia Dependente de Piridoxina Tratamento

- ✓ **DOSE INICIAL:** 100 mg EV
 - Sem resposta: doses adicionais 100 mg
 - Até total de 500 mg
 - Na dúvida sobre uma resposta parcial: manter 15-30 mg/kg/dia por 7 dias
- ✓ **MANUTENÇÃO**
 - Suplementação diária de piridoxina por toda a vida: 5 a 15 mg/kg/dia
 - Em geral, 50-100 mg/dia
 - Máx: 200 mg em crianças e 500 mg em adultos
 - Uso excessivo de piridoxina neuropatia sensorial reversível, apneia e hipotonia
- ✓ **Tratamento pré-natal** – dose de 100 mg de piridoxina /dia parece ser segura
- ✓ Ácido fólico falta de resposta à piridoxina (3-5mg/kg/d a 10-30mg/d)
- ✓ **Dieta com restrição de lisina**- difícil, poucos estudos

Van Karnebeek CD et Jaggamantri S. Curr Treat Options Neurol 2015;17:335.

Epilepsia Dependente de Piridoxina Fenótipo - Evolução

- ✓ Os fenótipos clínicos de epilepsia dependente de piridoxina podem ser classificados em três grupos:
 - Grupo 1 consiste em pacientes com controle completo das crises, com piridoxina e desenvolvimento normal
 - **O grupo 2 consiste em pacientes com controle completo das crises com piridoxina, mas com atraso no desenvolvimento**
 - Grupo 3 consiste em pacientes com convulsões persistentes e atraso no desenvolvimento, apesar da piridoxina.
- ✓ Apesar de extensos estudos, as correlações entre o genótipo e essas categorias fenotípicas ainda não foram estabelecidas

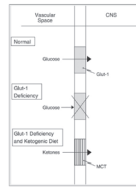
Van Karnebeek CD et Jaggamantri S. Curr Treat Options Neurol 2015;17:335.

CASO CLÍNICO 2

- Criança do sexo masculino com 8 meses de idade
- Filha de pais não consanguíneos, sem antecedentes pré e perinatais importantes.
- Aos 4 meses a mãe observou que não interagía com o meio. Nesta mesma ocasião percebeu movimentos rotatórios dos olhos e crises epilépticas caracterizadas desvio dos olhos e da cabeça para a esquerda, nistagmo e postura tônica dos MMSS, com duração de 5-10s, cerca de 20x ao dia. Utilizou fenobarbital clonazepam sem controle das crises.
- Exames
- **Glicemia – 98 mg/dL**
- **LCR – glicose 38 mg/dl**
- **Relação glicose LCR/glicose sangue: 0,38 (N=1,1-0,4 ou 0,6)**
- Exame genético confirmou o diagnóstico

Síndrome de Deficiência de GLUT1 Defeito do Transportador de Glicose (Síndrome de De Vivo)

- ✓ O cérebro é dependente de glicose existindo nove transportadores para vencer a barreira hemato-encefálica incluindo o GLUT1
- ✓ O gene *SLC2A1* (1p35-31.3) codifica o GLUT 1
- ✓ A deficiência de Glut-1 é geralmente autossômica dominante mas têm sido descritos casos de herança autossômica recessiva

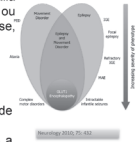


Adaptado de: Kass et al. Epilepsia 2016;57:1631-1633

Kass HR, et al. Seizure 2016 Feb;35:83

Síndrome de Deficiência de GLUT1 Defeito do Transportador de Glicose

- ✓ **Síndrome de deficiência de GLUT1**
- Crises refratárias de início precoce, RDNPM, microcefalia adquirida, anormalidades do tônus muscular (hipotonia ou espasticidade) e distúrbios do movimento, como coreoatetose, ataxia e distonia
- ✓ **O espectro clínico da deficiência de GLUT1 é mais amplo:**
- RDNPM, epilepsia e formas familiares e esporádicas de discinesia induzida por exercício paroxístico
- Diferentes graus de comprometimento cognitivo associados a disartria, disfluência e déficits de linguagem expressiva são características adicionais



Kass HR, et al. Seizure. 2016 Feb;35:83

Paroxysmal eye-head movements in Glut1 deficiency syndrome.



Estudo retrospectivo do primeiro evento neurológico (Columbia University n = 133)

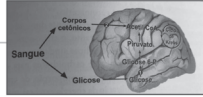
- ✓ Crise epiléptica – 61%
- ✓ Movimentos oculares anormais – 38%
- "rolar os olhos", "tremor dos olhos", "opsochonus"
- 85% apresentaram os primeiros movimentos oculares em torno de 6 meses



- Os movimentos oculares são sacádicos e geralmente conjugados
- cada três desvios de olhar, é seguido por um movimento da cabeça na mesma direção.
- Existem períodos de fixação entre as sacadas

Neurology, 2017 Apr 25;88(17):1666-1673

Síndrome de Deficiência de GLUT1



TRATAMENTO

- ✓ Dieta cetogênica
 - Rica em gorduras, adequada em proteínas e pobre em carboidratos
 - Determina cetose, mimetizando o jejum
 - Dieta cetogênica clássica: 4gr de gordura, 1gr de carboidrato e proteína
- ✓ FISIOPATOLOGIA: fonte alternativa de energia para o cérebro
 - Boa adesão
 - Controle eficiente de crises
 - Melhor do alerta e da atividade
 - Em alguns casos pode ser necessário manter os FAE
- ✓ Criança citada iniciou tratamento com dieta cetogênica
 - **Evoluiu com controle das crises epiléticas e melhora do desenvolvimento.**
 - Iniciado redução PB.

Kara HR, et al. Seizure. 2016 Feb;35:83
Sampaio LPB. Tratamento medicamentoso das epilepsias /ed Yacubian/Contreras-Calcado/ Rios-Pohl , 2014 pg207

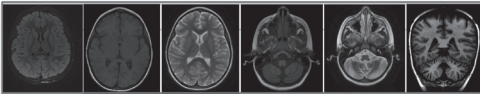
CASO CLÍNICO 3



Caso Clínico

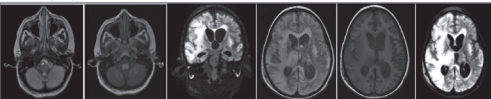
- ✓ Criança do sexo feminino, 8 anos, sem antecedentes perinatais
DNPM: adequado, exceto por discreto atraso da linguagem
- ✓ Aos 13 meses de idade com história de **anemia** iniciou crises epiléticas focais motoras disperceptivas frequentes e refratárias a vários esquemas terapêuticos. Seguiu-se involução do DNPM, aparecimento de crises generalizadas sendo internada em mais de uma ocasião em estado de mal epilético. Persistiu piorando necessitando de traqueostomia.
- ✓ LCR - **aumento de lactato**
- ✓ EEG - desorganização difusa da atividade elétrica cerebral, por maior teor de ondas lentas teta; paroxismos de espículas e ondas agudas, de projeção centroparietal bilateral, com difusão para as regiões anteriores
- ✓ HD- MELAS? Lipofuscinose ceróide neuronal?

RNM 30/05/2014



- Proeminências dos espaços líquidos ao redor do cerebelo, sugerindo redução volumétrica
- Espectroscopia com redução da relação NAA/Cr na substância branca e cinzenta parieto-occipital podendo representar perda e/ou disfunção neuroaxonal

RNM 27/11/2014



- Redução volumétrica encefálica, múltiplas lesões cortico-subcortical nos hemisférios cerebrais e cerebelares, na substância branca periventricular, região nucleocapsular e tálamos.
- Espectroscopia com aumento do lactato
- Lesões compatíveis com insulatos isquêmicos em diferentes territórios e fases evolutivas, podendo-se considerar a possibilidade de hipóxia secundária ao referido ou mitocondriopatia.

Encefalopatia Epilética Responsiva à Uridina (CAD)



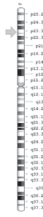
- ✓ Distúrbio por mutações do CAD*
- CAD codifica uma enzima multifuncional (CPSase / ATCase / DHOase) envolvida na biossíntese de novo de pirimidina.
- As pirimidinas também podem ser recicladas a partir da uridina.
- ✓ Características clínicas
 - Atraso / regressão do desenvolvimento neuropsicomotor
 - Encefalopatia epilética grave
 - Aos 4 anos de idade – restritos ao leito, rebaixamento do nível de consciência
 - **Anemia**
- ✓ Literatura refere quatro crianças com RDNPM, encefalopatia epilética e anemia
 - Duas faleceram pós um curso de 4-5 anos de doença neurodegenerativa
 - Duas receberam suplementação com uridina oral: cessação imediata das crises melhora dramática cognitiva e motora e resolução da anemia.

*CAD protein (carbamoyl-phosphate synthetase 2, aspartate transcarbamylase, and dihydroorotase)

Koch J et al. Brain. 2017 Feb;140(2):279

Encefalopatia Epiléptica Responsiva à Uridina (CAD)

- ✓ EXOMA- Duas variantes em heterozigose no gene CAD
 - Chr 2:27.445.462 C>T -> Substituição da arginina na posição 191 por um códon de parada. Definidamente patogênica
 - Chr 2:27.462.599 G>A -> Substituição da arginina na posição 1810 por glutamina. Provavelmente patogênica
- ✓ Tratamento via oral com uridina controle da anemia e melhora da epilepsia



CASO CLÍNICO 4

- ✓ AF- Pais consanguíneos. Irmã com quadro semelhante diagnosticada quando o paciente já tinha a doença
- ✓ DNPM – normal até 4 anos de idade exceto discreto atraso de linguagem
- ✓ Aos 4 anos iniciou com ataxia e mioclonias resistentes aos tratamentos evoluindo com piora progressiva dos sintomas e involução do DNPM deixando progressivamente de sentar, andar e falar. Ficou restrito ao leito persistindo as mioclonias. Evoluiu para óbito aos 8,5 anos de idade



Youtube - CLN2 Batten Disease progression - Noah's Hope



Frederick Batten
1903

Lipofuscinose Ceróide Neuronal DOENÇA DE BATTEN

Frequência

- ✓ Uma das doenças neurodegenerativas herdadas mais comuns da infância
- ✓ Prevalência e incidência dependem de ascendência e região geográfica:
 - Prevalência (/população) → 1:1.000.000 em algumas regiões a 1:100.000 nos países escandinavos;
 - Incidência (/nascidos vivos) → 1:67.000 (Itália e Alemanha) a 1:14.000 (Islândia).
- ✓ 13 genes descritos e mais de 500 mutações listadas
- ✓ 14 formas da doenças
- ✓ As mais prevalentes são: CLN3 - fenótipo juvenil clássico, seguido por CLN2 - fenótipo infantil tardio.

Schulz A, et al. Biochim Biophys Acta. 2013;1832:1801-1806; Haltia M et Goebel HH. Biochim Biophys Acta. 2013; 1832: 1795; Williams RE. NCL incidence and prevalence data. In: The Neuronal Ceroid Lipofuscinoses (Batten Disease), 2nd edition; Moir SE, Williams RE, Goebel HH (Eds). Oxford: Oxford University Press; 2011. pp. 361-365; Simonati et al., Current Molecular Medicine 2014, 14, 1042-1051

Classificação e características das LCNs

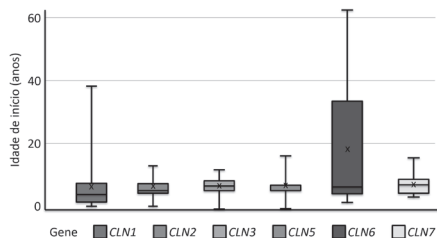
Doença*	Manifestação e fenótipo clínico	Gene	Proteína
CLN1	Clássica infantil, infantil tardia, juvenil, adulto	CLN1 (PTF1)	Proteína polifenol fosforase
CLN2	Fenótipo clássico infantil tardia; fenótipos atípicos: infantil, juvenil, prolongado; SCAR2 T	CLN2 (TPP1)	Triptofano pirimidase 1
CLN3	Clássica juvenil	CLN3	Proteína transmembrana
CLN4	Adulto (autossômico dominante)	CLN4 (DNAJC5)	Proteína do núcleo de citosina adenosil
CLN5	Variante infantil tardia, juvenil, adulto	CLN5	Proteína salivável lisossomal
CLN6	Variante infantil tardia, adulto (Kufs tipo A)	CLN6	Proteína transmembrana
CLN7	Variante infantil tardia	CLN7 (MFSD8)	Proteína transmembrana
CLN8	Variante juvenil tardia	CLN8	Proteína transmembrana
CLN9	Variante juvenil	—	—
CLN10	Clássica congênita, infantil tardia, juvenil, adulto	CLN10 (CTSD)	Catepsina D
CLN11	Adulto	CLN11 (C9orf72)	Progranulina
CLN12	Juvenil	CLN12 (PPI3A2)	ATPase
CLN13	Adulto (Kufs tipo B)	CLN13 (CTSF)	Catepsina F
CLN14	Infantil	CLN14 (PCTD1)	Proteína do canal de potássio

* Doenças LCN conhecidas. Os genes de LCN adicionais ainda devem ser identificados.

Schulz A, et al. *Biochimica et Biophysica Acta*. 2013;1832:1801-1806. OMM database. TPP1: <http://www.omim.org/entry/607998>. Accessed July 14, 2016. OMM database. Kufor-Rakeb Syndrome: <http://www.omim.org/entry/606693>. Accessed July 14, 2016. OMM database. CTSD: <http://www.omim.org/entry/611726>. Accessed July 14, 2016.

Classificação e características das LCNs

Idade de início em pacientes com LCNs por genótipo (não foram descritos os genótipos com <5 indivíduos)



Adaptado de: G. Aungaroon et al. / *Pediatric Neurology* 60 (2016) 42x48

Lipofuscinaose Ceroide Neuronal TIPO 2 CLN2

Doença	Epônimo	Nº OMIM	Fenótipo	Nome abreviado
CLN2	Jámsky-Bielschowsky	204500	Infantil tardia clássica Juvenil	LINCL

Cromossoma	Gene	Produto do Gene	Proteína Acumulada
11p15	TPP1/CLN2	TPP1	SCMAS

Lipofuscinaose Ceroide Neuronal Tipo 2 (CLN2)

- ✓ Um subtipo da doença de Batten
- ✓ Herança autossômica recessiva (gene *CLN2*)
- ✓ É uma das doenças de depósito lisossômico
- ✓ Incidência estimada: 0,22 a 9/100.000 nascidos vivos dependendo da região geográfica
- ✓ A neurodegeneração é o resultado da deficiência ou ausência da atividade da enzima TPP1
- ✓ A ausência ou atividade reduzida da enzima TPP1 é associada ao acúmulo de lipopigmento autofluorescente lisossômico (lipofuscina ceroide)
- Com o tempo, ocorre disfunção e morte celular, atrofia neuronal e da retina.



Doença do cor de imagem licenciada à Batten.

Chang M, et al. *CLN2*. In: Mole S, Williams R, and Goebel H, eds. *The neuronal ceroid lipofuscinoses (Batten Disease)*. 2nd ed. Oxford, United Kingdom: Oxford University Press; 2011:80-109. Hattis M. *Biochim Biophys Acta*. 2006;1742:850-856. Anderson GW, et al. *Biochim Biophys Acta*. 2015;1852:1807-1826.

FISIOPATOLOGIA ATIVIDADE ENZIMÁTICA

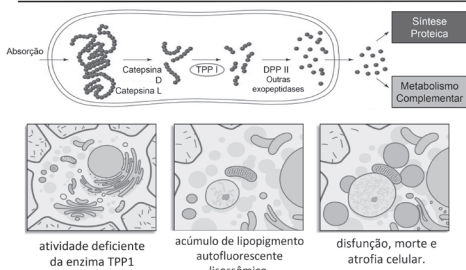
✓ CLN-> 4 enzimas lisossomais foram identificadas como deficientes em leucócitos, fibroblastos e vilo corial:

- Palmitoil-proteína tioesterase 1 (PPT 1) codificada por *PPT1 (CLN1)*
- **Tripeptidil-peptidase 1 (TPP-1) codificado por *TPP1 (CLN2)***
- Catepsina D (CTSD) codificado por *CTSD (CLN10)*
- Catepsina F (CTSF) codificado por *CTSF (CLN13)*

Neverman NJ et al. *Biochim Biophys Acta* 2015; 6:S925

Envolvimento da Tripeptidil-peptidases na degradação proteica

Degradação de proteína lisossomal



Adaptado de Tomkinson B, Tripeptidyl Peptidases: Enzymes That Count, *TIBS* 24 - SEPTEMBER 1999, p355-356, PI: 0960-0040/99/241425-6

Lipofuscina

- ✓ Lipopigmento autofluorescente de origem glicoproteica
- ✓ Pigmento fino, castanho-dourado, que resulta da digestão incompleta dos glóbulos sanguíneos danificados (resíduos celulares)
- ✓ Este pigmento serve para detectar o tempo de vida celular. Ele está presente em células que não se multiplicam muito e têm vida longa, como as musculares do miocárdio e os neurónios
- ✓ Normalmente, quanto mais lipofuscina presente, mais velha é a célula
- ✓ Ceroide – que tem aspecto de cera

Brunk UT1, Terman A, *Free Radic Biol Med.* 2002 Sep 1;33(5):611-9.

Lipofuscina Ceroide Neuronal Tipo 2 (CLN2) Diagnóstico Clínico

A doença CLN2 é uma patologia de progressão rápida que apresenta um conjunto de sintomas

- ✓ **Atraso de linguagem** recentemente identificado como um sinal inicial da doença CLN2, na maioria dos pacientes.
- ✓ **Crises epiléticas** de início entre as idades de 2 e 4 anos no fenótipo clássico
- ✓ **Perda completa das habilidades cognitivas, função motora e visão:**
 - A perda da visão ocorre com o avanço da doença.

Exemplo de progressão da doença CLN2



18 meses 3 anos de idade 5 anos de idade 7 anos de idade 10 anos de idade

Nickel M, et al. Poster session presented at: The 12th Annual WORLD Symposium; February-March 2016; San Diego, CA; Andell E, et al. *Epilepsia*. 2015;156:180-181; Worgall S, et al. *Hum Gene Ther*. 2006;19:663-674; Chang M, et al. CLN2. In: Mole SE, Williams R, and Goebel H, eds. *The neuronal ceroid lipofuscinoses (Batten Disease)*. 2nd ed. Oxford, United Kingdom: Oxford University Press; 2011:80-109.

Exemplo de uso do programa apresentado à ESCAN 2016

CLN2- DIAGNÓSTICO

Atraso Precoce de Linguagem

- ✓ 83% das crianças com a doença CLN2 apresentam atraso precoce de linguagem:
 - Menos de 25% das crianças entre 2 a 4 anos de idade que procuram cuidados médicos com crises epiléticas não provocadas de início recente também apresentam atraso da linguagem;
 - Em alguns casos, também pode ocorrer ataxia ou outras alterações do desenvolvimento, ou esses podem ser os primeiros sinais da doença CLN2.

Critérios para identificar atraso precoce de linguagem:

Primeiras palavras isoladas aos 18 meses (ou mais tarde/nunca)

Primeiras frases de duas palavras aos 24 meses (ou mais tarde/nunca)

Primeiras frases completas aos 36 meses (ou mais tarde/nunca)

Nickel M, et al. Poster session presented at: The 12th Annual WORLD Symposium; February-March 2016; San Diego, CA; Andell E, et al. *Epilepsia*. 2015;156:180-181; Worgall S, et al. *Hum Gene Ther*. 2006;19:663-674; Chang M, et al. CLN2. In: Mole SE, Williams R, and Goebel H, eds. *The neuronal ceroid lipofuscinoses (Batten Disease)*. 2nd ed. Oxford, United Kingdom: Oxford University Press; 2011:80-109.

CLN2 - DIAGNÓSTICO

Crises Epiléticas Não Provocadas De Início Precoce

- ✓ Na maioria das crianças com a doença CLN2, crises epiléticas não provocadas surgem entre os 2 e 4 anos de idade;
- ✓ Embora as crises epiléticas sejam frequentemente não provocadas, podem ocorrer crises febris;
- ✓ Mioclonias - tanto epiléticas quanto não epiléticas - são predominantes;
- ✓ Crises tônico-clônicas generalizadas, de ausência, clônicas, tônicas e atônicas também podem ocorrer;
- ✓ As crises epiléticas persistem durante o curso da doença e são refratárias ao tratamento.

Schulz A, et al. *Biochim Biophys Acta*. 2013;1832:1801-1806; Schulz A, et al. Poster session presented at: The Society for the Study of Inborn Errors of Metabolism (SSIEM) Annual Symposium, September 2015; Lyon, France.

CLN2- DIAGNÓSTICO

Características Da Involução Psicomotora

- ✓ A involução pode ser descrita em fases:
 - 1ª fase → perda das sentenças, geralmente aos 3 anos de idade;
 - 2ª fase → perda da capacidade de andar e da comunicação verbal;
 - 3ª fase → perda da capacidade de sentar, do uso das mãos, do controle esfinteriano. Ao redor de 5 anos de idade tornam-se cadeirantes e, em meses, disfágicos.

Pérez-Poyato MS et al. *J Child Neurol* 2013;28(4):470

CLN2- DIAGNÓSTICO

Outros Sintomas Neurológicos

- ✓ Ataxia;
- ✓ Espasticidade;
- ✓ Movimentos involuntários:
 - Mioclonias (epilépticas e não epilépticas) são uma das características da CLN2;
 - Distonia e espasticidade também são achados comuns; coreia, atetose e tremores também podem ser vistos. *Status distonicus* e *status mioclônico* podem ser complicações com risco de vida;
 - Parkinsonismo, ataxia e coreia proeminentes têm sido relatados em fenótipos atípicos.

Chang M, et al. CLN2. In: Mole S, Williams R, and Goebel H, eds. The neuronal ceroid lipofuscinoses (Batten Disease). 2nd ed. Oxford, United Kingdom: Oxford University Press; 2011:80-109. Perez-Poyato MS, et al. *J Child Neurol* 2012;28:470-478; Steinfield R, et al. *Am J Med Genet* 2002;112:347-354; Schulz A, et al. *Biochim Biophys Acta* 2013;1832:1893-1895; Worgall S, et al. *Hum Gene Ther* 2009;19:463-474.

CLN2- DIAGNÓSTICO

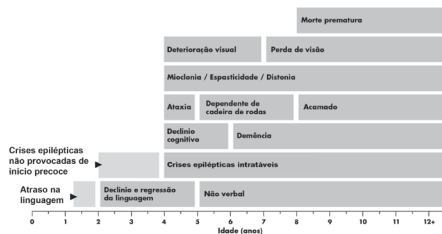
Diagnóstico visual

- ✓ Perda de visão na CLN2 ocorre secundária a degeneração progressiva da retina de fisiopatologia incerta;
- ✓ As manifestações oftalmológicas da CLN2 estão intimamente relacionadas com o grau de função neurológica e a idade do paciente, sendo úteis na avaliação de novas estratégias terapêuticas;
- ✓ **Avaliação:**
 - **Potencial visual evocado:** aumento da latência. Intensificado cedo na doença, mas reduzido no estágio final da doença;
 - **Tomografia de coerência óptica:** Avalia a progressão através de degeneração da retina (ex.: acúmulo de material hiperrefletivo, afinamento da retina com perda de fotorreceptores, aspecto de olho de boi);
 - **Eletroretinograma:** Pode ser reduzido antes da deterioração visual ser clinicamente detectada.

Chang M, et al. CLN2. In: Mole S, Williams R, and Goebel H, eds. The neuronal ceroid lipofuscinoses (Batten Disease). 2nd ed. Oxford, United Kingdom: Oxford University Press; 2011:80-109. Mole SE, et al. *Neurogenetics* 2005;6:197-208; Orlin A, et al. *PLoS One* 2013;8:e73128; Mole SE, et al. 2001 Oct 10 [updated 2013 Aug 1]. In: Pagon RA, et al., eds. *GeneReviews*.

Crianças apresentam perda significativa das funções à medida que os sintomas evoluem com a idade

Linha do tempo da manifestação de sintomas da doença CLN2 clássica



Chang M, et al. CLN2. In: Mole S, Williams R, and Goebel H, eds. The neuronal ceroid lipofuscinoses (Batten Disease). 2nd ed. Oxford, United Kingdom: Oxford University Press; 2011:80-109. Perez-Poyato MS, et al. *J Child Neurol* 2012;28:470-478; Steinfield R, et al. *Am J Med Genet* 2002;112:347-354; Schulz A, et al. *Biochim Biophys Acta* 2013;1832:1893-1895; Worgall S, et al. *Hum Gene Ther* 2009;19:463-474.

FORMAS ATÍPICAS DA DOENÇA CLN2

- ✓ Os fenótipos atípicos são mais raros, caracterizados por idades de início variadas e/ou maior expectativa de vida, como por exemplo:
- **Forma Juvenil:** evolução mais benigna, predomínio de sintomas extrapiramidais como coreia, distonia, parkinsonismo;
- **Forma do Adulto:** variante de ataxia espinocerebelar 7 (SCAR7), pode não apresentar epilepsia.

Fietz M et al. Mol Genet Metab. 2016 ;119:160;
Kohan R, et al. Biochim Biophys Acta. 2015;1852:2301

Lipofuscinose Ceroide Neuronal Tipo 2 (CLN2) Exames Complementares

O eletroencefalograma (EEG)

- ✓ EEG é o primeiro exame que deve ser realizado;
- ✓ Atividade de fundo alentecida (pode ser normal na 1ª fase da doença), com alterações epileptiformes generalizadas que predominam nas áreas posteriores;
- ✓ Fotoestimulação intermitente (FEI) a 1-2Hz deve ser solicitada sempre;
- ✓ É importante testar todas as frequências para não perder as características informativas do EEG.

Fietz M et al. Mol Genet Metab 2016;119:160-167

4

Como solicitar o EEG

Solicito:

EEG em vigília, smolência e sono com estimulação fotica enfatizando os seguintes bancos de fotoestimulo - 0,5/s; 1/s; 2/s, 3/s

Arquivo pessoal da Dra Elza Márcia Yacubian. Usado com permissão.

Fotostimulação de baixa frequência

- ✓ Pontas gigantes occipitais em paciente com a doença CLN2
- Ocorrência de potenciais evocados gigantes com maior amplitude nas regiões occipitais, em resposta ao estímulo fótico de 3 lampejos/seg., com frequência idêntica à estimulação.

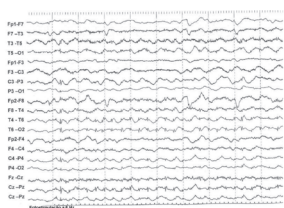


Arquivo pessoal da Dra Elza Márcia Yacubian. Usado com permissão.

4

Fotostimulação de baixa frequência

- ✓ Pontas gigantes occipitais em paciente com doença CLN2
- Estes potenciais apresentam redução em amplitude e menor correlação com os lampejos conforme a frequência dos últimos é aumentada.



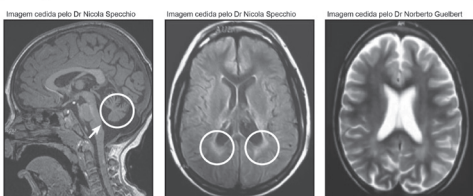
Arquivo pessoal da Dra Elza Márcia Yacubian. Usado com permissão.

Photosensitivity is an early marker of neuronal ceroid lipofuscinosis type 2 disease (Specchio N, et al., Epilepsia 2017 Jun 20)

- ✓ N = 14 pacientes, 2005-2015. Idade de início aos 3,0 (2,0-3,8) anos;
- ✓ Sintomas:
 - Atraso ou regressão do DNPM, 100% aos 3 anos de idade;
 - Início da epilepsia (50%) aos 3,2 anos de idade (2,6-3,8) e a primeira crise foi:
 - Generalizada: mioclônica em 36%, TGC em 29%, atônica em 22%;
 - Focal com sinais motores em 14%;
 - Marcha independente, 100% aos 12 meses de idade.
- ✓ Exames:
 - EEGs com resposta fotoparoxística → 93%;
 - Atrofia cerebelar na RM → 100%;
 - Alteração da substância branca na RM → 79%.

Achados de ressonância magnética

RM de paciente CLN2



Atrofia Cerebelar

Hiperintensidades periventriculares na substância branca

Atrofia cerebral

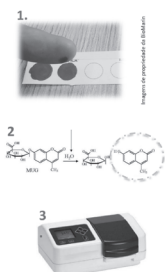
Chang M, et al. CLN2. In: Mole S, Williams R, and Goebel H, eds. The neuronal ceroid lipofuscinoses (Batten Disease). 2nd ed. Oxford, United Kingdom: Oxford University Press; 2011:10-109. 2. Mole SE, et al. Neurogenetics. 2005;8:107-126.

DOSAGEM DA ATIVIDADE DA ENZIMA TPP1

✓ CLN2: deficiência na enzima tripeptidil-peptidase 1 (TPP1);

✓ Processo:

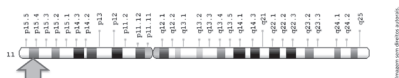
1. A atividade pode ser medida em leucócitos, fibroblastos, vilosidades coriônicas e fluido amniótico;
 - Adaptado para gota de sangue seca (DBS).
2. A enzima TPP1 cliva o substrato artificial em pH ácido;
3. Composto fluorogênico 7-amino-4-metilcumarin é liberado e medido no fluorímetro.



Miller et al. Poster presented at ASHG 2016; Fietz M, et al. Mol Genet Metab. 2016;119:160-167; Giugliani R, et al. Mol Genet Metab. 2016;117:561, Abstract 143.

SEQUENCIAMENTO DO GENE CLN2/TPP1

✓ O gene CLN2/TPP1 é localizado no cromossomo 11p15.4, contém 13 éxons e tem 6,7kbp de comprimento;



✓ Sequenciamento de todos os éxons e regiões flanqueadoras associadas para detecção de variantes patogênicas (SNPs e pequenos indels);

- Next generation sequencing (NGS) → Técnica padrão;
- Sanger sequencing → Confirmar variantes novas e regiões perdidas.

✓ Importante confirmar que variantes patogênicas sejam encontradas nos dois alelos (em homocigose ou heterocigose composta em trans).

Miller et al. Poster presented at ASHG 2016; Fietz M, et al. Mol Genet Metab. 2016;119:160-167; Giugliani R, et al. Mol Genet Metab. 2016;117:561, Abstract 143.

Orientação genética e planejamento familiar

✓ Doença com padrão de herança autossômico recessivo;

✓ Avaliar consanguinidade na família;

✓ Avaliar risco para irmãos, novas gestações, parentes em primeiro grau etc.;

✓ Diagnóstico precoce é de fundamental importância para avaliar risco genético para futuras gestações.



Williams RE, et al. Poster session presented at: The 12th Annual WORLD Symposium; February-March 2016; San Diego, CA.

Lipofuscinose Ceroide Neuronal Tipo 2 (CLN2) Tratamento

SEGUIMENTO: CONDUTA PADRÃO

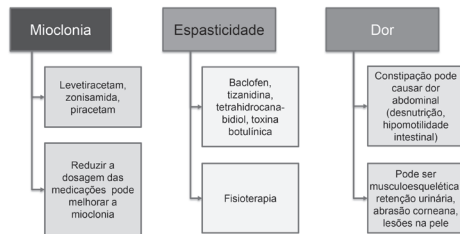


O atendimento multidisciplinar promove melhor acompanhamento para crianças com a doença CLN2

Adaptado de: Williams RE, et al. Poster session presented at The 12th Annual WORLD Symposium, February-March 2016, San Diego, CA.

CONDUTA NA CLN2 TERAPIA SINTOMÁTICA

Sugestão de especialistas em LCNs para tratamento dos sintomas da CLN2



Adaptado de Schulz A. Biochim Biophys Acta. 2013;1832 :1801.

Existem oito ensaios clínicos voltados a NCLs (clinicaltrials.gov)

Tipo de CLN	Terapêutica	Mecanismo de ação	Estudos pré-clínicos	Fase do teste
JNCL	Anti-inflamatório Micoletato mofetil	Neuro inflamação Produção de AC	Seehafer 2011	Recrutamento
LINCL	Gene terapia AAVrh10CUH/CLN2	Engenharia -> células para produzir TPP1 sem mutação	Sandhi 2007 2008 e 20012	Recrutamento
LINCL	Gen terapia AAVrh10CUH/CLN2	Engenharia->Células para produzir TPP1 sem mutação	Sandhi 2007 2008 e 20012	Recrutamento
LINCL	TRE (Terapia de Reposição enzimática) BMN 190*	Fonte de TPP1 funcional combinante absorvidas por célula doente	Vuilleumet 2014, 2014	Ativo
LINCL	Gen terapia AAV2CUH/CLN2	Engenharia -> células para produzir TPP1 sem mutação	Sandhi,2005 Passini 2006	Ativo
INCL	Células tronco SNC humano	Células tronco como fonte de PPT1 e TPP1 funcionais (~TER)	Tamaki 2009	Completo
INCL	Pequena molécula Cystagon	Limpa lisossoma de material de depósito	Zhang 2001	Completo
INCL	Células tronco SNC humano	Células tronco como fonte de TPP1 funcional (~TER)	Vuilleumet 2014, 2014	Ativo

Gerzets RD et al. J Rare Dis. 2016;11:40

*Produto não registrado no Brasil

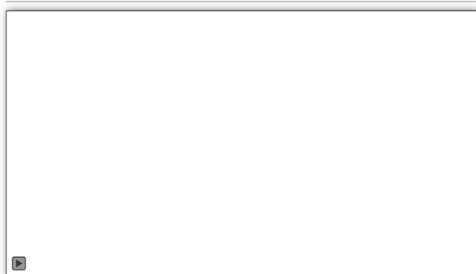
Modelos animais de CLN2 reproduzem a doença humana

- ✓ Camundongos TPP1-knockout (KO) apresentam tremores, ataxia e perda neuronal;
- ✓ Dachshunds de TPP1-null apresentam déficits visual e cognitivo, ataxia, tremores, crises mioclônicas e atrofia cerebral;
- ✓ Depósito de corpos auto-fluorescentes no SNC em ambos os modelos;
- ✓ Expectativa de vida reduzida: camundongo, 120 dias; dachshunds, 10-11 meses.



Katz ML, et al., Journal of Neuroscience Research 92:1591-1598, 2014; Sleat et al. Neurobiol Dis 2004; Awano et al. Mol Genet Metab 2006

Terapia em cães com TPP1-null (cont.)*

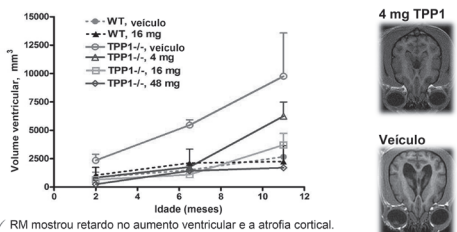


*Produto não registrado no Brasil

Vídeo cedido pelo Dr. Katz ML.

Terapia em cães com TPP1-null*

Efeito do tratamento com rhTPP1 no volume ventricular cerebral



✓ RM mostrou retardado no aumento ventricular e a atrofia cortical.

*Produto não registrado no Brasil

Adaptado de Katz ML, et al., *Journal of Neuroscience Research* 92:1891-1898, 2014; Sleat et al. *Neurobiol Dis* 2004; Awano et al. *Mol Genet Metab* 2006

TRATAMENTO DA CLN2

- ✓ **BRINEURA[®]**
- ✓ Aprovada pela FDA, EMA e ANVISA



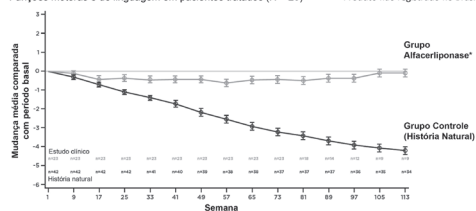
- ✓ **Reposição Enzimática: Alfa-cerliponase**
- ✓ Reposição da enzima: TPP1 humana (**produzida por engenharia genética**);
- ✓ Alfa-cerliponase por via intracerebroventricular (ICV);
- ✓ Dosagem: 300 mg dose fixa;
- ✓ Frequência: a cada duas semanas.



Data on file (FDA): https://www.accessdata.fda.gov/drugsatfda_docs/nda/2017/761052Orig1s000TOC.cfm
http://www.ema.europa.eu/en/medicines/human/medicines/020206/summar_phil_020211_135Andr/WC901aw050001r124-Vu
 Heemroot BR et al. *Mol Genet Metab*. 2015;114:281-293; Hallia M. *Biochim Biophys Acta*. 2006;1752:850-856; Vujkiewicz BR et al. *Toxicol Appl Pharmacol*. 2014;277:48-57

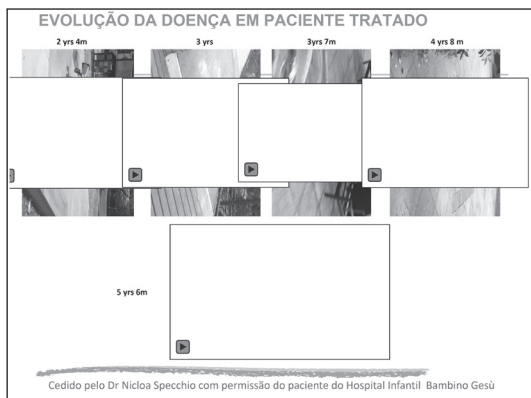
Em humanos, alfacerliponase^{*} estabilizou a evolução clínica da doença CLN2 na maioria dos pacientes em 48 semanas comparados com a história natural da doença

Mudança na média comparada com o período basal na escala de evolução clínica da CLN2 Funções motoras e de linguagem em pacientes tratados (N = 23) *Produto não registrado no Brasil



- ✓ No estudo 190-201, o declínio médio nos pacientes tratados com alfacerliponase 300mg a cada 2 semanas foi 0,40 pontos em 48 semanas, sendo que a taxa esperada de declínio apontada no grupo de história natural é de perda de 2 pontos a cada 48 semanas.

Data on file (FDA): https://www.accessdata.fda.gov/drugsatfda_docs/nda/2017/761052Orig1s000TOC.cfm; Schulz A, et al. *International Conference on Neuronal Ceroid Lipofuscinosis*. Abstract O-48, 2016.



Resumo

- ✓ A doença CLN2:
 - Para crianças com essa patologia neurodegenerativa de progressão rápida, 2 anos até o diagnóstico é muito tempo;
- ✓ Deve-se suspeitar da doença CLN2 em crianças entre 2 a 4 anos de idade com:
 - crises epiléticas não provocadas de início precoce;
 - histórico de atraso precoce de linguagem.
- ✓ Teste enzimático e/ou molecular deve ser usado para diagnosticar a doença CLN2;
- ✓ EEG com FEI de baixa frequência pode ser usado para a suspeita da doença CLN2;
- ✓ O diagnóstico precoce acelera o acesso ao tratamento multidisciplinar específico para a doença CLN2, o que melhorar a qualidade de vida, tanto da criança, como da família.

Schulz A, et al. *Biochim Biophys Acta*. 2013;1832:1801-1806. Mole SE, et al. 2001 Oct 10 [Updated 2013 Aug 1]. In: Pagon RA, et al., eds. *GeneReviews*. Nickel M, et al. Poster session presented at: The 12th Annual WORLD Symposium; February-March 2016; San Diego, CA. Perez-Poyato MS, et al. *J Child Neurol*. 2012;28:470-478. Fietz M, et al. Poster session presented at: The 12th Annual WORLD Symposium; February-March 2016; San Diego, CA.

ATENÇÃO

1-ATRASO NA FALA -> acompanhar com atenção

2- EPILEPSIA DE INÍCIO RECENTE -> pesquisar etiologia

PARA ALGUMAS DOENÇAS HEREDODEGENERATIVAS EXISTE TRATAMENTO

MAS

O DIAGNÓSTICO PRECOCE É FUNDAMENTAL

Schulz A, et al. *Biochim Biophys Acta*. 2013;1832:1801-1806. Mole SE, et al. 2001 Oct 10 [Updated 2013 Aug 1]. In: Pagon RA, et al., eds. *GeneReviews*. Nickel M, et al. Poster session presented at: The 12th Annual WORLD Symposium; February-March 2016; San Diego, CA. Perez-Poyato MS, et al. *J Child Neurol*. 2012;28:470-478. Fietz M, et al. Poster session presented at: The 12th Annual WORLD Symposium; February-March 2016; San Diego, CA.


FACILIDADES PARA O DIAGNÓSTICO DA CLN2

REDE DLD BRASIL- Projeto CLN2

Serviço de Genética Médica – Hospital de Clínicas de Porto Alegre
Rua Ramiro Barcelos 22350 - CEP 90035-903- Porto Alegre - RS- SP

Fone gratuito 0800 6438011
Fone (051) 33598010 e Fax (051) 33598010
dld@ufrgs.br

PROJETO “Epilepsia e Genética”



✓ **Entre em contato com o Mendelics:**

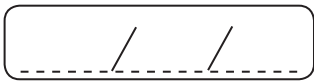
- 1- Ligue ou envie um e-mail para o Mendelics
- 2- Solicite a ficha de critérios de elegibilidade;
- 3- Depois siga as instruções informadas pelo Mendelics.

✓ +55 11 5096-6001 contato@mendelics.com.br

OBRIGADA



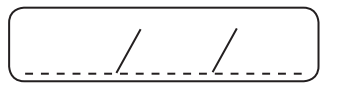
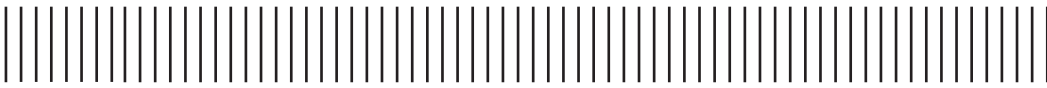
BIOMARIN



PRESENTATION OF RESEARCH PROJECTS



Lined writing area consisting of 20 horizontal lines.



GOODBYE TO THE 13TH LASSE



Lined writing area consisting of 20 horizontal lines for text entry.

